Predictive Modelling of Ash Particle Deposition in a PF Combustion Furnace

By

Mohammed Usman Degereji

Supervised by

Professor Mohamed Pourkashanian
Professor Derek B. Ingham
Professor Alan Williams
Dr. Lin Ma

Submitted in accordance with the requirements for the degree of PhD

Advanced Power Generation Technology Group
Centre for Computational Fluid Dynamics
School of Process, Environmental & Materials Engineering
Faculty of Engineering

University of Leeds

July, 2011

ACKNOWLEDGEMENTS

I would like to express my gratitude to God for giving me the health and ability to carry out this research. Also, my sincere appreciation goes to the Nigerian Government for funding this research work. The support I enjoyed from PTDF and FCE Yola is highly appreciated.

I am highly indebted to my supervisors, namely; Professor Mohamed Pourkashanian, Professor Alan Williams, Professor Derek B. Ingham and Dr Lin Ma, for their continued support, patience, guidance, direction and understanding during the period of this PhD research study.

I wish to acknowledge with thanks all the support and assistance I received from the staff and friends of the University throughout my research period. Special thanks to Professor Jim Williamson of Imperial College London for his helpful comments on some part of my research findings.

Finally, I would like to thank my parents, my wife and children, and all the members of the Degereji family who have been encouraging and motivational, to me, in completing this PhD research. Not to forget, many thanks to my colleagues and friends who have been so kind and supportive to me in this research.

This thesis has fulfilled the wish of my late father, Alh. Usman Ahmad Degereji, and therefore it is dedicated to his memory.

ABSTRACT

Slagging and fouling during the combustion of pulverised coal in boilers is a major problem as power generators strive to improve the efficiency of plants. The coal type has a major influence on the slagging propensity in furnaces. The correlation between predicted results using some of the existing slagging indices and the actual observations made in most conventional boilers has been poor, especially when their use is extended to different coals.

In this thesis, a numerical model to predict coal ash particle deposition rate in pulverized coal boilers has been developed. The overall sticking probability of the particle is determined by its viscosity and its tendency to rebound after impaction. The deposition model has been implemented in the Fluent 12.1 software, and the effects of swirling motion ash particle viscosity on deposition rates have been investigated. The predicted results are in good agreement with the reported experimental measurements on the Australian bituminous coals.

Also, a novel numerical slagging index (NSI) which is based on ash fusibility, ash viscosity and the content of ash in the coals has been developed. The incoming ash shows significant influence on slag accumulation in boilers. The results of assessment of the slagging potential using the NSI on a wide range of coals and some coal blends correlate very well with the reported field performance of the coals. The NSI has been modified to predict the slagging potential of some coal and biomass blends with < 20% biomass ratio. The results of predictions using the modified index on coals blended with sewage sludge and saw-dust are in good agreement with the experimental data.

TABLE OF CONTENTS

LIST OF FIGURES

LIST OF TABLES

NOMENCLATURE AND ABBREVIATIONS

Nomenclature

A_p	surface area of a droplet (m^2)
c	intercept
C_D	spherical drag coefficient
C_i	component i by condensation
C_m	coefficient of mass exchange
C_s	coefficient of thermal slip
C_t	coefficient of temperature jump
C_P	particle specific heat (kJ/kg.K)
D	ratio of maximum deformation to actual particle diameters
d_P	burning particle diameter (m)
D_o	diffusion rate (moles/sec)
d_{po}	initial coal particle diameter (m)
E_x	particle excess energy (J)
f	mixture fraction
F_D	drag force ($Pa.m^2$)
F_i	body forces (N)
F_s	correlating factor
$f_{v,o}$	initial mass fractions of the volatiles in a particle (kg)
$f_{w,o}$	initial mass fractions of evaporating material in wet combustion (kg)
F_x	virtual mass forces (N)
g_x	gravitational force (N)

H enthalpy (J/kg)

i specific internal energy (J/kg)

I_i component i by inertial impaction

I_b black body emission coefficient

$\bar{I}$ in-scattering coefficient

k Boltzmann constant

k fluid thermal conductivity (W/m.K)

k_p particle thermal conductivity (W/m.K)

K_a absorption coefficient

m slope

m_i mass of component i in the deposit

m_p char particle mass (kg)

m_{po} initial coal particle mass (kg)

$\dot{m}_{trj,i}$ trajectories of i^{th} particle

p fluid pressure (N/m^2)

P_{ox} partial pressure of the oxidant species (N/m^2)

q_c convective heat transfer coefficient

Q_c rate of heat gain of loss by particle per unit mass by convection (W/kg)

Q_r rate of heat gain of loss by particle per unit mass by radiation (W/kg)

R kinetic rate (moles/sec)

R_i component i by heterogeneous reactions

R_e Reynolds number

R_S slagging index (B/A multiplied by S)

S dry sulphur content in coals (wt % db)

S_i internal energy source

S_m momentum source

S_x proposed numerical slagging index

t particle residence time (s)

T local fluid temperature (K)

$T_{250(ox)}$ 250 poise temperature for oxidizing conditions (°C)

$T_{1000(red)}$ 1000 poise temperature for reducing conditions (°C)

T_i component i by thermophoretic effect

T_p particle temperature (K)

T_∞ bulk phase temperature (K)

U fractional degree of burnout

$\mathbf{u}$ velocity vector

u x-velocity component (m/s)

u_f fluid velocity (m/s)

u_i fluid phase velocity (m/s)

u_p particle velocity (m/s)

v y-velocity component (m/s)

w z-velocity component (m/s)

W_e Weber number

Z_i elemental mass fraction for the element i (mole)

α particle static contact angle (degrees)

α_s swirl factor

β fractional degree of burnout

γ ash loading in coals (MJ^{-1})

Γ diffusion coefficient

κ_i particle sticky probability

μ	fluid molecular viscosity (Pa.s)
μ_c	critical (reference) viscosity (Pa.s)
μ_f	fluid molecular viscosity (Pa.s)
μ_p	particle viscosity (Pa.s)
μ_{to}	turbulent viscosity without swirl (Pa.s)
ρ_f	fluid density (kg/m^3)
ρ_p	particle density (kg/m^3)
σ_{ij}	stress (N/m^2)
σ_s	out-scattering coefficient
δ	particle surface energy (N/m)
τ	elapsed laboratory time (s)
τ_p	particle relaxation time (s)
ϕ	property of transported quantity
Φ	dissipation function
Ω	characteristic swirl number
μm	micron

Abbreviations

ACF American coal foundation

ACIRL Australian coal industries research laboratories

AFT ash fusion test

ASTM American society for testing and materials

B/A basic to acidic ash oxides ratio

BR Biomass ratio

CCS carbon capture and storage

CFD computational fluid dynamics

CPD chemical percolation devolatilization

CPU central processing unit

CV calorific value

DO discrete ordinate

DPM discrete phase model

DRW discrete random walk

EIA energy information administration

Exp experimental measurement

FC fixed carbon

HHV higher heating value

HT hemispherical temperature

IDT initial deformation temperature

IGC international geology congress

LHV lower heating value

NSI numerical slagging index

NTA Nigerian television authority

PDF probability density function

PF pulverized fuel

RNG renormalized group theory

RTE radiative transfer equations

SEM scanning electron microscopy

SN swirl number

SR silica ratio

ST softening temperature

TMA thermo-mechanical analysis

UDF user-defined function

VM volatile matter

WCI world coal institute

WSGGM weighted-sum-of-grey-gases model

PAPER PUBLICATIONS AND CONFERENCE ATTENDANCE

Paper Publications

1. Degereji MU, Ingham DB, Ma L, Pourkashanian M, & Williams A. *Prediction of ash slagging propensity in a pulverized coal combustion furnace.* Fuel (2011), doi:10.1016/j.fuel.2010.12.038.

2. Degereji MU, Ingham DB, Ma L, Pourkashanian M, & Williams A. *Numerical assessment of coals/blends slagging potential in pulverized coal boilers.* Submitted to Fuel Journal (April, 2011).

3. Degereji MU, Gubba SR, Ingham DB, Ma L, Pourkashanian M, & Williams A. *An assessment of slagging potential during co-firing of coal with sewage sludge and woody biomass.* In preparation for 'Fuel Processing Technology' (July, 2011).

Conferences Attended

1. 8th European conference on coal research and its applications, ECCRIA, 6-8 September 2010, Leeds – UK. A paper on coal ash deposition rates has been presented.

2. Fifth international conference on clean coal technologies CCT2011, 8-12 May 2011, Zaragoza – Spain. A paper on slagging index has been presented.

CHAPTER 1

INTRODUCTION

1.1 General Background

The availability of energy in reliable and economical form is considered as a major pre-requisite for national development and it remains a major challenge for energy engineers (Mshelia, 1997). The world's energy demand is continuously growing, with higher growth rates in developing countries than in the developed ones. Energy suppliers are faced with numerous challenges, including environmental and operational related ones, and these challenges need to be fully understood before resolving them.

In order to solve the problems related to energy generation, experimental and numerical techniques are been developed, and some of the features of the power generation facilities and their operational conditions are modelled in order to enhance the understanding of the system. So far, tremendous achievements in the use of numerical techniques have been recorded. However, still a lot needs to be done considering the increasing demand for energy and the fast depletion of some of the available energy resources.

The increasing demand for energy is apparent in view of the population increase and technological advancements across the globe. In the International Energy Outlook for 2010, the Energy Information Administration (EIA, 2010)

projected that world energy consumption will increase by 49% from the year 2007 to the year 2035, with the largest projected increase in energy demand from the developing countries.

According to the EIA report, China and India, being the least affected by the current economic recession, continue to lead the world's economic growth and energy demand. The report also projected that the world marketed energy consumption by the year 2015 will be 543 quadrillion Btu as against 495 quadrillion Btu in the year 2007 (EIA, 2010).

According to Pimentel *et al.* (1994), the United States (US), with only 4.7% of the world's population, consumes approximately 25% of the total world's fossil fuel used each year. They described this situation as critical in view of the fact that US now imports about half of its oil from other countries. They further stated that the domestic fossil fuel reserves in the US are rapidly being depleted, and their coal supply could be used up in a period shorter than the projected 100 years.

Electric energy demand shows similar escalating trends. Estimates show that the total world energy and electric energy consumption will double in a couple of decades' time. According to some research reports, the doubling period is much shorter for developing countries, particularly those countries undergoing development programmes with a relative high population growth rates (Mshelia, 1997).

The available sources of energy include the non renewable, such as, oil, gas, coal and nuclear, and the renewable, such as, biomass, geothermal, hydro power, solar and wind. These resources are distributed in different quantities and in different parts of the world. Although these energy resources are available in sufficient quantities, the financial and technological constraints hinder the successful harnessing of the resources in order to supply the energy that will meet its increasing demand. Also, it has become apparent that the processes of generating energy using most of the existing resources are accompanied with numerous challenges.

Basically, energy is used for industrial processes, transportation, space heating and electricity generation. Electricity generation is more popular because of its direct application by billions of users from all parts of the world. The technological advancement makes it more difficult to meet the demand for electricity supply. Therefore, it has become necessary to explore all available options of generating electricity. However, the cost of generation electricity remains a major concern even in the developed countries.

One of the most important ways of generating electricity is the burning of coal to generate the required steam to turn the turbines. Wigley & Williamson (1998) anticipated that coal will remain the major source of energy for electricity generation in the foreseeable future. Owing to its high heating value, coal is the most preferred source of energy despite its emission problems. Also, if not because of its alarming environmental impact, the burning of coal is considered as a relatively cheap means of electricity generation.

With the emergence of clean coal technologies, such as coal gasification and carbon capture & storage (CCS) technique, which are being used in order to minimize environmental issues on coal combustion, the need for more research work on coal combustion optimization should not be overstressed since the use of coal for energy generation is on the increase.

According to the American Coal Foundation (ACF, 2010), nine out of every ten tons of coal being mined in the US today is used to generate electricity, and more than 50% of the total electricity in the country is coal generated. In another projection, the World Coal Institute (WCI, 2010) suggests that coal will fuel about 44% of the world electricity in the year 2030, and this prediction further highlights the important role of coal in the energy generation sector.

The study of the combustion process is generally based on the laws of thermodynamics, chemical kinetics, heat and mass transfer, and fluid flow. It is considered as one of the most important processes in engineering, which involves turbulent flow, heat transfer, chemical reactions and other complicated physical and chemical processes (Versteeg & Malalasekera, 2007). Most of the processes involved in the combustion of coals are physically difficult to measure for individual particles due to high temperatures in boiler situations. This further complicates the process and informed the need for the use of numerical techniques.

With the advent of highly technical modelling capabilities, several problems encountered in the combustion processes, including ash-related problems, are being investigated. More often, the ash generated through the combustion of

solid fuels, such as pulverized coal, stick to the heat exchange surfaces and this results in operational problems, such as slagging and fouling which results in increased cost of maintenance (Naganuma *et al.*, 2009; Huang, Norman, Pourkashanian & Williams, 1996; Rushdi, Gupta, Sharma & Holcombe, 2005; Mueller, Skrifvars, Backman & Hupa, 2003). Also, slagging and fouling affect the availability of the energy due to untimely shutdowns.

The influence of ash deposition in boilers leaves the energy engineer with the choice between coal quality and cost (Wigley & Williamson, 1998), and the need for an effective mechanism for the removal of deposits on the boiler surfaces in order to protect the downstream superheaters from damage due to fouling and erosion (Zhang & Ahmadi, 2001).

Although it is very difficult to effectively determine the ash deposition processes at operating conditions close to actual boilers in the power stations (Su, Pohl, Holcombe & Hart, 2001b), Benson, Sondreal & Hurley (1995) summarized the behaviour of ash formation and deposition in coal combustion as dependent on the physical transformations that are involved in a high temperature suspension, which include:

i. Selective elemental vaporization and subsequent condensation to form surface coating.
ii. Coalescence of mineral grains within hot reactive char particles.
iii. Char fragmentation and partial coalescence of included mineral grains.
iv. Shedding of particles from the char surface.
v. Fragmentation or fusion of liberated mineral grains.

vi. Convective transport of the volatile species within and between the char particle.

vii. Formation of thin-walled ash spheres.

However precise such a summary of ash behaviour can be, the understanding of the ash deposition process at high temperatures is still inadequate (Naruse *et al.*, 2005). Therefore, it is desirable to intensify studies on all the individual mechanisms responsible for ash particle deposition in pulverized fuel (PF) boilers. This is considered as a viable means of understanding the ash deposition processes in full.

To overcome the difficulty of the experimental study of the ash deposition processes in high temperature combustion, several efforts have been made towards developing an acceptable and robust numerical prediction model (Rushdi *et al.*, 2005). The performance of the developed predictions tools have been tested using both pilot-scale and industrial facilities. Although the results obtained are encouraging, still a lot more need to be done.

Although the problem of ash deposition is still not fully understood, it is generally agreed that the ash deposition is due to the cumulative effect of four main processes, namely; inertial impaction due to particles of large sizes, heterogeneous reactions, condensation of flue gas in the convective region of the boiler and change in temperature gradient which is referred to as thermophoretic effect (Huang *et al.*, 1996; Lee & Lockwood, 1999).

Each of the ash deposition pathways plays a significant and distinct role in the overall deposition rate of ash particles. Although several attempts are being made to understand or predict the ash deposition processes (Lee & Lockwood, 1999; Baxter & DeSollar, 1993; Rushdi *et al.*, 2005), a comprehensive approach that may effectively reveal the effects of individual deposition pathways is required. However, modelling the individual pathways will enhance the understanding of how they influence the overall deposition process.

In an attempt to understand the effect of individual parameters contributing to the overall deposition process of the ash particles during coal combustion, the thermophoretic particle deposition mechanism has been studied by several researchers.

Most research results on ash deposition reveal that for fine particles sizes (0.3-1.3 μm), the thermophoretic force plays a significant role in their deposition process (Lin, Tsai, Tung & Chiang, 2008; Byers & Calvert, 1969), and such fine particles are said to be enriched with sodium and potassium elements (Takuwa, Mkilaha & Naruse, 2006).

Condensation is the mechanism by which vapours in the boiler are cooled and deposited to the heat exchange surfaces. However, condensation process mostly occurs in the regions of low temperatures, especially in the downstream boiler region. Both condensation and chemical reactions are strongly dependent on temperature, giving rise to spatial variations in the composition of the ash deposits (Baxter and DeSollar, 1993).

Baxter and DeSollar (1993) identified three different ways that lead to condensation, namely, heterogeneous condensation of vapour on the boiler walls, homogeneous nucleation of vapours resulting in fume formation which deposit on the walls, and vapours condensing on other particles that are already deposited on the heat exchange surfaces. All the three processes require that the vapour has to transverse the boundary layer and hit the boiler walls before deposition takes place.

Large particles (≥ 10 μm) are often transported to the furnace walls by inertial forces (Huang *et al.*, 1996; Strandstorm, Mueller & Hupa, 2007; Zhao & Wu, 2006; Costen, Lockwood & Siddique, 2000), and such particles are assumed to have sufficient inertia to transverse the gas streamlines and hit the furnace walls (Baxter & DeSollar, 1993).

Several investigations on the deposition patterns for both fine and coarse coal ash particles, considering inertial impaction, thermophoretic effect and other deposition mechanisms, such as, condensation and kinetic reactions, have been conducted (Lin *et al.*, 2008; Rushdi *et al.*, 2005; Lee & Lockwood, 1999).

However, it should be noted that the ash deposition mechanisms are mainly responsible for the transportation of particles to the heat exchange surface, and therefore, there is the need to numerically determine what will be the fate of the ash particles after impaction on the heat exchange surfaces.

Thermal conditions and the aerodynamics have been identified as some of the principal factors that can influence ash deposition characteristics in a furnace (Su, Pohl, Holcombe & Hart, 2001a). Also, these important features are being influenced by several other factors, such as, furnace input variables, swirling motion, coal type and properties, burner design, etc., which also need to be investigated (Rushdi *et al.*, 2005).

Any study on ash deposition processes that do not consider deposition characteristics due to the temperature and the operating conditions of a system is considered as a poor indicator of deposition (Nutalapati, Gupta, Moghtaderi & Wall, 2007). In addition to other deposition factors, such as coal type, reaction atmosphere (oxidizing process) and flow dynamics, the temperatures of the ash particle and the heat exchange surface have been emphasized (Naruse *et al.*, 2005).

The use of particle viscosity to determine the capture efficiency of the ash particles has been reported (Huang *et al.*, 1996; Lee & Lockwood, 1999). However, the choice of the reference viscosity, the varying wall temperatures and the ash particle composition bring about inconsistencies in the research results.

The choice of suitable application models in the existing commercial software packages, in order to simulate a particular experiment, is also considered as a major challenge for the modelling engineers. More often, some assumptions are made to represent some of the situations that are very difficult, or sometimes

even impossible, to measure in real boilers. The accuracy of such assumptions always affects the prediction results.

In the FLUENT software for example, the available discrete phase model (DPM) boundary conditions include reflect, trap, escape, wall-jet, wall-film and interior types. It is also possible to monitor particle erosion and accretion rates. The erosion rate is a function of the particle diameter, impaction angle and particle relative velocity. However, both the available wall boundary conditions and the erosion rates do not effectively account for the particle capture efficiency, which is very significant in ash deposit growth.

In a related development, research activities on the problems being caused by coal mineral impurities in large boilers have received some attention (Raask, 1979; Wigley, Williamson & Jones, 1990). However, the choice of coal has been the pre-combustion priority, and several attempts to produce a more reliable slagging and fouling indices are being made. When coals that are more suitable to the design of a particular boiler are identified, the operational problems related to ash deposition may be minimized.

The prediction of coal ash deposition characteristics has been traditionally related to the chemistry of the bulk ash and ash fusion temperatures (Gupta, Wall, Creelman & Gupta, 1998). Also, the ash shrinkage rate is used to characterize the ash behaviour in boilers.

The general ash fusion test (AFT), the basic to acidic ash oxides ratio (B/A) and the ash viscosity have been widely used as tools for the characterization of coal ash in boilers. However, these slagging indices do not reliably predict the field slagging performance of all coals (Lawrence, Kumar, Nandakumar & Narayanan, 2008), and hence the need for a generic and more acceptable tool.

In recent times, empirical research reports reveal that the ash shrinkage rate can be correlated with the field performance of the coal since it depends on the ash viscosity (Raask, 1979; Gupta *et al.*1998; Lawrence *et al.*, 2008). Although this is a laboratory-scale test which may not account for the dynamic boiler situations, at least, it accounts for the ash chemistry and the effect of changing temperature gradients.

The techniques of blending different coals and the co-firing of coal/biomass blends in existing coal facility are widely used for the generation of electricity. Although the practice of blending has significant advantages, such as, ensuring fuel availability, cost and emissions reduction, etc., slagging, fouling and boiler corrosion remain critical issues to contain with. Therefore, careful selection of the fuels for the blends is necessary in order to minimize operational problems.

1.2 Statement of the Problem

The main concern for a power system engineer is to generate electricity in a more reliable, economical and uninterrupted manner. In pulverized coal fired power stations, ash deposition on heated surfaces is an important factor in

determining the combustion performance. This problem, which is associated with slagging, fouling and other boiler drive problems, often results in untimely power outages and high maintenance cost. In view of the importance of energy supply in our global industrialization efforts, untimely outages are considered unacceptable.

In order to eliminate, or minimize, unwanted power outages, the ash deposition mechanism needs to be well understood. However, in a high temperature environment, such as a pulverized coal combustor, the behaviour of ash particles is difficult to predict. This is because of the uncertainties caused by the turbulence eddies in the boiler and the changing physical properties of the fuel. Therefore, understanding particle trajectories, or predicting the ash particles deposition behaviour during pulverized coal combustion in boilers, is a major challenge.

Despite several research studies in the field of ash deposition, the problem is yet to be fully understood. Since the combustion mechanism is virtually the same for all solid fuels, solutions to particle tracking problems in coal combustion will apply to other pulverized or pelletized fuels, such as biomass, co-firing of coal and biomass, etc., when the fuel properties are fully evaluated and integrated.

In another approach, the problems of coal ash in boilers can be minimized by careful selection of the coal. However, most of the existing coal selection tools (the coal slagging indices) have been established for particular types of coal,

specifically, American and European coals. Furthermore, most of the existing coal slagging indices do not account for ash loading in predicting coal slagging potential despite its significant contribution in the accumulation of ash deposits in boilers.

Although there are several investigation reports on coal slagging and fouling assessment tools, the search for a generic and more reliable coal slagging index continues. The use of coal blends and the co-firing of coal and biomass will add more pressures. Thus, the search for a better fuel selection tool will continue as long as scientists and engineers manipulate the available energy resources in order to supply a more efficient, reliable, and cost-effective energy that will meet the demands of the increasing world population.

Coal slagging indices that are developed based on the properties of different coals may have their use been extended to coal blends and to even coal/biomass blends provided that the properties of the individual fuels and the interaction between them are properly accounted for.

1.3 Research Motivation

The world's energy demand is continuously growing and demand figures are doubling by decades. Although predictions show rapid depletion of fossil fuels, several researchers have predicted that the use of coal for electricity generation will remain dominant in decades to come. However, environmental problems, such as emissions, and operational problems, such as slagging and fouling,

have been identified as the major challenges in coal combustion processes, and these problems need to be fully understood in order to profound possible solutions.

A number of research studies have already been performed in coal ash deposition. Several experiments have been conducted and various simulation techniques were applied, all in an attempt to fully understand the problem of ash deposition mechanism. However, this problem is still not completely understood and it remains a major impediment in the power generation industry.

Large countries, such as America and China, use coal for more than 50% of their electricity generation. The story is the same even in the developing countries. For example, the Nigerian government, in the first quarter of 2011, has announced on its state media, i.e. the Nigerian Television Authority (NTA), a plan to establish five coal-fired plants in the country in order to boost power generation.

The problems associated with coal combustion are extremely difficult to physically investigate because of the high temperature situations. However, the advent of new prediction techniques, such as Computational Fluid Dynamics (CFD), has encouraged researchers to work for better results while using different approaches to investigate combustion problems. It is expected that the efficiencies of coal and biomass combustors will one day reach a new optimal stage.

Several commercial software packages have recently been put into practice. These packages contain some parametric values that are likely to yield better prediction results. However, the use of the commercial software packages to obtain better prediction results depends, to a large extent, on the skills and the ability of the user. For example, the accuracy of the results obtained using the FLUENT software is largely dependent on the manipulative skills of the person implementing the simulations.

Also, identifying a suitable fuel to burn in a given combustion facility will significantly reduce the ash slagging tendency in the boiler. One of the reliable ways of selecting fuel is by the use of assessment tools in order to distinguish between a good and a bad fuel. This is one of the reasons why several slagging and fouling indices are being developed and improved upon. In the meantime, there is no universally accepted slagging and fouling indices for coal/biomass blends, instead, some of the existing coal slagging indices are used to predict the slagging potential of the blends.

1.4 Research Objectives

The aim of this study is to numerically investigate how some of the physical and chemical properties of the coal, such as bulk ash chemistry and ash particle viscosity, influence the behaviour of coal-ash in boilers. In order to achieve this objective, a numerical model to predict ash particle deposition rates during pulverized coal combustion, in particular in the burner region where the

temperatures are very high (≥ 1500 K), is developed on the basis of ash viscosity, among other factors.

Inertial force is assumed to be the key pathway for ash particles to transverse to the wall boundary layer and reach the boiler walls. When the particles hit the heat exchange surfaces, the ash particle viscosity, surface energy and static contact angle are some of the factors considered in determining the fate of the particles in contact with the surfaces. Particle rebound tendency at impaction is also considered in determining the overall sticking probability of the ash particles.

Some of the factors that have sufficient influence on the ash behaviour in a boiler, such as the swirling motion and the viscosity of the ash, are investigated in order to determine how they influence the ash slagging process under dynamic boiler situations.

Another popular method for minimizing slag formation in boilers is the use of a reliable tool in selecting coal fuel before combustion. Also, this research study is aimed at developing a numerical slagging index (NSI) to predict the slagging potential over a wide range of coals. The NSI is to account for the effects of ash fusibility, ash viscosity and ash loading, in predicting the slagging potential of the coals.

The slagging index is flexible such that can be used to predict the slagging potential of coal blends. Also, it is expected to predict coal/biomass blends if

additional work to account for the complex properties of biomass ash is done. In this thesis, attempt is made to extend the use of the coal slagging index to predict slagging potential of co-firing blends.

CFD techniques are used in the implementation of the developed numerical models. The ash deposition model is hooked as DPM boundary condition in the FLUENT 12.1 commercial software in order to determine the fate of the ash particles upon impaction on the heat exchange surfaces. Although the NSI can be implemented using simple tool, such as Excel and MATHLAB, the execute-on-demand command in the FLUENT software was used. The two models are validated using the available experimental measurements on coal combustion and co-firing.

1.5 Scope and Limitations

The ash particle deposition processes involve several steps; complete fuel combustion, particle trajectories and deposition processes are the key. Ash deposition is a cumulative effect of four main processes. These processes include both chemical and physical pathways, namely; inertial impaction, thermophoretic attraction, condensation and heterogeneous reaction between the ash particles and the deposition surface (Huang *et al.*, 1996).

The first part of this research study is mainly concerned with the determination of the fate of coal ash particles that may impact on the heat exchange surfaces of the furnaces. The numerical model developed is to determine whether a

particle sticks to the furnace walls upon impact or not. The existing models for combustion and particle transport are used in order to establish the required gas phase and particle trajectories in the boilers.

The available combustion facility that has relevant experimental measurements is modelled, and a computational grid is generated from the available test facility using the design tools provided by the University of Leeds. Furnace dimensions and experimental operating conditions, as provided, are used in the simulations.

The slagging performance of different coal types is assessed, and some important parameters, such as the swirl velocity and reference viscosity, are varied in order to assess the sensitivity of the model. The outcome of this is expected to be helpful in furthering our understanding of ash-related boiler problems.

The second part of this research is basically to examine the various coal properties and propose a numerical technique that can be used to assess the slagging potential over a wide range of coals. This is to complement the numerous attempts that are being made towards the development of a more acceptable and robust coal slagging index.

The coal ash fusibility, the ash viscosity and the content of ash in coals are some of the physical properties to be examined along side the bulk ash

chemistry in order to correlate the coal properties to its slagging field performance.

The numerical models developed in this research are tested using the only available experimental data (Su *et al.*, 2001b). No experimental investigation has been performed in order to generate any measurements for further validation of the proposed numerical models. The results of the comparison between the measured and predicted data have been analysed.

1.6 Thesis Outline

This thesis contains a research report that is presented in eight chapters. The first chapter, which is the introduction, presents the basic information on the research activities, including the background information on the research, a statement of the problem, the motivation for the research, the objective of the research, and the scope and limitations of the research. This chapter provides an insight in to the general content of the thesis.

In chapter two, a review of the existing literature on related research areas is been reported. The ranks of the coals, coal properties, coal combustion and combustion characteristics are some of the reviewed areas. Also under this chapter, the available numerical techniques for investigating coal combustion processes have been examined. Some of the reported existing coal deposition models and numerical slagging indices have been summarized and presented in separate tables.

The numerical steps adopted in developing the ash deposition model are reported in chapter three. The mathematical equations representing the various stages of coal combustion and ash deposition, such as, devolatilization, char burnout, turbulence, heat transfer, particle trajectories, etc, are also explained in this chapter. Basically, chapter three deals with the governing equations and their respective roles in the coal combustion processes. Most importantly, the chapter three contains one of the novel ideas (numerical equations) that is been developed during the course of this research.

In chapter four, a procedural explanation on the test case used in validating the coal ash deposition mathematical model has been made. The geometrical modelling and grid generation processes are also described in this chapter. To make it more explicit, the chapter is further divided into three sections. Section one discusses the modelling of the test facility used in this study, while in section two, the properties of the tested fuels and the operating conditions used are reported.

All the necessary steps for the implementation of the numerical models on the test facility, using the FLUENT 12.1 software are described in section three. These computational steps are very important since they determine the accuracy of the calculations.

Chapter five contains the numerical results and discussions on the ash deposition model. The results of predictions using the ash particle deposition model are compared with the available experimental data, and analyses and

some conclusions are made. This chapter is divided into two sections. The first section discusses the results of calculations using the two-dimensional (2D) domain, while the three-dimensional (3D) calculations using the same ACIRL furnace and the Australian coals are reported in the second section.

In the sixth chapter, the modelling of the NSI and the results of the assessment of the slagging potential of different coals using the NSI and six other existing slagging indices are presented. Also, in this chapter, the results obtained from the prediction of the slagging performance of some coal blends using the proposed coal numerical slagging index are reported. All the reported results are therefore analysed, comparatively. Also, the properties of the coals used and the performance of some of the existing slagging indices are reported in this chapter.

In chapter seven, the coal NSI has been modified in order to predict the slagging potential of coal/biomass blends with a low biomass ratio. Also, the results of predictions using the modified coal NSI on some coal/biomass blends are reported in this chapter.

Chapter eight is the final chapter which contains the conclusions from the entire research study and the suggested future work. Reading chapter eight will give an insight into the findings and the general conclusions that have been made at the end of the investigation. Also, the suggested areas for future work are discussed in details in this chapter.

CHAPTER 2

LITERATURE REVIEW

2.1 Coal Combustion

Looking at various concepts, combustion could be seen as a sequence of exothermic reactions that take place when fuel and oxidant come into contact. These chemical reactions are complex in nature and they are accompanied by the production of heat and sometimes light, depending on the nature of the fuel and the combustion process.

The study of combustion is generally based on thermodynamics, chemical kinetics, heat and mass transfer, and fluid flow. "It is one of the most important processes in engineering, which involves turbulent flow, heat transfer, chemical reactions, radiative heat transfer and other complicated physical and chemical processes" (Versteeg & Malalasekera, 2007).

Some of the types of combustion include smouldering, slow, rapid, etc. One of the most common types of combustion is the rapid form where oxidation is fast and temperatures are high (1320-1800K) (Murphy & Shaddix, 2006). This type of combustion situation is of significant interest to power generators. The chemical reaction between any form of fuel and oxidizer usually involves a significant release of heat energy. Although the fuel type determines, to a large extent, the combustion technology to be used, and to some extent, the

maximum flame temperature that is expected (Rushdi *et al.*, 2005). In reality, the actual energy-releasing reactions occur in the gaseous phase.

The combustion of pulverized coal is a complex process that involves gas mixing, dispersion of particles, mass transfer, particle heating, gas and particle reactions, heat transfer, swirling and re-circulating fluid mechanics, pollutant formation, and mineral phase transformation (Brewster, Baxter & Smoot, 1988). However, it is important to note that most of the world's energy comes from the combustion of fossil fuels.

It was estimated that, in 2007, fossil fuels constitute 86.4% of the world's primary sources of energy (EIA, 2010). Energy is required for transportation, heating, industrial processes and most importantly for electricity generation. Coal combustion plays a significant role in the power generation sector because of its high calorific value. In 2006, the World Coal Institute (WCI, 2006) reports that coal constituted 41% of the total world electricity generation (see Fig. 2.1).

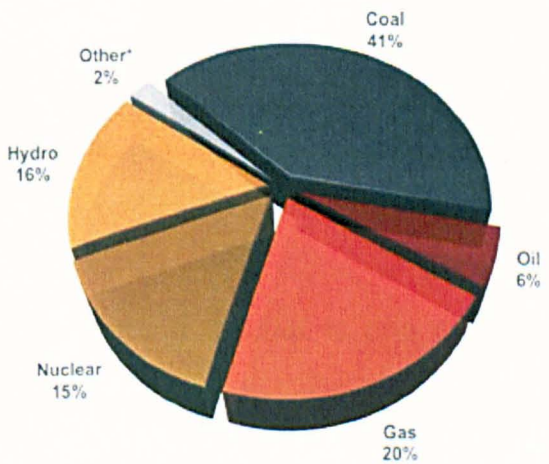

Fig. 2.1 Total world electricity generations by fuel in 2006.

*Others include solar, wind, combustible renewable, geothermal & waste (IEA 2008 data). **Source:** Coal & Electricity, World Coal Institute.

The EIA Energy Outlook (2010) puts the world recoverable coal reserves as at January 1, 2008 at 909.4 billion short tons. The availability and uses of coal also motivate further research into the potential and challenges of coal combustion.

The coal fuel is being used in different ways, ranging from electricity generation to manufacturing and other industrial uses. The WCI gave a breakdown of the available reserves according to coal ranks and uses in Fig. 2.2 (WCI, 2010).

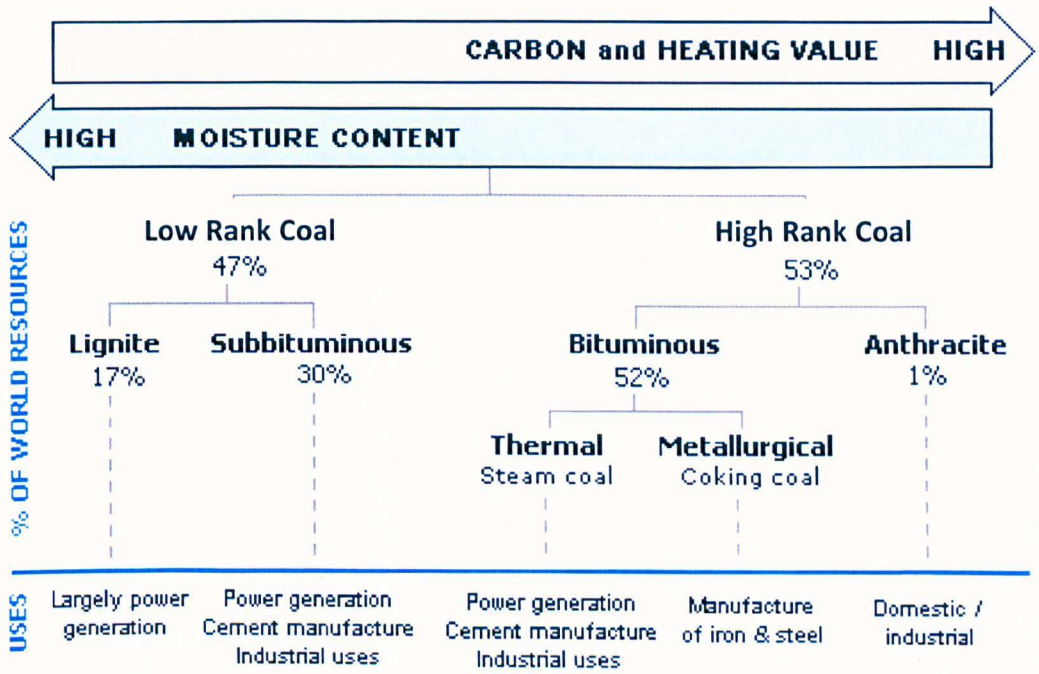

Fig. 2.2 Typical uses and the estimated percentage of the world's coal reserves by rank. (CC) Image: World Coal Institute

Although the burning of coal is one of the most popular ways to generate electricity, the process has severe environmental and operational problems. The environmental challenges facing the coal combustion communities are as diverse and heterogeneous as the coal itself (Scaroni, 1989). All the processes

involved in coal combustion, from mining to burning and waste disposal, are not environmentally friendly.

Finkelman (2004) enumerated some of the problems caused by surface and in-ground coal fires as follows:

- Visual blight and loss of potentially valuable acreage;
- Destruction of the nearby ecosystem;
- Forest fires;
- Sources of windblown dust and siltation of streams;
- Deterioration of cultural infrastructure by acid gases;
- Disruption of families and communities;
- Physical hazards from collapse and explosion;
- Health hazard due to respiration of dust and aerosols, exposure to acid gases, potentially toxic trace elements, and organic compounds;
- Pollution of surface and ground water;
- Loss of valuable energy resources;
- Significant source of CO_2, a major greenhouse gas.

The operational problems associated with coal burning are equally complex. Scaroni (1989) states that coal is very difficult to ignite when compared to other types of fuel. He is also of the opinion that: the kinetic and pyrolysis process is not fully understood by the researchers, especially the temperatures of rapidly devolatilizing coal particles that are universally acceptable have not yet been established. It may be true that a little more is known about the fundamentals of char burnout than of the pyrolysis; and the products of coal combustion, such as

ash and gaseous pollutants, are of serious concern to both the coal combustion communities and the power engineers. He then states that the burning of coal has been practised for centuries and misunderstood for centuries.

2.1.1 Coal classification

Coal is generally classified by rank, and this is a broad-based measure which depends on the average carbon content of the particular coal (Williams, Pourkashanian & Jones, 2000). The rank of the coal refers to its degree of maturity, or its age. Adequate knowledge of the coal rank enables an assessment of the most important properties of the coal that are likely to affect the efficiency of the combustion process, or suitability of the coal to other industrial processes.

The coal properties, such as, volatile matter – which determines coal ignitability, and calorific value – which relates to the available heat in the coal and the physical changing stages of the coal during combustion (the swelling, caking and clinkering) are some of the important bases for coal classification.

The early research studies revealed that coal classification could be based on the ratio of the fixed carbon to the volatile combustible matter (FC:VM). Frazer (cited in Moore, 1922) noted that it is only possible to classify coals according to their fuel ratio within wide limits, and he suggested the following divisions:

Hard-dry anthracite	100-12 (FC/VM)
Semi-anthracite	12-8 "
Semi-bituminous	8-5 "
Bituminous	5-0 "
Lignite	< 5 "

Frazer's ratio limits did not distinguish subbituminous and lignite coals from bituminous coals and this is a pointer to the deficiency of his ratio limits in modern use. Moore (1922) gave a general way of coal classification which was adopted by the International Geology Congress (IGC), and this is presented in Table 2.1.

Table 2.1 Moore's coal classification system adopted by IGC (Speight, 2005).

Classes of Coal	**FC/VM**	**CV (cal/kg)**	**Mean Composition (%)**		
			C	H	O & N
Anthracite	12 +	8000 – 8330	93 – 95	2 – 4	3 – 5
Semianthracite	7 – 12	8300 – 8600	90 – 93	4 – 4.5	3 – 5.5
Anthracitic & high carbon bituminous	4 – 7	8400 – 8900	80 – 90	4.5 – 5	5.5 – 12
Bituminous	1.2 – 7	7700 – 8800	75 – 90	4.5 – 5.5	6 – 15
Low carbon bituminous	2.5 – 3.3	6600 – 7800	70 – 80	4.5 – 6	18 – 20
Cannel	Yield 30 – 40% VM, with a resinous fracture of porous coke				
Lignitic (subbitiminous)	1.8– 2.5	5500 – 7200	60 – 75	6 – 6.5	20 – 30
Lignite	20% moisture	4000 – 6000	45 – 65	6 – 6.8	30 – 45

One of the latest ranking schemes evolved in America and was adopted by the American Standards Association, originally known as the American Society for Testing and Materials (ASTM). This scheme identifies four main categories of coal, namely; anthracite, bituminous, sub-bituminous and lignite, as presented in Table 2.2 (Speight, 2005).

Brief descriptions of the ranks of coal are summarized by Schobert (cited in Habib, 2001) as follows:

Lignite coal: This is the lowest rank of coal. It has high moisture and volatile contents and produces smoky-flames. It is considered low quality coal due to its low heating value.

Sub-bituminous coal: This is an intermediate rank of coal which tends not to have an apparent woody texture. It burns cleaner than lignite.

Bituminous coal: This is the most widely used class of coal for power generation and other applications. It has a lower content of moisture and volatile matter. It has a high heating value and burns out with a clear and hot flame.

Anthracite coal: This is the highest rank of coal. It possesses low volatile matter content and burns out with a hot, clean and uniform flame, with little or no smoke or soot.

Table 2.2 ASTM coal classifications by rank.

Class or Rank	Group	FC [b] (wt % dry mmf)		VM [b] (wt % dry mmf)		Gross CV [c] (MJ/kg moist mmf)	
		≥	<	>	≤	≥	<
Anthracitic	Meta-anthracite [d]	98			2		
	Anthracite [d]	92	98	2	8		
	Semi-anthracite [d]	86	92	8	14		
Bituminous	Low-volatile bituminous [d]						
	Medium-volatile bituminous [d]	78	86	14	22		
	High-volatile A bituminous	69	78	22	31	32.55	
	High-volatile B bituminous		69	31		30.23	32.55
	High-volatile C bituminous [e]					26.74	30.23
	High-volatile C bituminous [f]					24.41	26.74
Sub-bituminous	Sub-bituminous A					24.41	26.74
	Sub-bituminous B					22.09	24.41
	Sub-bituminous C					19.30	22.09
Lignite	Lignite A					14.65	19.30
	Lignite B						14.65

(a) Percentage by weight on a dry and mineral matter free basis (mmf).
(b) Gross Heating Value multiply MJ/kg by 430.11 to convert to Btu/lb.
(c) Coals containing 69 wt % or more fixed carbon on a dry mmf basis are ranked according to their fixed carbon content regardless of their Gross Heating Value.
(d) A high-volatile C bituminous coal that may be agglomerating or non-agglomerating.
(e) A high-volatile C bituminous coal that is an agglomerating coal, which means that it tends to become sticky and to cake when heated.

Source: http:\\www.knovel.com

2.1.2 Proximate and ultimate analyses

The fuel content of a coal is its actual heating value. The heating value can be calculated based on the chemical composition of the coal, and this could be defined in terms of proximate and ultimate (elemental) analyses.

Proximate analysis: Moisture, volatile matter, ash and fixed carbon contents are the parameters used in determining the proximate analysis of a coal. The moisture in coal tends to reduce its heating value during combustion. It is basically regarded as the incombustible residues after burning coal to a constant weight.

The rank of coals increases with decrease in its moisture content. For example, it is shown in Table 2.1 that the lignite (low rank) coal has 4000-6000 cal/kg with up to 20% moisture content, while the anthracite (high rank) coal has about 8000 calories. In order to reduce the moisture content, coals are subjected to pre-combustion drying processes.

Ash is a measure of inorganic content of a coal and it also reduces the coal heating value. Some of the problems of high ash content in coals include the following: environmental problems in ash disposals; the cumulative effect of the ash on the performance of the boiler; and the issues related to slagging and fouling, such as corrosion and high maintenance cost.

The ash content in coals varies according to the rank of the coals. Four US coals of different ranks have been investigated and their properties are shown in Table 2.3. The properties of the US bituminous discussed by Murphy and Shaddix (2006) correspond with the properties presented in Table 2.3.

Table 2.3 Properties of US coals of different ranks on moisture and ash free basis, wt % (Murphy & Shaddix, 2006; Coal science, 2011).

Coal	HHV (Btu)	FC	VM	Ash	Moisture
Anthracite	13,500	79	7	10	4
Bituminous	12,900	48	38	9	5
Sub-bituminous	8,250	33	35	7	25
Lignite	6,800	29	27	6	38
	Ash analysis (wt %)				
SiO_2	**Al_2O_3**	**Fe_2O_3**	**TiO_2**	**P_2O_5**	**CaO**
57.11	32.74	5.60	1.37	0.08	1.23
MgO	**SO_3**	**Na_2O**	**K_2O**	**MnO**	
0.73	0.92	0.40	2.31	<0.01	

Table 2.3 shows that the ash content is not always a good indicator of good coals, since the anthracite and the bituminous coals are reported to have high ash content (10 and 9 wt %, respectively). However, the moisture and fixed carbon contents are considered as good indicators of coal rank (Lee *et al.*, 2010). High coals have high FC and low moisture contents, while low rank coals have low FC and high moisture contents as shown in the Table 2.3.

Also, in Table 2.3, the composition of coal ash is shown under ash analysis. The content of the individual species may vary depending on the type of coal.

The report of an investigation on the effect of high ash content in pulverized coal combustion suggests that, although the effect of high ash on char reactivity is negligible, the overall diffusion rate of the oxidant to the surface of the char is reduced significantly. This is due to the presence of a thick ash layer covering the char particle (Jayanti, Masheswaran & Saravanan, 2007). However, they reported that the flue gas temperature is relatively insensitive to the high ash content in the coal.

The volatile matter (VM) is a measure for the tendency of a substance to vaporize at a given temperature. The volatiles are burnt out through the devolatilization process. High VM content helps to easily ignite coal combustion. Also, high volatile release during coal combustion enhances flame stabilization, and reduces the level of NOx emission (Lee *et al.*, 2010). According to Lee *et al.* (2010), the major reason for the reduction of the NO with the increase of VM content in the coal is the production of hydrogen fuel, in the form of hydrogen cyanide (HCN), during the process of devolatilization.

The solid combustible matter that remains after coal devolatilization is called fixed carbon. The higher the fixed carbon (FC) content in a coal, the higher is its heating value. Fixed carbon is determined as subtracting the sum of ash, volatile matter and moisture content from the total content of the coal. The coal rank increases with an increase in its fixed carbon content. For example, the anthracite is the highest ranking coal and it has about 80-90 wt % of FC content as shown in Table 2.2.

In coal combustion, a high FC content may results in delayed ignition, which implies that greater activation energy is required (Kucukbayrak, Acma, Mericboyu & Yaman, 2001). Although the combustion of coal with a high FC content takes longer time than the coal with a low FC content, it yields higher energy content.

Ultimate analysis: This is also referred to as the elemental analysis and it gives a quantitative determination of the carbon, hydrogen, sulphur, nitrogen and oxygen within the coal. The sulphur and nitrogen contribute to air pollution problems and frequently requires removal from the stack gases of utility boilers (Turns, 2006). Carbon and hydrogen are considered as the most important constituents of coal. Carbon amounts to 70-95% and hydrogen 2-6% by weight of the organic content of the coal (Speight, 2005).

In order to have an effective control of emissions during the combustion of coal, a comprehensive data on the content of sulphur in the coal is essential (Speight, 2005). Usually, the sulphur content in coals is presented in two forms, namely, the dry sulphur content in coal before burning, and the content in the combustion by-products.

The dry sulphur content in coal is a significant factor in the prediction of the ash behaviour in a boiler. For example, the ratio of the basic to acidic oxides of the ash is multiplied by the content of dry sulphur in coal, and it is being used as a slagging index (Lawrence *et al.*, 2008)

Most importantly, the ultimate analysis of coal is used in determining the heating value of the coal. A formula for the calculation of the heating value of coal from its carbon, hydrogen, sulphur and ash content has been suggested by Mason and Gandhi (1983). They described the proposed formula as being advantageous for use in modelling and monitoring coal conversion processes.

2.1.3 Calorific value

This is the specific energy of the fuel, also referred to as its heating value. It is the amount of heat per unit mass of the fuel released on combustion. The calorific value can be expressed as gross or net. When performing a combustion test in the laboratory, the higher heating value (HHV) realized is gross. While during the actual combustion in a furnace, only the net value is realized and it is considered as a lower heating value (LHV).

The heating value of solid fuels has a great importance, especially in the conversion of such fuels to energy (Mason & Gandhi, 1983). The high heating value of coal is one of the principal reasons why coal is still considered as a viable energy option despite its environmental impact.

2.1.4 Types of flame

In general, combustion occurs in non-flame and flame modes. The concept of non-flame and flame combustion has well been described in the literature

(Turns, 2006). Combustion flames are categorized into non-premixed, premixed and partially premixed types.

Non-premixed flames: In the non-premixed (diffusion) flames, the fuel and the oxidizer diffuse into each other at an interface and flames occur. In this case a fuel and oxidizer are introduced to the combustion zone in two or more separate streams and subsequently brought together due to diffusion and mixing prior to combustion.

The modelling of the non-premixed combustion involves solving the transport equations for one or two conserved scalars (mixture fractions). Instead of solving equations for individual species, the non-premixed model considers species concentration from mixture fraction fields. The thermo-chemistry calculations are pre-processed and then tabulated for look-up. An assumed-shape probability density function (PDF) is used to account for the interaction of the turbulence and the chemistry.

The non-premixed modelling approach is specific to the simulation of turbulent diffusion flames with fast chemistry. For such systems, the non-premixed model is of enormous advantage over the eddy-dissipation method. It allows for possible species prediction, disassociation effects and rigorous turbulence-chemistry coupling. It is also computationally efficient since it does not require the solution of a large number of species transport equations.

Premixed flames: Contrary to the non-premixed flames, in the premixed flames, the fuel and the oxidizer are mixed at the molecular level before any significant chemical reaction occurs. Since the fuel and the oxidizer are mixed before coming into the combustion zone, reactions start at the combustion zone where the unburnt reactants and the burnt combustion products are separated.

Application of the premixed model in some commercial software packages, such as FLUENT, has some limitations, which include the following:

- The model is only available in the density-based solver.
- It is valid for turbulent and sub-sonic flows only.
- It cannot be used in conjunction with the pollutants, e.g. soot.
- It cannot be used to simulate the reacting discrete-phase particles.

Partially premixed flames: When the fuel-oxidizer ratio is non-uniform, the flame is referred to as partially premixed. This model is considered as a simple combination of the two models discussed above, i.e. the non-premixed and the premixed models. When applying the non-premixed and the premixed models in combination, it is worth noting that the single-mixture fraction approach requires two inlet streams, while the two-mixture-fraction approach requires three inlet streams. This approach will also require additional computational work.

2.1.5 Devolatilization

Coal is usually prepared before being fed into the burner. The preparation, which is called pulverization, is a process of grinding of the coal to smaller

sizes, generally, in the range of 75 to 300 μm (Lawn, 1987). The minerals interaction in the initial burning of the coal particle is complex, and of particular interest to this research is the decomposition of the inorganic materials to form ash and then slag (Williams *et al.*, 2000). The processes involved in coal combustion are depicted in Fig. 2.3, where the left-hand side shows the heterogeneous steps, and the homogeneous reactions are shown on the right-hand side.

Devolatilization is always considered as the first step in thermally driven coal conversion and utilisation processes and has a profound effect on the course of the combustion process (Brewster *et al.*, 1988). For combusting particles, devolatilization occurs when the particle mass is in excess of its non-volatile size, and its temperature reaches the vaporisation stage (Baum, 1971).

When heated to a temperature range of 400 and 600 °C, coal starts to decompose, giving out a mixture of combustible gases and non-combustible gases (Strezov, Lucas, Evans & Strezov, 2004). With an increase in temperature, the rate of devolatilization also increases significantly.

The rate and extent of the thermal decomposition of coal particles is important in combustion processes. This is because about 50% of the coal feed may be volatile materials that are expected to burn in the gas phase (Badzioch & Hawksley, 1970). Therefore, adequate knowledge on the thermal decomposition rate is very important not only for investigating the ignition

process but also to have accurate information on subsequent heat releases in the furnace.

According to Smith (1982), the combustion of most solid fuels involves thermal decomposition at the initial heating stage and the subsequent combustion of the porous solid residue from the first step. He added that, the decomposition of PF in flames take place within the order of 0.1s, while the char burn-out time, which is usually longer, is about 1s.

Strezov *et al.* (2004) describe coal decomposition as an intrinsic chemical reaction step, and the effect of the process is of great importance for combustion optimization and increased efficiency. They further stated that the heating rate is one of the most important parameters that affect the devolatilization process. However, Fletcher & Kerstein (1990) are of the opinion that it is difficult to study the effect of heating rate on the yield of volatiles independently of the final temperature.

In the numerical analysis of combustion, coal particles are assumed to be perfect spheres. They are also assumed to have a uniform density, while their burning diameters are reduced by an amount equivalent to the consumed carbon (Baum & Street, 1971). Numerical models that represent the interaction of the chemistry and turbulence often assume that coal VM has a constant elemental composition and heating value. To justify this assumption, Brewster *et al.* (1988) pointed at the uncertainties that exist in devolatilization and state

that the major elements, such as, carbon, hydrogen, nitrogen and sulphur, are released in proportion to the total mass evolution.

Aslanyan & Maikov (1994) used the constant rate devolatilization model in simulating pulverized coal combustion in turbulent flows. This model requires the setting of the vaporization temperature which controls the onset of the devolatilization. The single rate model assumes that the rate of devolatilization is first-order and dependent on the volatiles remaining in the particle, and it is widely used in coal combustion (Rushdi *et al.*, 2005; Lee & Lockwood, 1999).

The two-competing rates model is used to reproduce the observed temperature dependence on the volatile yield. Truelove & Holcombe (1990) used this model by setting the rate constant and the stoichiometric factors in order to set up their predictions for the devolatilization of bituminous coals.

The chemical percolation devolatilization (CPD) model was developed in order to explain coal devolatilization on the basis of the initial chemical structure of the coal (Fletcher & Kerstein, 1990). The CPD model allows for a temperature-dependent competition between the formation of side chains and char, which leads to changes in the yield of volatiles as a function of the heating rate.

2.1.6 Char combustion

Char combustion processes commence during or after devolatilization. This process is slower and it takes much more time than the devolatilization. In coal

combustion, the char oxidation process, which depends on the physical structure of the coal, is very important. At temperatures near 900 °C, most of the volatile matter has been evolved. With the supply of sufficient air being mixed into the jet, burning is ignited.

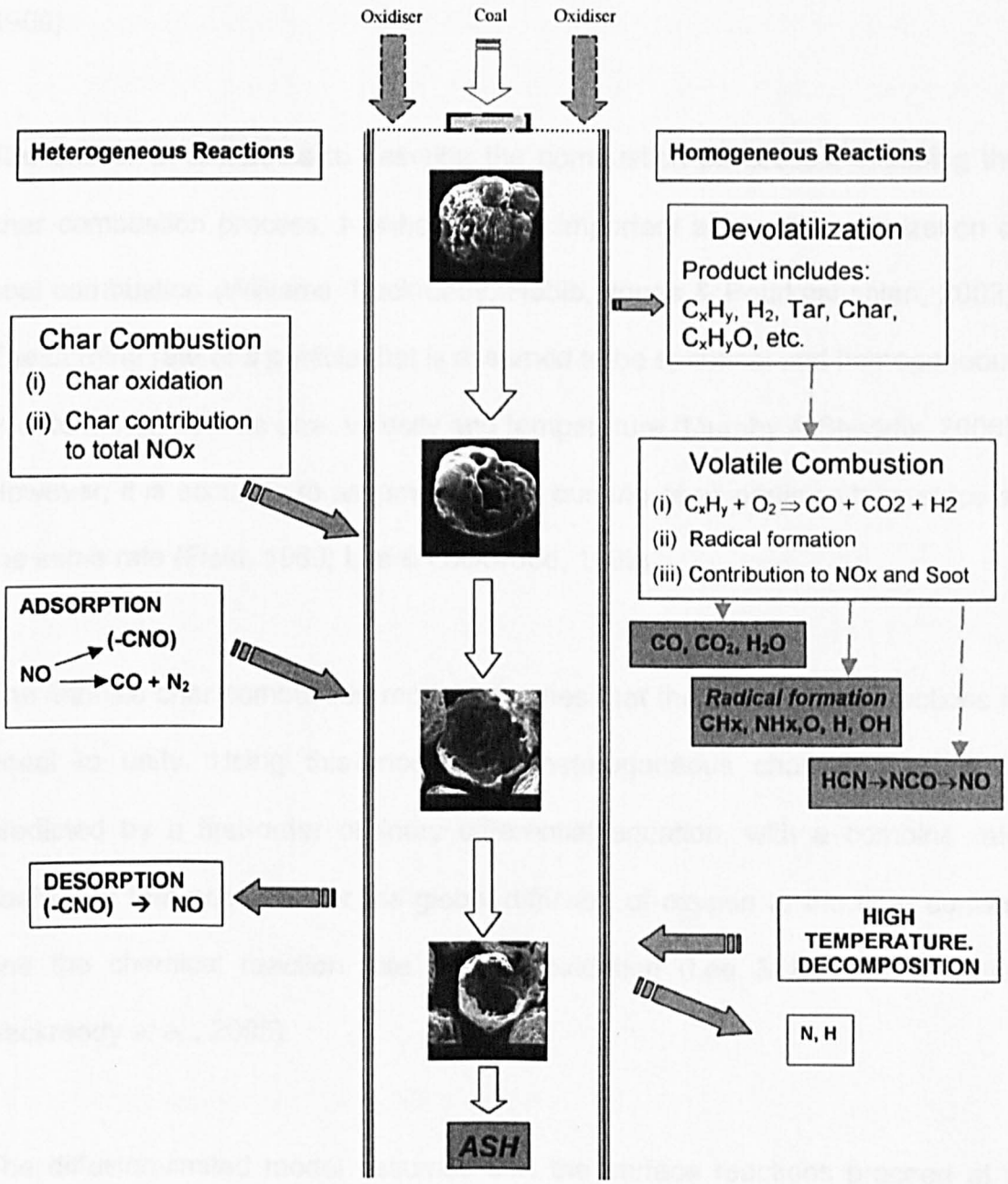

Fig. 2.3 Combustion processes of a single particle of bituminous coal in a one-dimensional drop tube (Williams *et al.*, 2000).

The rate of coal char combustion can be affected by its mineral matter content, and since coal is not a homogeneous substance, it is characterized by wide variations in its properties and composition. A successful implementation of coal combustion simulations depends on a proper application of fundamental knowledge of combustion and modelling skills (Eghlimi, Lu, Sahawalla & Harris, 1999).

The use of CFD models to describe the combustion processes, including the char combustion process, has become an important aid in the optimization of coal combustion (Williams, Backreedy, Habib, Jones & Pourkashanian, 2002). The burning rate of a particle that is assumed to be spherical and homogeneous is determined from its size, velocity and temperature (Murphy & Shaddix, 2006). However, it is accurate to assume that the burning of all particles take place at the same rate (Field, 1969; Lee & Lockwood, 1999).

The intrinsic char combustion model assumes that the order of the reactions is equal to unity. Using this model, the heterogeneous char combustion is predicted by a first-order ordinary differential equation, with a combine rate coefficient that accounts for the global diffusion of oxygen to the char surface and the chemical reaction rate of char oxidation (Lee & Lockwood, 1999; Backreedy *et al.*, 2005).

The diffusion-limited model assumes that the surface reactions proceed at a rate determined by the diffusion of the gaseous oxidant to the surface particle (Dhumal & Saha, 2007). The model ignores the kinetic contribution to the

surface reaction and also assumes that the diameter of the particle remains constant (Eghlimi *et al.*, 1999).

The kinetic/diffusion-limited model assumes that the surface reaction rate includes the effect of both the bulk diffusion and chemical reactions. This model is widely used for coal combustion (Xu, He, Azevedo & Carvalho, 2002; Li, Wei & Jin, 2003), and it is assumed to be a simple model (Sheng, Moghtaderi, Gupta & Wall, 2004). In this model, the rate of oxidation is limited by the kinetics and the rate of diffusion are coupled, where the flux of oxygen depends on the gradient of the available oxygen supplied by the decrease of oxygen with depth (Elberling, Nicholson & Scharer, 1994).

With the multiple surface reaction model, the chemical state of the surface can be described by a set of surface coverage which specifies the fraction of the surface that is covered by a particular species (Miessen, Behrendt, Deutschmann & Warnat, 2001). The multiple surface reaction model has some limitations. For example, in the FLUENT software, the model is only available with the steady tracking and species transport options, and therefore it is not applicable with the premixed, non-premixed and partially premixed combustion models (Fluent Inc., 2009).

2.2 Combustion of other Solid Fuels

The burning of other solids, such as biomass, as a fuel in PF furnaces, is gaining more acceptance as a means of reducing emissions in the power

generation industry (Ma, Pourkashanian, Williams & Jones, 2006). Biomass fuels contain inherent inorganic elements that are involved in reactions leading to ash slagging and fouling in boilers (Jones, Darvell, Bridgeman, Pourkashanian, & Williams, 2007). In view of the two strong competing factors, CO_2 emissions reduction and slag formation, the co-firing of coal and biomass has been advocated for years as being advantageous both environmentally and economically (Backreedy *et al.*, 2005).

Although this thesis is mainly on coal combustion, an insight into biomass combustion and co-firing of coal and biomass is given. Also, the slagging potential of coal and biomass blends is investigated. This has become essential due to the fact that the combustion of solid fuels, especially biomass, follows a similar pattern to coal combustion (Williams *et al.*, 2000).

However, the huge difference in terms of the physical and chemical properties of biomass and coal, and the difference in the properties of their ashes need to be acknowledged if only we want to enhance the processes of co-firing.

2.2.1 Biomass combustion

Biomass is considered as a complex organic-inorganic solid product generated by natural and anthropogenic processes (Vassilev, Baxter, Anderson & Vassileva, 2010). Biomass fuel is CO_2-neutral and can be a good alternative to fossil fuels in view of the decreasing resources of the fossil fuels and their negative environmental effect (Zhou, Jensen & Frandsen, 2007). Using biomass

as a fuel in PF furnaces has been recognised as an important measure that is taken in order to reduce emissions in the power generation industry, and an industrial test of firing 100% biomass as a fuel has been performed (Ma *et al.*, 2006).

Similar to coal, the proximate analysis in biomass is a measure to determine its moisture, ash, volatile matter and fixed carbon contents. The ultimate (elemental) analysis in biomass also measures Cl, in addition to other similar coal properties such as C, H, N, O and S.

In order to optimize the burning of biomass as a fuel, some important considerations have to be made. Some of these considerations include the following:

- Choice of biomass fuel type and its calorific value.
- Processes of drying, devolatilization, etc., towards reaching its available energy.
- Problems such as slagging, fouling, corrosion, pollution, safety, ash handling, etc.

Some of the issues mentioned above, coupled with other operational difficulties create bottle necks for the use of biomass as a fuel. Ma *et al.* (2006) noted that firing biomass presents a number of technical problems that substantially limits its use in existing coal fired plants and the formation of deposits is one of the key issues.

Deposition of ash particles on furnace and boiler surfaces leads to corrosion and a reduction of the heat transfer, which can cause subsequent plant shutdowns and increased operational costs (Joller, Brunner & Obernberger, 2005; Plaza, Griffiths, Syred & Rees-Gralton, 2009).

In order to increase the use of biomass for energy production, the ash related problems must be reduced (Forstner *et al.*, 2006). The relative large size of biomass fuel particles, and their high moisture content, may also affect its rate of combustion. Owing to the large size biomass particles, inertial impaction becomes the most important mechanism for ash deposition (Mueller *et al.*, 2005).

Deposition characteristics of biomass fuel can be related to its ash content, which ranges from 2 to 20% depending on type and the growth conditions and handling (Nutalapati *et al.*, 2007). However, to fully understand the deposit formation process in both biomass and coal combustion plants, several researches are ongoing (Mueller *et al.*, 2005). With the increasing computational power in recent years, attempts are being made to describe deposition formation and build-up in boilers with combustion simulations using CFD techniques (Forstner *et al.*, 2006).

2.2.2 Coal / biomass co-firing

The European Union (EU) initially set a goal to increase the total amount of energy from renewable sources from 6 to 12% by 2010 (Sroda, Makipaa, Cha &

Spiegel, 2006). However, this goal was not achieved and now a new goal of 20% total energy from renewable sources by 2020 has been set by the EU (Munir, 2010c), and co-firing is considered as a good option for the utilisation of biomass and coal to deliver the renewable energy option (Heinzel, Siegle, Spliethoff & Hein, 1998). A great variation of biomass fuels, from wood pellets to straw co-fired with coal is used in combustion units with a thermal power ranging from a few kW to several hundred MW (Backreedy *et al.*, 2005).

Co-firing offers a short-term, low-cost and high-social benefit energy option that is much required in the energy market (Baxter, 2005). According to Ghenai & Janajreh (2009), the advantages of biomass co-firing include the following: it is the fastest means of increasing the use of biomass for power generation; it minimizes cost by using the existing coal-fired infrastructure; and it offers environmental advantages, as well as benefiting from efficiencies of scale.

However, the implementation of co-firing in existing coal-fired facilities is still under investigation. So far, feasibility of different combustion systems has pointed out the management of ash-related problems as the major area requiring a better understanding (Heinzel *et al.*, 1998). The different types of biomass sources intended for co-firing include wood residue, agricultural residues, energy crops and sewage sludge.

Although each form of biomass has its different composition and properties, typical biomass fuel has a lower inorganic content than coal, but the alkalis in biomass could change the properties of the fuel when co-fired with coal, thus

resulting to higher deposition rate (Wigley, Williamson, Malmgren & Riley, 2007). Ma *et al.* (2006) are of the opinion that the presence of inorganic species in biomass, particularly potassium, can increase its deposition tendencies by significantly lowering its fusibility.

Therefore, it is suggested that the use of biomass fuel in combustion systems comes with added operational difficulties related to ash deposition (Lokare *et al.*, 2006) and the implementation of co-combustion in existing coal power plants and its engineering consequences are some of the problems being investigated (Heinzel *et al.*, 1998). The results of these investigations can be used to minimize deposit formations.

The different mineral matter composition of biomass may results in increased slagging and fouling tendency in the boilers. Also, biomass has higher content of moisture, volatile matter and oxygen, and it has a lower density, ash content and heating value than the coal (Molcan *et al.*, 2009). Although there is no available index that predicts the slagging and fouling of biomass, unequivocally, some of the coal slagging indices are used for biomass (Munir, Nimmo & Gibbs, 2010a).

2.3 Boiler Furnace Design

In boiler furnace design considerations, heat generation and heat absorption are key issues. A typical boiler furnace is enclosed by a water wall. The burner fires the fuel in flames and the resultant heat is radiated to the furnace walls. In

some boiler furnaces, superheater, reheater and economiser surfaces are added in order to cool the flue gas leaving the furnace.

The general requirements of furnaces are summarized as follows (Basu, Kefa & Jestin, 1946):

- The furnace should provide the physical space and time required to complete the combustion of the fuel.
- To ensure the safe operations at the downstream convective area, the furnace should have adequate radiative heating surfaces to cool the flue gas.
- The air motion in the furnace should prevent flame impingement on the water walls to ensure uniform heat distribution.
- The furnace should provide reliable conditions for natural circulation of water through the water walls tube.
- There is the need to optimize the use of steel or any other materials used in constructing the furnace.

Swirl burners usually generate swirling combustion air with the use of guiding vanes. The swirling air creates recirculation zones which assist in igniting the fuel and this accelerates the process of combusting the air and fuel. In an axial vane burner, the intensity of the swirling secondary air is regulated by moving the axial vane wheel, which allows a fraction of the secondary air to flow straight without passing through the axial vane. While in a tangential vane swirl burner, the intensity of the secondary air is adjusted by changing the inclination angle of the tangential guide vanes (Basu *et al.*, 1946).

The swirling jets are helpful in controlling the flame shape, flame stability and temperature distribution in combustion chambers (Kwark, Jeong, Jeon & Chang, 2004). The swirling influences axial pressure gradients in the region of swirl decay which may be strong enough to set up recirculation flow zone near the jet exit (Alecci, Cammarata & Petrone, 2005).

The swirling flows are normally classified as strong, medium and weak swirling, depending on the strength of the recirculation flow zone they can create, and swirl intensity can be quantified by an exponential parameter called swirl number, SN, (Alecci *et al.*, 2005). The SN is defined as a non-dimensional number representing the ratio of the angular momentum flux and the axial momentum flux (Kwark *et al.*, 2004).

The swirl number could therefore be varied by varying the ratio of axial and tangential bulk flow rates. Non-premixed flames are efficiently stabilized by the swirling motion; hence swirl burners are widely used. However, the uncertainties in the inlet conditions of a swirl burner limit the use of some good measurements for validating the computational models (Hubner, Tummers, Hanjalic & Van der Meer, 2003).

2.4 Ash Particle Deposition

Ash deposition in boilers makes it almost impossible for the engineer to supply a sufficient and uninterrupted power. Generally, slagging deposits occur on the surfaces directly exposed to the flame radiations, such as, the furnace walls in

the burner region, while fouling are deposits in regions not directly exposed to flame radiations, such as, in the convection section of the boiler (Lawn, 1987). Slagging deposits are molten, while fouling deposits are sintered.

Fig. 2.4 shows a simple schematic diagram of a typical coal-fired boiler. The furnace region where temperatures are high is directly exposed to the flame radiations, and that is where slagging takes place. The high temperature region is the main concern of this investigation.

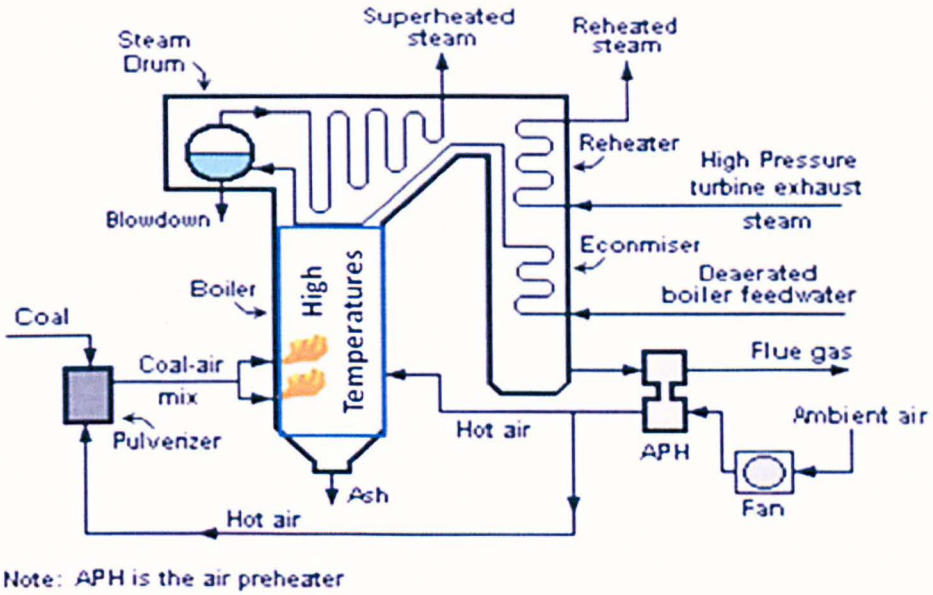

Fig. 2.4 A simple schematic diagram of a typical coal-fired power plant steam generator-boiler. Source: http://en.wikipedia.org/wiki/File:Steam_Generator.png

The deposition that takes place at the convective section of the boiler (fouling) affects the boiler walls, as well as the super heaters, reheaters and the economisers. Fouling is mainly due to thermophoretic effect on fine ash particles (Lin *et al.*, 2008). When the fine ash particles are transported to the

heat exchange surfaces, they condense and agglomerate into sintered deposits (Naganuma *et al.*, 2009).

The thermal efficiency of boilers is highly affected due to slagging. Other deposit factors, such as corrosion, also affect the physical properties of the boilers. Several researchers agree that during coal combustion, the slagging propensity is usually measured by indices derived from the chemical properties of coal and or ashes (Lee & Lockwood, 1999; Rushdi *et al.*, 2005).

Experimental methods for measuring ash deposition are not easy because of the high temperatures involved and the uncertainties in the high turbulence situation. Although Laursen, Frandsen & Larsen (1998) in their coal burn test, based their selection of sub-bituminous coal on its combustion behaviour rather than the ash deposition propensity, they classified the deposits collected on the probe into porous, powder, iron-rich, semi-fused slag and fused slag.

The slag classification described above depends on the properties of the coal and the location of the probe in the boiler. Therefore, it only gives an idea on the contribution of individual ash elements to the formation of the slag, and not on the deposition mechanism.

In a separate study on slagging propensities of coals/blends, Su *et al.* (2001b) agree that different coals yield different types of slag. The photographs of the slag produced by some of the coals they have tested are shown in Fig. 2.5. Also, their report indicates that more molten and sintered deposits were formed

in the burner region and this was attributed to the high temperatures in that region.

Figure 2.5 shows some deposit samples of various Australian coals. The photographs show the visual characteristics of the slagging deposits of coals with different ash material contents, presented as types A, B, C & D. For example, deposits from coal type D in Figure 2.5 appear brighter and this may be due to its high silicon oxide (SiO_2) content. The silica content in coal ash is significant in determining the ash behaviour (Huang *et al.*, 1996), unlike the case of biomass where potassium plays a pivotal role (Jones *et al.*, 2007).

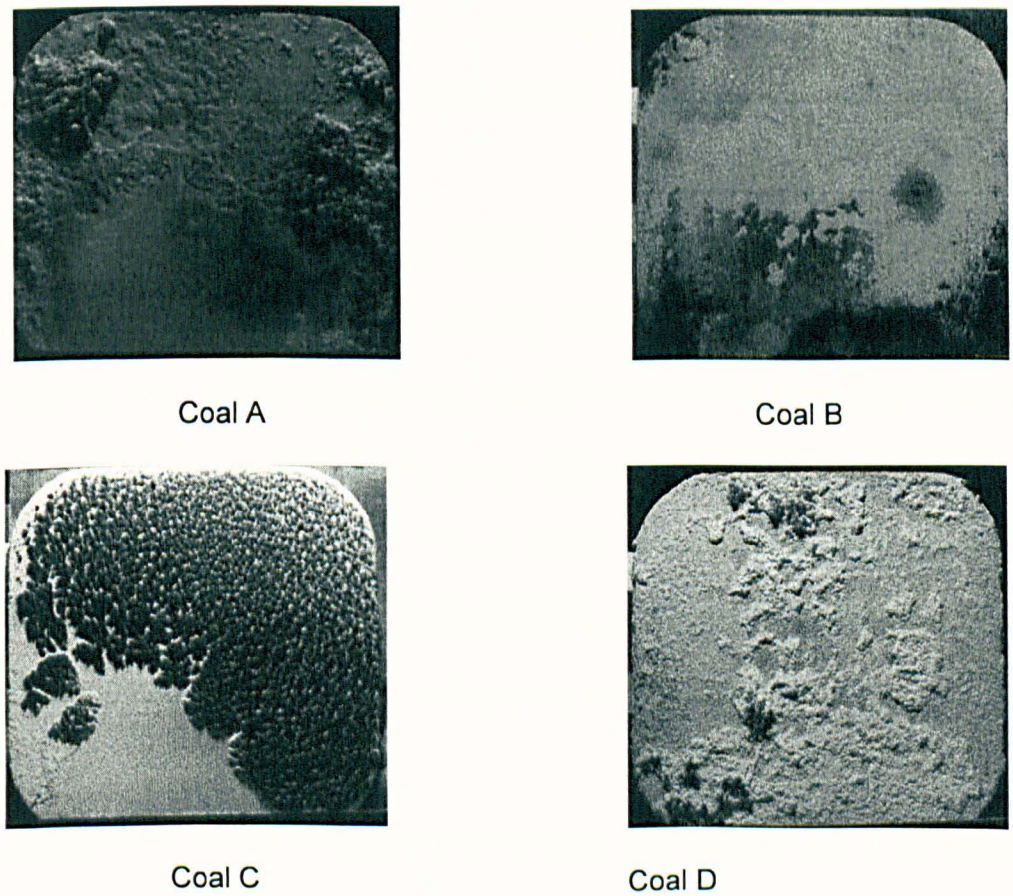

Fig. 2.5 Photographs of molten and sintered deposits of Australian coals (Su *et al.*, 2001b).

On the mechanism of deposition, Huang *et al.* (1996) agreed with the high-temperature high-deposit propensity assumption. They also suggested that an increase in the particle diameter results in a rapid increase in the impaction temperature. Similarly, high-density particles are assumed to have less heat dissipation and thereby impacting furnace walls at high temperature (Huang *et al.*, 1996). Therefore, large sizes of particles and high temperatures increase the particles sticking propensities.

However, the deposition of large particle in the region of high temperatures is mainly due to unburnt carbon. Coal particles that are not completely burnt may become molten and sticky at high temperatures, and due to their high density they can posses sufficient inertial force to transverse the boundary layer and impact on the heat exchange surface (Ma *et al.*, 2006).

The ash particle transport to cooled boiler surfaces, the thermo-chemical properties of particle, particle sticking tendency, local steady state deposit thickness and particle rebounding probability have also been identified as some of the necessary parameters to be considered while quantifying deposit growth rates (Mueller *et al.*, 2005). For a better understanding of the deposition mechanism, it is important to understand the extent of the influence of the above mentioned parameters on ash particle deposition rate.

The thermo-chemical properties of the coal ash particle are used as slagging indices. For example, the ratio of the basic to acidic oxides of the ash is used to predict the ash behaviour in a boiler (Lawrence *et al.*, 2008). Also, the content

of silica and iron oxide in the ash are good indicators of the slagging potential of coal.

According to Walsh (cited in Forstner *et al.*, 2006), the ash particle sticky probability at impaction can be expressed as a function of the sticky probabilities of both the particle and the impact wall. This suggests that the impacting particle will stick if either the particle or the wall is sticky. They further argue that around the boiler section of the furnace, the cooled walls have temperatures low enough to condense a considerable amount of ash forming vapour and this may result in a sticky wall that may capture silicon based fly ash particles.

In order to model the mechanism for the deposition of ash particle in a boiler, an understanding of the outcomes of empirical investigations on the deposition processes of the ash particle is necessary. The experimental measurements will reveal most of the data required for the modelling, and where there is insufficient data due to measurement difficulties, correct assumptions and/or approximations are possible.

The slagging and fouling potential of coal ash can be empirically determined in a number of ways. Basu *et al.* (1946) have described some empirical methods: the alkali components of ash can guide us towards the determination of the fouling tendencies of coal ash, sodium oxide (Na_2O) has the greatest influence on the deposition surface in a furnace; another approach is to use the deformation of ash cone to measure the ash deformation temperature, and the

ash deformation temperature can also be used to characterize the slagging tendency; and the third criterion is by determining the ash viscosity, which depends on the deposit temperature and ash composition.

The latter approach requires physical measurement of particle temperature inside the boiler, which makes it difficult to implement experimentally (Basu *et al.*, 1946), but an empirical correlation can be used to obtain the slag viscosity (Huang *et al.*, 1996).

2.4.1 Review of existing deposition models

This review is limited to ash deposition models that use coal chemical properties. In fluid dynamics, the particle behaviour is of considerable importance. In the combusting situation, the particle velocities and trajectories are more complicated due to the effects of high temperatures and large eddies (Williams *et al.*, 2000).

However, the knowledge of the statistical properties of particle tracers influenced by turbulent flow is very important for stochastic Lagrangian modelling (Biferale, Boffetta, Celani, Lanotte & Toschi, 2005). For particles with a small Reynolds number (R_e), Stokes linearly approximated the drag coefficient to be $24/R_e$. However, Morsi & Alexander (1972) observed that this is not always the case, especially at sufficiently high values of R_e. They argue that at very high values of R_e, the drag coefficient becomes constant at a value of approximately 0.4.

Several attempts have been made to accurately compute the paths of particles in a fluid; these have resulted in the development of a set of governing equations. Amongst the set of equations, those presented by Morsi & Alexander are validated and widely used by researchers (Huang *et al.*, 1996; Lee & Lockwood, 1999).

To this development, Lapple & Shepherd (1940) observe that all such equations, except those for the motion in a centrifugal field, are developed for the motion of particles in a fluid at rest. However, they accepted that the equations will still apply for a fluid medium in motion provided all particle – velocity terms are redefined as relative to the fluid.

In modelling particle tracking, a combined two phase flow model can be used (Li *et al.*, 2003) or one can use the Eulerian gas and Lagrangian particle models (Huang *et al.*, 1996; Ma *et al.*, 2006).

A number of research attempts have been made to accurately predict ash deposition rates in boiler situations. Results of such research works continue to improve with the introduction of better techniques and mathematical models. The significant influence of boiler operation conditions and temperatures in modelling coal ash particle deposition rates may be one of the reasons why researchers use the ash particle viscosity to determine the capture efficiency of the ash particle at impaction on the boiler walls (Huang *et al.*, 1996; Lee & Lockwood, 1999; Rushdi *et al.*, 2005).

However, the choice of values for the reference viscosity and combustion codes, the varying wall temperatures and the properties of the coal fuel used, cumulatively, left the particle viscosity approach in the ash deposition research open-ended. Any variation in the parameters listed above may result in significant difference in the results obtained.

Israel & Rosner (1983) used the generalized Stokes number technique to determine the capture efficiency of a non-Stokesian particle from a compressible gas flow. This technique uses a non-Stokes drag correction factor which is defined as a function of the particle R_e. In one of the reported investigations, a coal ash deposition model was developed using the ash particle viscosity and the generalized Stokes' number to determine the particle stickiness and drag coefficient, respectively.

Although the model described above was successfully implemented in a drop-tube furnace and a pilot-scale combustor, significant discrepancies between experimental and predicted results were reported at high temperatures (≥ 1327 K), which was attributed to ash build-up that affects the effective heat transfer to the tube (Huang *et al.*, 1996).

Wang and Herb (1997) developed a deposition sub-model that included the affects of both the ash chemistry and operating conditions. The particle stickiness was calculated based on the particle temperature and composition. The model was implemented with both pilot-scale and utility-scale facilities, and fairly good results were reported.

However, the use of the particle cloud method by Wang and Herb (1997) in order to determine the impaction rates is based on the assumption that all the particles in a single computational parcel have the same properties (Smoot & Smith, 1985). Therefore, this approach has failed to account for the deposition processes of individual particles.

Several similar research activities have been reported, with various levels of success. Most studies consider only the ash particle viscosity to determine the particle collection efficiency (Rushdi *et al.*, 2005; Costen *et al.*, 2000). The surface energy and static contact angle of the ash particle are also essential in determining the particle's overall sticking probability.

The effect of the above mentioned factors on particle stickiness have been examined in biomass combustion and a strong influence was reported (Ma *et al.*, 2006; Strandstorm *et al.*, 2007). In the area of coal combustion, very little has been reported on the effects of the particle surface energy and static contact angle on its stickiness at impaction on heat exchange surfaces of a boiler.

Although a wide range of values for the static contact angle is reported to produce the same or similar effects (Mao *et al.*, 1992), the inclusion of the static contact angle in the model makes it more comprehensive.

The assumptions embedded in various combustion codes have a great influence on the predicted results. For example, in devolatilization, some

models assume that volatiles are being released at a constant rate, while others assume that the release of volatiles is first-order dependent on the amount of remaining volatiles in the particle (Field, 1969; Baum & Street, 1971; Stephenson, 2003).

Also, during devolatilization process, the heated coal particle behaves in an unsteady manner. Therefore, the devolatilization process is better described by a model that accounts for the exchange of heat between the surface of the particle and the surface of the heat exchanger (Komatina, Manovic & Saljinikov, 2006).

In char burnout, factors such as chemical reactions and diffusion rates of oxidant are considered by different models (Lee & Lockwood, 1999; Muller *et al.*, 2003) and they show significant differences. In the diffusion and reaction model, the burning of the char particle is considered to take place at constant size with mainly carbon monoxide as the first product of the surface oxidation (Lee & Lockwood, 1999). While the diffusion rate model assumes that the surface reaction is determined by oxidant diffusion to the surface of the particle (Backreedy *et al.*, 2006).

Therefore, a suitable choice of combustion model enhances the quality of the predicted gas temperature which has a direct influence on the radiant heat fluxes and deposition rates (Su *et al.*, 2001a). In modelling the ash particle deposition rates, the combustion model may also be modelled, and where they are not, the existing combustion models are used.

In order to highlight the differences between some of the existing coal ash particle deposition models and the one that have been proposed in this thesis, a summary of the reviewed deposition models and the one been proposed are presented in Table 2.4. The various approaches used in determining the particle impaction and collection efficiencies are presented in the Table 2.4.

Also, presented in the Table 2.4 is a brief description on individual model, and in the last column, the mathematical representation of the models are shown. In this investigation, the mathematical equation presented in the last row in Table 2.4 has been developed and implemented using the FLUENT software in order to determine the fate of ash particles that hit the heat exchange surfaces of a boiler.

The proposed ash deposition model has accounted for the effects of particle impact temperature, ash viscosity and the rebound tendency of the particle that may impact on the heat exchange surfaces in order to determine if the particle sticks to the surfaces. The Watt- Fereday viscosity method is used to determine the viscosity of the particle, while the rebound tendency of the particle is obtained using the particle static contact angle and surface energy. The proposed deposition model is discussed in more detail in Chapter 3.

Table 2.4 Summary of some of the coal ash deposition models.

Author(s)	Impaction efficiency	Collection efficiency	Model description	Deposition Model
Baxter & DeSollar, 1993	Inertia, thermophoresis, condensation & chemical reaction	Particle residence time & composition	The 4 deposition pathways & stickiness are modelled w. r. t. τ and t	$\frac{dm_i}{d_i} = I_i G_i + T_i + C_i + T_i$
Huang et al., 1996	Inertia & thermophoresis	Watt-Fereday viscosity model	Inertial deposition in terms of particle density and size	$m = \int_0^\infty \int_0^\infty I(\rho_i, x_i) d\rho dx$
Wang & Herb, 1997	Particle cloud model incorporated in PCGC-3	Viscosities of both particle & impact wall,	Heat fluxes; particle impaction rates, size and composition	–
Lee & Lockwood, 1999	Particle arrival rate, $y^+ = 5$	Urbain viscosity model	Deposits in terms of inertial deposition rate & time interval	–
Costen, Lockwood & Siddique	Particle arrival rate, $y^+ = 11.63$	Kalmanovitch viscosity model	Deposit surface temperature & heat fluxes	$Q = \frac{K}{x}(T_s - T_w)$
Rushdi et al., 2005	Particle impact velocity	T-shift viscosity method	Inertial deposit in terms of particle density & size	$M_D = R_{Dep} A_t$
Proposed	Inertial & thermophoretic forces	Viscosity, surface energy, contact angle & rebound tendency	Deposition rate in terms of particle trajectories & sticking probability	$\dot{M} = \frac{1}{A_f} \sum_{i=0}^{n} (\dot{m}_{trj,i} \cdot \kappa_i)$

2.5 Slagging Indices

Slagging refers to molten ash deposition in the furnace region of the boiler where the heat transfer is predominantly by radiation (McLennen, Bryant, Bailey, Stanmore & Wall, 2000), while sintering is sintered deposits at the convective section of the boiler (Erickson *et al.*, 1995). These processes are better described as the fast melting of particles in the flame zone of high

radiation, and low sintering of agglomerated particles at low temperatures (Raask, 1979).

The ash fusion temperature, ash particle viscosity and ash chemistry are three popular bases of characterizing coal ash deposition and slagging (McLennan *et al.*, 2000). Most of these indices use laboratory ash to measure the properties of interest (Wigley *et al.*, 1990).

2.5.1 Coal fusibility

Different researchers have used different characteristics temperatures, but in general, fusion temperatures and cone melt down testing have been employed in evaluating the slagging behaviour of coal ash, yet the criterion did not yield a better tool for selecting good coal (Lawrence *et al.*, 2008). Coal with a low ash fusion temperature is said to have a high slagging potential (McLennan *et al.*, 2000).

Although estimating ash fusion temperature from coal chemical composition is complex because the relation between most of the interacting factors are unknown (Yin, Luo, Ni & Cen, 1998), several researchers agree that the increased percentage of basic oxides in coal will lower its fusibility (Lawrence *et al.*, 2008; McLennen *et al.*, 2000). Ash fusibility can be expressed in terms of the initial deformation temperature (IDT) and the hemispherical temperature (HT) of coal, and coals with fusibility greater than 1343 °C are said to have a low slagging potential (McLennen *et al.*, 2000).

Research reports indicate that the use of the fusion temperature as a criterion to distinguish between good and bad coals can lead to detrimental situations. According to Lawrence *et al.* (2008), the AFT which determines the temperatures at which the various stages of ash softening, melting and flow take place, is considered more as an observation rather than a measurement and hence is susceptible to subjective assessment. Therefore, it may not accurately predict the coal performance in real boiler situations (Lawrence *et al.*, 2008).

2.5.2 Ash viscosity

The range of ash particle viscosity is an important factor in determining the extent of the capture and consolidation of the ash particles on furnace walls (Wigley *et al.*, 1990). Although the viscosity of the slag in a boiler has to be low enough to ensure smooth flow and operations, most coals exhibit a continuous increase in viscosity with a decrease in temperature, and therefore the viscosity is a major physical property that affects the deposit strength in regions of high temperature (> 1093 °C) (Arvelakis, Folkedahl, Dam-Johansen & Hurley, 2006).

At high temperatures, coal ash slag behaves as a Newtonian fluid and its measured viscosity is independent of the shear rate. However, as the slag is cooled and forms solid crystals, its viscosity becomes non-Newtonian (Browning, Bryant, Hurst, Lucas & Wall, 2003), and therefore, viscosity is no longer linearly-dependent on the temperature. In Fig. 2.6, the viscosity of a coal/biomass blend was measured against temperature in two separate

experiments, with different viscometer bob speed, and the results show that at critical temperature (approximately 1150°C) the slag is no longer Newtonian as the temperature decreases (Arvelakis *et al.*, 2006).

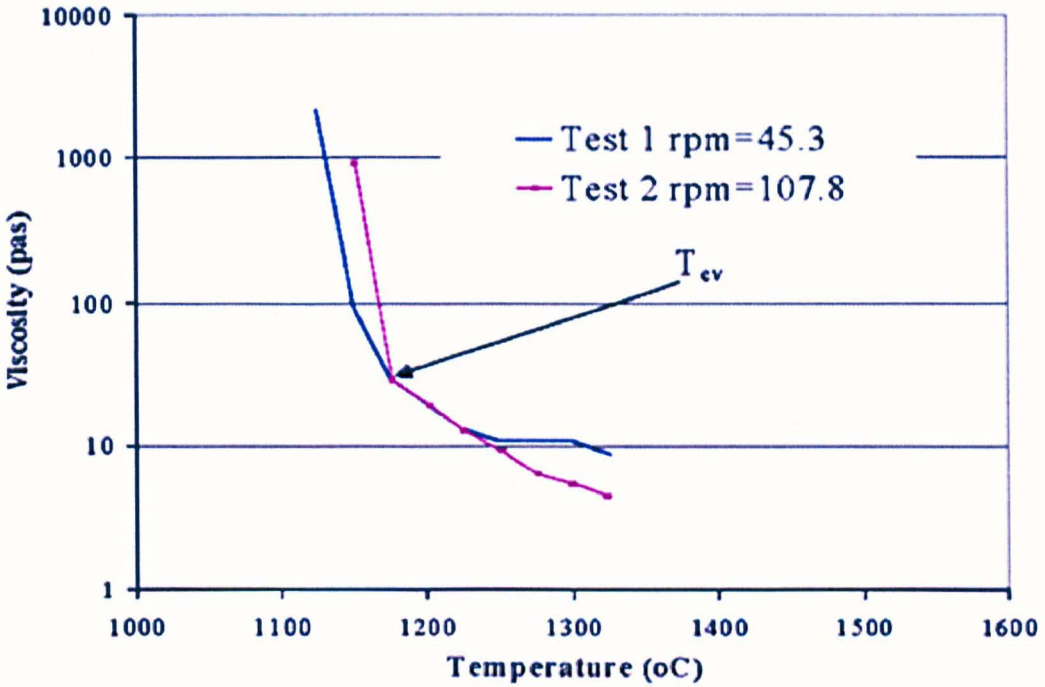

Fig. 2.6 Temperature-dependent viscosity for synthetic coal/corn slag showing critical viscosity, T_{cv}, (Arvelakis *et al.*, 2006).

Several models to predict the ash slagging using the viscosity method have been developed. These models include those developed by Urbain and other, Watt-Fereday, Raid-Cohen and Kalmanovitch-Frank (Vargas, Frandsen & Dam-Johansen, 2001). However, the viscosity models are also facing criticism from researchers.

According to McLennan *et al.* (2000), the application of the viscosity of slag to predict the slagging potential is limited to viscosities measured accurately for a sample that is predominantly liquid. They added that if a limited portion of the

bulk ash melting at a lower temperature is responsible for slagging, then the bulk ash viscosity measurement may not be indicative of the slagging potential.

Further investigations on the viscosity models are also focusing on non-homogeneous products, where solid crystals are formed at lower temperatures and the fluid is treated as a mixture of liquid and solids. According to Kondratiev and Jak (2001), the viscosity of the mixture is determined in terms of the solid concentration and the composition of the liquid.

The determination of the solids concentration is performed using a prediction code (Kondratiev and Jak, 2001), and since this method is subjected to the performance of a prediction tool, it may not always be accurate.

2.5.3 Ash chemistry

Coal ash has high levels of silicon and aluminium. Silicon and aluminium oxides make up to 80 to 90% of the total ash (McLennan *et al.*, 2000). Silicon, aluminium and titanium oxides form the acidic oxides of coal ash. The basic oxides of coal ash have a high percentage of iron oxide, which is the third abundant element in coal ash chemistry.

From the ash properties, the basic oxides are those of iron, calcium, magnesium, potassium and sodium, while acidic oxides are those of silicate, aluminium and titanium. The ratio of the total sum of the basic oxides to that of the total sum of the acidic oxides, which gives the ratio B/A, also assists in

distinguishing between good and bad coals. An increase in the B/A of coal, lowers its fusibility and hence increases the slagging potential. Coals having B/A ≤ 0.11 are considered as good coals (Lawrence *et al.*, 2008).

The empirical slagging index (R_s), which has been derived by multiplying the percentage of dry sulphur content in the coal, S, by the ratio B/A was developed based on American and European coals, where iron is typically present in iron sulphite (FeS_2) as pyrite. However, in low sulphur coals, where there is strong correlation between iron and carbonate ($FeCO_3$) as siderite, including Australian coals, it was suggested that the slagging index be better defined as the product of B/A and Fe_2O_3.

According to McLennan *et al.*, (2000), if the slagging index of a coal, determined using the product of B/A and dry S, is less than 0.6, the coal is said to have low slagging potential. Since this index is based on particular coal properties, the misleading results when it is tested on other coals are not unexpected McLennan *et al.*, 2000).

Other criteria that are used for the selection of coals which are based on ash chemistry include the percentage of iron oxide in the ash and the percentage of silica in the ash. The most successful coals have their iron level in ash below 6%, and for silica content, 72-80% is considered the range for good coals (McLennan *et al.*, 2000; Lawrence *et al.*, 2008).

2.5.4 Ash shrinkage

According to Lawrence *et al.* (2008), the AFT does not always accurately predict the performance of coal in PF combustion, because the test is more of observation than measurement. Although the AFT is still the most widely accepted means of assessing the slagging and fouling characteristics of coals, of particular concern is the estimation of the IDT (Gupta *et al.*, 1998).

Others slagging indices, such as the B/A, iron percentage and silica percentage, are established for particular types of coal properties and therefore their use is not necessarily reliable when extended to other types of coals, (Lawrence *et al.*, 2008). Neglecting the ash loading in coal may result in a misleading result, (Rushdi *et al.*, 2005).

In an attempt to correlate the slagging index to the field performance of the coals, Lawrence *et al.* (2008) conducted a laboratory test to study the relationship between various shrinkage events due to the melting of ash pellets on heating. They reported different stages of shrinkage pattern when ash the pellets are heated from an ambient temperature to 1400 °C. Their report indicated that a 5% to 40% shrinkage occurs at temperatures between 1120 °C and 1200 °C, which they attributed to particle initial deformation process.

On the basis of their experimental results, Lawrence *et al.* (2008) proposed an empirical slagging index based on the relative shrinkage rate of ash and the weight of ash per Mkcal. They concluded that the slagging in boiler furnace

depends on the combined effects of the liquid forming tendency of the ash, the temperature experienced in the furnace and the ash loading in coal.

In another similar experiment on Australian coals, Gupta *et al.* (1998) conducted a mechanistic study, in which coal is heated with its shrinkage rate measured continuously up to a temperature of 1600 °C. They reported four maximum shrinkage rates with different temperatures. A summary of their report is as follows:

- At temperatures below 900 °C, there was no significant shrinkage in most coal ash samples.
- Lower temperature peaks up to 1100 °C were related to activities in the SiO_2 - $Al2O_3$ - K_2O system.
- At 1200 °C, peaks were observed and they were related to the SiO_2 – Al_2O_3 - FeO system.
- Peaks between 1220 °C and 1440 °C have been correlated to the FeO/CaO reaction with various proportions of SiO_2 and Al_2O_3.

They concluded that since the viscosity, calculated from the ash chemical composition, gives estimations for the temperatures for the ash particle to be sticky, it can therefore be related to the extent of the shrinkage measured at these temperatures. Therefore, the shrinkage level is appropriate as a criterion for the ash stickiness.

Attempts to correlate ash shrinkage to the slagging of coal started some decades ago. According to Raask (1979), the ash shrinkage measurements can

give useful information on the sintering potential of the ash. He reported a method which could be used for the studies of the coalescence of hot ash particles as a routine test of the slagging characteristics.

A summary of some of the existing coal slagging indices, which are based on the fusibility, viscosity and chemistry of the ash, are presented in Table 2.5. The available literature suggests that most of the existing slagging indices have been developed based on some specific properties of the coals, and this calls for the need to search for a more robust slagging index.

A more generic slagging index is expected to account for the effects of various physical and chemical properties of ash, such as, chemical composition, fusibility, viscosity and content in coal. Such a model should be able to predict the slagging potential over a wide range of coals.

Also, the parameters of a robust slagging index should be made flexible such that it can accommodate the properties of different solid fuels. As shown in the last row of Table 2.5, the proposed numerical slagging index is based on the weight of the incoming ash and the viscosity of the ash. In determining the weight of the incoming ash, the ash content of the coal and its heating values are considered. Also, the ash viscosity is computed based on some important properties of the ash, such as, the ash softening temperature, the bulk ash chemistry, etc. The wide range of ash properties considered in modelling the NSI makes the model very sensitive and flexible. Refer to Chapter 6 for further details.

Table 2.5 Summary of some of the coal ash slagging indices.

Author(s)/ reported by	Basis	Slagging index	Slagging potential			
			Low	***Medium***	***High***	***severe***
McLennan *et al.* Energy & fuel 2000	Fusibility	$AF = \frac{4IDT + HT}{5}$	> 1343 °C	1232 – 1343 °C	1149 – 1232 °C	< 1149 °C
Yin *et al.* Fuel 1998	Fusibility	$ST = a(SiO_2) + b(Al_2O_3) + c(Fe_2O_3) + d(CaO) + e(MgO) + f(\alpha) + g$			-	-
Watt & Fereday J. Inst. Fuel 1969	Viscosity	$Log(\mu) = \frac{m.10^7}{(T-150)^2} + c$				
Lawrence *et al.* Fuel 2008	Silica ratio	$SR = 100(SiO_2 / SiO_2 + Fe_2O_3 + CaO + MgO)$	72 – 80	65 – 72	50 - 65	-
McLennan *et al.* Energy & fuel 2000	Percentage of Fe_2O_3	Index = % Fe_2O_3 in ash	< 6 %	6 – 7 %	> 7 %	-
Lawrence *et al.* Fuel 2008	B/A ratio	$B/A = \frac{Fe_2O_3 + CaO + MgO + K_2O + Na_2O}{SiO_2 + Al_2O_3 + TiO_2}$	< 0.11	0.11 - 0.14	> 0.14	-
Lawrence *et al.* Fuel 2008	Sulphur content	$Index = (B/A) \times S$	< 0.6	0.6 - 2.0	2.0 - 2.6	> 2.6
Lawrence *et al.* Fuel 2008	Shrinkage rate	$Index = \frac{R_m}{T_m} \times W_t$	No standard scale shown, but from the report, ≤ 55 shows no slagging relative to others			
Proposed NSI	Viscosity, fusibility & ash loading	$S_x = \gamma / Log(\mu)$	High index-value = high slagging potential			

CHAPTER 3

MATHEMATICAL MODELLING

This chapter discusses the general approach and specific steps followed in the development of the theoretical models used in the calculations. The basic principles underlying the existing models that have been adopted and/or developed, including the ash particle deposition rates model, are presented in this chapter.

3.1 Governing Equations

In modelling combustion systems, the conservation laws of physics are adopted to numerically represent the entire governing system of equations. The law of conservation of mass, Newton's second law of motion and the first law of thermodynamics are the fundamental laws (Versteeg & Malalasekera, 2007). The basic variables to be considered in the modelling of the fluid dynamics for a non-reactive gaseous flow are the velocity components and the thermodynamic properties.

3.1.1 Fluid flow equations

A summary of the conservative form of the governing equations of fluid flow (representing the continuity, equation (3.1); momentum, equations (3.2)-(3.4); and energy, equation (3.5)), are given as follows (Versteeg & Malalasekera, 2007):

$$\frac{\partial \rho}{\partial t} + div(\rho \mathbf{u}) = 0 \tag{3.1}$$

$$\frac{\partial(\rho u)}{\partial t} + div\,\rho(u\mathbf{u}) = -\frac{\partial p}{\partial x} + div(\mu\, grad\, u) + S_{mx} \tag{3.2}$$

$$\frac{\partial(\rho v)}{\partial t} + div\,\rho(v\mathbf{u}) = -\frac{\partial p}{\partial y} + div(\mu\, grad\, v) + S_{my} \tag{3.3}$$

$$\frac{\partial(\rho w)}{\partial t} + div\,\rho(w\mathbf{u}) = -\frac{\partial p}{\partial z} + div(\mu\, grad\, w) + S_{mz} \tag{3.4}$$

$$\frac{\partial(\rho i)}{\partial t} + div(\rho i\mathbf{u}) = -p\, div\,\mathbf{u} + div(k\, grad\, T) + \Phi + S_i \tag{3.5}$$

where S_m, S_i and Φ are the momentum source, internal energy source and dissipation function, respectively, k is the Boltzmann constant, ρ is the fluid density, $\mathbf{u}$ is the velocity vector, u, v and w are the velocity components, p is the fluid pressure, T is the temperature of fluid, and i is the specific internal energy.

For a transported quantity with property ϕ, its transport process is represented as follows

$$\frac{\partial(\rho\phi)}{\partial t} + div(\rho\phi\mathbf{u}) = div(\Gamma\, grad\,\phi) + S_\phi \tag{3.6}$$

The rate of change and the convective terms are presented on the left hand side of the equation (3.6), while the diffusive and the source terms are on the right hand side of the equation, and Γ is the diffusion coefficient.

3.1.2 Energy equation

Heat transfer can take place through three main methods; conduction, convection and radiation. The total energy (in terms of temperature), includes sensible energy, chemical energy and kinetic energy. It is the total energy per unit mass, also referred to as the specific energy.

For the non-adiabatic non-premixed combustion models, the total energy (enthalpy, H), from the energy equation, is given by

$$\frac{\partial}{\partial t}(\rho H) + \nabla \cdot (\rho v H) = \nabla \cdot (\frac{k_t}{c_p} \nabla H) + S_h \tag{3.7}$$

The first term on the right hand side of equation (3.7) represents the ratio of turbulent thermal conduction (thermal diffusivity) term to the species diffusion term, while the second term which appears in non-conservative form, represents the contributions from the viscous dissipation and the radiation source terms where applicable (Barths, Hasse and Peters, 2000; Fluent Inc., 2009).

3.1.3 Radiation model

The radiative heat transfer is always considered when the radiative heat flux is large compared to the heat transfer due to conduction and convection. The P-1 Radiation model and Discrete Ordinate (DO) model are commonly used in coal combustion (Ma *et al.*, 2006; Huang *et al.*, 1996; Lee & Lockwood, 1999).

The P-1 radiation model is a simplified case of the P-N model which is expressed in terms of normalized spherical harmonics (Sazhin, Sazhina, Saravelon and Wild, 1996). The P-1 model is not Central Processing Unit (CPU) intensive and it is mostly applicable for combustion models with large optical thickness (Lee & Lockwood, 1999).

On the other hand, the DO model is more intensive in terms of CPU demand, but it has the advantage of spanning the entire range of optical thicknesses. Also in the DO modelling, the energy transfer due to radiation, I(r,s), as a function of position, r, and direction, s, is governed by the Radiative Transfer Equations (RTE) given as follows (Chui & Raithby, 1993):

$$\frac{dI(r,s)}{ds} = -(K_a + \sigma_s)I(r,s) + K_a I_b(r) + \sigma_s \bar{I}(r,s) \qquad (3.8)$$

where K_a and σ_s are the absorption and scattering coefficients, I_b and $\bar{I}$ are black body and in-scattering coefficients, respectively. Therefore, the four terms on the right hand side of equation (3.8) represent the absorption, out-scattering, emission and in-scattering coefficients, respectively.

3.2 Turbulence Modelling

In modelling combustion, the two flow phases are calculated separately. Based on the CFD techniques, the Eulerian reference frame is used to calculate the gas phase of the combustion, while the Lagrangian reference frame is used to calculate the particle motions and combustion. In turbulent flows, the particle

velocity is decomposed into its steady mean value, u, with a fluctuating component, u', (Versteeg & Malalasekera, 2007), namely;

$$U(t) = u + u'(t) \tag{3.9}$$

This conventional Reynolds decomposition method can be used in a constant density turbulent fluid flow. However, in combustion, the heat release leads to density fluctuations which give rise to more uncertainties. Therefore, the density weighted averaging is used to cater for the fluctuating terms.

In turbulent fluid flows, the continuity equation, along with the Navier-Stoke (N-S) equations, is characterized by a dimensionless parameter called the Reynolds number. This is the ratio of the convective to diffusive terms and is defined as follows (Turns, 2006):

$$\mathrm{R_e} = \frac{\rho u L}{\mu} \tag{3.10}$$

where u and L are the velocity and length scales, respectively, while ρ and μ are the density and viscosity, respectively.

3.2.1 Averaging method

Reynolds averaging:

In the Reynolds averaging approach, the conserved scalar ϕ is defined as follows:

$$\phi = \overline{\phi} + \phi' \tag{3.11}$$

Favre averaging:

Here we average as follows:

$$\tilde{\phi} \equiv \overline{\rho\phi} / \overline{\rho}$$

and this implies that

$$\phi = \tilde{\phi} + \phi'' \tag{3.12}$$

where ϕ'' is the superimposed fluctuation.

The Favre fluctuation averaging is of advantage considering the elimination of the density-velocity cross product terms in the momentum equations (3.2) – (3.4), which is an effective way to account for the effect of density fluctuations due to turbulence (Habib, 2001).

3.2.2 RANS equations

Averaging the density and velocity, leads to averaged forms of the general equations. Representing the momentum conservation, continuity and scalar, for high Reynolds number, we obtain the following (Versteeg & Malalasekera, 2007):

$$\frac{\partial}{\partial t}(\rho u_i) + \frac{\partial}{\partial x_j}(u_i u_j) = \frac{\partial}{\partial x_j}\sigma_{ij} + F_i \tag{3.13}$$

$$\sigma_{ij} = -p\delta_{ij} = \mu\left(\frac{\partial u_i}{\partial x_j} + \frac{\partial u_j}{\partial x_i}\right) \tag{3.14}$$

$$\frac{\partial \rho}{\partial t} + \frac{\partial}{\partial x_i}(\rho u_i) = 0 \tag{3.15}$$

where

$$\delta ij = \begin{cases} 0 & for\ i \neq j \\ 1 & for\ i = j \end{cases} \tag{3.16}$$

$$\frac{\partial}{\partial t}(\rho\phi) + \frac{\partial}{\partial x_i}\left(\rho u_i \phi - \Gamma \frac{\partial \phi}{\partial x_i}\right) = S \tag{3.17}$$

The equations (3.13), (3.15) and (3.17) represent the momentum, continuity and scalar transport, respectively. Equation (3.14) is part of the momentum equation, representing the Newtonian fluid. Further, u_i represents the fluid velocity, σ_{ij} represents the stress, and F_i represents the body forces.

3.2.3 κ- epsilon model

Modifying the governing equations introduces additional variables, and a turbulence model is required in order to determine these variables in terms of known quantities. The κ-ε model is the most popular, because it is robust, economical and reasonably accurate for many flows involving turbulence.

The assumption in the κ- ε model is that the flow is fully turbulent and the effect of molecular viscosity is negligible. This method is based on modelling the transport for the turbulence kinetic energy (κ) and its dissipation rate (ε). The turbulent viscosity in the high R_e limit is calculated as follows:

$$\mu_t = \rho C_\mu \frac{\kappa^2}{\varepsilon} \tag{3.18}$$

and the default value of the constant, C_μ, is 0.0845, which is very close to the value in the standard κ- ε model (Launder & Spalding, 1972).

To improve upon the standard κ-ε model, the RNG κ-ε model was derived from a statistical technique called the 'renormalized group theory'. Most importantly, the RNG κ-ε model includes the effects of swirling flows and it also accounts for low values of the R_e. Modifying equation (3.18) to account for swirling effects (Backreedy, Fletcher, Ma, Pourkashanian & Williams, 2006), gives the RNG κ-ε model as follows:

$$\mu_t = \mu_{to} f(\alpha_s, \Omega, \frac{K}{\varepsilon}) \tag{3.19}$$

The turbulent viscosity without swirl and the characteristic swirl number are represented by μ_{to} and Ω, respectively, while the swirl factor α_s takes a default value of 0.07. However, for strong swirl flows, the swirl factor can assume a higher value. Numerically, the striking difference between the standard and RNG κ- ε models is that the RNG model has an additional term in the ε equation (Orszag, 1993 quoted in Fluent inc., 2009).

3.3 Combustion Modelling

3.3.1 Non-premixed model

Modelling the mixing and transport of the chemical species can be achieved by solving the conservation equations that describe the convection, diffusion and reaction sources for each component species. However, the non-premixed combustion model is considered more suitable for pulverized coal furnaces. It is specific for the simulation of turbulent diffusion flames with fast chemistry,

computationally it is efficient, and it takes a pre-processed thermo-chemistry through the PDF table (Versteeg & Malalasekera, 2007).

The non-premixed model works under the assumption that the thermo-chemistry can be reduced to a single parameter (mixture fraction) representing the mixture fraction of the local mass fraction of burnt and unburnt fuel stream elements (Jones & Whitelaw, 1984). The mixture fraction, f, is determined from:

$$f = \frac{Z_i - Z_{i,ox}}{Z_{i,fuel} - Z_{i,ox}} \tag{3.20}$$

where Z_i is the elemental mass fraction for the element i. The subscripts ox and $fuel$ represent values of Z_i at the oxidizer and the fuel stream-inlets, respectively. Equation (3.20) was derived from the generalized relation for species concentration (mass fraction) given by Sivathanu & Faeth (1990). They stated some relationship functions for hydrogen reacting with the oxygen-nitrogen mixture, and for the mass fractions of oxygen, carbon dioxide and water vapour.

The non-premixed model requires some inputs in creating the look-up PDF table. The non-adiabatic systems require the computational process to update the properties, such as density, temperature, species mass fraction and enthalpy from the PDF table in order to account for the varying pressure of the system. The PDF table accounts for the interaction of the turbulence and chemistry (Williams *et al.*, 2000).

The double delta PDF and the beta PDF are the two types of PDF commonly used in commercial software packages. The double delta PDF is considered to be faster, while the beta function may be a more accurate representation of the PDF (Fluent Inc., 2009).

3.3.2 Single rate devolatilization model

The single rate devolatilization model assumes that the rate of devolatilization is first-order dependent on the amount of volatiles remaining in the particle (Rushdi *et al.*, 2005). Based on this assumption, the devolatilization rate of the combusting particle is expressed as follows:

$$-\frac{dm_p}{dt} = k[m_p - (1 - f_{v,o})(1 - f_{w,o})m_{p,o}] \tag{3.21}$$

where m_p and $m_{p,o}$ are the current and initial particle masses, and $f_{v,o}$ and $f_{w,o}$ are the mass fractions of the volatiles initially present in the particle and that of the evaporating or boiling material in wet combustion. Badzoich & Hawksley (1970) gave the fundamental equations representing the volatile matter of char, the change in volatile matter, char yields and the weight loss during initial coal heating. The results of their research work led to equation (3.21).

In the discrete phase modelling, the exchange of mass from the discrete phase to the evaporating phase due to the devolatilization of combusting particle occurs. Therefore, in the non-premixed model, the DPM mass source is equal to the DPM burnt-out plus DPM evaporation.

3.3.3 Kinetic/diffusion limited model

The kinetic/diffusion-limited model assumes that the surface reaction rate includes the effect of both bulk diffusion and chemical reactions. This model, was derived from two separate equations; one representing the diffusion rate, D_o, and the other representing the kinetic rate, R. The two equations were described by Baum & Street (1971) and Field (1969), respectively:

$$\frac{dm_p}{dt} = -A_p P_{ox} \frac{D_o R}{D_o + R} \tag{3.22}$$

where the surface area of a droplet and the partial pressure of the oxidant species surrounding the combusting particle are denoted by A_p and P_{ox}, respectively.

3.4 Deposition Model

Several research attempts have been made in order to improve the accuracy of predicting the coal ash deposition in utility boilers. The viscosity method is widely used in the prediction of ash behaviour in boilers. However, the different approaches employed by researchers and the selection of prediction software packages result in inconsistent prediction results.

For example, the particle cloud method has been used to predict the effect of turbulence on the dispersion of particles in the furnace (Wang and Herb, 1997). However, this method assumes that particles in a single stream have the same properties and are considered as a single parcel instead of being treated

individually. Also, some deposition models use only one or two parameters in determining the fate of an ash particle upon impaction on the heat exchange surfaces. Baxter and DeSollar (1993) used particle residence time and composition to predict collection efficiency. In many case, only the particle viscosity is used to determine the sticking probability of the particle (Huang *et al.*, 1996; Wang & Herb, 1997; Lee & Lockwood, 1999; Rushdi *et al.*, 2005).

The technological advancement has produced more flexibility with the recent CFD tools, such as, FLUENT 12.1 commercial software. In the past, software packages which have more limited modelling capabilities, such as TEACH have been used in predictions (Rushdi *et al.*, 2005).

In this section, a numerical model to predict the ash particle deposition rates in the burner region of coal-fired furnace is developed. Most the existing coal ash deposition models that uses viscosity method do not consider the rebound tendency of the particle after impaction, and the rebound tendency is significant for particle with excess energy at impaction (Ma *et al.*, 2006).

Therefore, the ash particle stickiness in the proposed deposition model is computed based on the particle viscosity, surface energy and static contact angle, where the overall sticking probability of the ash particle at impaction is determined based on the particle stickiness and its tendency to rebound after impaction.

The viscosity of the particle is determined from the chemical properties of the ash and the impact temperature of the particle, and then the particle viscosity is compared with a reference viscosity in order to determine its stickiness. Combustion codes in the new FLUENT 12.1 software have been used to implement the proposed ash particle deposition rates model.

3.4.1 Impaction efficiency

To calculate the discrete phase particle trajectories in a Lagrangian frame of reference, the force balance equations for the x-direction can be written in terms of the drag force, F_D, gravitational acceleration, g_x, and other forces, F_x, (such as the change in the pressure gradient and the thermophoretic force), as follows (Huang, *et al.*, 1996):

$$\frac{du_p}{dt} = F_D(u - u_p) + g_x\frac{(\rho_p - \rho)}{\rho_p} + F_x \tag{3.23}$$

The drag force acting on a particle ash, which is determined in terms of particle relaxation time (τ_p), is given as follows:

$$F_D = \frac{C_D \mathrm{R_e}}{\tau_r 24} \tag{3.24}$$

$$\tau_r = \frac{d_p^2 \rho_p}{18\mu} \tag{3.25}$$

The relative Reynolds number $\mathrm{R_e}$ is defined as follows:

$$\mathrm{R_e} = \frac{\rho d_p |u_p - u_i|}{\mu} \tag{3.26}$$

and the drag coefficient is given as

$$C_D = \frac{a_1}{\mathrm{Re}} + \frac{a_2}{\mathrm{Re}^2} + a_3 \tag{3.27}$$

u_f = fluid phase velocity

u_p = particle velocity

μ = fluid molecular viscosity

ρ = fluid density

ρ_p = particle density

d_p = particle diameter

a_1, a_2 and a_3 are constants (functions of Re) that apply to smooth spherical particles (Morsi & Alexander, 1972). For example, when Re is ≥10000, the constants take the following values a_1= -1662.5, a_2= 5.4167x10^6 and a_3= 0.5191.

The gravitational acceleration and the virtual mass forces are also included in the energy balance equation (3.23). Considering the forces due to the change in the pressure gradient and the thermophoretic effect, which are also acting on the particle, the virtual forces can be determined as follows (Talbot, in Huang *et al.*, 1996):

$$F_x = -\frac{6\pi d_p \mu^2 C_s (K + C_t K_n)}{\rho(1 + 3C_m K_n)(1 + 2K + 2C_t K_n)} \frac{1}{m_p T} \frac{\partial T}{\partial x} \tag{3.28}$$

where the Knudsen number $Kn = 2\lambda / d_p$ and the mean free path

$$\lambda = \left\{ \sqrt{\frac{\pi}{2}} \mu_g p \sqrt{RT} \right\}$$

$K = k / k_p$

k = fluid thermal conductivity

k_p = particle thermal conductivity

$C_s = 1.17, \quad C_t = 2.18, \quad C_m = 1.14$

m_p = particle mass

T = local fluid temperature

The energy balance equation of a fly-ash particle, which is solved along its trajectory to obtain the corresponding temperature at the point of impact, is given as follows (Lee & Lockwood, 1999):

$$\frac{d(m_p C_p T_p)}{dt} = q_c A(T_\infty - T_p) \tag{3.29}$$

C_p = particle specific heat

T_p = particle temperature

q_c = convective heat transfer coefficient

T_∞ = bulk phase temperature

Having subscribed to the popular opinion that inertial impaction (I_i), thermophoretic effect (T_i), condensation (C_i) and heterogeneous reaction (R_i) are the major processes of particle deposition, the rate of deposition of an ash particle at its residence time, t, relative to the injection time is determined as follows (Baxter & DeSollar, 1993):

$$\frac{dm_i}{dt} = I_i(t,\tau) + T_i(t,\tau) + C_i(t,\tau) + R_i(t,\tau) \tag{3.30}$$

The second time frame, τ, in the equation (3.30), is referred to as the elapsed laboratory time relative to an arbitrary time of the day, is independent of the particle residence time.

In the burner region, where the temperature is very high, there is little or no condensation of fly ash. Therefore, it has been assumed that the inertial impaction is the major pathway for the larger particle deposition. Although the particle may not be a perfect sphere, but using the spherical drag law, it is also assumed that the ash particle is spherical.

3.4.2 Collection efficiency

Particles may stick to the furnace walls after impaction if either the wall or the particle or both are sticky. However, in the burner region, where there is little or no condensation of ash-forming vapours due to the high temperatures, the sticky probability will largely depend on the impacting particle, because the sticky probability of such a wall is computed in analogy to the silicate particle sticky probability.

For particles rich in salts, typical in biomass, the sticky probability is determined by their melt fraction and/or softening temperature (Ma *et al.*, 2006). However, for silica-rich particles, as in coal, the sticky probability (κ_i) can be determined from the particle viscosity (μ_p) and a reference viscosity, called the critical viscosity (μ_c), as follows (Harb, Zygarlicke & Richards, 1993):

$$\kappa_i = \mu_c / \mu_p \quad \text{, where } \mu_p > \mu_c \tag{3.31}$$

$$\kappa_i = 1 \quad \text{, where } \mu_p \leq \mu_c \tag{3.32}$$

In determining the ash-particle viscosity, the particle temperature and its chemical composition are required as input. The particle viscosity is determined using the Watt & Fereday model as follows (Huang *et al.*, 1996):

$$Log_{10}(\mu_p) = [10^7 m/(T-150)^2] + c \tag{3.33}$$

where the slope, m, and the intercept, c, are functions of the bulk ash chemistry, and are been computed from the species concentration in weight percentages, as follows:

$$m = (0.00835)SiO_2 + (0.00601)Al_2O_3 - 0.109 \tag{3.34}$$

$$c = (0.0415)SiO_2 + (0.0192)Al_2O_3 + (0.0276)Equiv.Fe_2O_3 + (0.0160)CaO - 3.92 \tag{3.35}$$

The slope and intercept are determined on the basis that

$$SiO_2 + Al_2O_3 + Equiv.Fe_2 + CaO + MgO = 100(wt\%) \tag{3.36}$$

3.4.3 Reference viscosity

To assess the sticking probability of the ash particle using the viscosity method, a reference viscosity has to be chosen. It is sometimes called the critical viscosity, μ_c, and its value varies in different research studies. More often 10^4-10^8 (Pa.s) are reported (Rushdi *et al.*, 2005; Lee & Lockwood, 1999).

Yilmaz and Cliffe (cited in Rushdi *et al.*, 2005) conducted a laboratory-scale study in 1997, and they reported that deposition starts when the particle viscosity is less than 6.7×10^{9} (Pa.s). In this investigation, 10^{8} (Pa.s) has been chosen as the reference viscosity (Rushdi *et al.*, 2005).

3.4.4 Particle rebound

Particle with high impact velocity may possess excess energy to rebound. This is in addition to the sticky probability of the surface wall and the particle. The rebound tendency can be predicted as a function of viscosity, impact velocity and static contact angle of the particle. If a particle has excess energy, E_x, greater than zero, it is assumed to rebound, otherwise it sticks. The particle excess energy is calculated as follows (Ma *et al.*, 2006; Mao, Kuhn & Tran, 1997):

$$E_x = \frac{D^2}{4}(1-\cos\alpha) - \frac{3D^{2.3}}{25}(1-\cos\alpha)^{0.63} + \frac{2}{3D} - 1 \qquad (3.37)$$

where D is the ratio of the maximum deformation particle diameter to the particle diameter, determined as follows:

$$D = (12+We)^{1/2}\left[3(1-\cos\alpha) + 4(We/\mathrm{Re}^{1/2})\right]^{1/2} \qquad (3.38)$$

The Weber number is obtained from equation (3.39), while the Reynolds number has been redefined in terms of particle velocity in equation (3.40). α and δ are the static contact angle and the surface energy of the particle.

$$We = \frac{\rho_p u^2 d}{\delta} \qquad (3.39)$$

$$\mathrm{Re} = \frac{\rho_p u d}{\mu_p} \qquad (3.40)$$

3.4.5 Deposition flux

The deposition flux for a single particle that hits the wall of a furnace is evaluated from the mass flux of the particles, represented by their trajectories ($\dot{m}_{trj,i}$) (Forstner *et al.*, 2006), and the sticking probability of the impacting particle (κ_i). Therefore, on a wall face, the total deposition flux is determined as follows:

$$\dot{M} = \frac{1}{A_f} \sum_{i=0}^{n} (\dot{m}_{trj,i} \cdot \kappa_i) \tag{3.41}$$

3.4.6 Assumptions and limitations

The limitations of some of the existing deposition models that have been discussed in Chapter 2 include the following: the use of particle cloud to predict the properties of individual particle; the use of only viscosity to determine particle sticking tendency; and assuming a single deposition pathway. The model developed in this thesis addresses some of the limitations, such as particle rebound tendency and the effect of particle surface energy on its stickiness. Nevertheless, there remain the following assumptions and limitations:

i. Ash particles with viscosity less than or equal to the reference viscosity are considered to be sticky.
ii. Particles with possess excess energy (> 0) at impaction may rebound.
iii. The deposition panels are considered as clean surfaces.
iv. The reference viscosity of 10^8 (Pa.s) was chosen from empirical results.

v. The ash properties used in the calculations may change in a dynamic boiler situation.

3.6 Summary

In this chapter, the major theoretical models used in this numerical investigation are presented. The assumptions of both the adopted and the developed codes are also stated. The law of conservation of mass and the fundamental laws of thermodynamics are the governing equations for the fluid flow and the enthalpy calculations, while the effect of radiation is obtained using the DO model.

Turbulence is calculated according to the RNG κ-ε model, and the combustion is computed using the non-premixed model, which is found suitable for turbulent diffusion flames with fast chemistry. The thermo-chemistry is pre-processed using the β-function PDF lookup table. The rate of release of volatile matter is assumed to be first-order dependent on the amount of volatiles remaining in the particle, while the kinetic/diffusion-limited model which has been used includes the effects of bulk diffusion and chemical reactions.

The effects of the drag force, gravity and other forces, such as, thermophoretic force and pressure gradient are considered while calculating the particle trajectories. The overall sticking tendency of the particle is determined on the basis of its calculated viscosity at impaction on the boiler walls and its tendency to rebound after impaction. A reference viscosity of 10^8 (Pa.s) was used to define the state of the ash particle relative to its computed viscosity.

CHAPTER 4

IMPLEMENTATION OF THE DEPOSITION MODEL

In order to successfully validate the coal ash particle deposition rates model that has been developed in this investigation, comprehensive coal combustion codes are required in order to establish the gas phase temperature and velocity fields. Hence, the combustion models that are available in the FLUENT 12.1 commercial software (Fluent inc., 2009) have been used in computing the turbulent fluid flow, as well as the gas and particulate combustion phases. The proposed ash particle deposition rates model has been successfully implemented through the use of a user-defined function.

This chapter has been divided into four sections. The first section discusses the method adopted in the implementation of the ash deposition model. Section two describes the test case used in validating the model and, therefore, the furnace geometry, the computational grid, the fuel properties and the furnace operational conditions have all been explained. The third section of this chapter is mainly on the solver settings and the solution procedures that have been adopted. Finally, the fourth section contains a summary of the conclusions of the chapter.

4.1 Methodology

In an attempt to improve combustion efficiency, modelling and numerical simulations of PF combustion processes are considered as an important tool for

diagnostics and predictions of the operations and boiler situations (Filkoski, Belosevic, Petrovski, Oka & Sijercic, 2006). In order to predict the deposition mechanism of the ash particles, some important steps have to be followed. Therefore, this research study has been guided by the following salient steps:

- Generating a computational grid to represent the combustion furnace that has been used in the calculations, and identifying the furnace operational conditions. Also in this initial stage, the combustion fuel (coal) type and its properties have been identified.
- Setting up simulations using the available and suitable CFD codes in FLUENT 12.1 software, by selecting suitable models for the fluid flow and its various characteristics, such as, turbulence, heat transfer, chemical kinetics, etc., in an Eulerian frame of reference in order to establish the gas phase of the combustion process.
- In the second, discrete, phase of the combustion process, suitable sizes of the coal particles have been injected into the furnace. Simulations involving the interaction between the continuous and the discrete phases, including energy and radiation effects, have been iteratively solved. Also, the particle trajectories in a Lagrangian frame of reference, with the effects of drag and other forces acting on a particle in fluid, have been computed. A non-adiabatic PDF look-up table for the gas phase has been prepared in the FLUENT 12.1 software.
- In a sequel to the proceeding stage, the temperature distribution and velocity profiles, and some other properties of the gaseous phase, such as the heat fluxes, have been examined and reported.

- A theoretical model to predict the coal ash particle deposition rates in boilers has been developed. The model has been hooked into the FLUENT 12.1 software, as a UDF boundary condition in order to determine the fate of the ash particles that may impact on the surfaces of the heat exchanger. This stage is of major concern to this research study, being a test point for the effectiveness or otherwise of the proposed model.
- At this stage of the computational process, the particle trajectories and stickiness have been determined. The particle's stickiness has been defined based on the ash viscosity, the bulk properties of the ash and some other physical properties of the ash particles, such as the impact velocity, static contact angle and surface energy.
- The results of the predictions using the developed deposition code are compared with the available experimental data in order to validate the proposed code. This step was followed by the post-processing analyses and a discussion on the results of predictions using the proposed deposition model.

Fig. 4.1 depicts a flow chart illustrating an overview of the necessary computational steps for the prediction of the ash deposition rates in boilers which are based on the salient steps explained above. Fig. 4.1 shows that the required input into the commercial software for the initial set of calculations include a completed computational grid representing the various sections of the test boiler, the physical and chemical properties of the fuel, and the operational conditions of the boiler. When a converged solution of the first set of

computational iterations is obtained, the temperature and velocity fields, and the heat fluxes, are recorded and analysed.

The second phase of the calculations, as shown in Fig. 4.1, is basically on the particle trajectories and the determination of the fate of the particles when they are transported to the boiler walls. The particle trajectories are calculated under the influence of turbulence, particle dispersion effects, high temperature and pressure gradients, etc.

For the ash particle that possess sufficient energy and velocity to transverse the boundary layer and hit the boiler walls, the viscosity, surface energy and excess energy of the particle are computed in order to determine whether the particles stick to the walls or rebound.

4.1.1 CFD codes

The complexity of some engineering phenomena, such as combustion, makes it very difficult to have an accurate and precise measure of all the parameters involved. The need to study the characteristics of such vital engineering activities has led to the development of CFD codes.

CFD is the analysis of systems involving fluid flow, heat transfer and associated phenomena, such as chemical reactions, by means of computer-based simulations (Versteeg & Malalasekera, 2007). This powerful technique spans a

wide range of industrial and non-industrial application areas with acceptable performance results, and chemical processes such as combustion are inclusive.

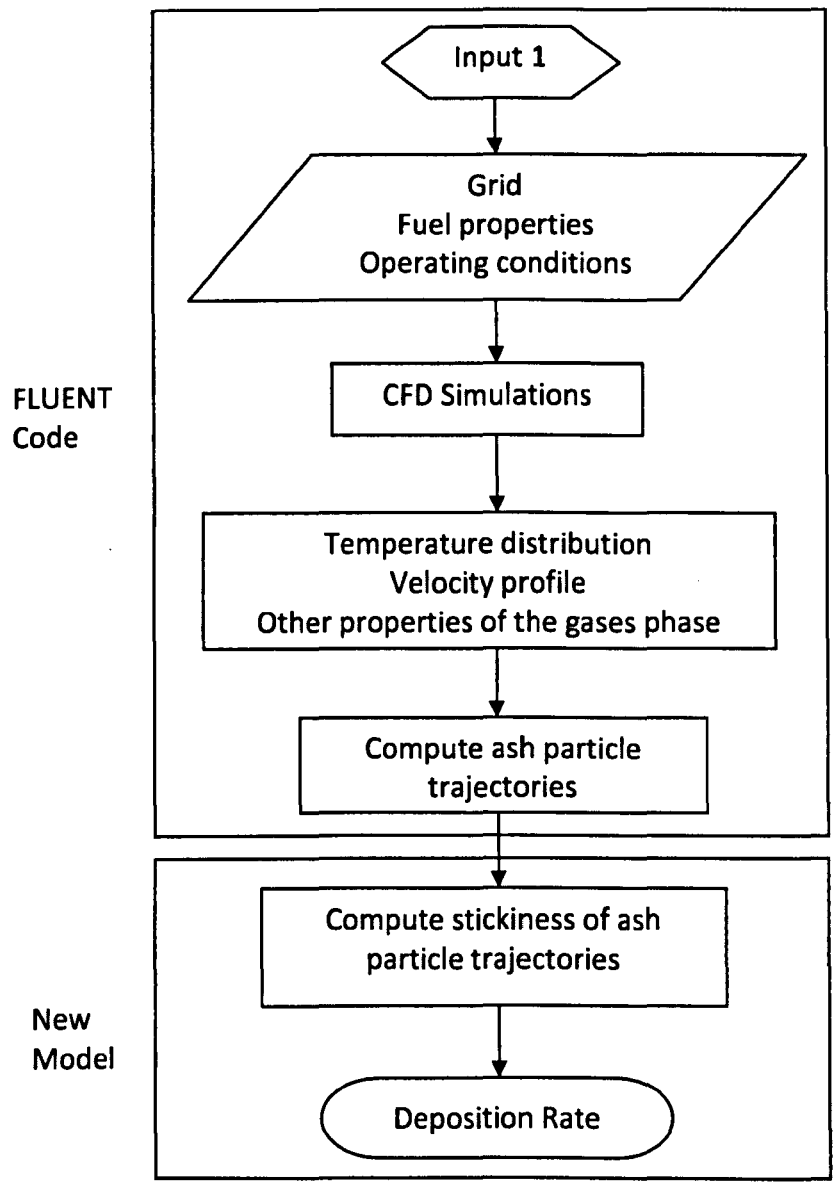

Fig. 4.1 Flow chart for the prediction of the ash particle deposition rates.

In relation to other computational processes, the CFD differential models based on solving the conservation equations, offer some local values of the relevant variables in the computational domain regarding the geometry and its operating

conditions, the fuel characteristics, and the complex operations of the plant (Filkoski *et al.*, 2006).

In general, modelling assists in solving problems that are related to PF combustion. Numerical predictions of boilers using CFD codes have been in the coal industry for some time, and reasonable advances have been made. Modelling and simulations of the processes of PF furnace combustion can be used to diagnose and predict the operational conditions in boilers, and the results obtained may be used to improve the combustion efficiency.

However, it is still not easy to use CFD techniques for detailed furnace design processes, and this is due to the increasing computational demands (Backreedy *et al.*, 2006). Therefore, the modelling engineers and scientists should know the potential, assumptions, limitations and the steps that are involved in CFD (Eaton, Smoot, Hill & Eatongh, 1999).

The CFD codes, which are structured around the numerical algorithms that can tackle fluid flow problems, consist of three basic stages, namely, pre-processor, solver and post-processor.

Pre-processor: This is mainly the input of the flow problem to a CFD program. The pre-processor stage is dominated by the user activities, such as:

- Defining the computational domain.
- Generating meshes for the domain.
- Selecting the physical and chemical processes to be modelled.

- Defining the fluid properties.
- Specifying the boundary conditions.

Solver: Based on the control-volume technique, the numerical algorithm consists of three basic steps:

- Integrating the governing equations of the fluid flow over the finite control volume of the domain.
- Discretizing the resulting integral equation into sets of algebraic equations.
- Iteratively solving the governing algebraic equations.

The choice of the solver, for example in the FLUENT software, is limited to the pressure-based or the density-based and the segregated or the coupled types of solver (Fluent Inc., 2009). The pressure-based solver was originally developed for low-speed incompressible flows. In this approach, the pressure field is extracted by solving the pressure equation which is obtained by manipulating the continuity and momentum equations (Versteeg & Malalasekera, 2007).

Post-processor: The CFD post-processing packages are capable of displaying the domain grid, vector plots, contours of measured quantities, particle tracking, animations of the dynamic results, etc. With the increasing popularity of engineering workstations, a large amount of developmental work has recently taken place in the post-processing field.

4.1.2 User-defined functions

The CFD models are usually developed based on several variables and assumptions, all in an attempt to investigate if the codes can closely predict the actual situations in the engineering field. The CFD codes are expected to provide reasonable engineering or scientific conclusions.

The user defined function (UDF) is a code, developed by a user, which can be dynamically loaded with the solver of a commercial software package, e.g. FLUENT, in order to further enhance the features of any of the existing codes. Also, the UDF can be used to incorporate user defined features, such as erosion rates, deposition rates and scalar values along the existing particle trajectories equations.

The ash deposition model has been incorporated into the FLUENT 12.1 software using the UDF, as a boundary condition, in order to customize the DPM to include additional body forces, such as particle collection efficiency at impaction.

Also, the numerical slagging indices for both coal and the coal and biomass blends have been implemented as a 'define-on-demand' UDF. Although the slagging models assess the slagging performance of the coals and blends before combustion, they are also considered as user-defined programs which are executable in the FLUENT software using the 'execute-on-demand' command.

4.2 Test Case

The deposition model has been tested on the ACIRL furnace using the Australian bituminous coals. The geometrical modelling, grid generation, fuel properties and the operational conditions are discussed in this section.

4.2.1 Geometry

The Australian Coal Industries Research Laboratories (ACIRL) swirl furnace has been modelled in these calculations in order to validate the proposed ash particle deposition rate model. The vertically fired pilot-scale furnace is being operated at a firing rate of 0.2 MW. The cylindrical furnace, which is 2.5 m long, has a diameter of 0.65 m, and has been found suitable for studying the slagging and fouling tendencies of coals (Su *et al.*, 2001a).

Three slag panels were designed on the furnace to represent water walls in the pulverized fuel boilers. The panels are water cooled to maintain an average temperature of about 773 K, assuming clean surface conditions (Rushdi *et al.*, 2005). Each panel has an area of about 0.038 m^2, and designed to collect the deposits. Determining the thermal conditions in the radiant section of a boiler is essential for the study of slagging propensities. Therefore, sampling of gas phase temperatures in the furnace was undertaken at the ACIRL during coal firing (Su *et al.*, 2001b). The ACIRL burner and furnace designs are schematically shown in Fig. 4.2 and Fig. 4.3, respectively.

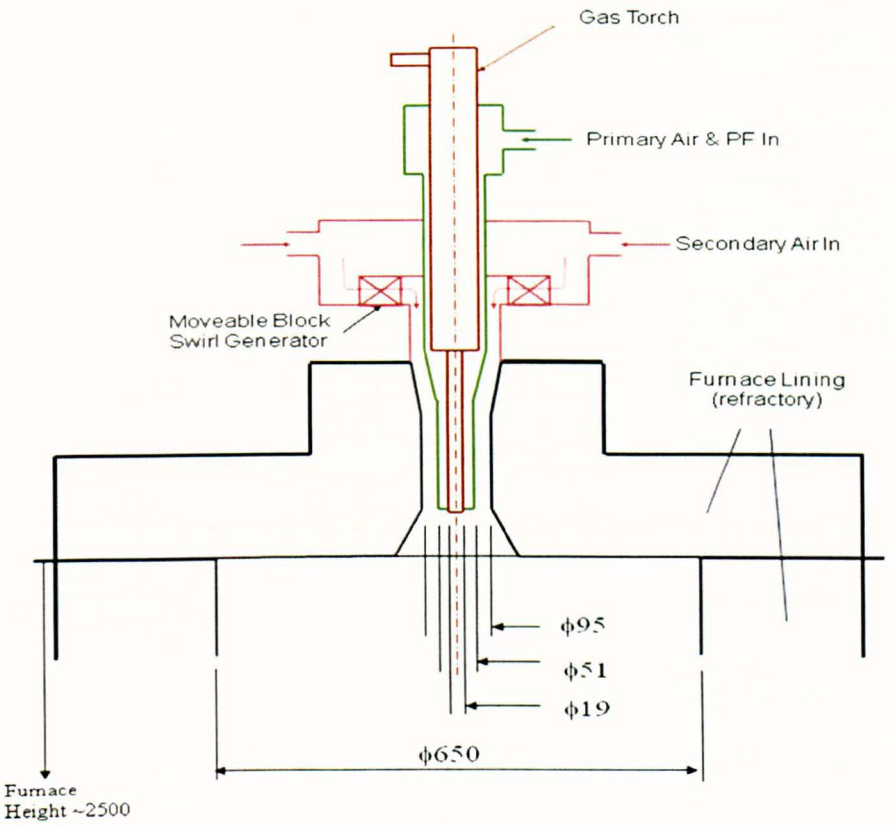

Fig. 4.2 Schematic of the ACIRL Burner with dimensions in millimetres (source: ACIRL, Australia).

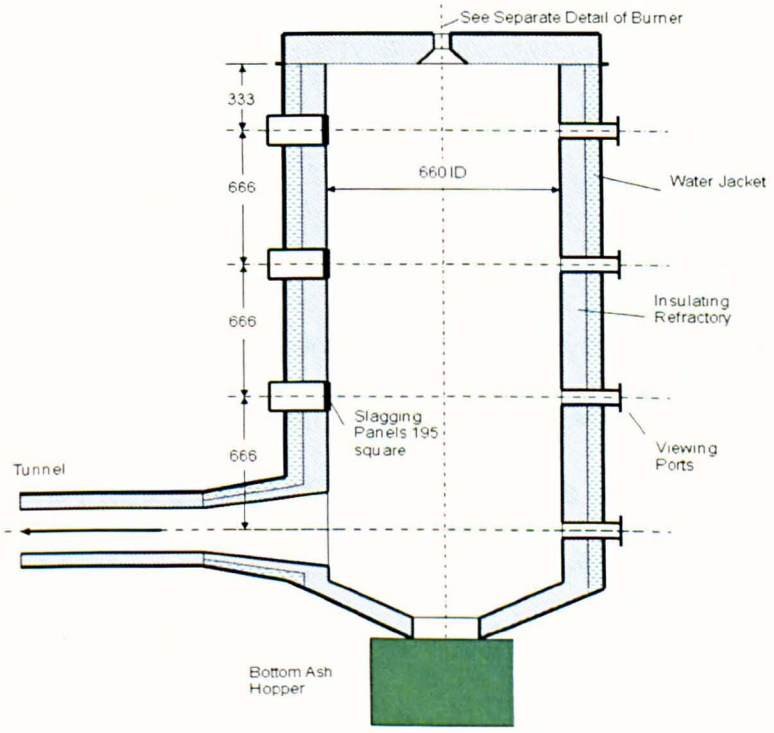

Fig. 4.3 Schematic of the ACIRL Furnace with dimensions in millimetres (Source: ACIRL, Australia).

The burner section, as shown in Fig. 4.2, consists of the gun torch, the primary air and fuel inlet, as well as the secondary swirl air inlet. The swirl burner has a conical shape at its exit, and it is designed to admit the secondary tangential air at an angle of 25° to the horizontal flow.

Fuel and primary air enters the vertically fired furnace from the horizontal primary inlet, while the secondary air enters vertically at a higher temperature (623 K) through the secondary inlet. The diameters of the gun torch, the primary inlet, the secondary inlet and the exit are 0.019, 0.051, 0.095 and 0.65 m, respectively.

The main furnace is shown in Fig. 4.3. The three slag panels, namely, panels 1, 2 and 3, are located at 0.333, 0.999 and 1.665 meters away from the burner exit, respectively. The rest of the walls are refractory lined to minimize the lost of heat.

4.2.2 Grid generation

The first step towards obtaining a CFD solution is the creation of a computational grid (Abolhassani & Stewart, 1994). A 2-dimensional (2D) axisymmetric set up of the ACIRL furnace has been modelled in these calculations. Although the modelling of pulverized coal combustion in an axisymmetric furnace with swirl is complex (Saljnikov, Komatina & Goricanec, 2006), the axisymmetric view of the ACIRL furnace modelled in these calculations is shown in Fig. 4.4.

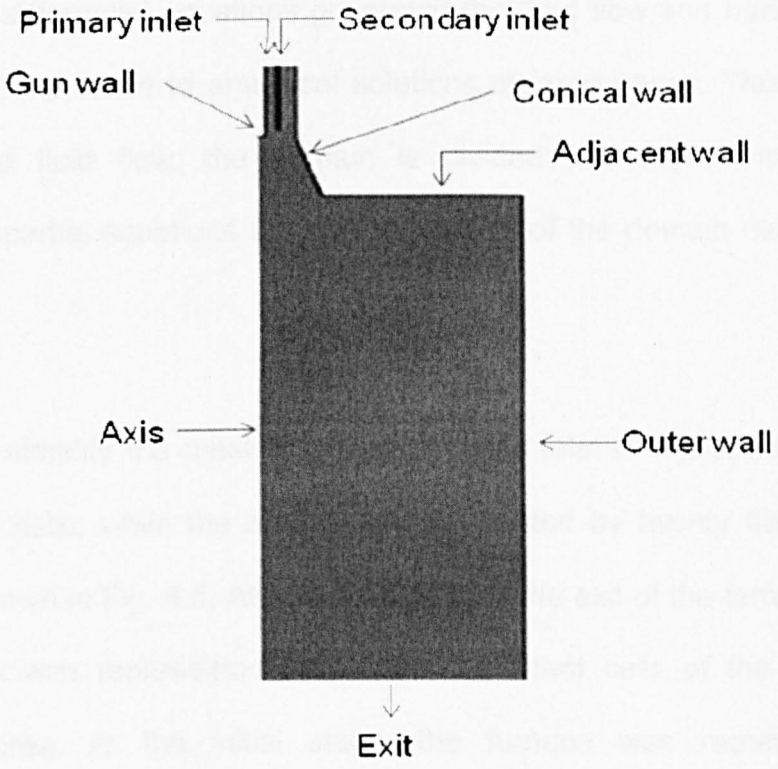

Fig. 4.4 Axisymmetric section of the ACIRL furnace that has been modelled.

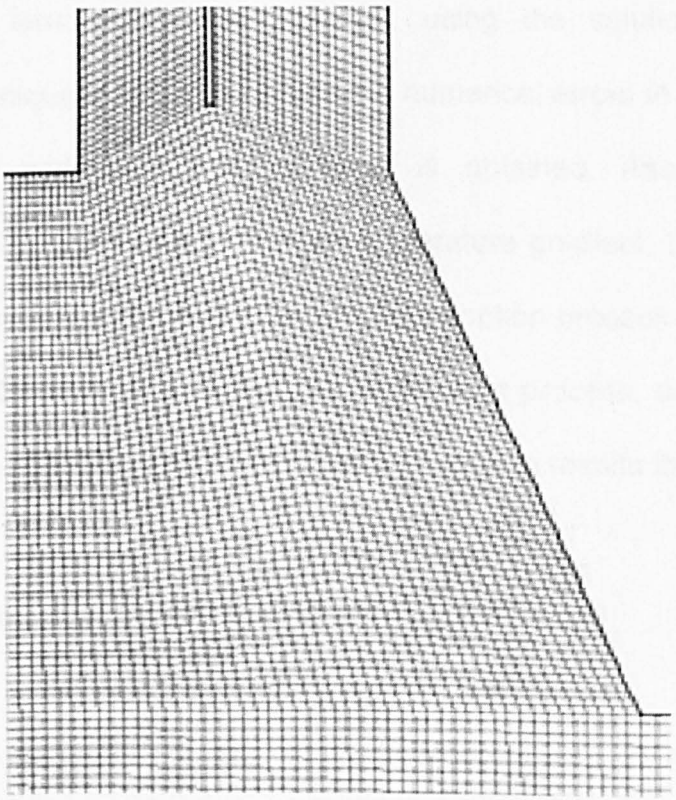

Fig. 4.5 Computational grid employed in the calculations.

The partial differential equations governing the fluid flow and heat transfer are not readily responsive to analytical solutions of large cases. Thus, in order to analyze the fluid flow, the domain is divided into sub-domains and the discretized partial equations are solved in each of the domain cells (Samareh, 1998).

In order to simplify the mesh structure, the fuel inlet is represented by fifteen rectangular cells, while the air inlet is represented by twenty five rectangular cells, as shown in Fig. 4.5. At about 1.6 m from the exit of the furnace onwards, the domain was represented by square-equivalent cells of the same cross-sectional area. At the initial stage, the furnace was represented by a computational grid consisting of about 0.05 million cells.

The grid was later refined continuously, using the solution-adaptive grid refinement technique in order to reduce the numerical errors in the solution and ensure that a grid-independent solution is obtained. Assuming that the maximum error is in the region of high temperature gradient, the evolving flow field information has been used to derive the adoption process (Habibi, Merci & Heynderickx, 2007). At the end of the refinement process, up to 0.25 million cells have been obtained with no significant change in results thereafter.

4.2.3 Fuel properties and operating conditions

The chemical properties of the coals (Rushdi *et al.*, 2005), the physical properties of the coals and the furnace operating conditions (Sheng *et al.*, 2004)

that have been used in these calculations are shown in tables 4.1 and 4.2, respectively. All the coals have heating values within the range of typical bituminous coals (~ 33 MJ/kg). Coal A has the highest volatile matter content (45.90 wt %), and it is next to the coal D in terms of the ash content value. This may result in increased slagging potential.

Although coal A has a relatively high content of SiO_2 in the ash, its high volatile matter content may yield a large amount of low-viscosity materials which may increase its slagging potential. Coal B has the lowest volatile matter content (25.70 wt %), and it also has a lower content of SiO_2 and a higher content of Fe_2O_3 in the ash than coal A (58.40 and 7.20 wt %, respectively).

The Australian coal C has a high content value for Fe_2O_3 and a low content value for SiO_2 in the ash (10.80 and 51.80 wt %, respectively). Its low ash content value (3.20 wt %) may reduce its tendency to accumulate slag in the boiler. Coal D has the highest content of ash and Al_2O_3 in the ash (12.70 and 36.80 wt %, respectively). Its volatile matter content and the content of SiO_2 in the ash are relatively low when compared with the other coals. The low SiO_2 content may increase the slagging potential of the coal.

The range of the coals tested in this investigation is relatively narrow, and therefore, a single value for the density, 1200 kg/m^3, and a single value for the specific heat, 1400 J/kg K, has been used for all the coals. Also, a swelling factor of 2 has been used, assuming that the final particle diameter doubles when all the volatiles have been released.

Table 4.1 Proximate, ultimate and ash analyses of the Australian coals A-D and their respective ashes tested using the ash deposition model (wt %, db) (Rushdi *et al.*, 2005).

ASH					COAL				
Ash	**Coal A**	**Coal B**	**Coal C**	**Coal D**	**Ultimate**	**Coal A**	**Coal B**	**Coal C**	**Coal D**
SiO_2	71.50	58.40	51.80	54.60	C	70.00	77.50	76.30	72.40
Al_2O_3	15.90	35.30	18.90	36.80	H	5.31	4.60	4.96	4.66
Fe_2O_3	1.80	7.20	10.80	2.80	N	0.97	1.83	2.08	1.91
TiO_2	2.20	1.80	1.30	1.60	S	0.39	0.40	0.38	0.61
CaO	4.20	2.60	7.10	0.90	O	13.70	7.87	13.10	7.72
MgO	1.30	0.70	2.50	0.42					
Na_2O	0.58	0.25	0.77	0.27	**Proximate**				
K_2O	0.27	1.30	0.42	1.00	Ash	9.60	7.80	3.20	12.70
Others	2.25	2.32	6.41	1.53	VM	45.90	26.70	38.50	12.70
CV MJ/kg	33.20	34.99	33.57	34.49	FC	44.50	65.50	58.30	56.70

Table 4.2 Physical properties of the tested coals & the operating conditions.

Property	**Value**
Density (kg/m^3)	1200
Specific heat (kJ/kg K)	1400
Vaporization temperature (K)	773
Thermal conductivity (W/m K)	0.33
Emissivity	0.9
Swelling coefficient	2
Coal mass flow rate (kg/s)	0.0075
Primary air mass flow rate (kg/s) @ 363K	0.0122
Secondary air mass flow rate (kg/s) @ 623K	0.0497

4.3 CFD Simulations

The CFD solver type, the solver settings and the solution procedures adopted in these calculations are discussed in this section. Also, in this section, the CFD codes employed for different combustion processes have been discussed and summarized.

4.3.1 Solver settings

The ANSYS FLUENT CFD Software version 12.1 has been employed in the calculations. The pressure-based solver is the only option available for the non-premixed coal combustion simulations in the FLUENT software. The segregated pressure-based solver, which requires low CPU memory and provides flexibility in solution procedures (Fluent Inc., 2009), has been employed in the calculations. The segregated solver algorithm, shown in Fig. 4.6, solves the energy equation after solving the momentum equations.

In the segregated pressure-based solver, the fluid properties, such as density, viscosity, etc. are updated along side the turbulent viscosity at the initial stage. Then, the solver computes the momentum equations sequentially using the updated fluid properties. The pressure correction is then obtained using the recently updated values for the pressure and face mass fluxes.

In the next step, the face mass flux, pressure and velocity fields are determined from the pressure correction. Subsequently, if any additional scalars, such as

the turbulent quantities, energy and radiation intensity exist, they are recalculated using the most recent values of the solution variables.

The source terms arising from different iteration phases, for example, the source term for the carrier phase due to the discrete particles, are updated. The final stage is the checking for the convergence of the equations. If the equations converge, the iterations terminate, otherwise the procedure starts all over again by updating the fluid properties.

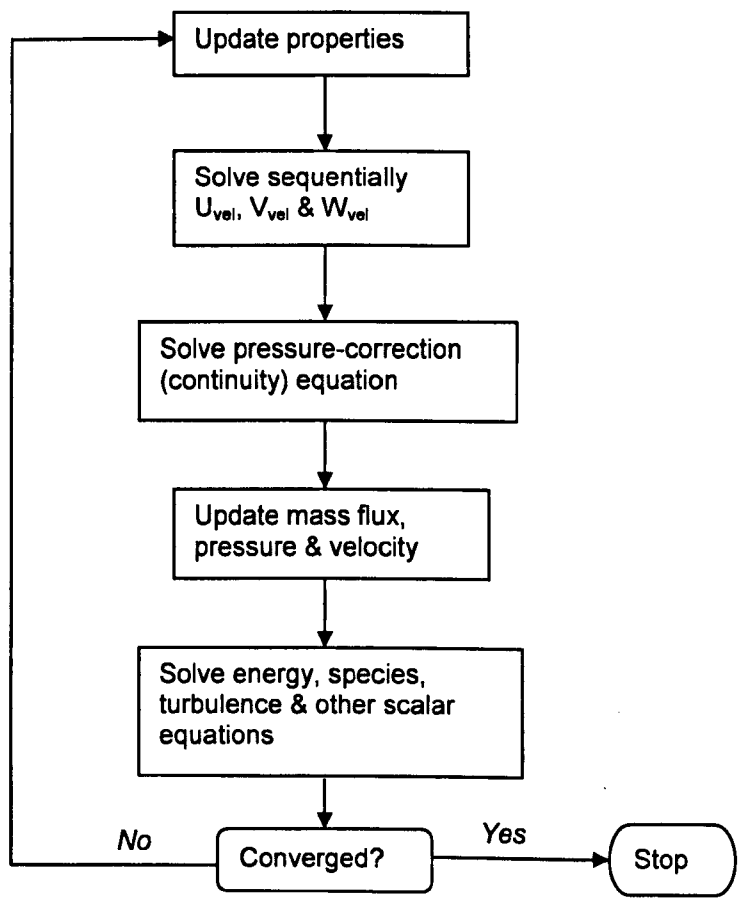

Fig. 4.6 Overview of the pressure-based segregated algorithm (Fluent Inc., 2009).

4.3.2 Models used

The non-premixed combustion model: The non-premixed model has been used for the reaction chemistry under an equilibrium state. The inlet diffusion option was selected for the non-adiabatic PDF table that has been used. The fuel is injected through the primary inlet and the species (mixture) transport phase was coupled with the dispersed phase to exchange mass, momentum and energy during the calculations.

The combustion simulation has been modelled using the PDF mixture fraction approach, where the non-premixed combustion model has been employed for the reaction chemistry. The non-premixed combustion model solves transport equations for one or two conserved scalars and mixture fractions (Barths *et al.*, 2000), and their concentrations have been derived from the predicted fraction distribution.

The properties of the species have been accessed through a chemical database (Fluent Inc., 2009), and the turbulence chemistry has been implemented using a β-shape PDF. While generating the PDF lookup table, it has been assumed that the mixture fraction can diffuse out of the domain through the inlets and the outlet (Fluent Inc., 2009).

Using the empirical fuel stream, the fuel composition has been defined in terms of the ultimate analysis. The heating value and the specific heat of the fuel are maintained as in Tables 4.1 & 4.2. The temperatures at the fuel and oxidizer

inlets are set to be 363 and 623 K, respectively (Rushdi *et al.*, 2005). The air oxidizer consists of 21% oxygen and 79% nitrogen (Fluent Inc., 2009). A maximum of 20 of the most prominent species are by default generated from the β-shape PDF, and these species have been considered after performing the equilibrium calculations. For the calculations of the enthalpy, a minimum temperature of 298.15 K was used (Habibi *et al.*, 2007).

The Weighted-Sum-of-Gray-Gases Model (WSGGM) has been employed in computing the absorption coefficient of the mixture of gases. In this approach, the non-gray gas has been replaced by a number of gray gases for which the heat transfer rates are calculated independently (Habibi *et al.*, 2007). The total heat flux was then determined by adding the heat fluxes of the gray gases as a function of certain weight factors. The WSGGM assumes that the total emissivity over a distance can be determined as a function of the emission and absorption coefficients of the gray gas (Fluent Inc., 2009).

Particles size distribution: The medium-volatiles combusting coal particles, represented by ten different size groups, have been injected into the boiler through the fuel inlet. The velocities of the particles are assumed to be the same as the primary air velocity at the inlet (Rushdi *et al.*, 2005).

The particles are spatially distributed at the inlet and the particle diameter distribution has been calculated according to the Rosin-Rammler distribution size model (Huang *et al.*, 1996), with 70 μm as the minimum particle diameter and 200 μm as maximum particle diameter.

The mean particle diameter was maintained at 134 μm and a spread parameter of 4.52 has been used according to the Rosin-Rammler particle diameter distribution. With 10 injection points, each representing a parcel of 10 particles, a total of 100 particles have been tracked in every discrete phase calculations. The assumed spherical particles are in constant interaction with the continuous phase while they are being tracked using the spherical drag law, see equation (3.24).

The effect of turbulence on the particles was compensated by the use of a dispersion stochastic sub-model; the Discrete Random Walk (DRW) model. The DRW model tracks representative particles from each aerodynamic size group for a defined number of times in order to simulate the ash particles dispersion by the fluid turbulence.

In order to improve the computational accuracy, an arbitrary number (10), for the stochastic tracks, has been used in the calculations. Although such a high number of tracks may increase the CPU demand and possibly introduce instabilities into the calculations, the under relaxation factors have been reduced. For example, DPM under relaxation factor was reduced to 0.25 in order to enhance the solution stability and convergence.

Single rate devolatilization: In modelling deposition rates, an accurate calculation of the temperature field is a key issue and this largely depends on the combustion models. The combustion model follows the approach previously used by some of the present authors (Backreedy *et al.*, 2006; Ma *et al.*, 2009).

The model uses a first-order devolatilization step for the coal followed by a global one-step reaction for the combustion of the volatiles.

The kinetic rate is defined according to the Arrhenius type pre-exponential factor and activation energy. The least amount of surmountable energy for a chemical reaction to occur was set at 7.4×10^7 J/kg mol (Li *et al.*, 2003). The coal vaporization temperature was initially set at 363 K (the same as that of the fuel inlet temperature) in order to enhance ignition. After the flame has stabilized, after a few iterations, the coal vaporization temperature of 773 K was then used.

Kinetics/diffusion-limited model: The char combustion begins when most of the volatiles are released and it is assumed that the reaction rate is dependent on either the chemical reactions or on the bulk diffusion (Backreedy *et al.*, 2005; Backreedy *et al.*, 2006). The particle size was assumed to remain constant, while the particle density decreases.

Both the char particles and the subsequent ash particles are subject to fragmentation processes but only in the experimental circumstances. In these calculations, the effect of the fragmentation process has been assumed to be insignificant (Backreedy *et al.*, 2006), and therefore the process was not included in the proposed ash particle deposition model. For the medium volatiles coals, the activation energy was set to be 7.9×10^7 J/kg mol (Williams *et al.*, 2002; Murphy & Shaddix, 2006).

The RNG κ-ε model: This turbulence model is said to be more suitable than the standard κ-ε model in similar calculations that have been reported, especially, considering the furnace size. This is because the model accounts for the effects of both small scales and swirl motions (Ma *et al.*, 2006; Ma *et al.*, 2009; Fluent Inc., 2009). The RNG is an anisotropic κ-ε model that includes the effects of strained flows, and this greatly improves the predictive accuracy (Eaton *et al.*, 1999).

Radiation model: Heat transfer between the particle and the boiler walls due to radiation is implemented using the Discrete Ordinates (DO) model (Ma *et al.*, 2009). Values higher than the default ones were chosen for the angular discretization in order to refine the computational steps for better results, but with additional computational cost (Fluent Inc., 2009).

To obtain more accurate results, the heat transfer calculations are repeated after every five calculations of the continuous phase. At the end of these calculations, the gas phase temperature and velocity fields have been established. Also the heat fluxes on the three slag panels were recorded.

Particle trajectories: The trajectories of the ash particles have been calculated in the Lagrangian approach. The simplified equation of motion for a particle moving in a viscous environment, equation (3.23) has been employed.

Ash particles deposition: The second part of the calculations, which is part of the original work in this investigation, is mainly to predict the behaviour of the

ash particles in the furnace using the established gas phase temperature and velocity fields. The ash particles deposition process includes the following: the transportation of the particles to the heat exchange surface; the tendency of each particle to stick to the surface upon impaction; and/or the particle's tendency to rebound after impaction.

Inertial impaction is the most prominent pathway for the transportation of the large particles (≥ 10 μm) to the heat exchange surface (Baxter & DeSollar, 1993). Inertial impaction can occur where the distance travelled by a particle before it adjust to the changes in the fluid velocity is greater than the length scale of an object submerged in the fluid, and the rate of inertial impaction mostly depends on the gas aerodynamics, particle size, and geometrical design (Naganuma *et al.*, 2009).

Although it has been assumed, in the region of high temperatures, that the inertial impaction is the major transport mechanism for the particles to the boiler walls, it is a common knowledge that the initial deposit layer is formed due to the condensation of the vapour of alkali metallization compounds, such as sodium, that occur during evaporation (Naganuma *et al.*, 2009).

The fine particles that make up the initial deposit layer are transported to the heat exchange surface by thermophoretic forces, which is part of the virtual forces represented in equation (3.28). The thermophoretic force is applied over a broad range of Knudsen numbers.

The impaction efficiency, which is defined as the ratio of the number of particles that hit the exchange surface to the number of particles that are directed at the surface from the free stream, is the main factor determined by equation (3.30). Each moving particle possesses a particular velocity, mass and composition, and the CFD code calculates the corresponding temperature for the particle according to equation (3.29).

The particle sticking probability when it hits the surface is determined using equations (3.31 & 3.32), by comparing the particle's viscosity to a reference viscosity. The Watt-Fereday model has been employed to determine the viscosity of the particle. In order to assess the sticking probability of the ash particle, a reference viscosity of 10^8 Pa s has been chosen.

The sticking probability of particles having a viscosity less than or equal to the reference viscosity has been assigned the value of unity. While for particles with a viscosity greater than the reference viscosity, the sticking probabilities are determined between the reference viscosity and their actual viscosity, and such particles are assumed to be non-sticky.

The probability for a particle to rebound after impacting on the wall surface depends on whether it possess excess energy or not, and this is determined by equation (3.37). The parametric values used in implementing the particle's excess energy calculations are $\alpha = 45^{\circ}$, $\delta = 0.7$N/m and $\mu_p = 10$ (Pa.s). These values are chosen from the results obtained from empirical investigations (Jung & Schobert, 1992; Forster et al., 2004; Melchior, Putz and Muller, 2009).

Particles with an excess energy after impact are assumed to rebound, otherwise they stick to the walls. The viscosity of each particle is calculated from its chemical composition and impact temperature.

The particles capture efficiencies are estimated based on their sticking and rebound tendencies. All particles with a viscosity less than or equal to the reference viscosity (10^8 Pa.s) and do not possess enough energy to rebound are assumed to stick to the walls. The code records the particle location along the walls of the furnace. Therefore, the particle rate of deposition on the heat exchange surface is directly proportional to their capture efficiencies, as in equation (3.41).

Naturally, the initial deposit layer is formed on a clean wall, while subsequent deposit layer are formed on the initial layer. However, in this investigation, it has been assumed that the subsequent deposit layers are also formed on similar clean walls. This assumption was made because the proposed ash particle deposition rate model did not account for deposit build-up.

Complete steady-state calculations are performed and the results of predictions obtained, using the proposed deposition model, have been compared with the available experimental data. A summary of some of the mathematical models used for various aspects of coal combustion in these calculations are shown in Table 4.3.

4.3.3 Solution procedures

The steady state RANS calculations have been performed using the ACIRL grid as described in section 4.2.2 of this chapter. A 2D-steady axisymmetric swirl case was set up, and the simulations were performed in two phases. The gas aerodynamics is solved using an Eulerian approach, while the ash particle trajectories and tracking were calculated separately in a Lagrangian frame of reference. An overview of the solution procedure is shown in Fig. 4.7.

Table 4.3 Summary of the combustion models employed in the calculations.

Activity	**Model Used**
Turbulence	RNG k-epsilon
Absorption coefficient	WSGGM
Radiation	Discrete ordinates
Combustion	Non-premixed (PDF)
Particle diameter distribution	Rosin-Rammler
Particle dispersion	Stochastic DRW
Devolatilization	Single rate
Char burnout	Kinetics/diffusion - limited.

The governing equations for the flow field, swirl velocity, turbulence, energy, DO and PDF have been solved sequentially. Since the equations solved are primarily nonlinear, suitable under-relaxation factors were selected in order to enhance the solution convergence.

The PRESTO pressure scheme, which accounts for the effect of the steep pressure gradient involved in swirling flows (Fluent Inc., 2009), with first-order discretization, was initially used in the simulations. After obtaining a converged solution, the second-order upwind discretization scheme was applied for more precise solutions. Using the pressure-based solver, the equations were solved iteratively in the natural variables of pressure and velocity using the SIMPLE method which caters for instabilities due to mesh skewness.

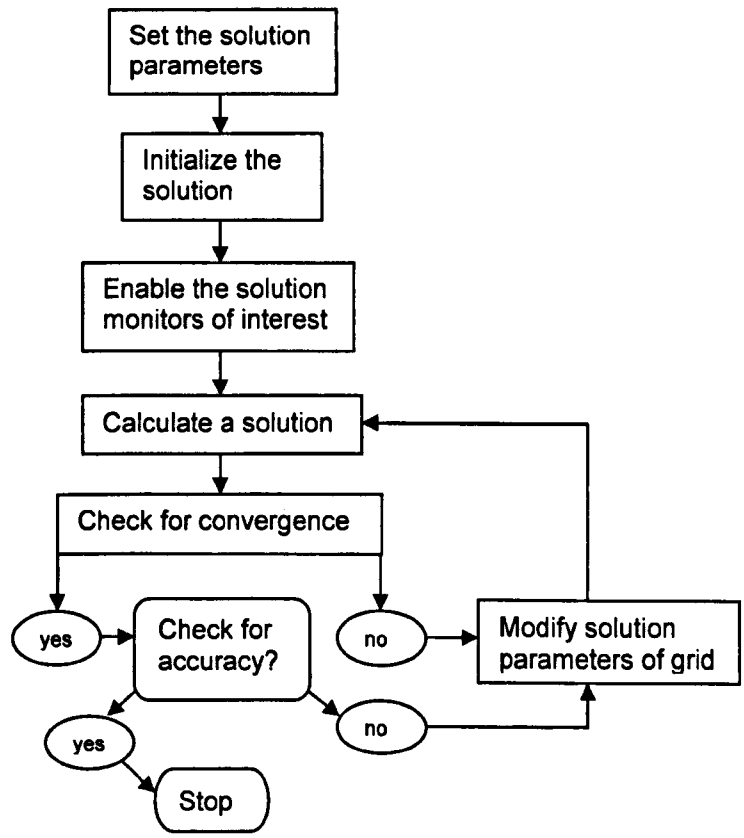

Fig. 4.7 An overview of the solution procedure.

The flexible linear solver has been implemented for all the variables. The choice of the under relaxation factors, which are used in order to stabilize the iterative process, is better made through experience. Therefore, the under relaxation

factors for the pressure, momentum, swirl velocity, turbulence, radiation, discrete phase sources, mixture fraction and mixture fraction variance, were maintained below unity. For example, the default under relaxation value 0.3 was maintained for the pressure, and 0.4, 0.95 & 0.25 have been set for the momentum, radiation and discrete phase sources calculations, respectively.

The solution limits for the magnitudes of the computed quantities were kept within reasonable values for all the quantities that have been evaluated. For example, the maximum absolute pressure was maintained at 5×10^5 Pa, while the maximum temperature was maintained at 5000 K (Fluent Inc., 2009).

After setting all the boundary conditions, especially, for the inlets, walls, outlet, etc., the solution was initialized. The iterative procedure, illustrated in Fig. 4.7, requires the initialization of all the variables before calculating a solution, and a realistic guess of the initial values improves the solution stability and convergence.

The accuracy of the converged solution is evaluated by validating the predicted results for the gas phase temperatures around the slag panels, heat fluxes on the panels and the ash deposition rates on the panels, against the experimental measurements (Williamson, Drake, Hack, Jakob & Swirz-trauber, 1992). The accuracy of the results is within ± 5%. Further accuracy evaluation has been done by varying some input parameters and observing how the predicted results change. The model was found to be most sensitive to swirling velocity and particle viscosity, and the results are discussed in Chapter 5. The model

had low sensitivity to particle swelling number and the gravitational effect, and therefore these results are not presented.

A good initial value guess is required for some of the variables. For example, a high temperature region is required in order to initiate the chemical reactions. Therefore, in these calculations, 1500 K has been used as the initial guess for the temperature field. For the other variables, such as the velocity components, turbulence, mean mixture fraction and mixture fraction variance, the default values in Fluent are maintained.

While performing the calculations, the solution convergence was determined both qualitatively and quantitatively. Monitoring the magnitude of the scaled residuals of all the species has been used in order to assess the solution convergence in qualitative terms.

The scaled residuals for the major flow fields established, such as the velocity components and continuity have decreased by 3 orders of magnitude from the initial value of a single order, while the scaled energy and radiation residuals decreased to 10^{-6} before convergence was achieved. The scaled residuals for the species have decreased to 10^{-5}, and this is necessary in order to have species balance. The converged solution has also been monitored quantitatively by ensuring that the properties conservation was satisfied. Some convergence difficulties have been experienced after switching to the second order discretization. However, when the under relaxation factor were reset to the values given above, the convergence was achieved.

4.4 Summary

The ash deposition model developed in this investigation has been successfully tested on the ACIRL vertical furnace using the Australian bituminous coals.

The coal combustion codes available in the FLUENT 12.1 software have been used in order to generate the required gas phase temperature and velocity fields.

The calculations have been performed in two separate phases. The time-averaged gas aerodynamics has been solved using an Eulerian approach, while the particle trajectories and tracking are determined separately in a Lagrangian approach.

The proposed ash deposition model has been hooked to the FLUENT 12.1 commercial software as a UDF boundary condition which determines the fate of the ash particles that may impact on the furnace walls.

A computational grid representing a single radian slide i.e. axisymmetric case of the ACIRL furnace has been employed for the calculations. The generated grid, the fuel properties and the furnace operating conditions have been used as simulation input for the commercial software.

Suitable solver parameters were set, and solution procedures that are amenable to the axisymmetric calculations have been followed. Converged solutions have been obtained.

The solution convergence was determined in two ways: firstly, by monitoring the magnitudes of the scaled residuals such that the residuals for all the properties except energy and radiation have decreased to 10^{-3}; and secondly, by checking the overall mass and energy balances, such that the net imbalance for each property is less than 0.2%.

Post-processing of the data from the converged solution has been performed and the results of predictions correlate with experimental measurements. The accuracy of the predicted results is between about 5%. Details of results and analyses are discussed in Chapter 5.

CHAPTER 5

RESULTS AND DISCUSSION OF THE DEPOSITION MODEL

The ash deposition model that has been proposed in this study has been implemented according to the procedures explained in the preceding chapter. The results of the predictions using the proposed ash deposition model have been compared with experimental measurements of Australian coals.

A comparison and discussion of the results are presented in this chapter. Also, some conclusions are drawn from the discussions and these are presented at the end of this chapter. Therefore, this chapter is mainly concern with discussion of the results of prediction using the deposition model which was described in the preceding chapter.

The discussion in this chapter has been divided into three sections. In the first section, the results of calculations using the 2D domain are presented and discussed. The second section discusses similar calculations in the 3D domain. Finally, conclusions are drawn from all the analyses in this chapter and these are presented in section three.

5.1 2D Calculations

In order to enhance the discussion, this section is further divided into seven sub-sections. In the first sub-section, the scaled residuals have been discussed. The predicted gas temperature and velocity fields have been compared with the

experimental measurements, and a comparative analysis is presented in the second sub-section.

Sub-section three discusses the particle temperature and residence times. In sub-section four, the predicted heat fluxes on the slag panels have been compared with the reported experimental data, while the predicted and measured ash deposition rates are compared and discussed in sub-section five. The effects of reference viscosity and swirl motion on ash deposition rates are discuss in sub-sections six and seven, respectively.

5.1.1 Scaled residuals

The scaling of the species residuals during calculations using FLUENT is automatically done by the software, as shown in Fig. 5.1 and Fig. 5.2, in order to give a measure of solution convergence. The results of the initial non-reacting solution calculations, shown in Fig. 5.1, indicate that the residuals for the velocity components and the turbulence fields are fast converging under a non-reacting flow after a few iterations. However, the solution was not allowed to converge completely since there is no particular interest in the non-reacting flow solution. Starting the with the non-reacting flow is a popular way of solving a reacting flow and it is known as a 'two step process' (Fluent Inc., 2009).

At the end of about 99 iterations, the DPM phase was set to interact with the continuous phase, with twenty continuous phase iterations per DPM iteration. This activates the discrete phase calculations.

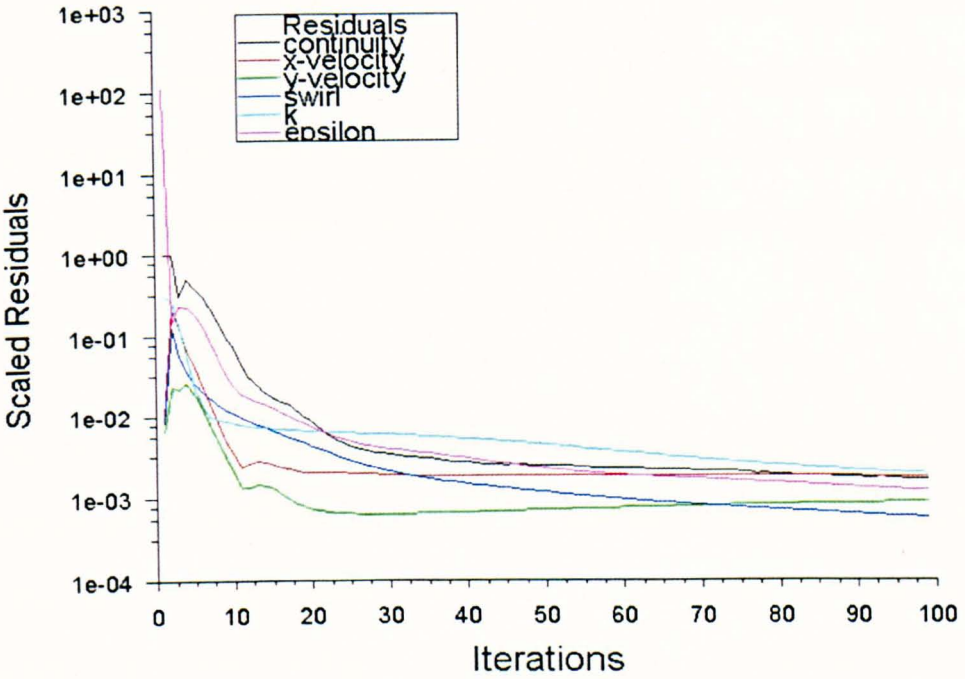

Fig. 5.1 The scaled residuals for the velocity and turbulence with non-reacting flow.

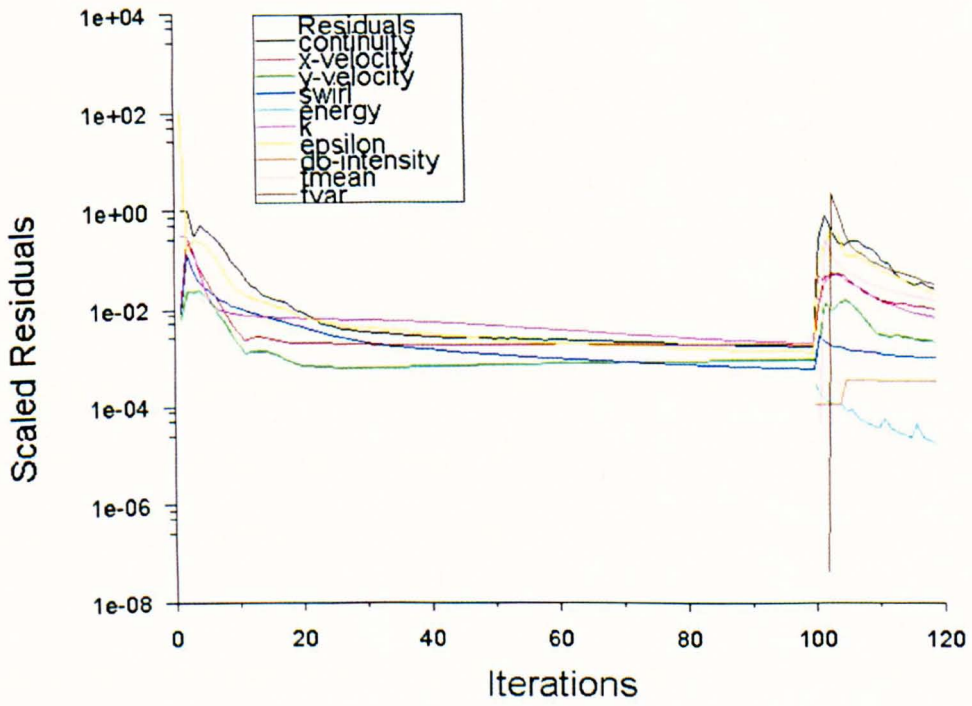

Fig. 5.2 The scaled residuals for all the fields in reaction flow after few initial iterations.

Also, at this point, the energy, radiation and PDF models were activated to make the flow a reacting one. Fig. 5.2 shows the residuals of the reacting flow after twenty iterations. The sudden change in velocity and turbulence fields may be due to the heat released when the pulverized coal was injected in to the boiler.

Injecting coal particles and the oxidant into the boiler, coupled with the initial temperature guess of 1500 K, ignites the combustion flame, and this resulted in large changes in the temperature which in turn introduces instability into the flow solution as shown in Fig. 5.2. To control this phenomenon, the under relaxation factors for the density and the species were reduced.

5.1.2 Gas phase temperature and velocity fields

The results of the calculations obtained revealed a characteristic recirculation zone near the exit of the burner, as shown in Fig. 5.3a. As stated earlier, this strong recirculation, which is caused by the swirling and turbulence effects in the furnace, is essential for the ignition of the fuel, and it also assists in maintaining the continuous and steady combustion of the fuel (Lee & Lockwood, 1999). Fig. 5.3b shows exactly where the recirculation in the ACIRL furnace occurs, i.e. at the entrance of the furnace.

The gas phase temperature and velocity profiles are shown in Fig. 5.4 and Fig. 5.5, respectively. Fig. 5.4 shows that the combustion of the injected particles starts immediately after the particles have mixed with the oxidizing air at the exit

of the burner. Also shown in Fig. 5.4 is the flame displacement in the horizontal direction which may be due to the influence of the strong swirling motion established in the furnace.

In pulverized-coal fired boilers, the adiabatic flame temperature is in the range of 1973 – 2273 K, but the exact value of the temperature remains a function of the furnace type and fuel quality (Lawn, 1987; Sheng *et al.*, 2004). For the medium-volatiles coals, such as the one used in these calculations, the flame temperature may be higher than 1800 K (Rushdi *et al.*, 2005). This is in good agreement with the result of this calculation, which shows a maximum flame temperature of 1920 K while simulating the combustion of Australian bituminous coal C.

A maximum velocity of about 6 m/s was obtained in the secondary air inlet through which the swirling air is introduced into the furnace. Fig. 5.5 depicts the contours of the velocity magnitude while simulating combustion using coal C, and inside the furnace, the interaction between the axial velocity and the swirling motion resulted in a lower velocity magnitude.

The influence of the swirl motion on the overall velocity magnitude is an indication that the strength of the swirl air has effect on the particle residence time. A strong swirl may lead to a strong recirculation zone in the furnace, and this may increase the particle residence time thereby enhancing the complete burning of the particle. In other words, particles have relatively longer residence time with higher recirculation of particle stream (Vuthaluru & Vuthaluru, 2006).

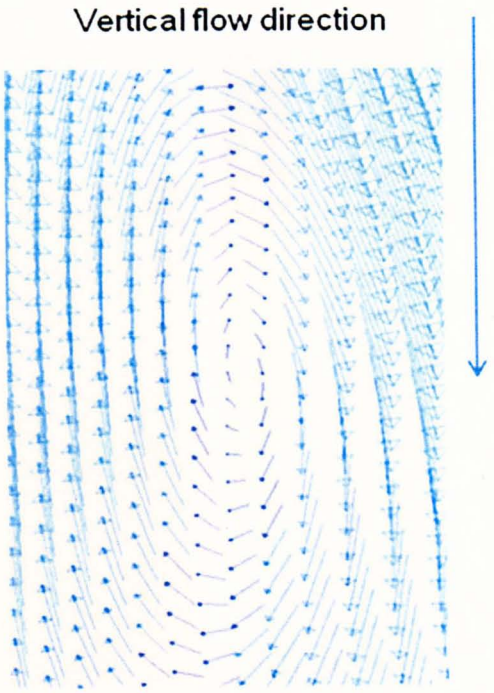

Fig. 5.3a A characteristic recirculation zone in the entry part of the furnace while simulating the combustion of coal C.

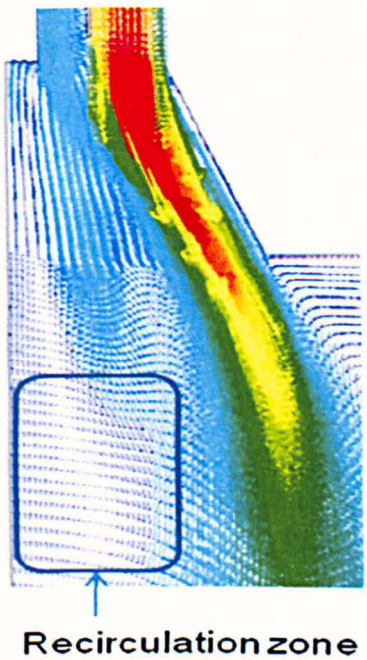

Fig. 5.3b A section of the ACIRL furnace showing the recirculation zone depicted in Fig. 5.3a.

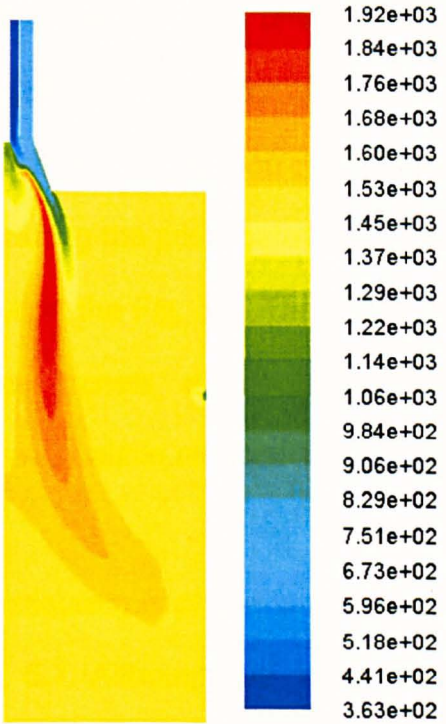

Fig. 5.4 Contours of the static gas phase temperature during the simulations of combustion with coal C (K).

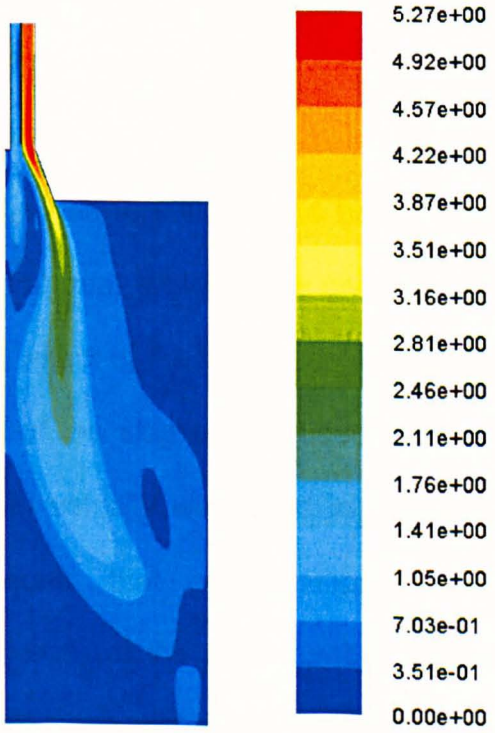

Fig. 5.5 Contours of the velocity magnitude during the simulations of combustion with coal C (m/s).

The Fig. 5.6 shows the predicted gas phase and particle temperatures around the slag panels while simulating the combustion of coal C. Also, the measured gas phase temperatures around the slag panel of the ACIRL furnace, measured for Australian coal C during the pilot-scale test at the firing rate of 0.2 MW (Su *et al.*, 2001a), are shown in the Fig. 5.6. The predicted flame temperatures in the regions of the slag panels are in agreement with the experimental measurements for coal C (within an accuracy of $\pm$ 5%) as shown in Fig. 5.6.

The predicted and measure gas phase temperatures for all the tested coals (A-D) are shown in Fig. 5.7. Although the numerical results are under predicted, the temperature difference for all the slag panels show similar trends. For example, the temperature difference between slag panels 1 and 2 for coal D, both measured and predicted, is about 80 K. Also, the temperature drop between slag panels 2 and 3 for both measured and predicted results on coal C is about 50 K.

The under-prediction of the gas temperature is better explained by the lower value of the swirl velocity (10 m/s), which is the given experimental value, used in the calculations and the effect of the water-cooled wall temperatures, in view of the corresponding size of the slag panels used for the axisymmetric case. Although the reported swirl velocity was used in the calculations in order to obtained deposition results that will compare to the experimental measurements, different values of the swirl number have also been tested in order to investigate the influence of the swirl motion on the deposition rates. The results are reported later in this chapter.

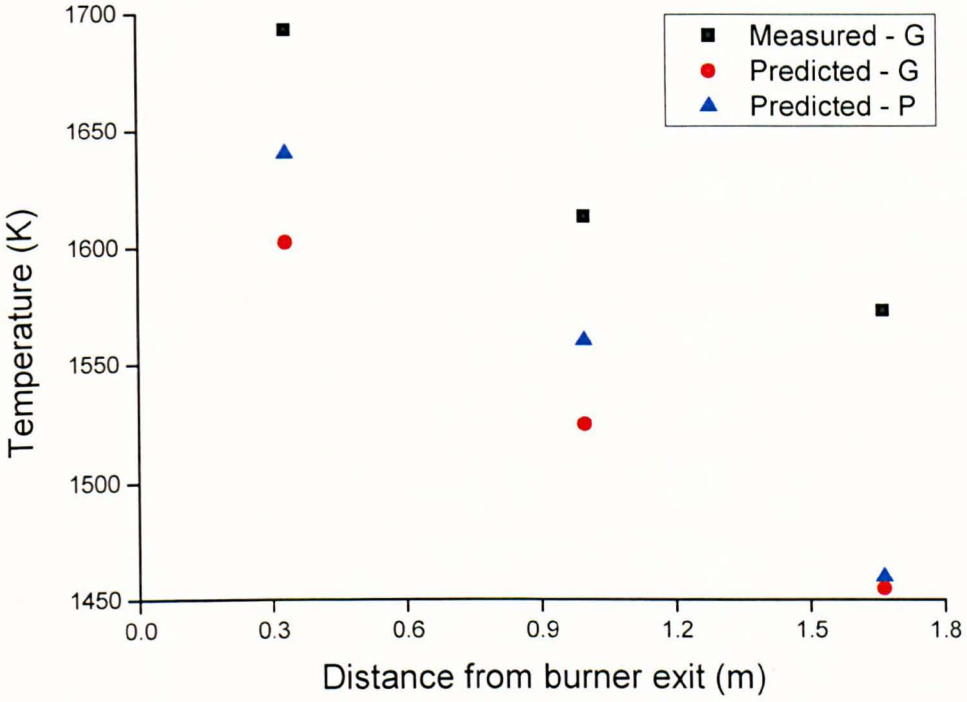

Fig. 5.6 Measured gas temperatures and predicted gas & particles temperatures - coal C.

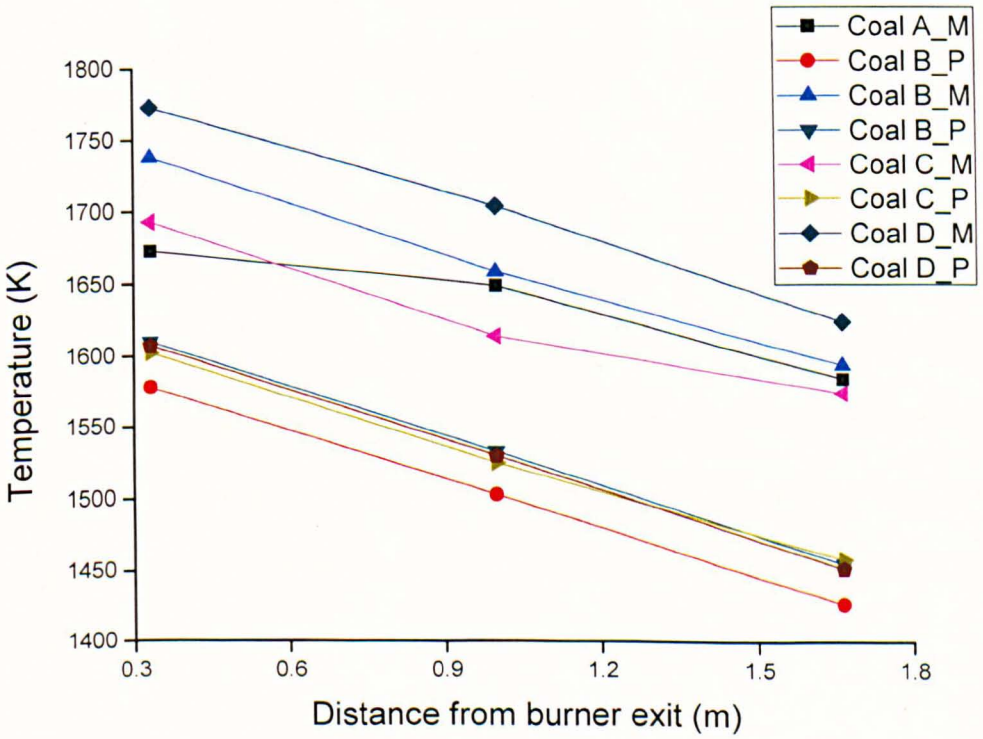

Fig. 5.7 Measured and predicted gas temperatures for coals A-D.

5.1.3 Particle temperatures and residence times

The particle static temperature and residence time for coal A are shown in Fig. 5.8a and Fig. 5.9a, respectively. Simulating the combustion of coal A has produced a peak flame temperature of 1910 K, and the burning particles have maximum residence time of 2.66 s. Particle traces for two injection streams (5^{th} and 10^{th}) are presented 5.8a, and the contours show that, in both cases, high temperature particles are traced near the exit of the burner. As the burning char particle is consumed, its temperature decreases gradually as shown towards the exit of the furnace.

As shown earlier in Fig. 5.4, the maximum flame temperature for coal C is about 1920 K, and the burning particles, with a maximum residence time of about 3 s, form part of the high temperature flame. Also, two injection streams each for particle temperature and residence time of coal C are traced as shown in Fig. 5.8b and Fig. 5.9b, respectively.

The particle temperature in the furnace is higher than the temperature of its surrounding gas. This is because the gas temperature is built up from the heat released by the burning particle. The predicted gas and particle temperatures for coal C are compared in Fig. 5.6, and the results show that there is a temperature difference between the burning char particle and its surrounding gas in the furnace.

The predicted results show that the particle temperature, especially in the burner region, is higher than the gas temperature. The particle is about 50 °C hotter than the gas phase, and this difference reduces to about 5 °C at a distance of about 1.6 m from the burner exit. The decrease in the temperature of the particle with time is due to the fact that it continuously releases its heat energy to the gas phase.

This prediction is in good agreement with the assumption that the gas phase takes its heat energy from the burning particles, and that the temperatures of the burning particle can significantly exceed the temperature surrounding the particle (by up to 300 °C, depending on the coal type) at the initial stage (Basu *et al.*, 1946).

The particle residence time is considered as a measure of the particle inertia and it denotes the time scale with which any slip velocity between the particle and the fluid is equilibrated (Srinivasachar, Helble & Boni, 1990). Particle with longer residence times have more tendency to penetrate the boundary layer due to the influence of recirculation forces. Also, if particles have longer residence time, the concentration of the VM in the environment increases, which may result in improved flame stability (Xiaohong *et al.*, 2011).

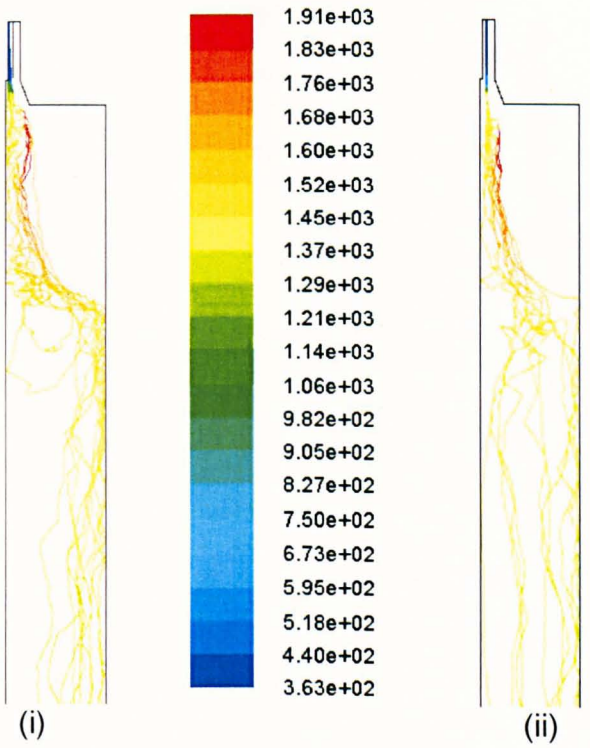

Fig. 5.8a Particle traces from the fifth (i) and tenth (ii) streams coloured by the static temperature (K) – coal A.

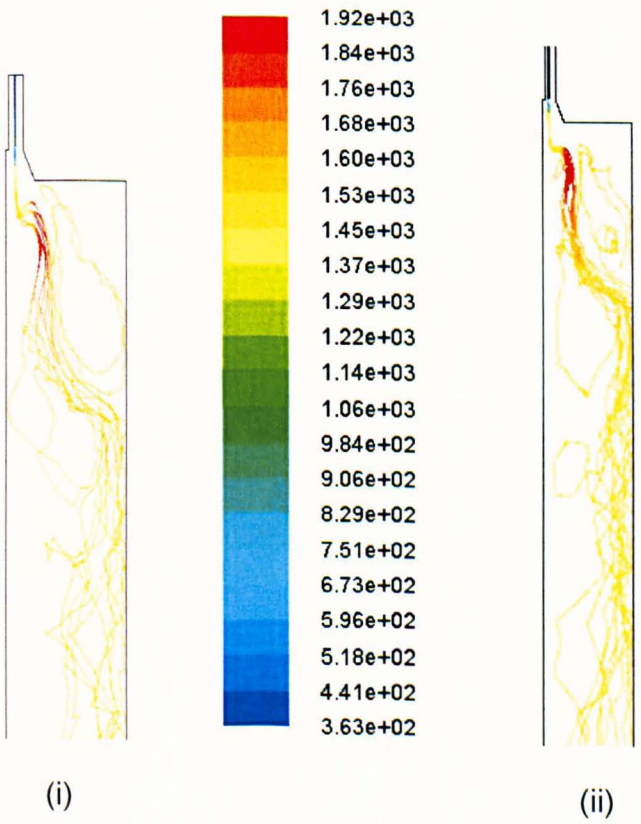

Fig. 5.8b Particle traces from the fifth (i) and tenth (ii) streams coloured by the static temperature (K) – coal C.

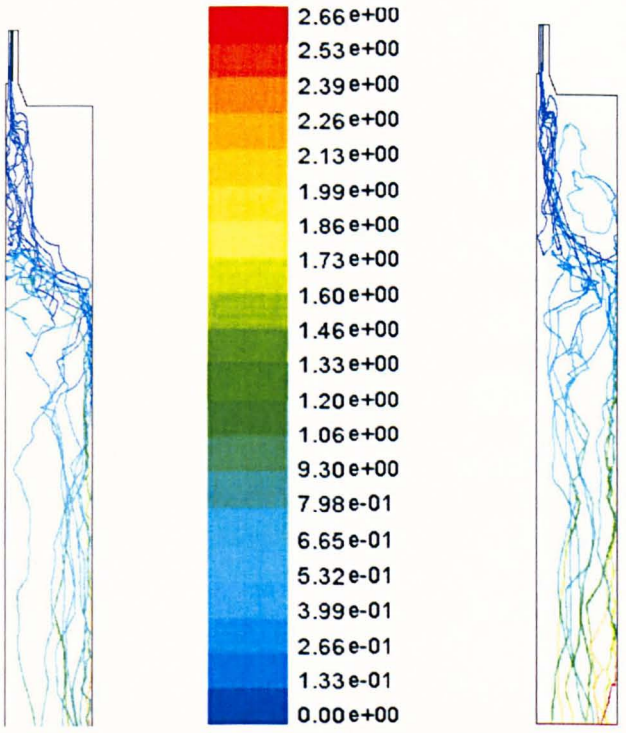

Fig. 5.9a Particles residence times (s) for the fifth (i) and tenth (ii) injection streams for coal A.

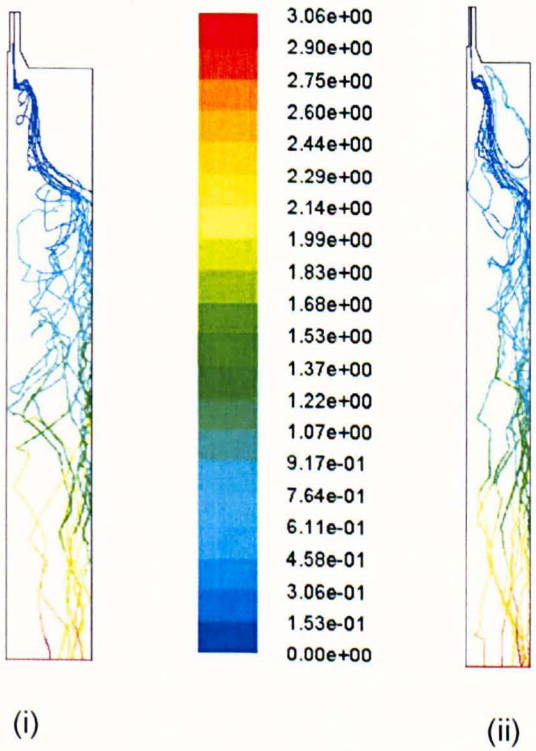

Fig. 5.9b Particles residence times (s) for the fifth (i) and tenth (ii) injection streams for coal C.

5.1.4 Heat fluxes

One of the significant influences on the slagging behaviour is the incident heat flux on the furnace walls, which can be used to determine the temperature of the deposit. The ratio of the net radiant heat flux to the incident heat flux could be used to characterize the amount of slagging deposits on the walls (Su *et al.*, 2001a). In conventional boilers, the incident heat flux from the flame is in the range of 400-700kW/m^2 (Chattopodhyay, 1995; Littler *et al.*, 1991 in Su *et al.*, 2001a).

Fig. 5.10 to Fig. 5.13 are comparing the incident radiant heat fluxes on the three slag panels for the four different coals. All the figures show a higher predicted value of the incident heat fluxes near the burner mouth. This is reasonable when compared with the experimental results as shown in the Fig. 5.10 to Fig. 5.13.

However, the general under prediction that have been reported may not be unconnected with the general characteristics of axisymmetric flows which assume that there are no circumferential gradients in the flow, but in reality there may be non-zero circumferential velocities during the calculations (Fluent Inc., 2009).

In Fig. 5.10, the measured and predicted heat fluxes on the three slag panels of the ACIRL furnace while burning coal A have been compared. On slag panel 2 for example, the difference between the measured and the predicted results is less than 20 kW/m^2. However, on the first and third slag panels, the difference

between the measured and predicted results is higher, and this may be due to the decrease in temperatures coupled with the cooling effect of the water walls.

The differences between the measured and the predicted results on the slag panel 1 may be due to the reported inaccuracy of the measurement data on the slag panel 1 (Su *et al.*, 2001a). For the slag panel 3, the discrepancy between the measured and the predicted results may be attributable to the low temperatures in that region of the furnace. The predicted furnace temperature around the slag panel 3 has been affected by the temperature on the water-cooled panel.

In similar results, the predicted heat fluxes for coals C and D have compared well with the measurement data, as shown in Fig. 5.12 and Fig. 5.13. However, Fig. 5.11 shows a fairly large discrepancy between the predicted and the measured results for coal B. Although this could not be explained numerically, but some levels of inconsistency in the experimental results of coal B have been reported (Su *et al.*, 2001a).

The heat flux from the flame to the slag panels can determine the deposit temperatures (Su *et al.*, 2001a), which can, in turn, determine the rate of slag accumulation on the panels. In some cases where the deposition rates are not measured directly from the experiment, the measured heat fluxes are used to characterize the coal ash behaviour under the boiler conditions (Su *et al.*, 2001a).

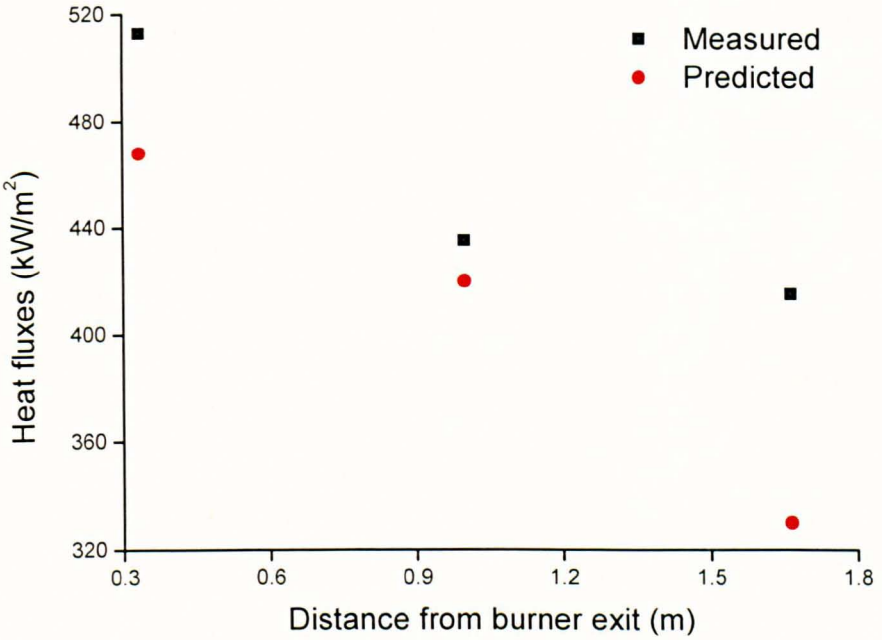

Fig. 5.10 Measured and predicted incident radiant heat fluxes on the slag panels with coal A.

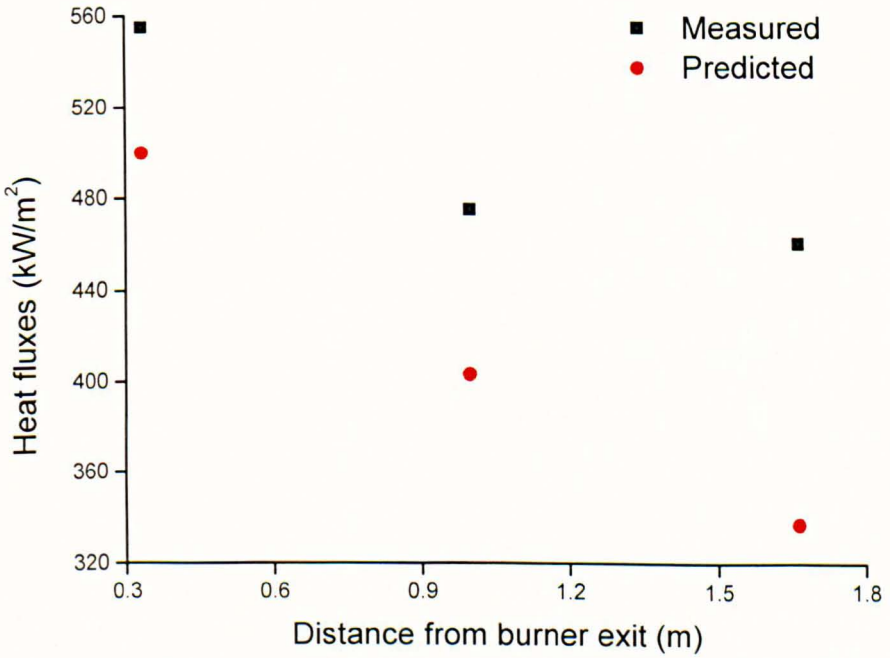

Fig. 5.11 Measured and predicted incident radiant heat fluxes on the slag panels with coal B.

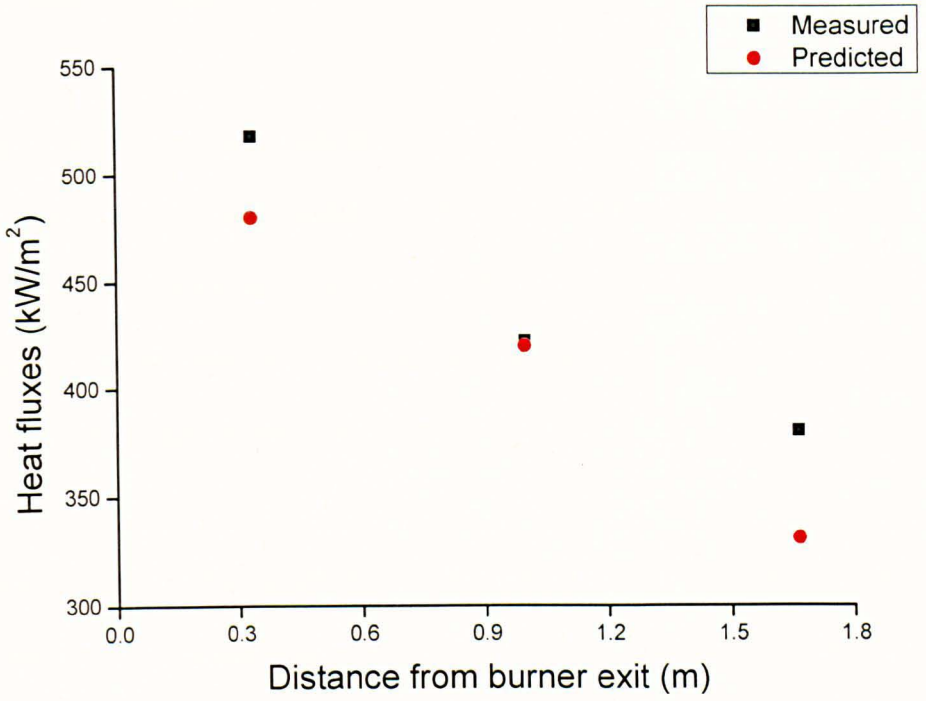

Fig. 5.12 Measured and predicted incident radiant heat fluxes on the slag panels with coal C.

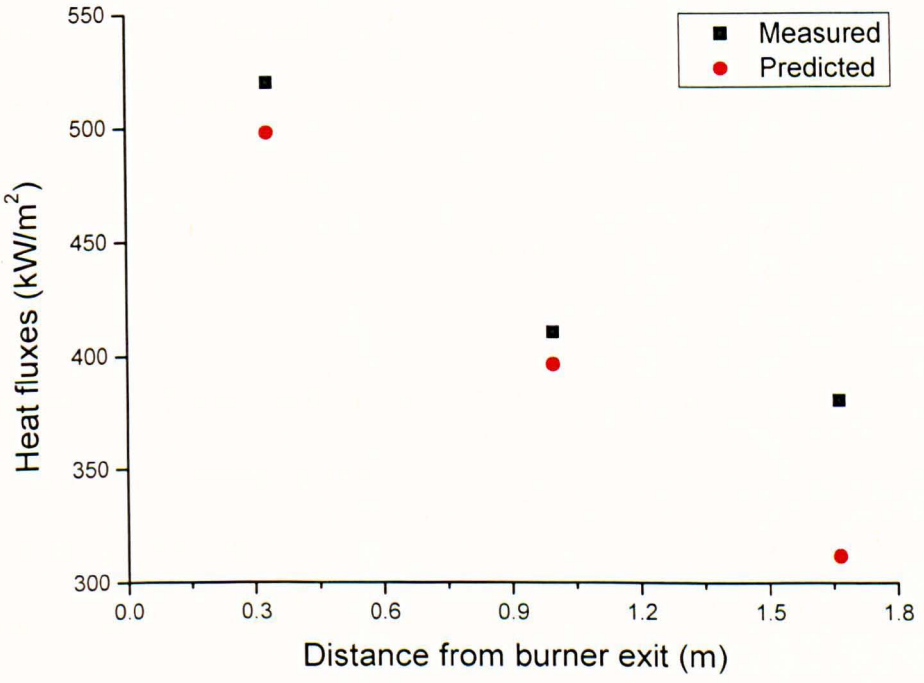

Fig. 5.13 Measured and predicted incident radiant heat fluxes on the slag panels with coal D.

5.1.5 Deposition rates

The main causes of ash deposition include the quality of the coals, boiler designs, and operational conditions, among others (Lee & Lockwood, 1999). Whatever the system and conditions of the coal combustion, there will always be problems with the ash, because the fate of the inorganic materials associated with coals is not fully understood.

The main concern of this investigation has been in ash deposition problems that are related to the boiler aerodynamics and fuel properties. The large pyrite particles that may hit the furnace walls before they are completed burnt are a major cause of deposition. This factor is significant in high temperature regions of furnaces where most particles are still burning.

The large particles that are not completely burnt may possess enough inertial force to transverse the boundary layer and impact the heat exchanger, and the high temperatures in the boiler region may soften the particles thereby increasing their tendency to stick to the walls.

The presence of iron, calcium, sodium and potassium in significant amounts may lower the melting temperatures of the coals, thus resulting in higher deposition tendencies. In the tested coals, the content of iron, calcium and sodium oxides are highest in coal C, while the content of potassium oxide is highest in coals B and D. These factors, according to the existing coal slagging indices, are expected to affect the slagging tendencies of the coals.

However, the content of ash in the coals poses more concern in terms of slag accumulation in boilers. This is because the weight of the incoming ash is one of the major determinants of the rates of the deposit accumulation in the furnace. The coals that have an insignificant amount of ash accumulate less deposit, even when their contents of iron, calcium, sodium and potassium oxides in the ash are significant. This has been shown in the performance of coal C.

The deposits on panels 2 & 3 on the ACIRL furnace were experimentally measured and presented in the works of Su *et al.* (2001b). However, they acknowledged that it is practically impossible to attempt to collect the ash deposits on slag panel 1 due to the high temperatures in that region which results in the deposit shedding. Therefore, the measured heat fluxes through panel 1 for all the coals are used in assessing the slagging propensities although the heat flux approach is not a reliable method for assessing the slagging propensities for all the coals (Rushdi *et al.*, 2005; Su *et al.*, 2001b). This may be the reason for the wide discrepancies between the measured and predicted results on slag panel 1 for all the coals investigated.

The predicted and measured deposition rates for coal A have been compared in Fig. 5.14. At distances of 0.999 and 1.665 meters away from the burner exit, where the slag panels 2 and 3 are located, respectively. The measured and predicted results have compared fairly well. For example, on slag panels 2 and 3, the predicted deposition rate results correlate with the experimental data better than on slag panel 1.

Similarly, the predicted and measured deposition rates for coals B, C and D are shown in Fig. 5.15, Fig. 5.16 and Fig. 5.17, respectively. For coal B, although the gas temperatures around slag panel 2 are over predicted, the deposition rates on the slag panel have been over predicted. These results appear inaccurate, but when compared with the performance of other coals, the predicted results are not unexpected. Therefore, this over prediction may be related to the reported measurement results.

Away from the exit of the burner, where the direct effect of the recirculation zone is minimal, the particle and gas temperatures are relatively close, and the predicted deposition rates correlate well with the measurement data as shown on slag panel 3 for coals B and D (Fig. 5.15 & Fig. 5.17).

In general, on slag panels 2 & 3, where the temperatures are relatively low, the measured and predicted deposition rates are in better agreement for all the tested coals, as shown in Fig. 5.18. For example, the measured results on panels 2 & 3 for coal B, which are 0.87e-5 and 0.65e-5 kg/m^2 s, respectively, are close to the predicted values of 1.50e-5 and 0.50e-5 kg/m^2.s, respectively. The wide change in the deposition rate from slag panel 2 to 1 in the measurement results for coal D (~4.0e-4) was not accounted for, but it has been assumed to do with experimental procedures.

In effect, the predicted ash deposition rates are consistent with the measured rates as discussed above. However, the predicted rates are slightly lower than the measured rates under similar operating conditions.

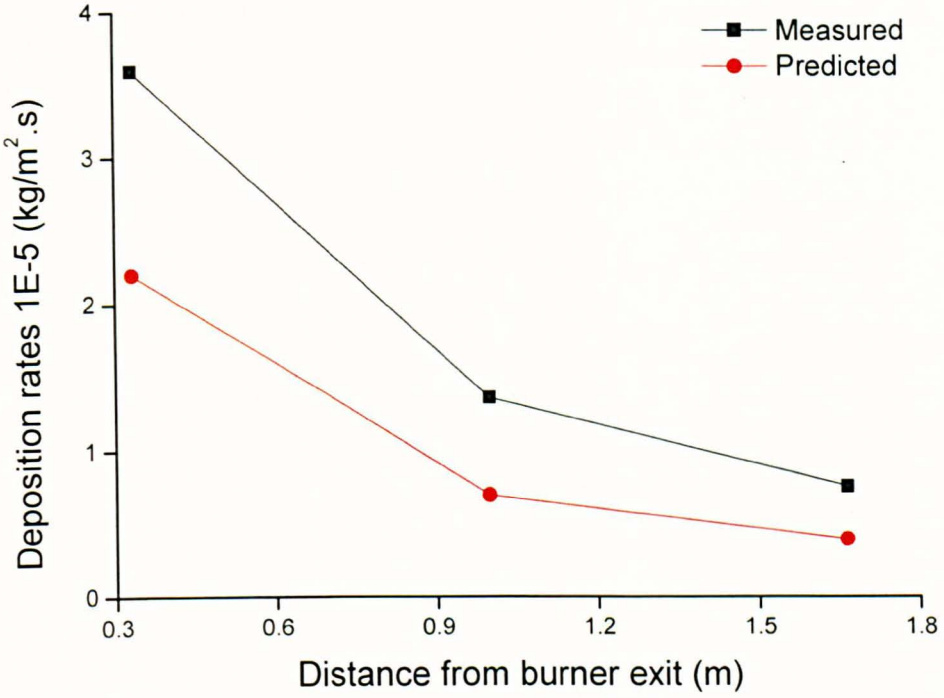

Fig. 5.14 Measured and predicted ash deposition rates for coals A.

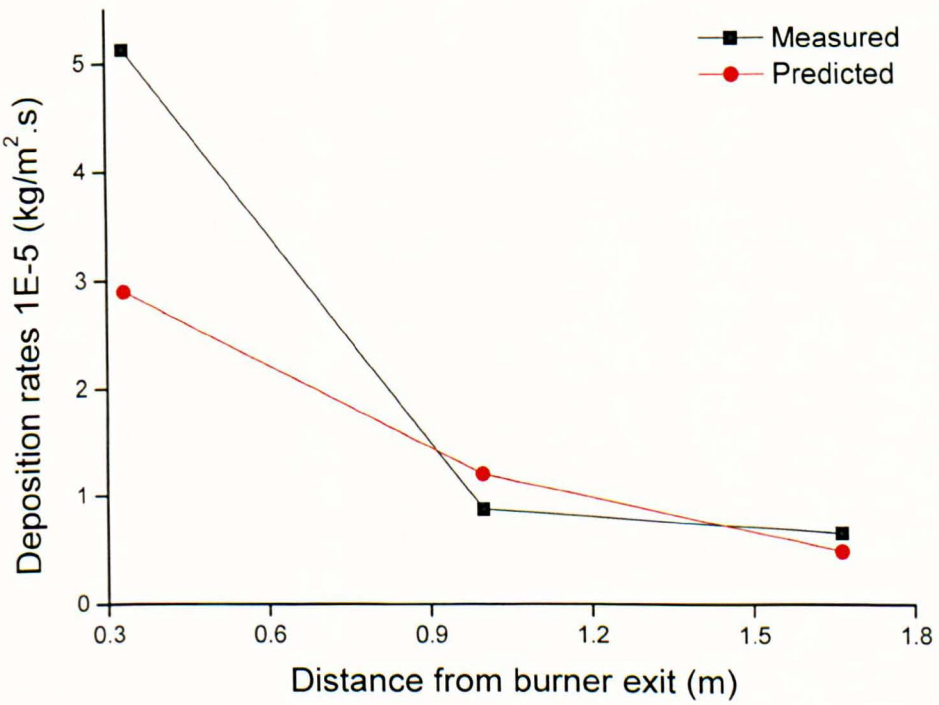

Fig. 5.15 Measured and predicted ash deposition rates for coals B.

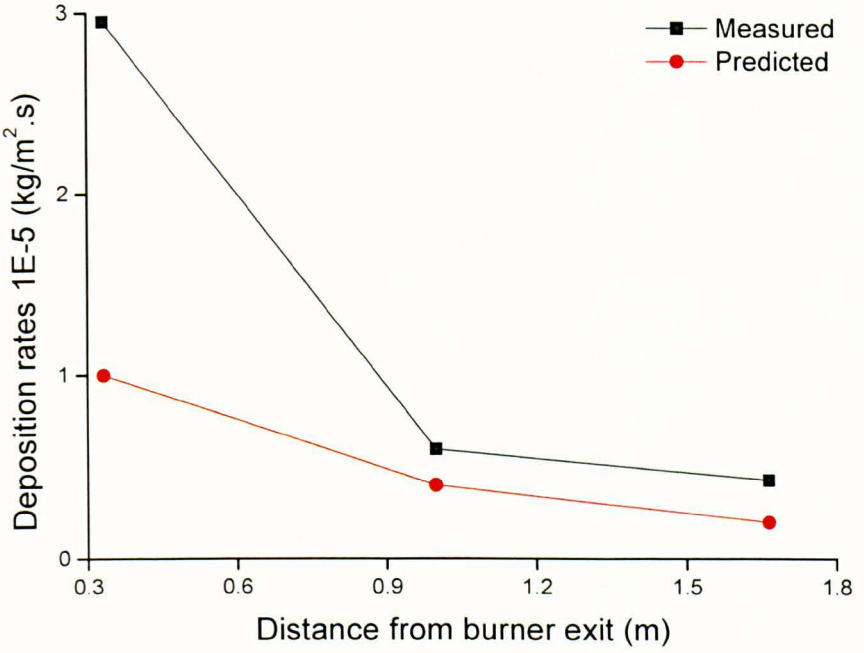

Fig. 5.16 Measured and predicted ash deposition rates for coals C.

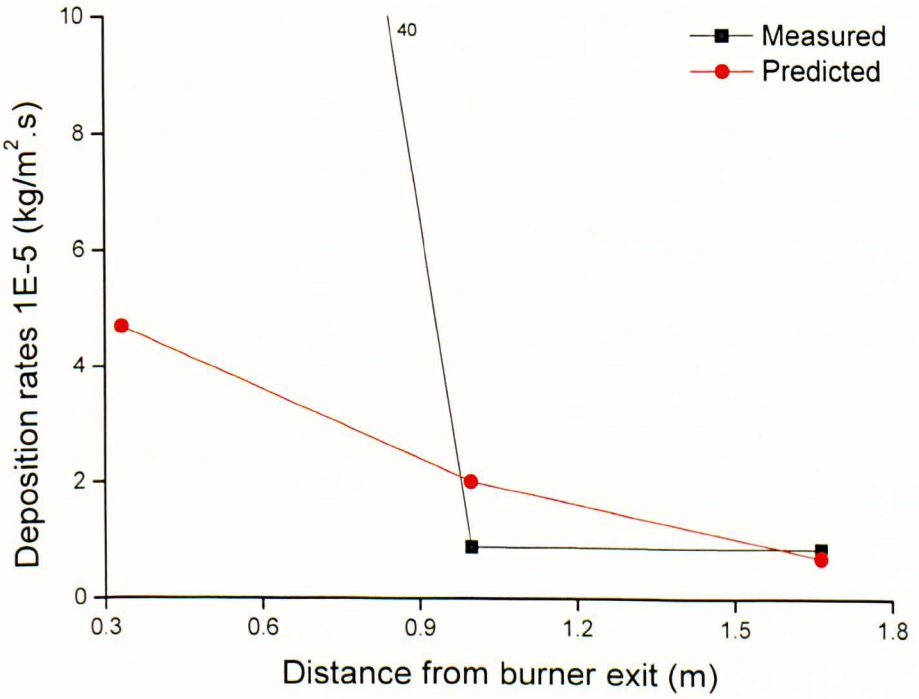

Fig. 5.17 Measured and predicted ash deposition rates for coals D.

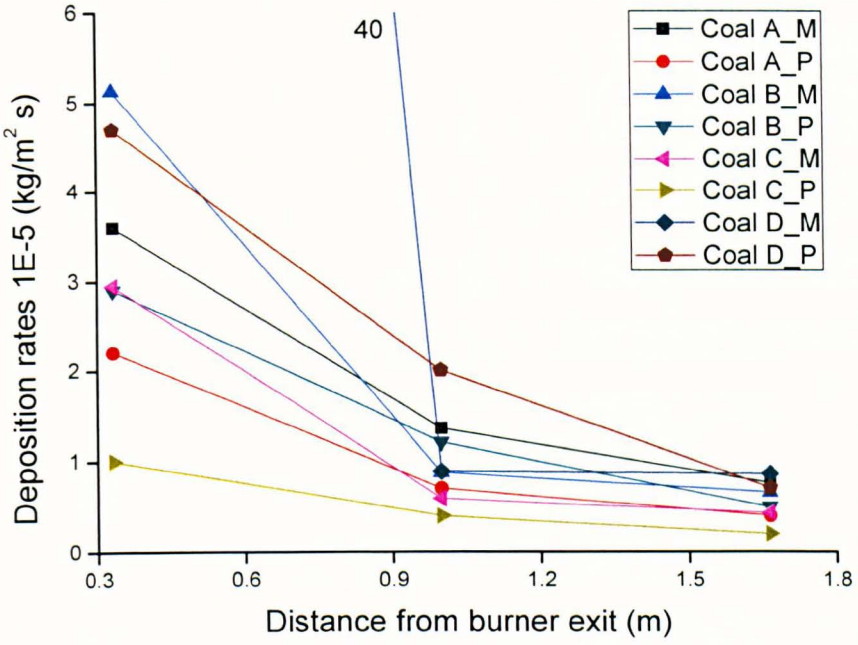

Fig. 5.18 Measured and predicted ash deposition rates for coals A – D.

5.1.6 Effects of reference viscosity on deposition rates

As reported in the literature, the value of the reference viscosity varies in many research studies. For example, it has been reported that the reference viscosity of ash particles range from 10^5 to 10^8 Pa s (Srinivasachar *et al.*, 1990). It is expected that by decreasing the value of the reference viscosity, the total deposition rate will also decrease (Rushdi *et al.*, 2005). Fig. 5.19 shows the deposition rates of coal A for different values of the reference viscosity. The prediction using the highest reference viscosity (10^8 Pa.s) produced results much closer to the experimental measurement.

The predicted results show that the deposition rates on the three slag panels decrease as the value for the reference viscosity gradually decreases from 10^8

to 10^4 Pa.s. When the particle temperature decreases, the viscosity of the particle increases, and in turn, the sticking tendency of the particle decreases.

In Fig. 5.19, the predicted results show no deposition rates on all the slag panels when the reference viscosity was reduced to 10^4 Pa s. Analysing this result, based on the viscosity model employed in these calculations, it indicates that either all the ash particles have a viscosity greater than 10^4 Pa s, or the viscosity model used in this investigation do not account for very low viscosity values. This phenomenon has been explained in the literature as follows:

i) Sodium-silica glass particles show that deposits are formed when particle viscosities are between 10^5 and 10^7 Pa s (Hunold & Bruckner cited in Senior & Srinivasachar, 1995).

ii) The critical viscosities for boiler conditions of interest are between 10^5 to 10^8 Pa s (Srinivasachar *et al.*, 1990).

iii) The difference in coal sticking coefficients is attributed to the differences in ash particle composition-based viscosities (Senior & Srinivasachar, 1995).

An increase in the reference viscosity from 10^4 to 10^5 Pa s has yielded some deposits on slag panel 1. However, further away from the burner exit, i.e. on slag panels 2 & 3, the temperatures have decreased and particles have gained more viscosity (> 10^5 Pa s), thus resulting in a zero deposition rate. In the range of viscosities (10^6 – 10^8 Pa s), varying levels of deposits are formed on all the three slag panels as shown in the Fig 5.19.

Also, a reference viscosity value of 10^9 Pa s has been tested, but the predicted results are the same with the results obtained using the reference viscosity of 10^8 Pa s.

5.1.7 Effects of swirling motion on deposition rates

The conical shape at the burner mouth is designed to admit swirling motion into the furnace, and the slagging process in the burner region is affected by the swirling motion. Fig. 5.20 illustrates the effect of the swirling motion on the predictions of the deposition model. From the Fig. 5.20, it can be observed that increasing the swirl number improves the CFD predictions.

When the swirl number was reduced from 0.67 to 0.27, the ash particle deposition model predicts a very low deposition rate on all the three slag panels when compared to the experimental measurements. Moreover, the predicted deposition rates on the slag panel 2 become higher than what was predicted on slag panel 1.

A gradual increase in the air swirling number increases the deposition rates on all the slag panels, where the maximum deposition rates are recorded on the uppermost slag panel. An increase in the swirl number strengthens the flow entrainment ability to transport more particles to the heat exchange surfaces walls (You & Zhou, 2006).

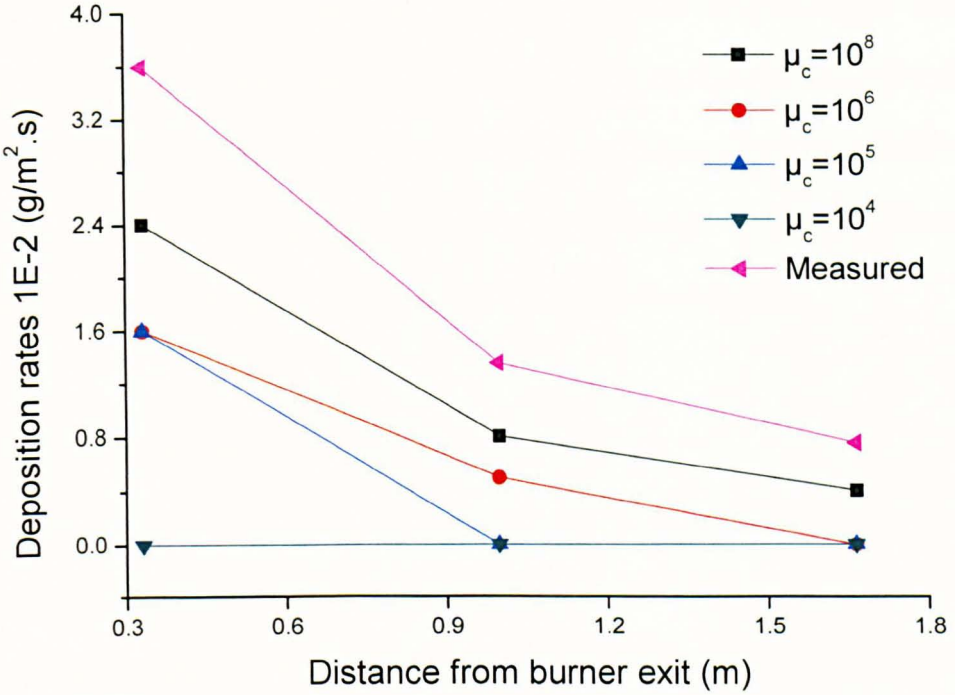

Fig. 5.19 Comparing the measured deposition rates on the slag panels and the predicted results using different values for reference viscosity - coal A.

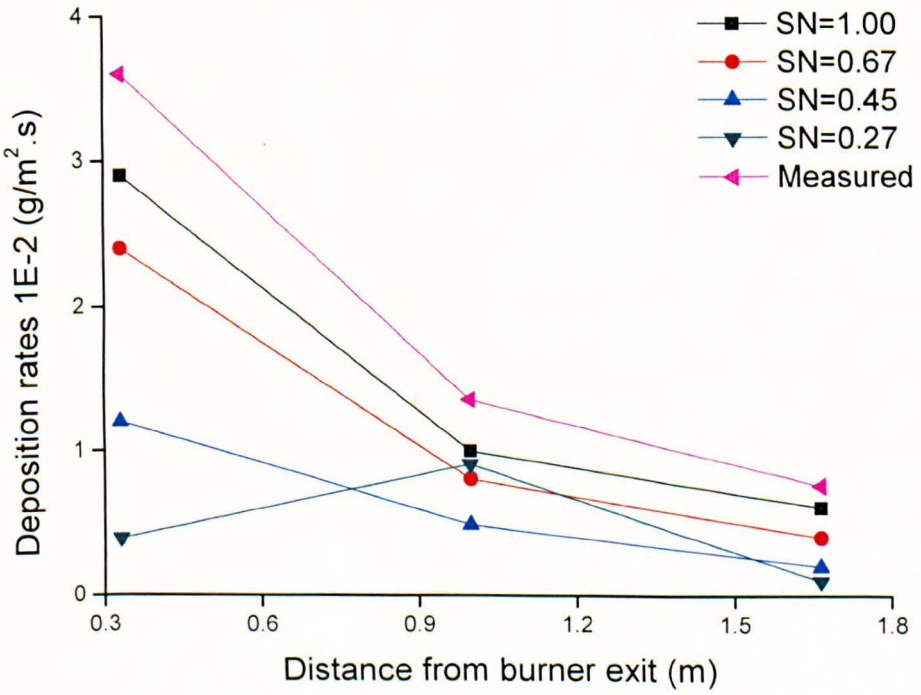

Fig. 5.20 Comparing the measured deposition rates on the slag panels and the predicted results using different swirl number (SN) - coal A.

However, it has been reported (You & Zhou, 2006) that increasing the swirl number may enhance the combustion of small particle due to proper mixing of the fuel and the oxidant by recirculation forces, and hence reducing the number of fine particles that may hit the heat exchange surfaces. This is evident in Fig. 5.20, which shows that prediction using the highest swirl number (1.00), yielded deposition results very close to the experimental measurement.

5.2 3D Calculations

Following the successful implementation of the ash deposition rates model in the two-dimensional domain of the ACIRL furnace, a 3D domain has been successfully modelled. The ash deposition model has been implemented in the 3D domain and results of calculations are obtained.

In general, the fundamental difference between the 2D and the 3D in terms of modelling is the space in which the object is defined, and the ability to render such an object as an image or shadow (Fluent Inc., 2009).

Although the 3D calculations have some advantages, such as flexibility and better representation of the physical system, it is more complex to model than the 2D case, and it is intensive in terms of CPU demand. The 2D assumption is sufficient to characterize a given 3D system taking into account that it may under estimate some of the flow features (Fluent Inc., 2009).

5.2.1 Grid generation

The full 3D geometry of the ACIRL furnace has been modelled and Fig. 5.21 shows the geometry of the furnace modelled using the GAMBIT software. The size and specifications of the furnace have been described in Chapter 4 of this thesis and therefore not repeated here.

In the initial stage, a computational grid consisting of 0.5 million cells was generated for the full furnace which is 2.5 m long and has a diameter 0.65 m. The grid has been refined continuously in search of a grid independent solution, and finally about 1.5 million grid cells have been obtained. Further refinement of the grid does not yield any significant change in the solution obtained during the calculations. Therefore, with 1.5 million cells it has been assumed that the grid is sufficiently fine for the 3D calculations.

Fig. 5.22 shows the final grid employed in these calculations. The meshes are mostly hexahedral with very negligible cell squish and skewness (< 1) although the cells are stretched where the flow is assumed to have been fully developed.

5.2.2 Operational conditions & settings

The 3D set-up was intended to run just a single set of calculations, with low swirl number (0.25), in order to assess the performance of the ash deposition model in a 3D domain. It may also provide a basis for comparison between the 2D and the 3D calculations under the same operating conditions.

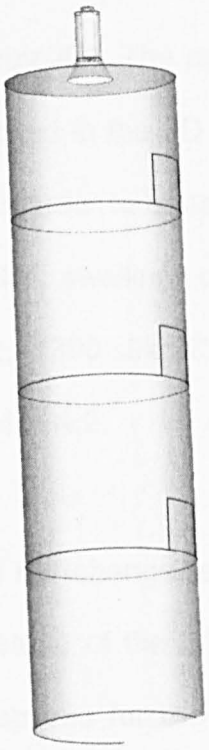

Fig. 5.21 The full 3D domain of the ACIRL furnace.

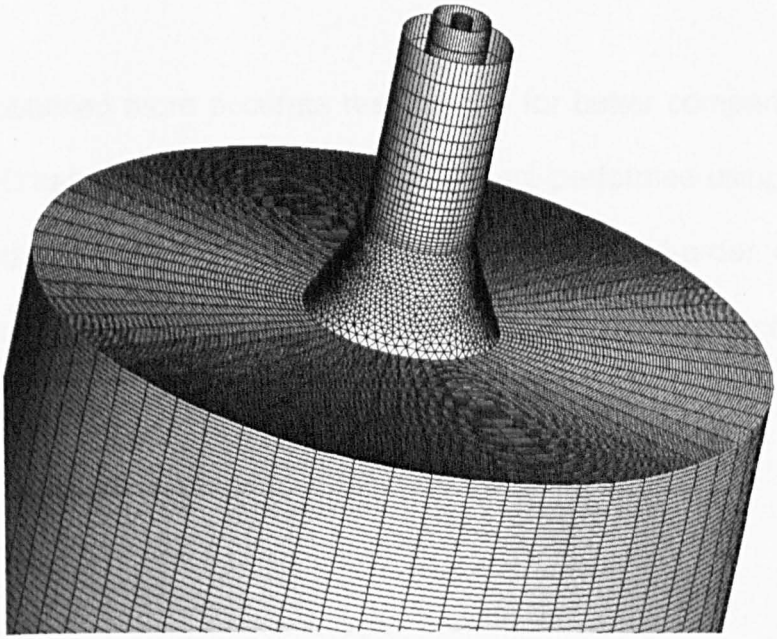

Fig. 5.22 The burner region of the 3D computational grid employed in the calculations.

The properties of the Australian coal C, which has been used in the 3D calculations, were presented in Table 4.1. The operating conditions used in the 2D calculations have been maintained in the 3D calculations, except some few changes in the parametric values in order to enhance solution convergence. For example, the value used for the swelling coefficient, specific heat and vaporization temperature are 1.2, 1300 J/kg-K and 700 K, respectively, as against the values presented in Table 4.2.

In general, the solver settings did not change, except that in the 3D case, the 3D solver has been employed instead of the 2D axisymmetric solver used for the 2D case. Thus, appropriate options for the 3D case in the FLUENT 12.1 software have been selected. However, the models used for energy, radiation, turbulence, etc., have been remained to be those employed in the 2D calculations.

In order to obtained more accurate results, and for better comparison with the completed 2D calculations, the 3D calculations are performed using the second-order upwind discretization scheme although the second-order discretization scheme requires fine grid cells, and hence, additional computational effort and time.

5.2.3 Solution procedure

After setting up all the required parameters in the software, non-reacting flow calculations were first performed for about 100 iterative steps. This was to

enable the successful initialization of the gas phase velocity field in the furnace before introducing the reacting materials.

The energy and PDF equations are then activated. Also, the discrete phase was set to continuously interact with the gas phase, i.e. allowing for the exchange of momentum, heat, etc., between the two phases. Initially, the reacting flow calculations have been performed using the first-order discretization scheme for all the properties and species involved. When the flow fields have been established and the calculations have become stable using the first-order discretization scheme, the second-order discretization scheme was then switched on for all the species. As earlier stated, the second-order discretization scheme is necessary in order to obtain more accurate solutions from the calculations.

5.2.4 Solution convergence difficulty

After about 0.4 million seconds of computations time on a 4GB memory processor, the radiation (DO) and the energy equations started to diverge. Although the calculations were started with 0.5 million grid cells, the grid was refined continuously in order to improve the solution. About 1 million cells were obtained after the initial refinement, and then additional calculations were performed. However, diverged solutions, similar to those described above, have been obtained. Further grid refinement yielded about 1.5 million gird cells, and a significant improvement in the solution convergence was obtained during the calculations.

Although there is no universally accepted settings for the under relaxation factors, the factors have been adjusted continuously, based on experience and reported setting in the literature (Tai, Hsieh & Chieng, 2005), in order to obtain a converged solution. For example, the under relaxation factors for momentum, DO and species concentration were reduced to 0.2, 0.9 and 0.15, respectively. This step, coupled with the low swirl number used, has produced a converged solution.

The effect of the swirl motion in the furnace is considered massive especially on turbulence effect (Rushdi *et al.*, 2005), and the 3D calculations with high swirling motion are always difficult to converge because most of the models that performed well in other conditions fail to perform under a high swirling motion (Dinesh, Malalasekera, Ibrahim & Kirkpatrick, 2005).

It is important to note that the converged solution at this stage is necessary before we can integrate the proposed ash deposition model into the FLUENT codes. Without the proper establishment of the gas phase temperature and velocity fields, and subsequent tracking of the particle trajectories in the discrete phase, the proposed ash particle deposition model can not be implemented as a boundary condition that determines the fate of an ash particle that may hit the boiler walls.

5.2.5 Discussion of the 3D simulations

The 3D non-reacting flow simulations have been successfully started in a similar way to the completed 2D calculations. All the species residuals tend to fast convergence after about 100 initial iterations. As shown in Fig. 5.23, the scaled residuals for the turbulence and all the velocity components have been reduced to about 10^{-2}.

Also, the introduction of the coal particles into the burner did not show any unusual flow from the scaled residual behaviour although the temperature and pressure gradients are expected to increase.

The surge in the scaled residuals at about 100 iterative steps in Fig. 5.24 was due to the ignition when the fuel and the oxidant are mixed in the burner region. Although the calculations are stable at this stage, the speed of the calculations has been reduced to less than a single iterative step in about two minutes.

Fig. 5.25 shows contours of the static temperatures in the furnace. The maximum flame temperature obtained is about 2180 K. The gas temperatures for the 3D case, the 2D cases and the experimental data are compared in Table 5.1. The peak flame temperature is not provided in the experimental measurement. However, 1973 – 2273 K has been used as the adiabatic flame temperatures for coal (Lawn, 1987).

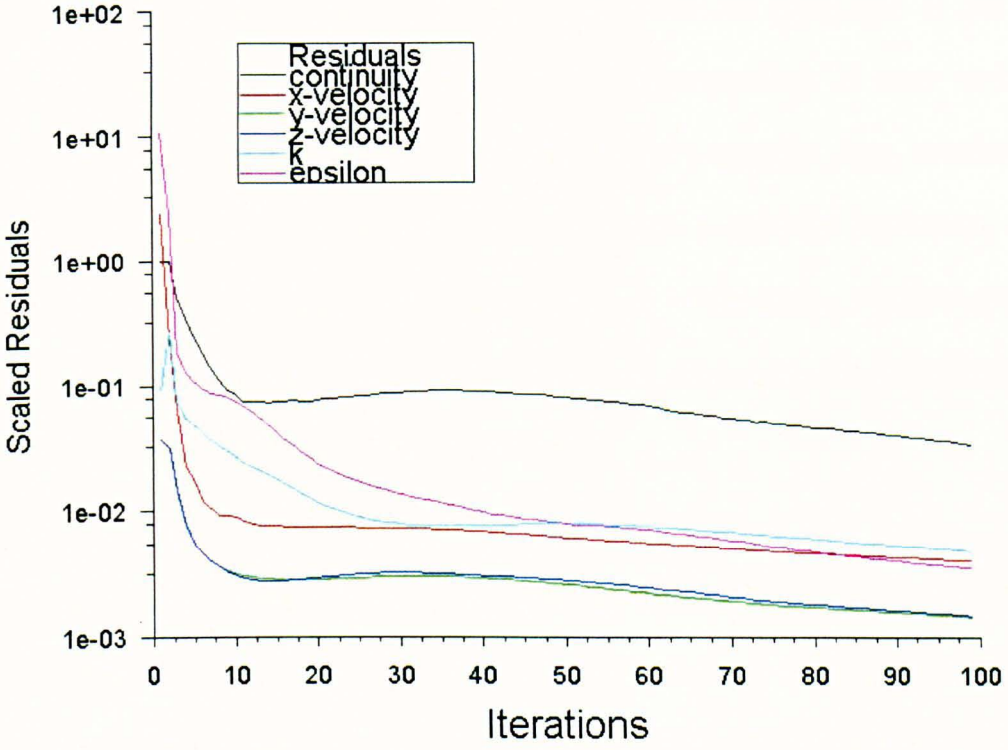

Fig. 5.23 Scaled residuals for the velocity and turbulence during the initial 3D non-reacting flow calculations.

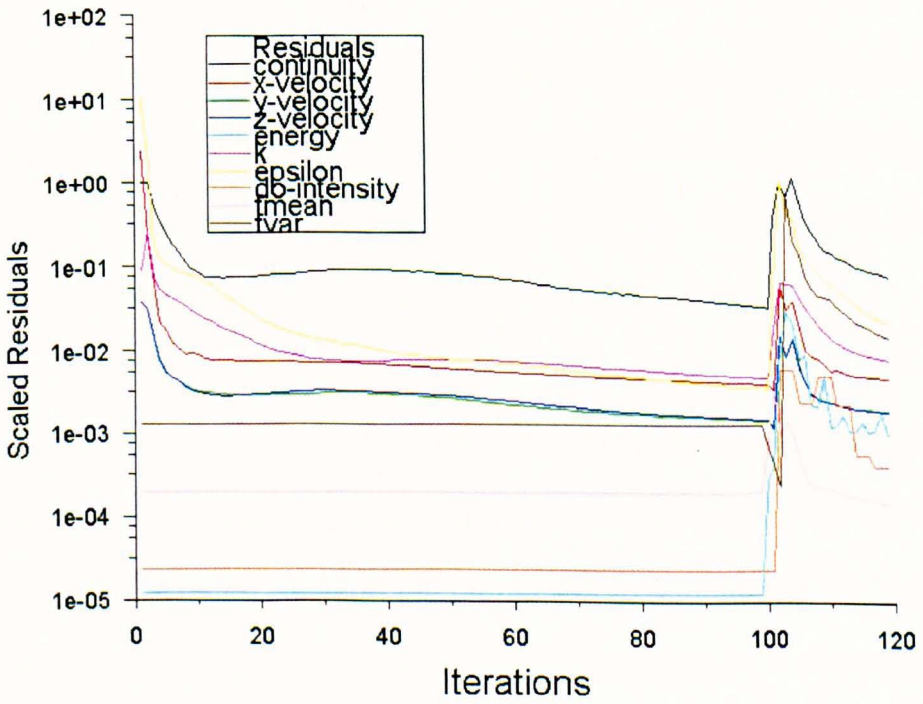

Fig. 5.24 Scaled residuals for the velocity and turbulence after a few iterations with the 3D reacting flow.

The results show that the maximum flame temperature predicted in the 3D domain is within the range of the adiabatic flame temperature of coal, while in the 2D cases the peak flame temperature was under predicted. Also, in different zones within the domain: flame zone 1 is about 0.3 m away from the burner exit, zone 2 is about 1.0 m away and zone 3 is about 1.7 m away, measurements have been taken. In all the flame zones, the results show over predictions in the 3D case and under predictions in the 2D cases.

In order to draw reasonable conclusions, the 3D results are compared with the results of the 2D Case 2. The 2D Case 2 calculations have been performed with exactly the same operating conditions and parameters with the 3D calculations. In this analysis, the 2D calculations earlier reported in section 5.1 of this Chapter five has been considered as 2D Case 1.

Although the same results are not expected from the 2D and 3D calculations since the difference in geometry can significantly influence the nature of the flow (Luo, Hinton, Liew & Tan, 2004), the 3D and the 2D Case 2 predicted temperatures in the flame zones 1 and 2 show a similar trend.

As shown in Table 5.1, the results indicate that the surrounding gas temperatures at 1.0 m away from the burner exit is higher than the temperature in the region that is much closer to the burner exit (0.3 m away). The case is not the same with the results of the experiment and the 2D Case 1 calculations.

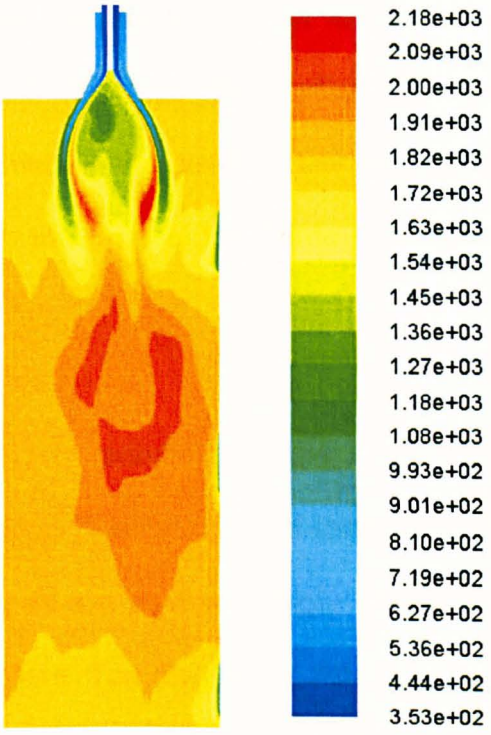

Fig. 5.25 Contours of the static temperatures (K) of the gas phase in 3D combustion simulations with Australian coal C.

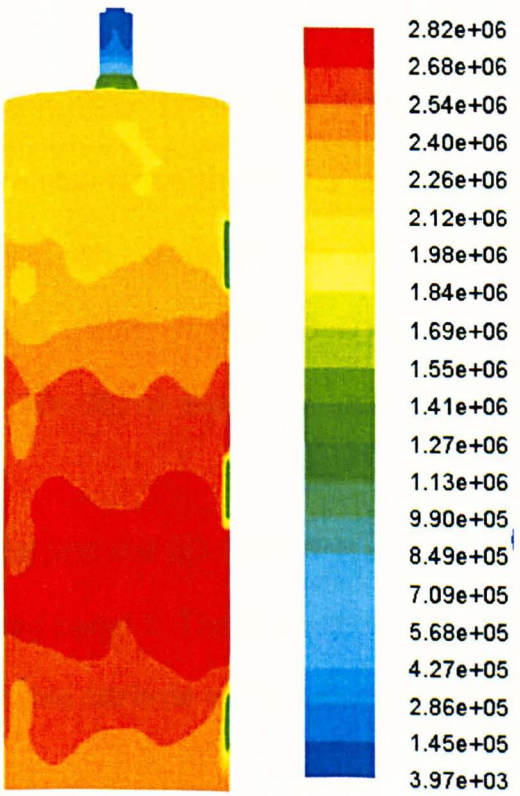

Fig. 5.26 Contours of the incident radiations (W/m^2) in the gas phase during 3D combustion simulations with Australian coal C.

The phenomenon described above is not unusual, and more often, it is attributed to the low swirl velocities which affects the particle residence times and the particle entrainment in the boiler. A low swirl number (< 0.4) results in a weak recirculation zone that affects the flame stabilization (Eldrainy, Jaafar & Lazim).

The contours of the incident radiations for the 3D calculations are presented in Fig. 5.26. The results show that the incident radiations are higher in flame zone 2 where the temperatures are also very high. The heat fluxes on all the slag panels show a similar trend. The slag panel 2 has the highest heat flux of about 666 ($kW/m^2.s$) as shown in Table 5.2. The heat flux on the slag panel 1 is the least in the 3D case. Also, the 2D Case 2 calculations produced similar results, where the highest heat fluxes are recorded on the 2^{nd} slag panel.

The contours of the ash deposition rates in the 3D domain while simulating the combustion with Australian coal C are shown in Fig. 5.27. The results show that slag panel 2 has the highest ash deposition rate of 9.5e-05 ($kg/m^2.s$), as shown in Table 5.3. Similarly, the results of the 2D Case 2 calculations show the highest deposition rate (1.10e-05) on the 2^{nd} slag panel.

However, the experimental and the 2D Case 1 results have shown the highest deposition rates on the slag panel 1. The deposition trend in the 3D calculations may not be accurate, and this attribute to the reduced swirling motion (Rushdi *et al.*, 2005).

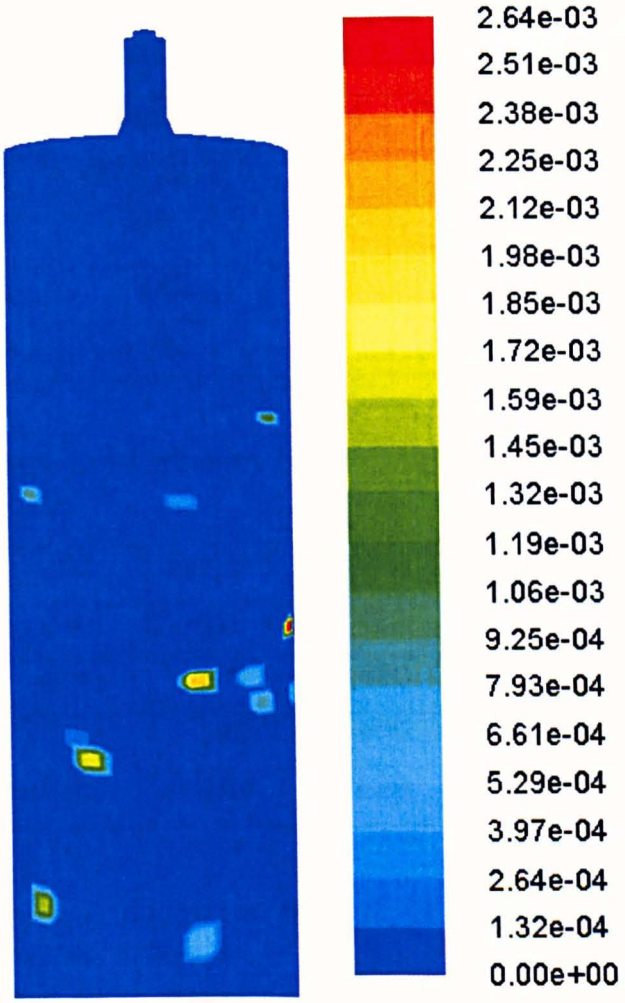

Fig. 5.27 Ash deposition rates (kg/m^2 s) in 3D combustion simulations with Australian coal C.

Although the prediction trend for the ash deposition in the 3D calculations is not consistent with the experimental results, they have correlated well with the 2D Case 2 calculations, and it is now evident that the deposition model has been successful in the three dimensional predictions. Therefore, the 3D and the 2D case 2 results are clear indications of the repeatability of the ash particle deposition model that have been developed in this investigation.

Table 5.1 Comparison of flame temperatures (K) in the 2D and 3D calculations with the experimental data.

	SN	Peak	Zone 1	Zone 2	Zone 3
Exp	0.45	1973-2273	1693	1613	1573
$2D_1$	0.45	1920	1602	1524	1455
$2D_2$	0.25	1910	1530	1608	1530
3D	0.25	2180	1724	1816	1724

Table 5.2 Comparison of heat fluxes (kW/m^2) in the 2D and 3D calculations with the experimental data.

	SN	Panel 1	Panel 2	Panel 3
Exp	0.45	518	422	380
$2D_1$	0.45	480	420	331
$2D_2$	0.25	388	400	344
3D	0.25	520	666	591

Table 5.3 Comparison of deposition rates (E-05 $kg/m^2.s$) in the 2D and 3D calculations with the experimental data.

	SN	Panel 1	Panel 2	Panel 3
Exp	0.45	2.95	0.59	0.42
$2D_1$	0.45	1.00	0.40	0.20
$2D_2$	0.25	0.30	1.10	0.80
3D	0.25	0.50	9.55	2.01

5.2.6 Remarks

The 3D calculations on the ACIRL furnace have been performed in order to further test the proposed ash particle deposition model. Advanced CFD techniques are used in the implementation of the model in FLUENT 12.1 commercial software. Although solution convergence difficulty has been

experienced, the predicted results obtained are reasonable within the available boundary conditions. Therefore, the following conclusions are made:

- The ash particle deposition model developed in this investigation has successfully predicted in both the 2D and 3D domains.
- The 3D results are over predicted when compared to both the 2D calculations and the experiment.
- Higher deposition rates are obtained on slag panel 2 instead of the slag panel 1 as reported in the experiment (Su *et al.*, 2001). This phenomenon is attributable to the low swirl number used in the calculations (Rushdi *et al.*, 2005) which results in the formation of a weak recirculation zone.
- The 3D calculations with higher swirl number may require further refinement of the gird cells, more computational time and, probably, the use of different combustion models or parameters.
- Further calculations using the 3D case could not be performed due to financial constraints. However, additional 3D calculations are recommended for future work since there is no available report on similar work using the ACIRL furnace.
- Although the 2D axisymmetric assumption of the test case is suitable for the intended investigations, the 3D results will offer a more flexible visualization and manipulation of the results.

5.3 Conclusions

The non-premixed combustion models, based on a CFD technique, have been implemented for pulverized coal fuel. The models were applied to the ACIRL furnace to establish the gas phase temperature and the velocity fields. This is a necessary step towards the study of slagging and fouling propensities. The measured and predicted results of the temperature profiles and heat fluxes in the ACIRL furnace have been compared.

A deposition model based on the temperature-dependent viscosity of the ash particles has been developed. The model has been validated against experimental data on four different types of Australian bituminous coal using 2D axisymmetric and full 3D cases of the ACIRL furnace.

Although modelling the ACIRL furnace using the axisymmetric assumptions has been recommended, especially where there time limitation, the 3D modelling provides added flexibility to the analysis of the results.

In general, the predicted results are in good agreement with the experimental measurements, and the following conclusions are made:

- The predicted thermal conditions, such as the gas temperatures and the heat fluxes, are in good agreement with the experimental data (± 5%). Therefore, the CFD set-up has been found to be suitable for the investigation of ash slagging tendencies.

- The ash deposition model developed in this investigation has been successful in the prediction of the deposition rates of the homogeneous coal ash slag in high temperature regions. However, in 3D calculations, convergence difficulty was experience with the experimental swirl number.
- The sticking tendencies of the ash particles downstream of the boiler, where the temperatures are low, have not been accurately predicted in this investigation.
- The reported experimental ash deposition rates on slag panels 2 and 3 are in a better correlation with the predicted results using the 2D case when compared to the results obtained for slag panel 1 which has no accurate deposit measurements.
- Strong recirculation zones have been established near the exit of the burner. The recirculation is due to the turbulence/swirl flow, and it enhances the ignition and flame stability.
- Both the flame temperature and the ash deposition rates have been under predicted with the 2D calculations. The under predictions may be attributed to the low swirl velocity and the low temperature of the slag panels that have been used in these axisymmetric calculations.
- The temperatures of the burning particles at the burner region are found to be higher than the temperatures of their surrounding gas. However, away from the burner region, the difference in particle and gas temperatures decreases.
- The choice of reference viscosity affects the ash deposition rates. When a higher value for the reference viscosity is chosen, more particles that

have sufficient inertia to hit the boiler walls have higher tendency to stick to the walls.

- The swirling motion helps in stabilizing the flame, resulting in a more even temperature distribution in the furnace. Higher swirling motion increases the temperature of the particles, and in turn, increases the tendency of the particles to stick to the heat exchange surfaces.
- However, lower swirl numbers reduces the particles residence times and weaker recirculation zones are created resulting in decreased tendency of particles entrainment.

CHAPTER 6

ASSESSMENT OF COAL SLAGGING POTENTIAL

In this chapter, the numerical modelling of the coal slagging index has been described. The model has been tested over a wide range of coals and some sets of coal blends in order to predict their slagging performance. Also, in this chapter, the results of the predictions using the proposed numerical slagging index (NSI) and some of the existing slagging indices on a wide range of coals have been presented and discussed. The chapter contains the results of predictions on some sets of coal blends using the NSI.

The chapter is divided into six sections. The numerical modelling steps are presented in the first section. The flow chart on the computational steps involved in predicting the slagging potential of coals and blend using the NSI has been explained in the second section. In the third section, the individual performance of the NSI and four existing slagging indices on four Australian bituminous coals has been presented.

Section four discusses, comparatively, the performance of the NSI (S_x) and six existing slagging indices, namely, ash fusion test i.e. deformation temperature (AFT), viscosity index (μ), the silica ratio (SR), percentage of iron oxide in the ash (%Fe_2O_3), basic to acidic oxides ratio (B/A) and the dry sulphur content index (R_s), on a wide range of coals. The use of the NSI has also been extended to coal blends. In section five, the results of predictions using the proposed NSI are compared with the reported performance of some existing

slagging techniques on coal blends. Finally, the conclusions drawn from the discussion made in this chapter are presented in section six.

6.1 Modelling of the Coal Slagging Index

At this stage, another numerical model has been developed. The proposed model is to predict the ash slagging potential of coals. In the development of the proposed numerical slagging index, the combined effect of some of the major contributing factors in the slag formation, namely; the viscosity of the ash, the ash fusibility and the weight of the incoming ash (the ash content in the coal), have been considered. Whereas most of the existing coal slagging indices are based on only the fusibility, viscosity or the chemistry of the ash (Lawrence *et al.*, 2008).

The slagging in a boiler furnace depends on the combined effects of the liquid forming tendency of the ash, the temperature experienced in the furnace and the ash loading in the coals (Lawrence *et al.*, 2008). Since the viscosity which is calculated from the ash chemical composition gives estimations of the temperatures of the ash particle to be sticky, it can therefore be related to extent of the shrinkage measured at these temperatures (Gupta *et al.*, 1998). Therefore, the shrinkage level is appropriate as a criterion for ash stickiness.

For effective modelling, the following assumptions have been made on the basis of the results of some empirical studies (Lawrence *et al.*, 2008; Wigley *et al.*, 1990; Gupta *et al.*, 1998):

- Peak shrinkage patterns are obtained at temperatures between 1100-1440 °C, and these temperatures fall within the softening temperatures of most coals.
- Since ash shrinkage is considered as an appropriate criterion for determining the ash particle stickiness, it can be related to the ash particle viscosity.
- In equation (3.33), T represents the ash particle temperature at impaction, and for a sticky particle, T is equal to the softening temperature of such particle, ST, which is also the temperature at which the ash particle is more plastic and has a high tendency to stick to the surface upon impaction.
- The accumulation of the slag in the boiler is directly proportional to the weight of the ash in the coal, while the slagging potential is inversely proportional to the slag viscosity.

The Watt-Fereday viscosity model has been used to calculate the ash particle viscosity using the ash composition and impact temperature, where the weight percentages of SiO_2, Al_2O_3, Fe_2O_3, CaO and MgO have been recalculated to 100%. However, the Watt-Fereday model did not account for the MgO content in the ash.

In order to account for the content of MgO as an important fluxing agent, the Bomkamp modified version of the Watt-Fereday model (equation (3.33)), which accounts for the content of MgO in the ash, has been used in evaluating the slope and intercept as follows:

$$m = 0.01404294(SiO_2) + 0.0100297(Al_2O_3) - 0.296285 \quad (6.1)$$

$$c = 0.0154148(SiO_2) - 0.0388047(Al_2O_3) - 0.0167264(Fe_2O_3) - 0.0089096(CaO) - 0.012932(MgO) + 0.04678 \quad (6.2)$$

The softening temperature is (°C) has been determined as follows (Chen & Jiang cited in Yin *et al.*, 1998):

$$ST = a(SiO_2) + b(Al_2O_3) + c(Fe_2O_3) + d(CaO) + e(MgO) + f(\chi) + g \quad (6.3)$$

where

$$\chi = 100 - (SiO_2 + Al_2O_3 + Fe_2O_3 + CaO + MgO) \quad (6.4)$$

and the values for the constants (a,b,c,d,e,f and g) in equation (6.3) are given based on the percentages of SiO_2, Al_2O_3 and Fe_2O_3 available in the ash content, as contained in Table 6.1 (not normalised).

Table 6.1 The values for the constants in equation (6.3) as a function of the content of silica, alumina and iron oxide in the ash (Yin *et al.*, 1998).

Content in ash	a	b	c	d	e	f	g
$SiO_2 \leq 60\%$ $Al_2O_3 > 30\%$	69.94	71.01	65.23	12.16	68.31	67.19	-5485.70
$SiO_2 \leq 60\%$ $Al_2O_3 \leq 30\%$ $Fe_2O_3 \leq 15\%$	92.55	97.83	84.52	83.67	81.04	91.92	-7891
$SiO_2 \leq 60\%$ $Al_2O_3 \leq 30\%$ $Fe_2O_3 > 15\%$	-3.01	5.08	-8.02	-9.67	-5.86	-3.99	1531
$SiO_2 > 60\%$	10.75	13.03	-5.28	-5,88	-10.28	3.75	453

The effect of the incoming ash has also been accounted for in the proposed NSI. The level of ash in coals is generally reported as a percentage (Lawrence *et al.*, 2008), but in practical boilers situations, the heating value of the fuel is more important. Therefore, the ash loading in pulverized coal fuel is determined

from the ultimate analysis and the heating value of the coal sample in terms of weight (kg) per MJ (dry ash basis), as follows:

$$\gamma = \frac{ash\,content\,kg\,per\,kg}{CV\,(MJ/kg)} \tag{6.5}$$

More often, the CV of the coals are given along side the coal properties. Where the CV is not given, it is determined, on dry ash basis, from the ultimate analysis of the coal as follows (Mason & Gandhi, 1983):

$$CV = 151.2(C) + 499.77(H) + 45.0(S) - 47.7(O) + 27.0(N) \tag{6.6}$$

where C, H, S, O and N are the carbon, hydrogen, sulphur, oxygen and nitrogen contents in the coal (dry ash basis), and the gross CV is calculated in Btu/lb.

At this stage, the weight of the ash has been determined in terms of the ash content and the heating value of the coal. The ash viscosity is determined from the bulk ash composition and the softening temperature, while in determining the softening temperature the properties of the bulk ash have been used. It is assumed that the slagging potential is directly proportional to the weight of the incoming ash, but inversely proportional to the ash viscosity.

Therefore, the proposed NSI, S_x, has been defined in terms of the ash viscosity, μ, and the weight of ash in the coal, γ, as follows:

$$S_x = \gamma / Log(\mu) \tag{6.7}$$

6.2 Implementation of the Proposed NSI

Fig. 6.1 shows a flow chart which illustrates the computational steps involved in predicting the slagging potential of the coals using the proposed NSI. The ash properties and the ash content in the coal, with the coal heating value, are first introduced into the code, as the initial input, in order to generate the weight of the incoming ash in kg per MJ, and the softening temperature of the ash in °C.

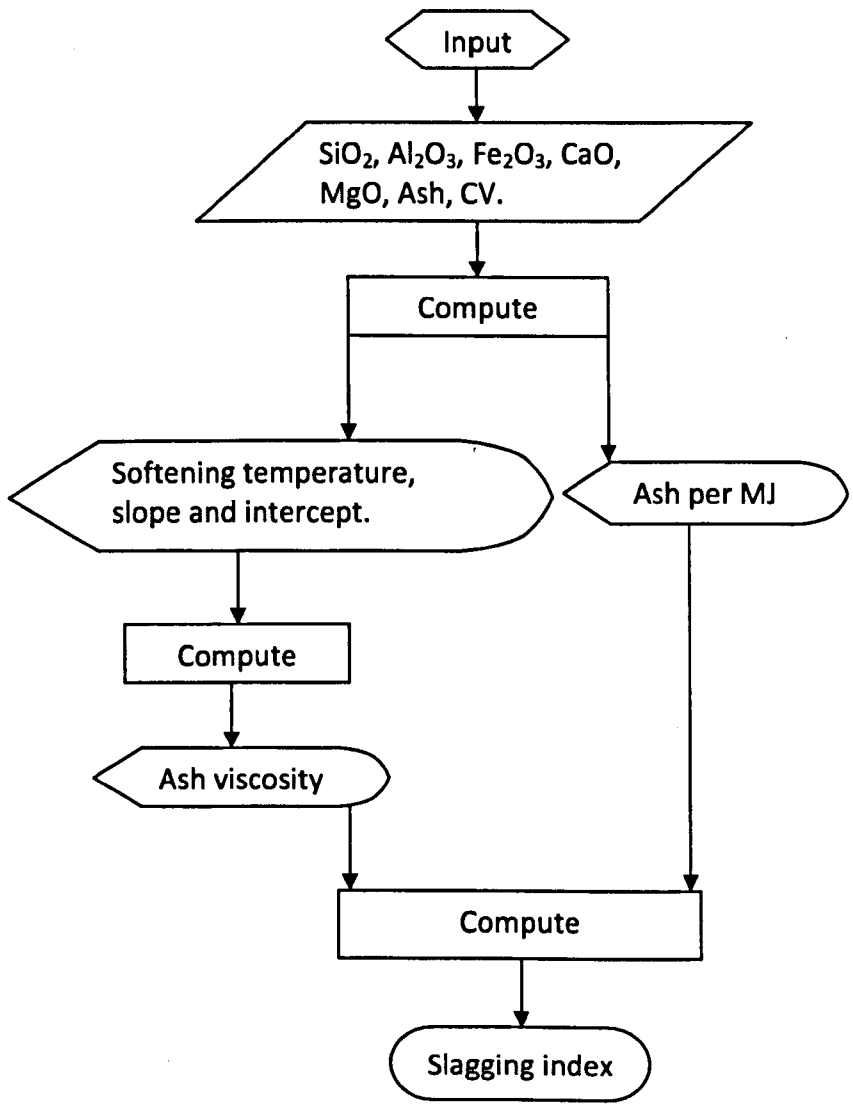

Fig. 6.1 Flow chart for the prediction of coal slagging potential using the proposed NSI.

However, where the heating value for the coal is not known, the ultimate analysis of the coal has been used as input for the code in order to generate the calorific value of the coal (in MJ/kg) according to equation (6.6) which has been described in this Chapter.

The ash softening temperature and other ash related parameters, such as, the slope and the intercept, which are described in equations (6.1) and (6.2), are considered as input data for the second phase of calculations using the developed coal ash slagging index. At this stage, the predicted ash viscosity and the weight of the ash which is determined according to equation (6.5) are automatically fed back into the code in order to finally predict the slagging potential of the coal that is been tested.

6.3 Performance of the Slagging Indices

In this section, the existing slagging indices, namely, AFT, μ, SR, $\%Fe_2O_3$, B/A and R_s, and the proposed coal NSI have been tested on a single set of four Australian bituminous coals in order to review and assess the *modi operandi* and the performance of the indices against the reported experimental data. (Rushdi *et al.*, 2005; Su *et al.*, 2001b)

The slagging performance of the tested coals has been reported (Su *et al.*, 2001b). Also, the proposed ash particle deposition rates model has been used to predict the performance of the coals. Therefore, the predicted results using the deposition model and the reported experimental results have been used in validating the slagging indices.

6.3.1 Test-coal properties

Four Australian bituminous coals (A-D) are tested for slagging using the existing slagging indices and the proposed NSI. The properties of the coals have been presented in Table 4.1. In general, the Australian bituminous coals have high heating values and low ash content. Details of the coal properties have been discussed in chapter four of this thesis.

6.3.2 Ash fusibility test

The results of the AFT on the investigated coals are presented in Fig. 6.2. The coals with low fusibilities are said to have high slagging potential (McLennan *et al.*, 2000). Fig. 6.2 shows that coal D has the highest deformation temperature of about 1493 °C, followed by coal A and then coal B. Coal C has the least value of fusion temperature, about 1278 °C. According to the AFT therefore, coal C is expected to have the highest slagging potential, while coal D is expected to have the lowest slagging potential. The low fusibility predicted for coal C may be due its high content of the basic oxides (Wigley *et al.*, 1990).

6.3.3 Viscosity slagging index

The viscosities for the four coals that have been investigated are presented in Fig. 6.3, which shows that all the coals exhibit a glassy behaviour due to the high content of SiO_2 (> 50%) and low content of Fe_2O_3 (< 10%) in their slag (Zhang & Johanshahi, 2001; Oh, Brooker, De Paz, Brady & Decker, 1995).

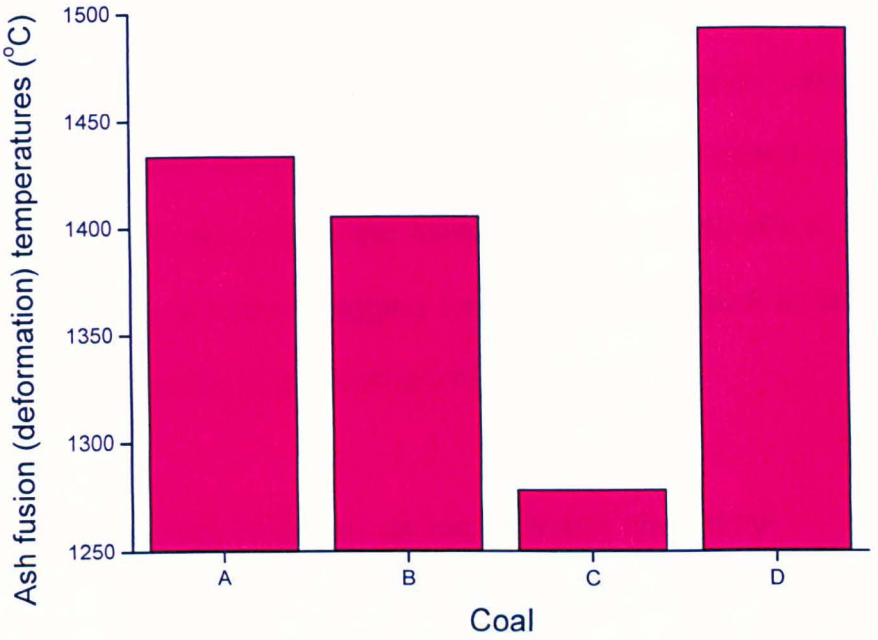

Fig. 6.2 Comparing the results of the ash fusibility test on the Australian coals A-D.

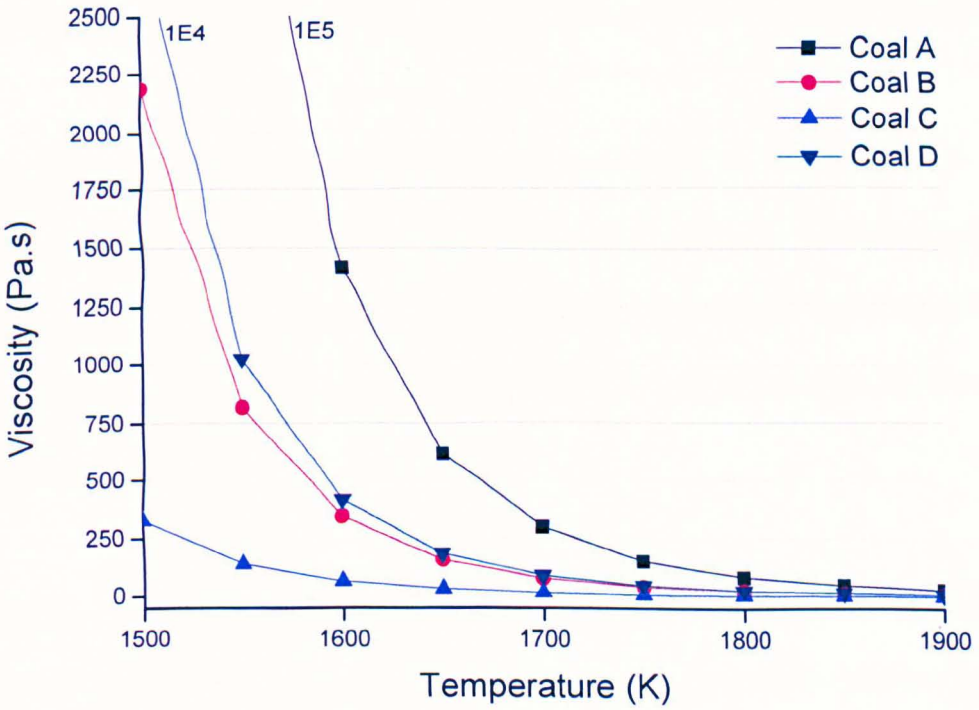

Fig. 6.3 Comparing the calculated temperature-dependent viscosity for the Australian coals A-D.

A large amount of silica in the slag results in a higher degree of polymerization, and this behaviour yields a liquid phase with a high viscosity, and hence a low slagging potential (Su *et al.*, 2001b). Coal A has the highest viscosity, followed by coal D, and then coal B and the least is Coal C. Guided by the viscosity index, the coal C, which has the lowest viscosity, ~250 (Pa.s) at 1550 K, is expected to show a higher slagging tendency, while coal A to have the lowest slagging tendency due to its relatively high viscosity.

6.3.4 Slagging indices based on the bulk ash chemistry

The performance of the slagging indices that are based on the bulk ash properties, such as, the SR, $\%Fe_2O_3$ and the B/A ratio, have also been investigated. Although the indices show similarity in their prediction characteristics, they yield inconsistent results in a few of the cases investigated.

Silica ratio: High silica content in coal increases its fusibility and hence decreases its slagging tendency (Lawrence *et al.*, 2008). The percentage of silicon oxide in the coals A-D, as shown in Fig. 6.4, indicates that coal A has the highest percentage of silica in the ash (71.50%), and then coals B, D and C in descending order.

Therefore, according to the silica ratio principles, the coals will have a reversed order in terms of the severity of their slagging potential, where coal C is expected to have the worst slagging potential and coal A to have the least slagging potential.

Percentage of iron oxide in ash: Another important parameter in determining the ash slagging potential is the percentage of iron oxide available in the ash. Higher iron oxide content usually lowers the slag viscosity (Zhang & Johanshahi, 2001), and this may result in a high slagging tendency. Coal ash with Fe_2O_3 < 6% has a low slagging tendency (Lawrence *et al.*, 2008).

The percentages of iron oxide for coals A-D have been computed and the results are also presented in Fig. 6.4. The results show that coal C has the highest content of Fe_2O_3 in the ash (10.80%), followed by coal B, and then coal C and coal A. Therefore, we expect their slagging propensities to take the same descending order from coal C.

Basic to acidic oxides ratio: The B/A ratios are also used in distinguishing between good and bad coals. An increase in the B/A ratio of the coal will lower its fusion temperature (Wigley *et al.*, 1990).

The computed values for the ratio of the B/A oxides for the four types of coals investigated are shown in Fig. 6.5. The results indicate that the slagging potential of coal C is expected to be the worst, and then coal B, coal A and coal D, in decreasing order.

Although the predicted results using the B/A ratio also suggest that the coal C has the highest slagging potential, as also predicted using the SR and $\%Fe_2O_3$ indices, the results in Fig. 6.5 suggest that coal D has the lowest slagging potential.

Ratio of basic to acidic oxides multiplied by the content of dry sulphur in the coal: The slagging index, R_s, for coals with more pyrite content than siderite, is the product of the B/A ratio and the percentage of dry sulphur in the coal. While for coals with more siderite than pyrite, the slagging index is the product of the B/A ratio and the percentage of iron oxide in the ash.

Notwithstanding the factor multiplied with the B/A ratio, the dry sulphur content in the coal or the content of iron oxide in the ash, the coals with $R_s < 0.6$ are said to have a low slagging potential (Lawrence *et al.*, 2008).

The results of predictions using the two slagging techniques described above on the set A-D of Australian coals that are investigated, are presented in Fig. 6.6. The results suggest that coals A and D have a low slagging potential, followed by coal B, then coal C in increasing order. These results are consistent with the results earlier predicted using the $\%Fe_2O_3$ index.

Although the predicted index values using the two indices discussed above are slightly different, the values show a consistent slagging trend for all the coals. Also, it is important to note that the results of the predictions using all the bulk ash based indices are similar, especially when tested on the same coal.

This suggest that the slagging indices that are based on the bulk ash chemistry can only accurately predict the slagging potential of coals whose properties are the bases on which they are established, otherwise they all produce misleading results.

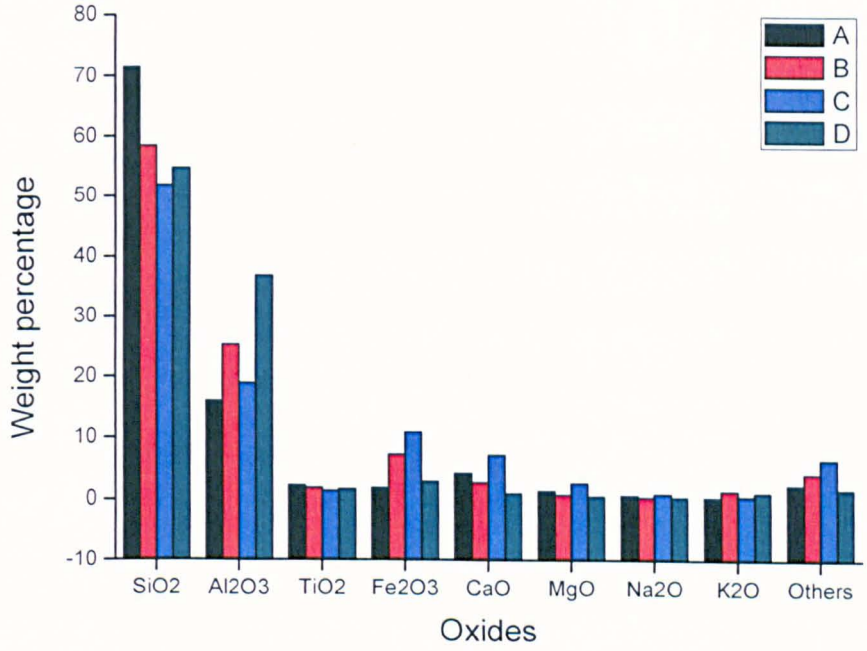

Fig. 6.4 Comparing the percentage oxides for the Australian coals A-D.

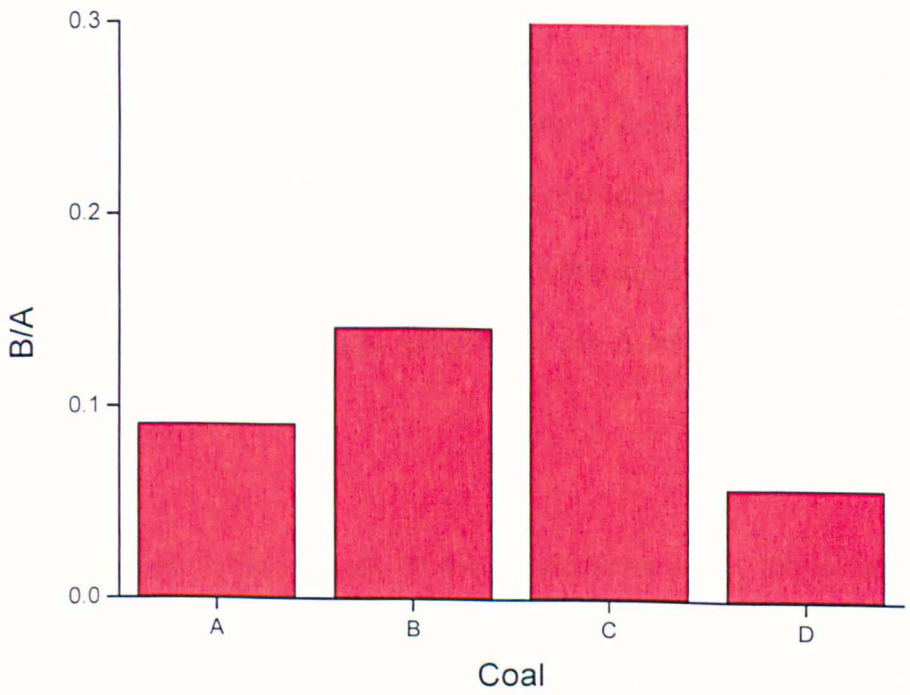

Fig. 6.5 Comparing the basic to acidic oxides ratios for the Australian coals A-D.

6.3.5 The proposed NSI

The results of predictions using the NSI have been compared with the results of predictions using four slagging indices, namely; $\%Fe_2O_3$, B/A, R_s and μ, that have been tested in this investigation, as shown in Fig. 6.7. The NSI prediction results suggest that the coal C has the lowest slagging potential, despite its very low ash viscosity. This may be due to the low ash content of the coal (3.20%) (Rushdi *et al.*, 2005).

The NSI also predicted coal D to have the highest slagging potential, followed by the coal A. These NSI predicted results are consistent with both the experimental measurements (M), and the results of predictions using the deposition model that was earlier developed in this study (P), as shown on the Fig. 6.7 (Su *et al.*, 2001b).

On the other hand, the existing coal slagging indices that have been tested in this investigation, show inconsistencies in predicting the field performance of the Australian coals, and this may be because the slagging indices are specifically established for coals other than the Australian coals (McLennan *et al.*, 2000).

The inconsistency in the results of the predictions using the existing slagging indices is a major concern in selecting good coals. These inconsistencies, especially when the application of the indices is extended to a wide range of coals, are what the proposed NSI seeks to address.

6.4 Performance of the Slagging Indices on a Wide Range of Coals

In order to establish the robustness of the proposed numerical slagging index, it has been tested on seventeen different coals, ranging from the Indian low rank coals to bituminous coals from Australian, Columbia, Indonesia, South Africa, UK and the US.

The properties and the slagging potential of the coals that have been investigated, both empirically, and in some cases, numerically, are reported by different research groups. In this section, the reported field performance of the tested coals has been compared with the results of the predictions using the NSI and the existing slagging indices.

6.4.1 Scaling of the Slagging Indices

Table 6.2 shows the scaling of the coal slagging indices discussed in this chapter (Lawrence *et al.*, 2008; Watt and Fereday, 1969; McLennan *et al.*, 2000). Although the proposed NSI has not yet been scaled, its relative measurements suggest that a higher index value represents a higher slagging potential, while for the viscosity index, a higher index value represents a low slagging potential.

From Table 6.2, it can also be seen that for the AFT, SR, and the μ indices, a higher index value represents a lower slagging potential. The coals with very low fusibility, < 1422 K, are expected to have severe slagging potential (Lawrence *et al.*, 2008).

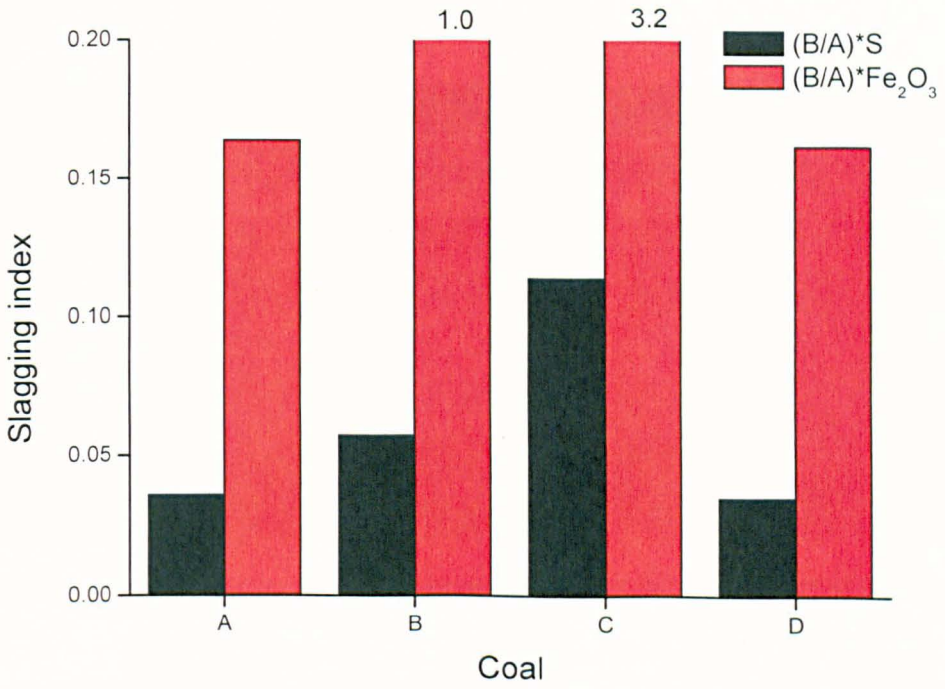

Fig. 6.6 Comparing the performance of the (B/A)×S and the (B/A)×Fe_2O_3 slagging indices on the Australian coals A-D.

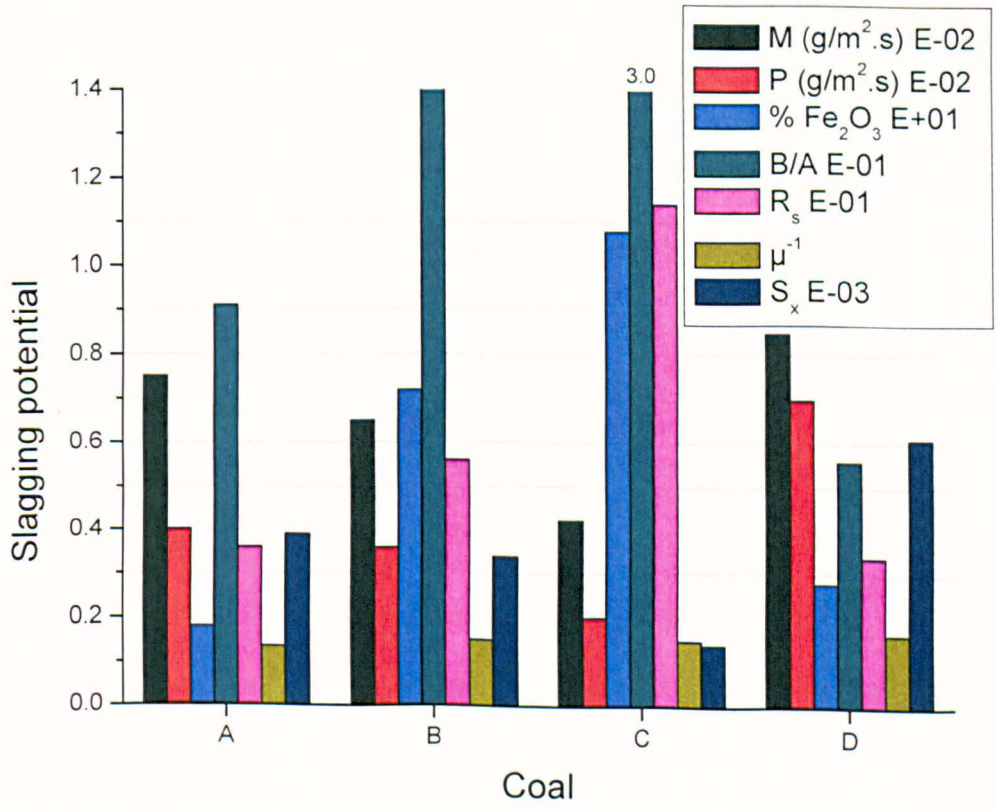

Fig. 6.7 Comparing the performance of the proposed NSI (S_x) against four existing indices on the Australian coals A-D.

Table 6.2 Scaling of some of the investigated coal slagging indices (Lawrence *et al.*, 2008).

	Low	Medium	High	Severe
AFT	> 1616 K	1505 – 1616 K	1422 – 1505 K	< 1422 K
SR	72 – 80	65 – 72	50 – 65	
Fe_2O_3	< 6 %	6 – 7 %	> 7 %	
B/A	< 0.11	0.11 – 0.14	> 0.14	
R_s	< 0.6	< 2.0	≥ 2.0	
μ	> 10^8 (Pa.s) †	10^5 – 10^8 (Pa.s) †	≤ 10^4 (Pa.s) †	
S_x	< 0.3 †	0.3 – 0.6 †	> 0.6 †	

† Indicative values derived on the basis of investigations reported in this thesis

6.4.2 Properties of the tested coals

Seven slagging indices, including the NSI, have been tested on seventeen different coals. The proximate analyses, the ash analyses and the heating values for the tested coals are shown in Table 6.3 (Lawrence *et al.*, 2008; Rushdi *et al.*, 2005; Degereji *et al.*, 2011; Laursen *et al.*, 1998; Lee & Lockwood, 1999; Zygarlicke, Pavlish, Gunderson and McCollor, 2000).

From Table 6.3, it is clear that the Indian coals have low heating values (13-17 MJ/kg) and medium-high volatile matter content. The Indian coal 1 has low ash content (2.42%) and a very high content of Fe_2O_3 and CaO in the ash (16.90 and 34.30%, respectively). The coal 1 may likely behave as a refractory material, and it may not yield to any slagging index predictions due to its high content of Fe_2O_3 and CaO in the ash.

All the Indian coals, except Indian coal 1, have high ash content (33 - 50%). The coal 5 has relatively low ash content (33.72%), and a low content of SiO_2 and Fe_2O_3 in the ash. The rest of the Indian coals have very high ash content, about 45% on average, and this may result in a high slagging potential. Indian coal 3 has a relatively low ash content (43.13%) and the highest heating value (17.04 MJ/kg) when compared with Indian coals 2 & 4, and this may reduce slagging tendency of the coal.

The properties of the Australian coals (1-4), as shown in Table 6.3, are the same with the properties of Australian coals (A-D) earlier discussed in Table 4.1. The coals have heating values above 33 MJ/kg, and this is within the range of values for typical bituminous coals.

Australian coal 3 has a high content value for Fe_2O_3 and a low content value for SiO_2 in the ash (10.80% and 51.80%, respectively). The low ash content of Australian coal 3 (3.20%) may reduce its tendency to accumulate slag in the boiler.

Although the Colombian, the Indonesian, and the South African coals are from different regions, they appear to have similar calorific values, with different levels of ash content. The Indonesian sub-bituminous coal has a slightly higher volatile matter (41.23%) compared with the Colombian and the South African coals, but it has low ash content (7.69%).

The Indonesian and the South African coals have a similar content of SiO_2 in the ash, while the content of Al_2O_3 in the ash is higher in the South African coal. The Fe_2O_3 content in the ash varies significantly for all the coals, with Indonesian coal having the highest content value (11.10%).

Table 6.3 Properties of the 17 tested coals (wt%, db) using the slagging indices (Lawrence *et al.*, 2008; Rushdi *et al.*, 2005; Degereji *et al.*, 2011; Laursen *et al.*, 1998; Lee & Lockwood, 1999; Zygarlicke, Pavlish, Gunderson and McCollor, 2000).

S/N	Coal	FC	VM	Ash	HHV (MJ/kg) (db)	SiO_2	Al_2O_3	Fe_2O_3	CaO	MgO
1	Indian 1	50.23	47.35	2.42	28.59	16.20	12.30	16.90	34.30	8.70
2	Indian 2	27.70	25.56	46.74	15.89	61.30	24.70	6.40	4.70	1.30
3	Indian 3	30.44	26.43	43.13	17.04	62.70	27.30	5.10	1.20	0.70
4	Indian 4	25.48	24.31	50.21	13.52	62.50	27.00	5.30	1.10	0.60
5	Indian 5	41.31	24.97	33.72	20.21	60.50	31.80	3.70	1.00	0.60
6	Australian 1	44.50	45.90	9.60	33.20	71.50	15.90	1.80	4.20	1.30
7	Australian 2	65.50	26.70	7.80	34.99	58.40	25.30	7.20	2.60	0.70
8	Australian 3	58.30	38.50	3.20	33.57	51.80	18.90	10.80	7.10	2.50
9	Australian 4	56.70	30.60	12.70	34.49	54.60	36.80	2.80	0.70	0.42
10	Indonesian 1	51.1	41.23	7.69	29.77	48.50	25.40	11.10	2.13	2.24
11	Columbian 2	52.29	34.67	13.04	29.17	61.00	20.40	7.60	3.07	0.63
12	S. African3	60.60	24.24	15.16	26.06	47.10	30.80	3.15	6.73	1.65
13	US 1	43.95	45.35	10.70	23.20	32.8	18.90	4.80	20.20	0.70
14	US 2	48.70	39.56	11.74	27.32	53.10	20.30	14.20	3.40	1.60
15	UK 1	51.35	30.29	18.36	33.92	53.10	25.70	12.00	1.90	1.10
16	UK 2	48.53	33.12	18.35	34.60	53.00	25.00	9.90	5.40	1.90
17	UK 3	49.18	32.82	18.00	34.62	45.7	25.0	25.0	1.10	0.60

The US coals appear to have a similar content in terms of volatile matter, fixed carbon and ash. However, the US coal 2 has a significantly higher content of SiO_2 and Fe_2O_3 in the ash when compared with the US coal 1, while the content of CaO in coal 1 is much higher than in coal 2.

The properties of the UK coals that have been investigated are very similar, except in the content of CaO and MgO in the ash, where Coal 2 is significantly higher than the two other UK coals. From Table 6.3, the UK coals have a higher content of Fe_2O_3 in the ash than all the other coals, and this has been reported (Lee & Lockwood, 1999).

6.4.3 Predictions results and discussion

The predicted results using the NSI and the existing indices, namely, AFT, SR, $\%Fe_2O_3$, B/A ratio, R_s and μ techniques, on seventeen different coals, have been compared with the reported field performance of the coals.

The coals investigated include five Indian low-rank coals, eleven bituminous coals from the UK, US, Columbia and South Africa, and a sub-bituminous coal from Indonesia. The slagging potential of coals is inversely proportional to the AFT, SR and μ indices, therefore, the inverse of their values have been plotted in order to enhance comparative analysis.

Indian coals: The field performance of the Indian coals has been reported in one of the references (Lawrence *et al.*, 2008). Lawrence and others also reported the performance of a new slagging index which was based on thermo-mechanical analyses (TMA). The TMA-based index has been defined in terms of the relative shrinkage rate of the ash and the weight of ash in the coals. The report show that the TMA results correlate with the field performance of the Indian coals.

In Fig. 6.8, the results of the predictions using the NSI and the six slagging indices mentioned above have been compared with the reported field performance of the Indian coals. The coal 1 appears not to fit well in these predictions, and this may be due to its unusual content of Fe_2O_3 and CaO in the ash (16.90 and 34.30%, respectively), as stated earlier in this chapter.

The Indian coal 4, which has the highest ash content in the ash (47.3%), has the highest slagging potential as predicted using the NSI when compared with other Indian coals tested in this investigation, while the Indian coal 3 has been predicted to have the lowest slagging potential.

The predicted results are in good agreement with the reported field performance of the Indian coals. All the other slagging indices that have been tested on these coals, predicted the Indian coal 2 to have the highest slagging potential, and most of the indices predicted the Indian coal 5 to have the lowest slagging potential assuming that coal 1 is exceptional due to high content of CaO and Fe_2O_3 in the ash which may make it behave as a refractory material.

Australian coals: For the Australian coals, an ash deposition model which was earlier developed in this study, equation (3.41), yielded results that agree very well with their field performance (Degereji, Derek, Ma, Pourkashanian & Williams, 2011).

In this investigation, the field performance of the coals has been compared with the predicted results using NSI and the existing slagging indices. As shown in

Fig. 6.9, the NSI predictions suggest that, amongst the Australian coals, coal 3 has the least slagging potential despite its low silica and high iron oxide content, and this result is in agreement with the measurement data.

The low slagging potential of coal 3 may be attributed to its very low ash content (3.20%), which can significantly affect the accumulation of slag in boilers. All the existing slagging indices tested on the Australian coals suggest that coal 2 is the second highest in terms of slagging. Similarly, all the indices, except the μ index which suggests coal 4 to have the worst slagging, predicted coal 3 to be the worst.

Columbian, Indonesian, and South African coals: In a study on the influence of probe temperatures on the composition of ash deposit, the deposition rates of three different coals (Indonesian sub-bituminous, and Colombian and South African bituminous coals), under the same operating conditions, have been reported (Laursen *et al.*, 1998). The reported deposition rates have been compared with the results of the predictions using the slagging indices that have been investigated.

The results of the predictions using the NSI suggest that coal 2 has the worst slagging potential, followed by coal 3. These predictions are in very good agreement with the reported boiler behaviour of the coals as shown in Fig. 6.10. Other slagging indices, such as, $\%Fe_2O_3$, B/A ratio and the μ index, all predicted coal 1 to have the highest slagging potential.

US coals: Zygarlicke and others have investigated the ash behaviour and the combustion performance during the co-firing of rice straw and coals (Zygarlicke *et al.*, 2000). They reported the ash deposition growth rates for two types of US coals (Absaloka and Illinois). The reported deposits growth rates of the tested coals have been compared with the results of predictions using the slagging indices that have been investigated.

As shown in Fig. 6.11, the results of predictions using the NSI correlate well with the reported measurement data. The US coal 1 has a very high level of slag compared to coal 2. The performance of the US coals was also accurately predicted by all the existing indices that have been tested in this investigation, except the $\%Fe_2O_3$ and the R_s indices.

UK coals: The deposition propensities of Bentinck, Daw Mill and Silverdale coals have been numerically investigated and some results from a test rig were reported (Lee and Lockwood, 1999). The reported results have also been employed in further validating the proposed NSI. The predicted results for the three coals using seven different slagging indices are shown in Fig. 6.12.

The NSI predictions suggest that coal 3 has the highest slagging potential with an index value of 0.93, and very close values have been predicted for coal 1 and coal 2 (0.86 and 0.84, respectively). Although all the predicted values are very close to the experimental measurements, the experiment indicates that coal 1 is better than the coal 2 in terms of slag formation. The AFT, SR and the B/A ratio accurately predicted the slagging behaviour of the British coals.

The overall prediction results: Fig. 6.13 compares the performances of all the slagging indices on all the coals investigated. In general, the proposed NSI suggests that the Australian coals have the least slagging propensity, followed by the Indonesian coals, and then, US, South African, UK, Columbian and Indian coals, in increasing order of slagging. From Fig. 6.13, the proposed NSI gives a better overall predicted result for all the coals when compared with the other slagging indices tested in this investigation.

The existing indices have only accurately predicted the slagging potentials of the US and the UK coals. The inability of the existing slagging indices to accurately predict the ash behaviour of other coals is not unexpected, since such indices were originally derived for the US and the European coals (McLennan *et al.*, 2000).

The results presented in Fig. 6.13 are further analysed in Table 6.4, which shows how the individual indices were able to rank all the tested coals. The coals are represented according to their numbering in Table 6.3. For example Indian coals 1, 2, 3, 4 & 5 are in the first five columns in Table 6.4. The performance of the coals are arranged in the order of decreasing slagging propensity.

According to the reported field performance of the Indian coals, coal 4 (#4), has the worst performance, while coal #1 has the best relative slagging performance. The reported results are in good agreement with the results of the

predictions using the proposed NSI. The same analysis applies for all the remaining sets of coals that have been tested.

The last but one row shows the reported performance of the coals on a case-by-case basis. The first five columns in that row represent the Indian coals, as stated earlier, with coal 4 having the highest slagging potential, followed by coal 2, and then coal 3. The columns 6 - 9 are for the four Australian coals 1-4, columns 10 - 12 are for the Indonesian, Columbian and South African coals, columns 13 & 14 are for the US coals 1 & 2, and columns 15 -17 are for the UK coals 1-3 (Lawrence *et al.*, 2008; Degereji *et al.*, 2011; Laursen *et al.*, 1998; Zygarlicke *et al.*, 2000; Lee and Lockwood, 1999).

The last row in Table 6.4 shows the indices that have successfully predicted each set of the tested coals. The results show that it is only the proposed NSI that satisfactorily predicted the field performance of the Indian, Australian, Indonesian, Columbian and South African coals. On the other hand, the last two columns of the last row show that all the tested existing coal slagging indices were successful in ranking the UK and the US coals.

In the overall analysis, the proposed NSI predictions correlate well with the reported field performance of all the coal types that have been investigated in this study. On the other hand, the tested existing slagging indices, which are derived mostly on the basis of the ash chemistry, have only accurately predicted the slagging potential of the UK and the US coals. Such indices were originally derived for UK and US coals (McLennan *et al.*, 2000).

Sensitivity of the NSI: Fig. 6.14 shows the predicted effects of varying the percentage of incoming ash on the slagging potential of the coals. Using the Indian coal 2, the proposed NSI shows a steady and proportional increase in the slagging potential of the coal as the percentage of the ash loading increases.

The direct proportional increase in the slag build-up with an increase in the ash content suggests that the availability of low viscosity ash particles determines the rate of deposit accumulation on the water wall surfaces (Lawrence *et al.*, 2008).

For between 38 and 40% ash loading, the slagging potential increases sharply before it returns to a steady increase. This phenomenon has been described relative to the ash shrinkage rates and the ash loading. If either the ash shrinkage rate, or the ash content, is very high, while the other is very low, the overall slagging under furnace dynamic conditions may not be significant (Lawrence *et al.*, 2008).

In this investigation, the ash shrinkage rate is indirectly related to the ash viscosity, and the viscosity of Indian coal 2 is within the range of high slagging tendency, 10^5-10^7 Pa.s (Gupta *et al.*, 1998). Therefore, when both the ash content in the coal and the shrinkage rate are moderate, a high slagging potential is expected. However, if either the ash content or the ash shrinkage rate or both are low or high, a low slagging potential is expected (Lawrence *et al.*, 2008).

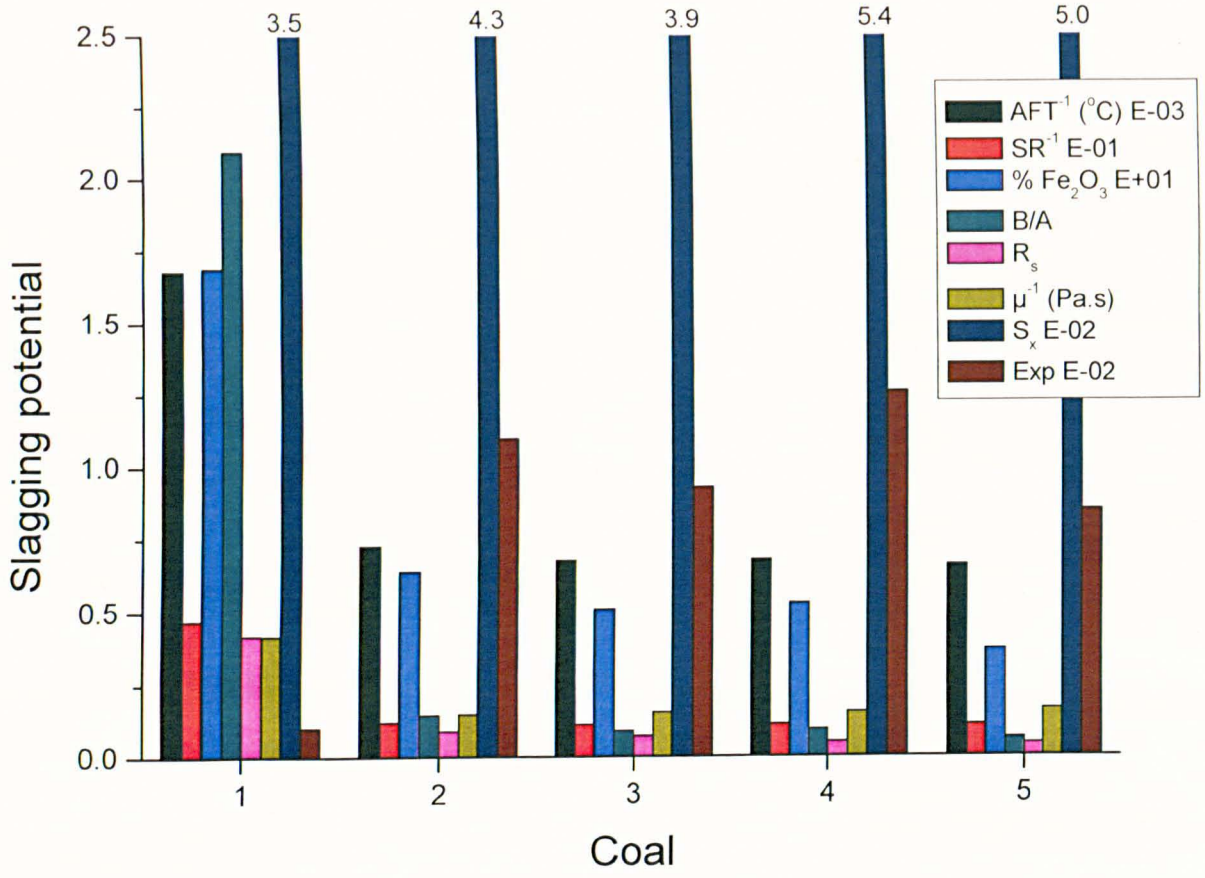

Fig. 6.8 Comparing the results of predictions using the NSI (S_x) and six existing slagging indices with experimental data (Exp) on five Indian coals.

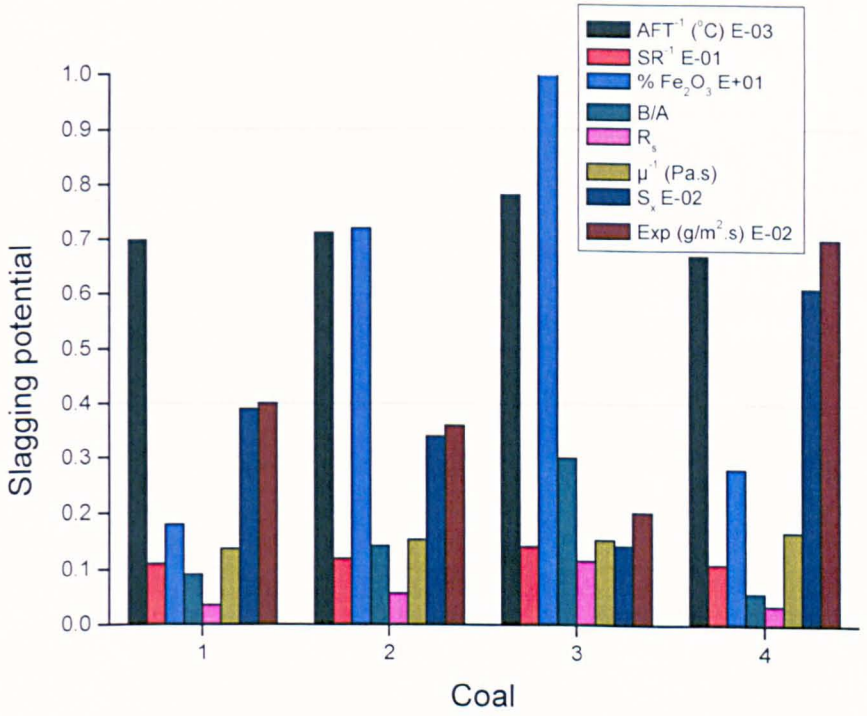

Fig. 6.9 Comparing the results of predictions using the NSI (S_x) and six existing slagging indices with experimental data (Exp) on four Australian coals.

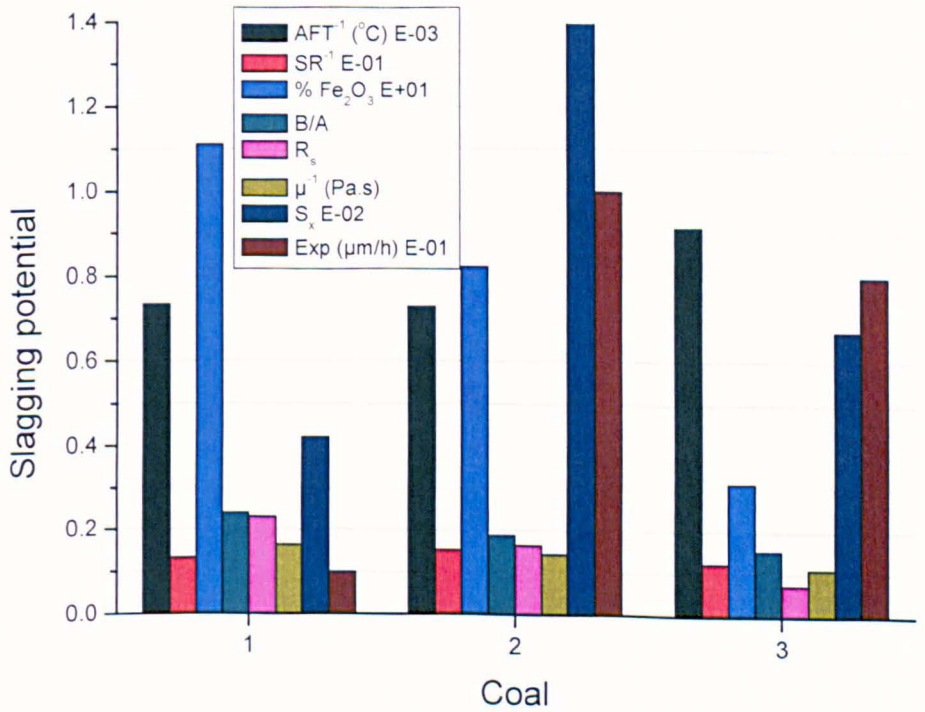

Fig. 6.10 Comparing the results of predictions using the NSI (S_x) and six existing slagging indices with experimental data (Exp) on Indonesian, Colombian and South African coals.

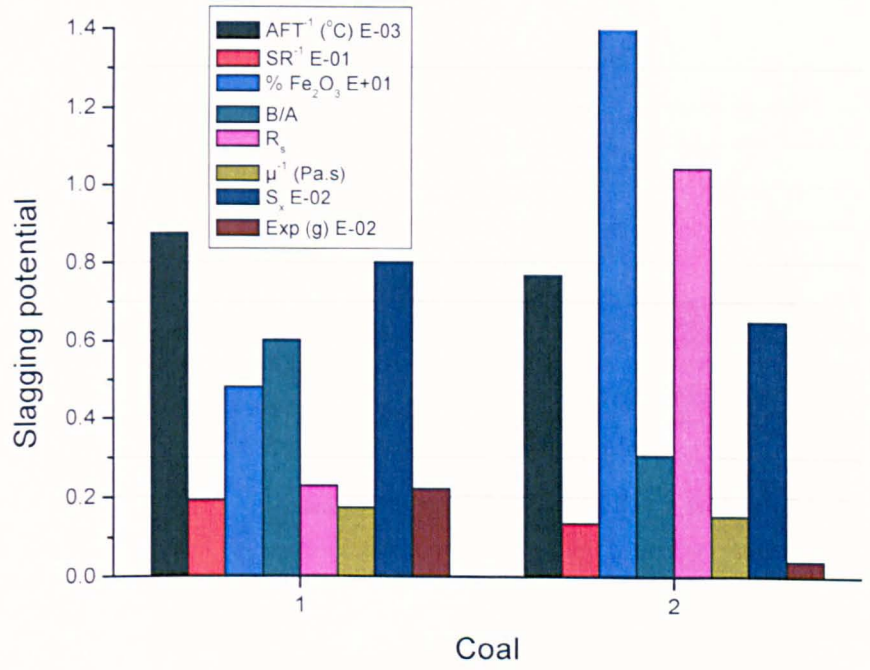

Fig. 6.11 Comparing the results of predictions using the NSI (S_x) and six existing slagging indices with experimental data (Exp) on two US coals.

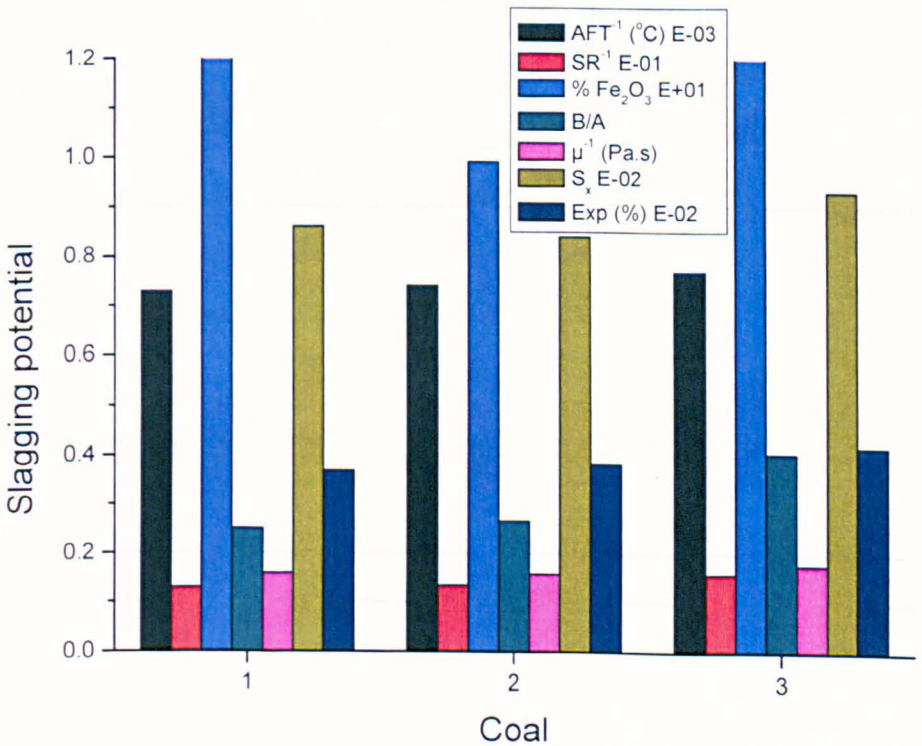

Fig. 6.12 Comparing the results predictions using the NSI and five existing slagging indices on three UK coals.

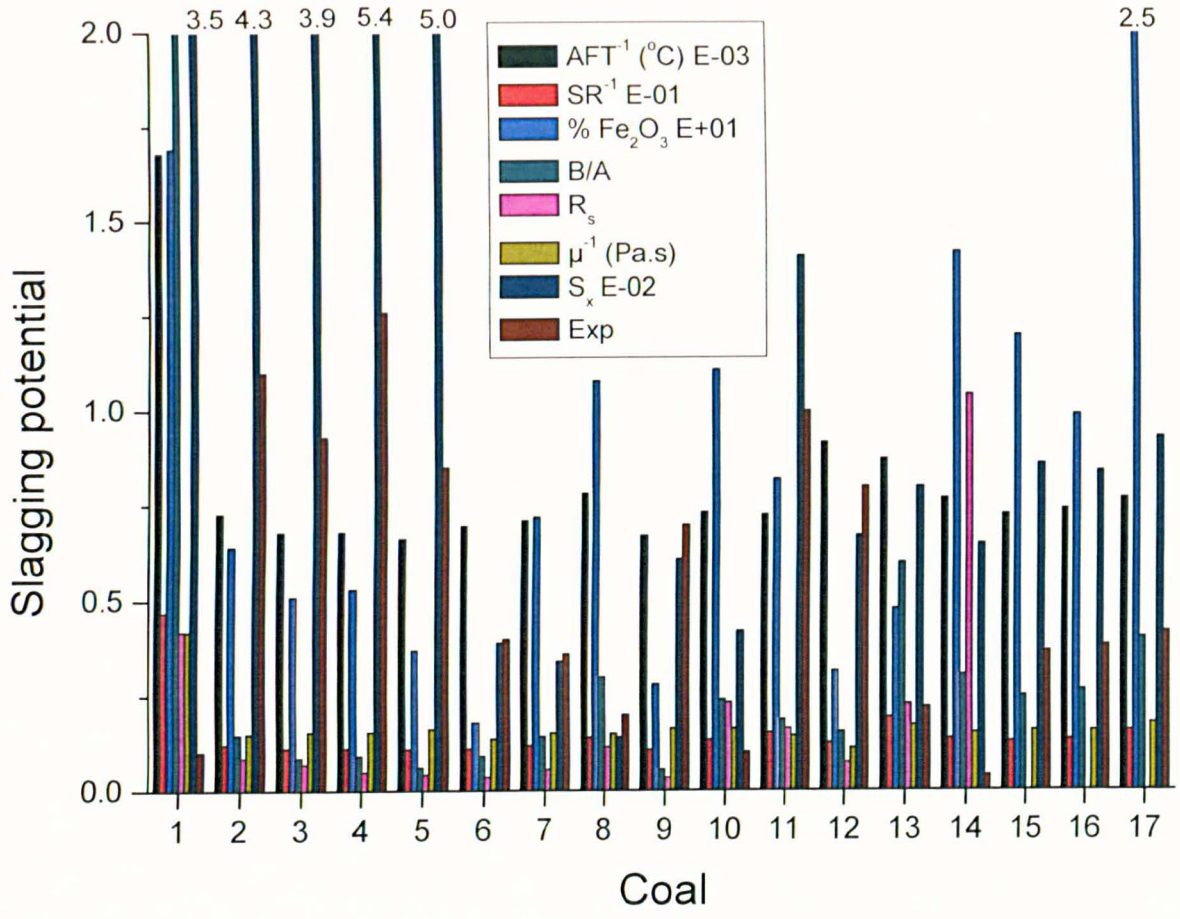

Fig. 6.13 The performance of the NSI and six existing slagging indices in predicting the slagging potential of wide range of coals.

Table 6.4 Performance of different coal slagging indices on 17 tested coals: tabular analysis of Fig. 6.13.

	Slagging potential of all the coals tested in decreasing order																	
Index	**Indian coals**					**Australian coals**				**Indonesian, Colombian & SA coals.**			**US coals**		**UK coals**			
AFT	1	2	4	3	5	3	2	1	4	3	1	2	1	2	3	2	1	
SR	1	13	17	11	8	3	2	1	4	2	1	3	1	2	3	2	1	
Fe_2O_3	17	1	14	15	10	3	2	4	1	1	2	3	2	1	3	1	2	
B/A	1	13	17	14	8	3	2	1	4	1	2	2	1	2	3	2	1	
R_s	14	1	10	13	11	3	2	1	4	1	2	3	2	1	-	-	-	
μ	1	17	13	9	10	4	2	3	1	1	2	2	1	2	3	1	2	
S_x	4	5	2	3	1	4	1	2	3	2	3	1	1	2	3	1	2	
Exp	**4**	**2**	**3**	**5**	**1**	**4**	**1**	**2**	**3**	**2**	**3**	**1**	**1**	**2**	**3**	**2**	**1**	
Correct predictions	S_x					S_x				S_x			SR, B/A,μ,S_x		ST, SR, B/A, μ, S_x			

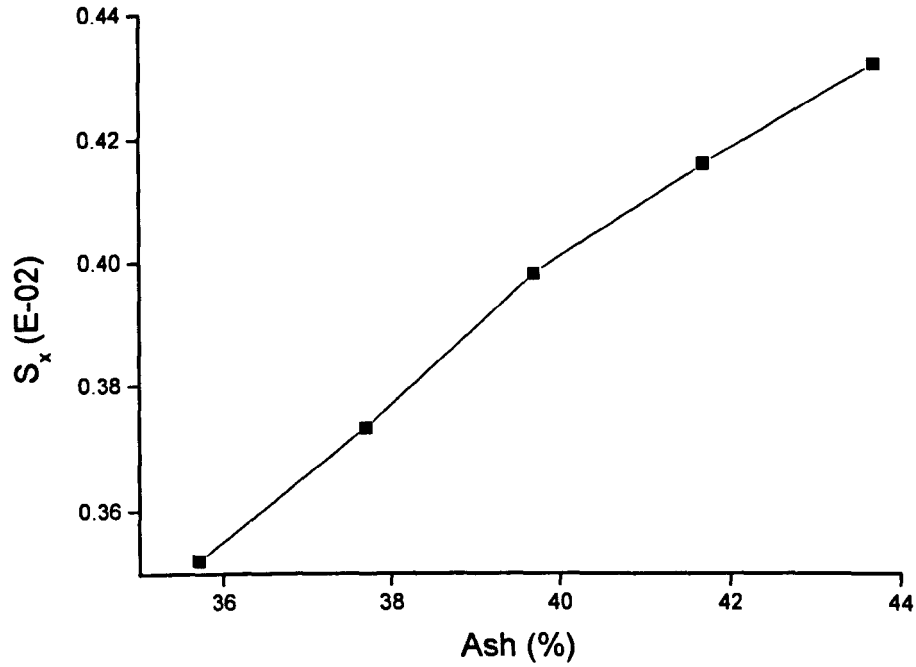

Fig. 6.14 The effect of ash loading on the slagging potential of coal 2 as predicted by the NSI.

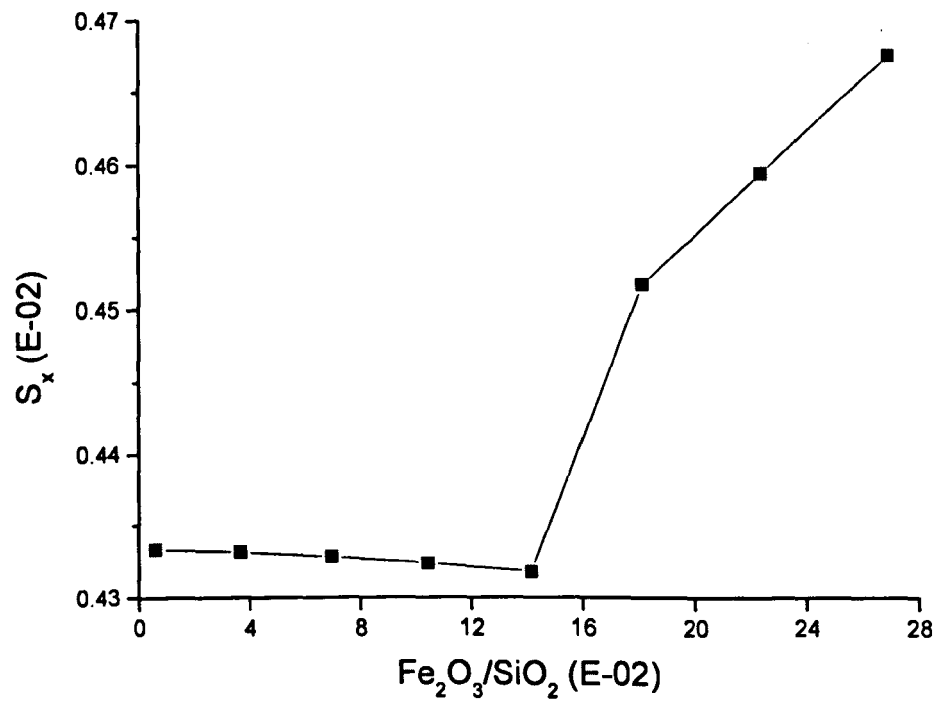

Fig. 6.15 The effect of varying the ratio of iron to silicon oxides on the slagging potential of coal 2 as predicted by the NSI.

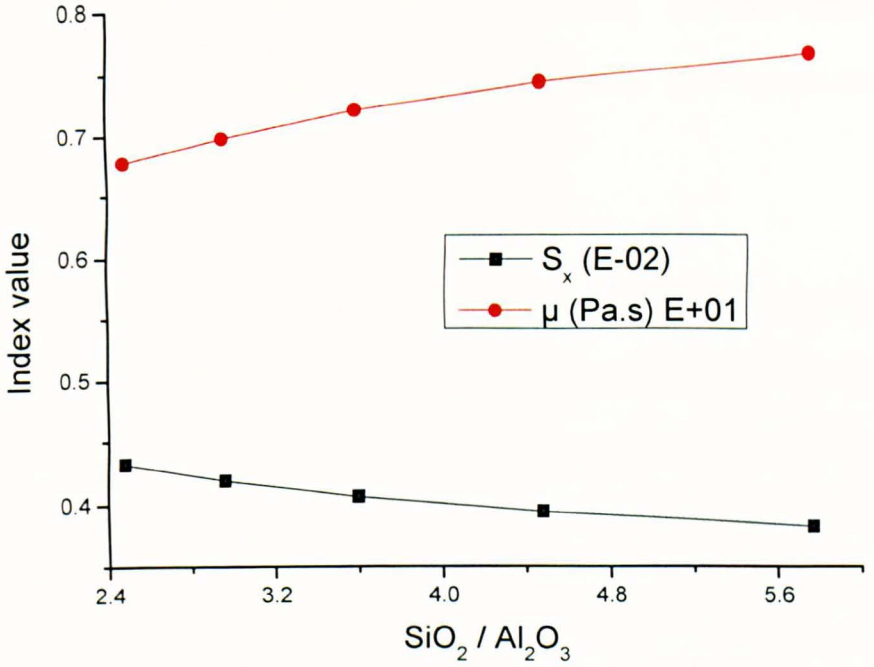

Fig. 6.16 The effect of varying the SiO_2/Al_2O_3 ratio on the slagging potential of Indian coal 1 as predicted using the NSI and viscosity index.

In Fig. 6.15, the ratio of the iron to silicon oxides, being the dominant basic and acidic oxides, respectively, was considered when investigating the sensitivity of the NSI. While gradually decreasing the weight percentage of the silicon oxide for Indian coal 2, from 61.0 and increasing that of the iron oxide above 6.4, the slagging index predicts a small but steady decrease in the slagging potential of the coal.

However, when the silicate was reduced to less than 59%, and the iron oxide increases to about 9%, the NSI predicts a sharp increase, which became steady afterwards. This trend is consistent with the prediction principles of the silica ratio and percentage of iron oxide.

The SiO_2/Al_2O_3 ratio affects the viscosity and melting characteristics of the coal ash (Luxsanayotin, Pipatmanomai & Bhattacharya, 2010). The low content of SiO_2 in the ash lowers the particle viscosity, which results in a higher sticking probability (Huang *et al.*, 1996).

The effects of SiO_2/Al_2O_3 have been investigated, and in Fig. 6.16 the predicted results using the NSI indicate an increase in the ash viscosity and a decrease in the NSI value as the SiO_2/Al_2O_3 ratio increases, and hence decreasing the slagging potential. This investigation was conducted on Indian coal 2, however the Australian coals have high SiO_2/Al_2O_3 ratios and they have been predicted to have a low slagging potential.

6.5 The Performance of the Proposed NSI on Coal Blends

The use of the NSI has been extended to coal blends in order to assess it flexibility. The reported field performance of a few coal blends have been compared with the results of the predictions using the NSI on those sets of coals and blends. A comparative analysis and conclusions on these tests are reported in this section. Also, in this section, the reported performance of some slagging techniques has been compared with the performance of the NSI, and a comparative analysis has been made.

6.5.1 Properties of tested coal blends

The properties of the parent coals and their blends are presented in Table 6.4. The parent coals A, B and E are Australian bituminous coals, and the properties

of coals A and B are the same as the properties of the Australian coals 1 and 2 in table 6.2. Although coal E has the least content of ash (7.4%), the proximate analysis data appears similar for all the coals.

The elemental ash content of the blends appears to be proportional to the blending ratio. For example, silica content for coals A and B are 71.5 and 58.4%, respectively, and for blend AB, with blending ratio 3:1, is 67.2%, while for blend BA, with blending ratio 1:3, is 62.7%. The blending ratio is shown in Table 6.5.

Also, this linearity has been observed in the computed weight of ash, as shown in the last column of Table 6.5. For example, coals A and B, and blends AB and BA have 0.32, 0.24, 0.30 and 0.27 weight factors, respectively. Ordinarily, one will expect the linearity shown in the ash elemental content of the parent coals and their blends, to extend to their respective ash behaviour in boilers. Table 6.6 shows some measured and derived properties of the tested coals/blends that have been discussed in this Chapter.

Table 6.5 Properties of the coals/blends tested using the NSI (wt%, db) (Rushdi *et al.*, 2004).

S/N	Coal / Blend	FC	VM	Ash	C	H	N	S	O	SiO_2	Al_2O_3	Fe_2O_3	CaO	MgO
1	A	45.5	45.9	9.6	70.0	5.3	11.0	0.4	13.7	71.5	15.9	1.8	4.2	1.3
2	AB	51.4	39.6	9.0	72.5	5.1	1.2	0.4	11.8	67.2	19.0	3.6	3.7	1.1
3	BA	58.6	33.0	8.4	75.0	4.8	1.5	0.4	9.8	62.7	22.2	5.4	3.1	0.9
4	B	65.5	26.7	7.8	77.5	4.6	1.8	0.4	7.9	58.4	25.3	7.2	2.6	0.7
5	AE	48.8	42.3	8.9	72.3	5.2	1.2	0.4	11.9	66.4	17.7	4.3	4.5	1.2
6	EA	54.4	37.5	8.1	75.5	5.0	1.5	0.4	9.6	59.5	20.2	7.6	4.9	1.0
7	E	58.7	33.9	7.4	77.8	4.9	1.8	0.3	7.8	54.4	22.0	10.1	5.2	0.9

Table 6.6 Measured and derived properties of the tested coals/blends (Rushdi *et al.*, 2004; Su *et al.*, 2001b).

Coal/Blend	Blending	Fe_2O_3/CaO Molar ratio	TMA Penetration %	Viscosity (Pa.s) Order	Ash content Factor (kg/MJ)
A	-	0.26	8.89	7.4	0.32
AB	67% A : 33% B	0.65	16.00	7.1	0.30
BA	33% A : 67% B	0.84	7.37	6.9	0.27
B	-	1.41	12	6.6	0.24
C	-	0.51	14.25	6.7	0.10
CD	75% C : 25% D	0.76	3.49	6.5	0.18
DC	50% C : 50% D	0.94	1.23	6.3	0.26
D	-	4.10	1.93	6.1	0.42
A	-	0.26	8.89	7.4	0.32
AE	67% A : 33% E	0.48	16.48	7.2	0.29
EA	33% A : 67% E	0.60	3.68	7.0	0.26
E	-	0.67	5.68	6.6	0.23

6.5.2 Results of slagging tests on coal blends

Two research groups have reported some slagging tests results on Australian bituminous coals/blends. One group has reported on the use of the scanning electron microscopy (SEM), thermo-mechanical analysis (TMA) and the ash bulk analysis, in testing the slagging potential of coals/blends (Rushdi, Sharma & Gupta, 2004). The other group has used the Fe_2O_3/CaO molar ratio to predict the slagging potential of the Australian coals/blends, and they compared the predicted results with deposit growth rate measurements from the ACIRL furnace (Su *et al.*, 2001b).

SEM method: The scanning electron microscopy has been used to obtain the average deposition layer thickness for the Australian coals and blends on alumina probe in a drop tube furnace. The results obtained using this technique was considered as the baseline data, which was used to validate the TMA and the bulk ash analysis results.

TMA method: The thermo-mechanical analysis was used to study the thermal behaviour of the ash from the same coals and blends, in terms of the slagging potential. This technique basically assesses the melting of the ash as a function of the temperature. It was reported that the results obtained using the TMA have good correlation with the baseline (SEM) data. According to the report, for the set of coals/blends A-B, the blend AB appears to have the highest slagging potential, followed by the parent coal B, and then the parent coal A (Rushdi *et al.*, 2004). As shown in Fig. 6.17, the reported results show consistency between the SEM and the TMA techniques.

In similar consistent reported results, in Fig. 6.18, both the SEM and TMA suggest that blend AE has the highest slagging potential for the set A-E. The parent coal A is the second highest in terms of slagging, and the blend EA has the lowest slagging potential.

μ and R_s methods: The use of the viscosity method and the product of the basic to acidic ratio and the dry sulphur content in the coal, to predict the slagging potential of the same sets of coals and blends, has been reported to be unsuccessful (Rushdi *et al.*, 2004).

Observation: In a separate investigation, Su and others have observed the deposit build-up rates for the same sets of Australian coals/blends on three slag panels of the ACIRL furnace (Su *et al.*, 2001b). The observed data has been used to validate the results of the slagging predictions using some of the existing coal slagging indices.

Fe_2O_3/CaO method: The Fe_2O_3/CaO molar ratio has been used to predict the slagging potential of the coals and blends. It was assumed that eutectics are formed between 0.3 and 3.0 ratio values, and severe slagging occurs at about 1.0. This index did not properly account for the molar ratio values that are above 1.0, or much less than 1.0. Although a satisfactory correlation between the Fe_2O_3/CaO molar ratio and the observed slagging propensity of coals and blends has been reported, it is clear from Fig. 6.19 that the blend BA has a ratio value 0.84, and therefore it is assumed to have the highest slagging potential. However, the observed data shows that blend AB has the highest slagging potential, and this is followed by the source coal A.

In Fig. 6.20, the reported molar ratio values for all the coals and blends in set A-E, are less than 1.0, and therefore it was reported that there was no slagging problem for this pair of blends (Su *et al.*, 2001b). However, the measurement data reveals that the source coals A and E have the highest and the lowest relative slagging potentials in that set.

It is important to mention here that, although the correlation between the SEM and the TMA analyses is better than that of the Fe_2O_3/CaO molar ratio when compared with the observed data, the SEM results are inconsistent with the results of several investigations on the same source (Australian) coals (Rushdi *et al.*, 2005; Su *et al.*, 2001b; Degereji *et al.*, 2011). For example, the above references have reported that the parent coal A has a higher slagging potential than the parent coal B, and this is consistent with the observed results reported in Fig. 6.19. Therefore, in view of this, the observed deposition rates in the

ACIRL furnace (Su *et al.*, 2001b) are considered as the baseline data for this investigation.

However, within the reported investigations, when one attempts to compare the performance of the TMA and the Fe_2O_3/CaO molar ratio techniques using the observed deposit growth rates for the set of coals and blends (A-B), it appears that the TMA predictions are far better in accuracy when compared to the Fe_2O_3/CaO predictions, as shown in Fig. 6.21. The TMA technique predicted blends AB and BA have the worst and the least slagging potentials, respectively, and this is in agreement with the observed data. On the other hand, the Fe_2O_3/CaO predicts the source coals B and A to have worst and least slagging potentials, respectively, which is inconsistent with the observed data.

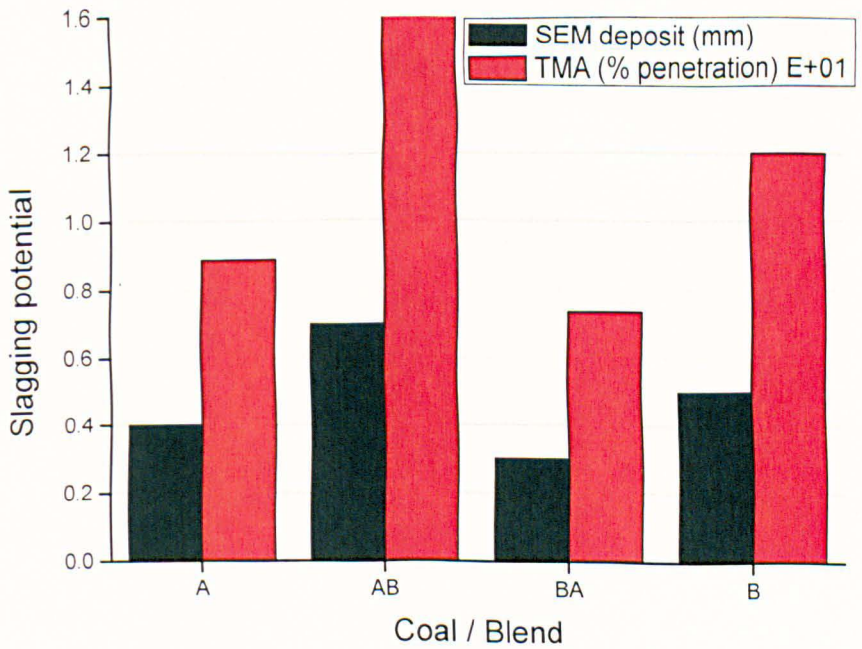

Fig. 6.17 Comparing ash deposit measured using the SEM and the percentage penetration obtained using the TMA technique for coals/blends set A-B (Rushdi *et al.*, 2004).

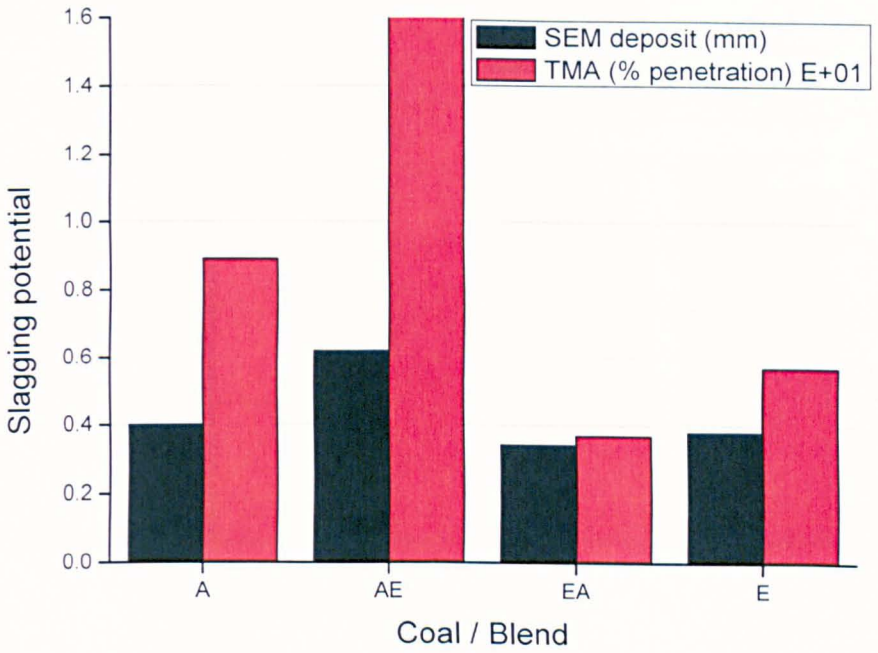

Fig. 6.18 Comparing ash deposit measured using the SEM and the percentage penetration obtained using the TMA technique coals/blends set A-E (Rushdi *et al.*, 2004).

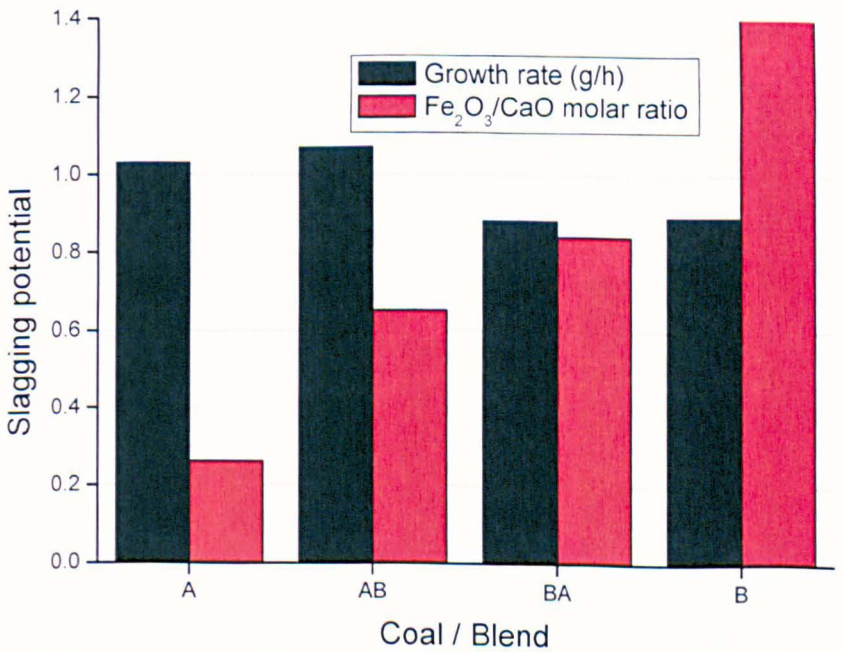

Fig. 6.19 Comparing ash deposit growth rate measurement with the results of predictions using the Fe_2O_3/CaO molar ratio for coals/blends set A-B (Su *et al.*, 2001).

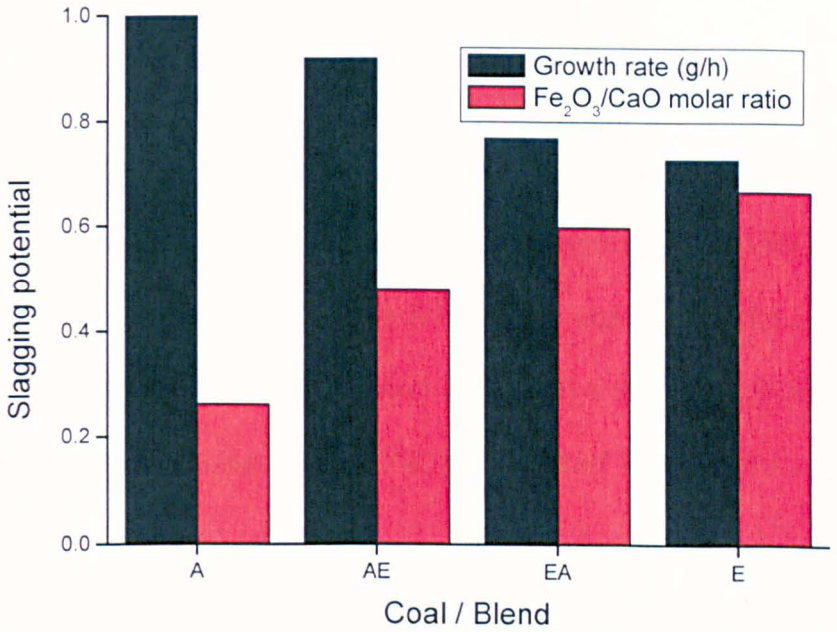

Fig. 6.20 Comparing ash deposit growth rate measurement with the results of predictions using the Fe_2O_3/CaO molar ratio for coals/blends set A-E (Su *et al.*, 2001).

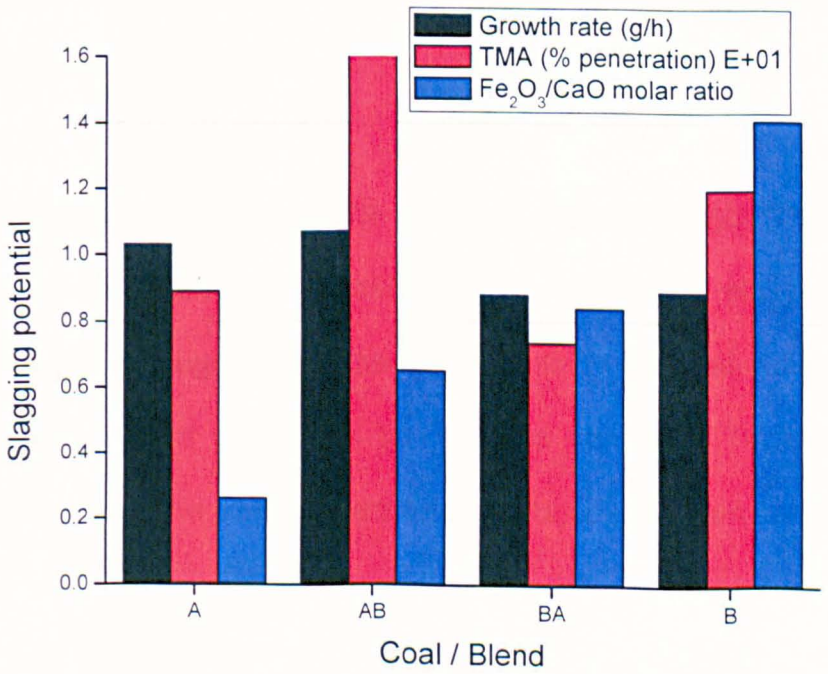

Fig. 6.21 Comparing measured ash deposit growth rate with the results obtained using the TMA and Fe_2O_3/CaO molar ratio for coals/blends set A-B (Su *et al.*, 2001; Rushdi *et al.*, 2004).

6.5.3 Results and discussion of the predictions using the NSI on coal blends

The results of the prediction using the NSI have been compared with the measurement data on the Australian coals and blends in set A-B, as shown in Fig. 6.22. The reported growth rate measurements show that the blend AB has the highest slagging potential, while the source coal B has the lowest slagging potential. The NSI predicted the blend BA to have the second highest slagging potential, while the measurement data show that the source coal A has the second highest slagging potential.

In the second set of coals/blends (A-E), in Fig. 6.23, the growth rate measurements show that the parent coal A has the worst slagging potential and the parent coal E has the least slagging potential, while the proposed NSI predicted blend AE to have the worst slagging potential and the source coal E to have the least.

The results of predictions using the proposed NSI also suggest that the source coal A has the second highest slagging potential, while the reported measurement data suggest that the blend AE is the second. The parent coal A has a higher content of SiO_2 in the ash, as shown in Table 6.4, which is expected to reduce the slagging tendency of the coal A when compared to other coals.

Also, the blend AE, has a higher content of Fe_2O_3 in the ash (4.3%), compared to that of the parent coal A (1.8%), and this is another pointer that the blend AE

may have a higher slagging than the parent coal A. The ash content in the coals is another important factor that affects the accumulation of slag in boilers, and Table 6.4 shows that the ash content of the source coal A is slightly higher than that of the blend AE by 1.5%. Although all these are significant indicators of the slagging tendency, it is reported to be difficult to predict the ash behaviour of the coal blends relative to their parent coals (Su *et al.*, 2001b).

Fig. 6.24 shows the performance of four coal blends, relative to one another. There is a very good correlation between the measurement data and the results of the predictions using the NSI for all the tested blends. This good correlation suggests that the NSI has successfully ranked the coal blends according to their field performance, irrespective of their source coals.

The results presented in Fig. 6.24 show that blend AB has the highest slagging, followed by the blends AE, BA, and then EA in descending order. Some of the properties of the coal blends also suggest that the predicted slagging potentials are satisfactory. For example, coals with high ash content are expected to yield high slag accumulation. From Table 6.4, blends AB, AE, BA and EA, have 9.0, 8.9, 8.4 and 8.1 weight percentages of ash content, respectively.

The better set of predictions results obtained, using the proposed NSI, may be attributed partly to the ability of the model to account for the following conditions: if either the ash shrinkage rate or the ash content in coal is high, while the other is less, the overall slagging, under furnace dynamic conditions, may not be significant.

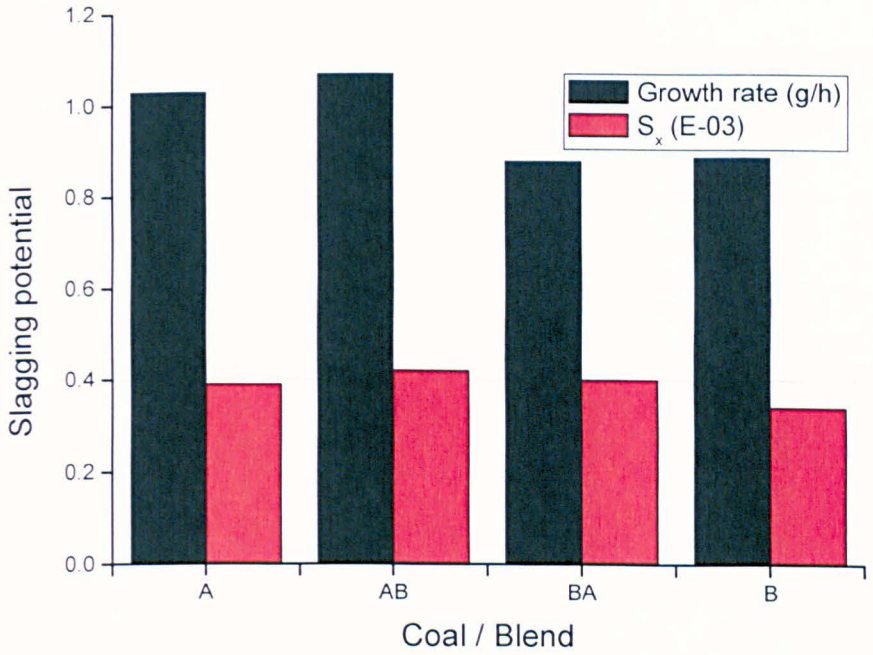

Fig. 6.22 Comparing ash deposit growth rate measurement and ash deposit thickness measurement with the results of predictions using the NSI for set of coals and blends (A-B).

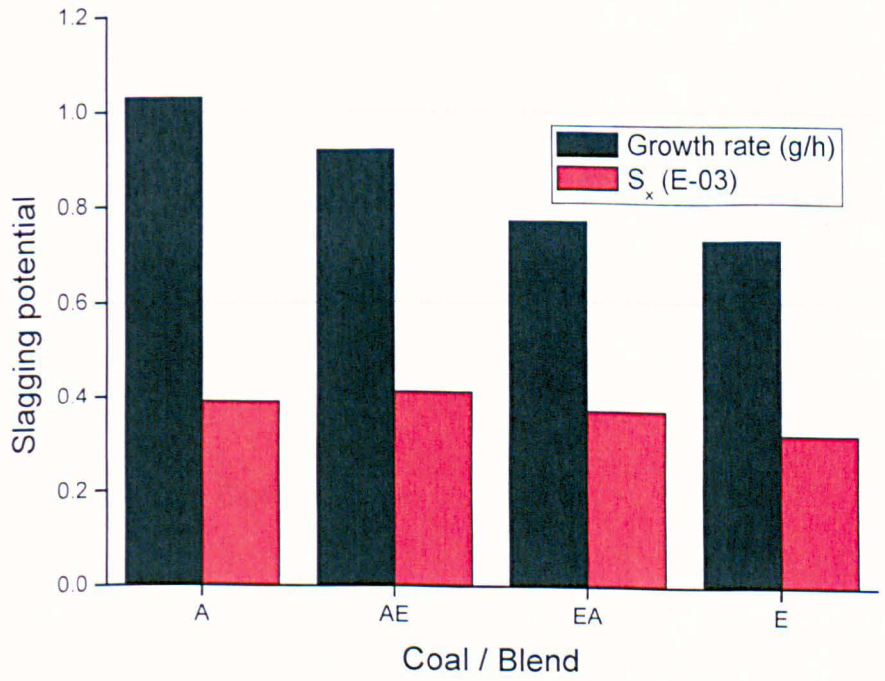

Fig. 6.23 Comparing ash deposit growth rate measurement and ash deposit thickness measurement with the results of predictions using the NSI for set of coals and blends (A-E).

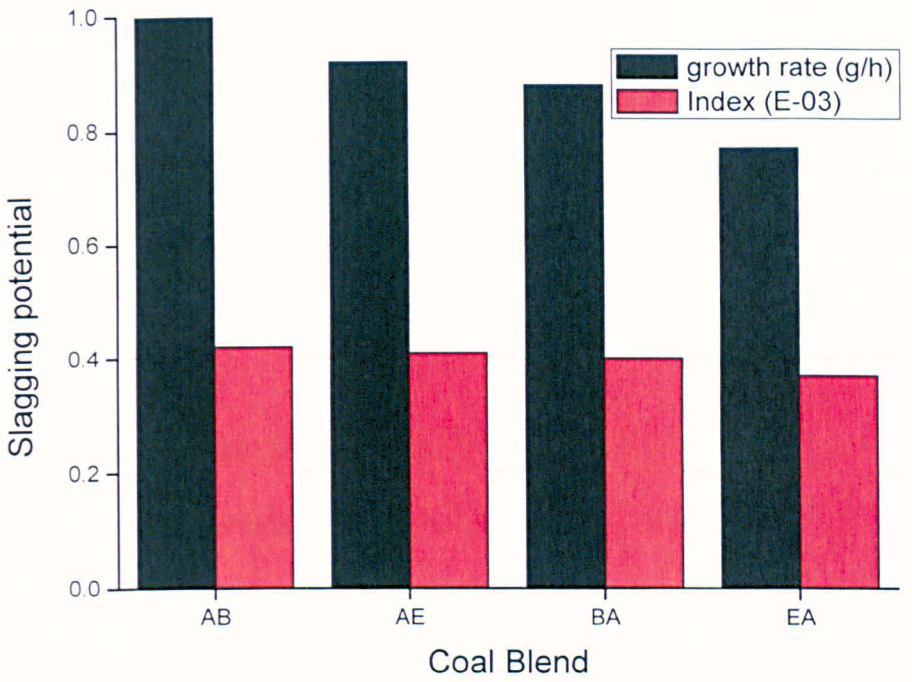

Fig. 6.24 Comparing ash deposit growth rate measurements with the results of predictions using the NSI for two sets of four coal blends (A-B and A-E).

However, if both the viscosity of the ash and the ash content are moderate, a high slagging is expected (Lawrence *et al.*, 2008); the viscosities of a high slagging tendency are within the value range of 10^5-10^7 (Pa.s), and such viscosity range is considered as moderate (Gupta *et al.*, 1998). The ash viscosity and the ash content techniques are also incorporated in the proposed NSI.

6.6 Summary and Conclusions

The burning of coal will remain the dominant source of power generation for many years to come. However, slagging and fouling in coal-fired boilers remain

a challenge for the energy engineers as they strive to optimize the combustion efficiency.

The selection of a suitable coal as a fuel has been identified as one effective way of tackling boiler problems that are related to ash. However, the existing coal selection tools yield misleading results when their use is extended to a wide range of coals.

Although the ash fusion temperature, the ash particle viscosity and the bulk ash chemistry are the three most popular bases for characterizing coal ash deposition and slagging, the content of ash in the coal, and the mineral matter transformation and associations can also influence slag accumulation in boilers, significantly.

In this investigation, a numerical slagging index has been developed based on the viscosity of the ash, the softening temperature of the ash and the ash content in the coal, with some basic assumptions. The Bomkamp modified version of the Watt-Fereday model has been used to determined the ash viscosity.

The particle softening temperature is determined from the bulk chemistry of the ash. The incoming ash is expressed in terms of kg per MJ, rather than weight percentage.

The NSI model has been implemented using the 'define-on-demand' UDF in the FLUENT 12.1 software, and it has been tested over a wide range coals,

including lignite and bituminous coals, and some sets of coal blends form different regions.

The general performance of the code on the tested coals and blends is very good when compared with the performance of the existing slagging indices.

The flexibility of the model has also been tested by varying the values of some important input parameters, such as the ash loading, the percentages of iron and silicon oxides, and the ratio of silica to alumina.

From the results of the predictions using the proposed NSI and some of the existing slagging indices, the following conclusions are made:

- A numerical slagging index has been developed based on the viscosity of the ash, the softening temperature of the ash and the ash content in the coal.
- The numerical slagging index has been successful in ranking about 90% of the seventeen different coals tested in this investigation.
- The six existing slagging indices that have been tested in this investigation, accurately predicted the performance of the UK and the US coals, but yielded poor performance when their use was extended to other coals, such as, the Australian, Indian and South African coals.
- The NSI has a better overall slagging prediction on all the coals tested when compared with the performance of the six existing slagging indices that have been investigated.

- The NSI has a better prediction of the performance of the sets of coals and blends that have been investigated, when compared with the reported performance of some of the prediction tools.
- The NSI has successfully predicted the performance of four coal blends that have been investigated.
- The proposed numerical slagging index is a step forward in the drive for a more generic method for predicting the pre-combustion slagging behaviour of coals in boilers.
- In addition to the chemistry of the ash, the mineral distributions and transformations, the ash loading in the coals have a significant effect on the rate of the ash accumulation in the boilers.
- The presence of low-viscosity materials and the ash content in coals/blends enhances the slagging propensity.
- The conclusion by Rushdi *et al.* (2004) and Su *et al.* (2001b), namely, the performance of blends may not be interpreted linearly from that of their parent coals, is upheld.
- It is important to note that the interaction of different ash particles on the deposit surface and how this affects deposit build-up needs to be well understood in order to provide a better prediction tool for coals and blends.

CHAPTER 7

ASSESSMENT OF CO-FIRING SLAGGING POTENTIAL

7.1 Introduction

The co-firing of biomass with pulverized coal in the existing coal fired facilities is widely used in order to reduce CO_2 emissions (Sami, Annamali & Wooldridge, 2001). It has been estimated that a reduction of about 300 Mt of CO_2 emissions can be achieved if only 5% of the total world energy generated using coal is substituted with biomass (IEA, 2009, cited in Munir *et al.*, 2010a). This estimation gives incentive to the co-firing practices.

However, the complex nature of the mineral matter composition of biomass may result in an increased slagging tendency during co-firing (Wigley, Williamson, Malmgren and Riley, 2007). Also, since biomass has a higher content of moisture, volatile matter and oxygen, and lower density, ash content and heating value than coal, an in-depth understanding of the characteristics of the blended fuels is necessary in order to achieve high co-firing efficiency (Molcan *et al.*, 2009).

Although several research activities, including the use of CFD techniques, are ongoing in order to fully understand the deposition mechanism in co-firing, still there is no available tool that predicts the slagging and fouling of biomass unequivocally, and therefore, coal specific ash fusibility correlations are used in practice for biomass (Munir, Nimmo & Gibbs, 2010b).

For blends with < 20% biomass, the ash mixture is still predominantly alumino-silicate, and the pure coal slagging indices can be used with caution, to predict the slagging potential of such blends (Tillman, Conn & Duong, 2009; Stam, Livingston, Cremers & Brem, 2009).

Using pure coal slagging indices to assess co-firing may not guarantee prediction accuracy. This is because the ash behaviour during co-firing is not yet fully understood (Shao *et al.*, 2010). Additionally, the composition of biomass differs from that of coal. For example, the inorganic matter in coal is in the form of minerals, while a substantial part of the alkali metals in biomass are present as salt (Zheng, Jensen, Jensen, Sander & Junker, 2007).

According to Heinzel *et al.* (1998), whether co-firing deposits show the behaviour of two single ashes or that of a mixture of ash under boiler conditions needs to be understood. Also, the knowledge of the nature of potassium release during biomass combustion is still inadequate. Although the release of potassium during co-firing is said to be mainly KCl in the fly ash, K_2SO_4, K-silicate and K-aluminium-silicates (Zheng *et al.*, 2007), other species, such as $CaSO_4$ which may possess lower mobility than the K_2SO_4, can also deposit on the boiler walls (Shao *et al.*, 2010).

In this thesis, the development of a numerical slagging index to predict the slagging potential of coals has been reported earlier. At this stage, the proposed coal slagging index has been modified such that it can predict the slagging

potential of coal and biomass blends by accounting for the introduction of a small percentage of biomass ratio (< 20%) in a coal fired plant.

Although the model is expected to predict the slagging potential of coal and biomass blends, more work still needs to be done, especially in integrating the effect of minerals transformation and association into the model in order to improve its performance.

7.2 Some of the Slagging Parameters

In order to understand the ash behaviour of coal/biomass blends, and to be able to come up with a reliable co-firing slagging tool, it is critical to evaluate the properties of both the coal and the biomass and the potential interaction between them (Tillman *et al.*, 2009).

The properties of coal and biomass in Table 7.1 are some of the factors that can influence slagging. Although the blends are made in percentages, in terms of either weight or energy, certain properties of the blends, such as reactivity may not necessarily behave according to the ratios of the fuels (Tillman *et al.*, 2009).

In Table 7.1, any of the parameters listed under coal can be used to characterize the slagging of coal, likewise for the biomass. However, any prediction tool that has been developed for a particular fuel, based on the cumulative effect of all the parameters listed under the fuel, may produce better

predictions, especially when compared to the results of predictions using a single parameter.

Table 7.1 Some of the fuel properties that have an influence on the slagging potential.

S/N	Coal	Biomass
1	Viscosity	Melt fraction
2	Softening temperature	Softening temperature
3	Ash loading	Ash loading
4	Ash elements (SiO_2, Fe_2O_3, etc.)	Ash elements (K_2O, P_2O_5, Na_2O, etc.)
5	Interaction and association of coal elements	Interaction and association of biomass elements
6	Interaction and association between coal and biomass elements	

In an attempt to answer the question 'whether the blend's ash behaves as two individual ashes or as a mixture ash', in this investigation, the ash of the blends is considered with dual characteristics. At the initial stage of calculations, the coal ash and the biomass ash are assumed to behave independently. At high levels of reactivity, the components of the individual ashes may interact and result in additional species. This has not been considered here.

The coal numerical slagging index earlier reported in chapter 6 of this thesis considers the viscosity, fusibility and the weight of the ash in the coal to assess the slagging potential of the coal. In a similar manner, the softening temperature, weight of the ash and the ash composition are considered in

assessing the biomass component of the blend. Also, the content of some important species, such as Fe_2O_3, K_2O and TiO_2, continue to change by varying the biomass ratio (BR) in the blend (Molcan *et al.*, 2009), as shown in Fig. 7.1.

In addition, the release of some elements, such as potassium, chlorine, sodium, etc., during and after devolatilization, coupled with the boiler thermodynamics, may strongly influence the slagging potential of the blends. Therefore, there is a need to establish the rates at which some of the alkali metals react with silicate, iron oxide and calcium oxide that are released from the coal ash. Also, the effects of the transformations and association of minerals are important.

7.3 Numerical Modelling

For effective modelling, it has been assumed that the individual properties of the fuels and the interactions between them under high temperatures are responsible for the ash slagging. Ash particles that transverse the boundary layer and hit the boiler walls may stick, and can cause slagging.

The stickiness of a silica-rich particle can be determined from its viscosity (Degereji *et al.*, 2011), while for a particle rich in salt, its stickiness can be determined from its softening temperature and/or melt fraction (Ma *et al.*, 2006).

Also, it was found that the content of alkali metals (K, Na & Ca), as well as Al_2O_3 and P_2O_5, were enriched in the deposited ash under co-firing conditions (Shao *et al.*, 2010). On the other hand, a significant decrease in the content of

Fe_2O_3 in the ash and an increase in TiO_2 content in the ash as the biomass ratio (BR) increases, are reported (Molcan *et al.*, 2009).

Although coal slagging indices are currently used to assess the slagging potential of coal/biomass blends with < 20% BR, in this chapter, the coal slagging index reported in chapter 6 has been modified in order to account for the effect of biomass blending.

The coal numerical slagging index in equation (6.7) is expressed in terms of the incoming ash, γ, and ash viscosity, μ, as defined in equations (6.5) and (3.33), respectively.

For coal/biomass blends, the effects of biomass addition on deposit sintering can be predicted by determining the viscosity of the blend ash from the ash content and ash chemistry of the individual fuels (Wigley *et al.*, 2007). Thus, the weight of the incoming ash has been defined in terms of the content of the ash and the heating value of the individual fuels as follows:

$$\gamma = x\gamma_c + y\gamma_b \tag{7.1}$$

where x, y, γ_c and γ_b are the ratio of coal in the blend, the ratio of biomass in the blend, the weight of coal ash and the weight of biomass ash, respectively. Also, the ash viscosity has been redefined to account for the softening temperatures of both the coal (T_c) and the biomass (T_b), analogous to equation (3.33), as follows:

$$Log(\mu) = \frac{10^7.m}{T_s^2} + c \tag{7.2}$$

Where T_s^2 represents the combined softening temperatures of the coal and biomass particles, which replaces T_c in equation (3.33), and is defined as:

$$T_s^2 = xT_c^2 + (y/k)T_b^2 \tag{7.3}$$

The individual softening temperatures of the coal and biomass particles are determined as (Degereji *et al.*, 2011; Ma *et al.*, 2006):

$$T_c = a(SiO_2) + b(Al_2O_3) + c(Fe_2O_3) + d(CaO) + e(MgO) + f(\alpha) + g + 150^oC \tag{7.4}$$

$$T_b = 1.81CaO + 4.20Al_2O_3 - 2.41K_2O + 5.31P_2O_5 + 1017^oC \tag{7.5}$$

In order to account for the interaction between the species of coal and biomass ash particle, results of some empirical studies have been reviewed. Molcan *et al.* (2009) reported the characteristics of some of the elements of the blends under high temperatures as shown in Fig. 7.1.

The Fig. 7.1 shows that the content of K_2O in the blend ash increases rapidly with increase in BR. However, this trend reverses when the BR is greater than 15%. On the other hand, the content of Fe_2O3 reducing characteristics as the percentage of BR increases. Also, it has been reported that devolatilization and incomplete condensation affect the concentration of K_2O and P_2O_3 in the ash deposit of blends (Wigley *et al.*, 2007).

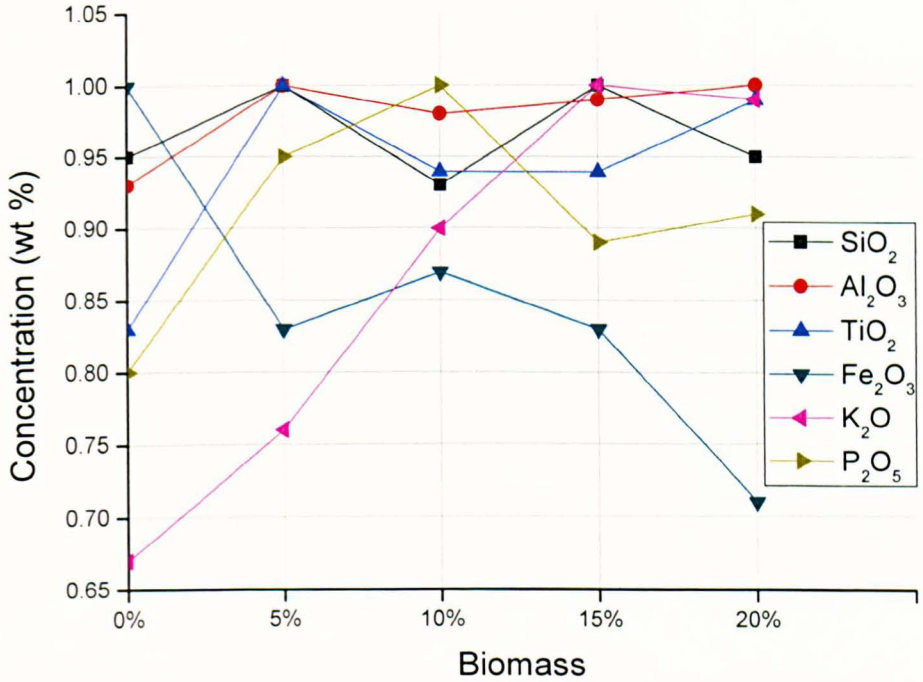

Fig. 7.1 Analysis of selected minerals in the inert matter of the coal/biomass blend from test Case 2.

In sequel to the review of the behaviour of some components of the blend ash as described above, four sub-models representing the softening temperature of the blend ash have been proposed are tested. The numerical results of the proposed sub-models are compared with experimental measurement as shown in Table 7.2.

Table (7.2) shows that the results of calculations using the sub-model with the k factor (serial number 2 in Table 7.2) gives better correlation with the experimental data when compared with the other sub-models. The sub-model predicts that slagging potential of the blend increases with increase in BR when the percentage of the BR in the blend is less than 20%.

Table 7.2 Comparing the slagging potential of coal/biomass blends using different softening temperature sub-models with experimental data - test Case 2 (Molcan *et al.*, 2009).

S/N	Sub-Model	0% BR	5% BR	10% BR	15% BR	20% BR
1	Experimental	0.75	0.81	0.82	0.95	1.00
2	$T_s^2 = xT_c^2 + (y/k)T_b^2$	0.89	0.96	0.93	1.00	0.90
3	$T_s^2 = (xT_c + yT_b)^2$	0.98	1.00	0.93	1.00	0.88
4	$T_s^2 = xT_c^2 + yT_b^2$	0.98	1.00	0.93	1.00	0.89
5	$T_s^2 = xT_c^2 + yT_b$	1.00	0.98	0.85	0.90	0.72

Therefore, the softening temperature sub-model in equation (7.3) is used in assessing the slagging potential of the coal and biomass blends according to equation (7.2), and the factor, k, is defined as follows:

$$k = (K_2O + TiO_2)/Fe_2O_3 \tag{7.6}$$

7.4 Test Cases

In order to validate the proposed co-firing slagging index, some reported experimental results on the slagging potential of some forms of coal / biomass blends have been used. The results of the predictions using the proposed co-firing slagging index are compared with the reported experimental measurements on some sets of coal and biomass blends. A total of three cases have been investigated as discussed below, and the properties of the tested blends are shown in Table 7.3.

7.4.1 Case 1

The deposition rates on the slag ports of a vertical slagging test rig during co-firing of South African bituminous coal with various percentages of sewage sludge, saw-dust and refuse derived fuel have been reported (Kupka, Mancini, Irmer & Weber, 2008). The slagging test was performed in a vertically fired reactor with ash collecting facility. The reactor is about 4.0 m long with a diameter of 0.25 m, and it has a nominal 50kW fuel input. Also, it has been reported that the reactor has very accurate control system and measurement equipment which results in very good repeatability.

The reactor was used to burn the blends of South African bituminous coal with sewage sludge (SS), saw-dust (SD) and refuse derived fuel (RDF), at different test times. The details of the properties of the fuels have been reported (Kupka *et al.*, 2008). The blending ratios of 5%, 10%, 15%, 20% and 100%, by energy (LHV), have been tested for both the SS and the SD. However, only 5% and 100% ratios of the refuse derived fuel tests have been reported in this Case (Kupka *et al.*, 2008).

The experimental results show high slagging with SS blends when compared with the SD blends and the pure coal. According to the report, the addition of SD to the coal appears to have reduced the slagging potential of the coal. Also, it has been reported that the gradual increase in the BR to 20% results in a linear increase in the slagging potential of both SS and SD blends (Kupka *et al.*, 2008).

7.4.2 Case 2

The concentration of fly ash collected from the flue section of a furnace during a co-firing test using the South African coal and pelletized saw dust (mixture of oak & pine woods), with BR of 0%, 5%, 10%, 15% and 20%, has been reported (Molcan *et al.*, 2009). A 3 MWth horizontally fired test facility has been used to characterize the biomass and coal co-firing. Saw-dust with 80% oak wood and 20% pine wood was blended with the South African coal.

The blending ratios are similar to those described in Case 1 (0-20%), but in this Case, the blending is by weight percentage. The fly ash collected during the co-firing has been analysed according to the weight of the unburned carbon, volatile matter and inert matter.

Also, the mineral analysis of the inert matter (ash) has been reported (see Table 7.3). According to the experimental data, the content of the fly ash is lower in pure coal combustion, and it keeps increasing linearly with increasing BR to 15%, and then, the content of the fly ash slightly reduces when BR was increased to 20%.

The experimental results further suggest that a complex characterization of the blends was produced which has been attribute to the varying properties of the biomass fuel.

7.4.3 Case 3

The superficial ash deposition rates during co-firing of white pine pellets and lignite coal, with BR of 0%, 20%, 50%, 80% and 100%, have been reported. (Shao *et al.*, 2010). The ash deposition study on co-firing biomass and coal was performed using a fluidized-bed combustor.

Although the blending ratios in this case are different from the two other cases, using a fluidized-bed reactor in this case may offer a basis for comparison between the test results using different facilities. The ash properties of the crushed lignite and the white pine pellets used in this test are shown in Table 7.3 (Shao *et al.*, 2010).

The test results show a slight increase in the deposition rates (0.5 $g/m^2/h$) as BR increases from 0% to 20% BR. It has been reported that the lignite has a higher surface deposition tendency, although the ratio of the ash feeding rate of the crushed lignite to the ash feeding rate of the blends shows that the combustion of 100% white pine pellets produced a slightly greater slagging than does 100% lignite coal (Shao *et al.*, 2010).

Also, it has been reported that the ash produced during the co-firing of the woody biomass and the lignite coal was found to be rich in some alkali metals, such as K, Na and Ca, as well as Al_2O_3 and P_2O_5.

Table 7.3 Mineral analyses of the inert matter from the three Cases investigated (Kupka *et al.*, 2008; Molcan *et al.*, 2009; Shao *et al.*, 2010).

	Mineral Content (% wt)											
% Biomass in the blend	**SiO_2**	**Al_2O_3**	**CaO**	**Fe_2O_3**	**SO_3**	**MgO**	**TiO_2**	**P_2O_5**	**K_2O**	**Na_2O**	**Ash content (% wt)**	**CV(MJ/kg)**
Case 1-SS											***(as received)***	***LHV***
0	40.49	32.21	12.29	5.02	0.72	3.86	1.81	1.73	0.93	0.94	10.64	26.54
5	36.38	28.39	13.07	7.71	0.17	4.01	1.60	6.53	1.22	0.91	12.49	25.32
10	34.20	26.15	13.18	9.36	0.32	3.79	1.49	9.30	1.31	0.90	14.17	24.22
15	32.48	24.30	13.40	10.73	0.49	3.73	1.38	11.21	1.37	0.92	15.70	23.21
20	30.29	22.48	13.16	11.22	2.95	3.76	1.30	12.43	1.48	0.94	17.10	22.30
Case 1-SD											***(as received)***	***LHV***
0	40.49	32.21	12.29	5.02	0.72	3.86	1.81	1.73	0.93	0.94	10.64	26.54
5	39.68	31.65	12.66	4.69	1.65	4.05	1.78	1.85	1.11	0.88	9.88	25.78
10	39.78	31.76	13	5.01	0.86	3.94	1.73	1.75	1.33	0.83	9.16	25.06
15	39.86	31.72	13.17	5.1	0.74	3.93	1.71	1.65	1.36	0.76	8.48	24.38
20	38.37	30.5	13.47	5.01	2.59	4.13	1.71	1.79	1.57	0.86	7.84	23.73
Case 2-SD											***(dry basis)***	***HHV***
0	42.50	29.40	8.09	5.72	2.54	1.64	1.40	1.35	0.64	0.10	14.60	27.80
5	44.90	31.50	7.51	4.76	1.47	1.39	1.68	1.59	0.66	0.10	14.10	27.29
10	41.90	30.90	8.76	4.95	1.66	1.64	1.57	1.68	0.78	0.13	13.59	26.77
15	44.90	31.10	6.60	4.74	1.16	1.11	1.58	1.49	0.87	0.07	13.09	26.26
20	42.60	31.40	9.23	4.07	1.60	1.85	1.67	1.53	0.85	0.13	12.58	25.74
Case 3-WPP											***(dry basis)***	***HHV***
0	38.05	15.33	7.51	0.76	0.60	12.26	9.26	5.27	4.63	0.81	22.00	21.80
20	35.28	18.34	8.41	0.84	0.52	16.58	3.64	5.27	5.53	0.65	18.22	21.56
50	35.60	16.88	7.11	0.60	3.38	12.92	4.21	4.95	4.39	3.17	12.55	21.20
80	28.93	12.48	6.21	0.52	6.56	13.81	5.43	6.66	3.49	4.72	6.88	20.84
100	29.58	4.33	25.44	0.19	0.37	8.85	18.47	2.59	1.70	1.22	3.10	20.60

7.5 Predicted Results and Discussion

The normalized results for the measured and the predicted slagging potential of coal and biomass blends for the Case 1 are reported in Fig. 7.2. The predicted results have a very good correlation with the experimental results for all the blend ratios. The results show an almost linear increase in the slagging potential with increasing BR. The maximum slagging potential is recorded when the ratio of the SS in the blend reaches 20%.

The poor slagging performance of the SS may be attributable to a number of factors. For example, the content of the ash in the SS is very high (29.93 wt %) when compared with the ash content in the coal (10.64 wt %) (Kupka *et al.*, 2008). Similarly, the SS has a higher content of sulphur (2.0 wt %) and a lower CV (13.8 MJ/kg) compared to the tested coal which has 0.83 wt % and 26.54 MJ/kg for sulphur content and CV, respectively. Also, its P_2O_5 content is high (12.43 wt %) for 20% BR.

Also, from the ash collected in the cyclone, it has been reported that the ash is enriched with some alkaline materials, such as K_2O (about 1.48 wt %) with 20% BR when compared with 100% coal (0.93 wt %). All these factors, coupled with some chemical reactions that might have not been accounted for, may result in the high slagging potential predicted. Therefore, one can conclude that the proposed co-firing numerical slagging index has successfully predicted the slagging performance of the sewage sludge and coal blend with BR up to 20%.

In Fig. 7.3, the measured and the predicted results of the slagging potential on saw-dust and coal blends are presented. The normalized results are in good agreement. The experimental results show that the maximum slagging potential occurs with 100% coal. It then decreases with 5% and 10% BR. The second peak is reached when the BR is 15%. Above 15% BR, the slagging potential begins to decrease again. The experimentalists reported that the continuous addition of the SD ratio in the blend may yield a lower slagging potential than that for pure coal (Kupka *et al.*, 2008).

The predicted results show that the slagging potential of the blend is highest with 15% BR, and it is lowest with 0% and 5% BR. Contrary to the SS, the reported properties of the SD show a very low content of ash (0.74 wt %). Also, the SD has a heating value (16.62 MJ/kg) greater than that of the SS (13.8 MJ/kg). The ash of the SD has a lower content of Na_2O, Fe_2O_3 and Al_2O_3 than that of the pure coal.

In another test using the woody biomass, the normalized values of the measured and predicted slagging potential of coal and saw dust blends for the Case 2 (Molcan *et al.*, 2009) are reported in Fig. 7.4. The predicted results have a good correlation with the experimental results, especially for BR ≤ 15%. For 20% BR, the model predicted a decrease in the slagging potential when compared with 15% BR, while the reported experimental data shows an increase.

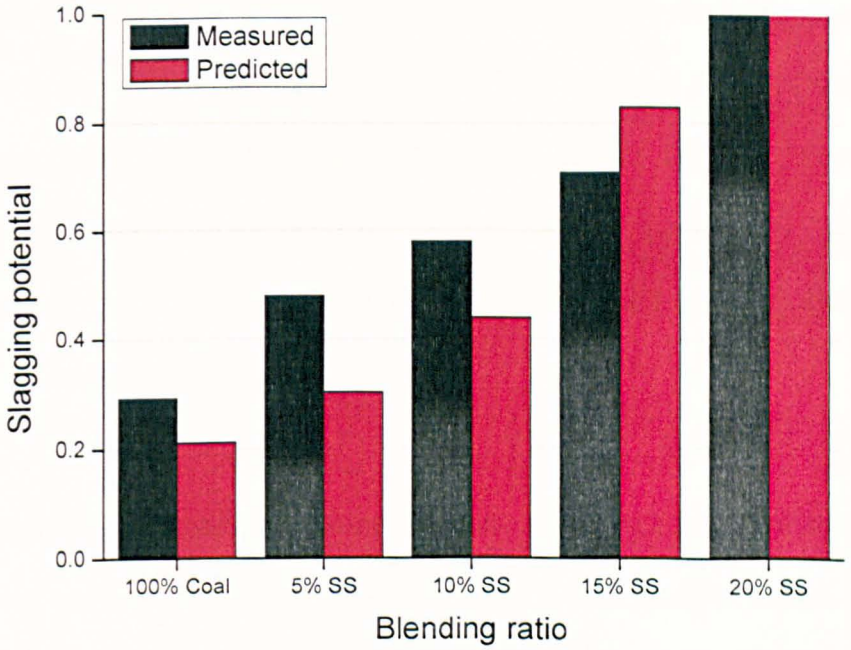

Fig. 7.2 Normalized values for the measured and predicted slagging potential of coal/biomass blends for test Case 1 (SS).

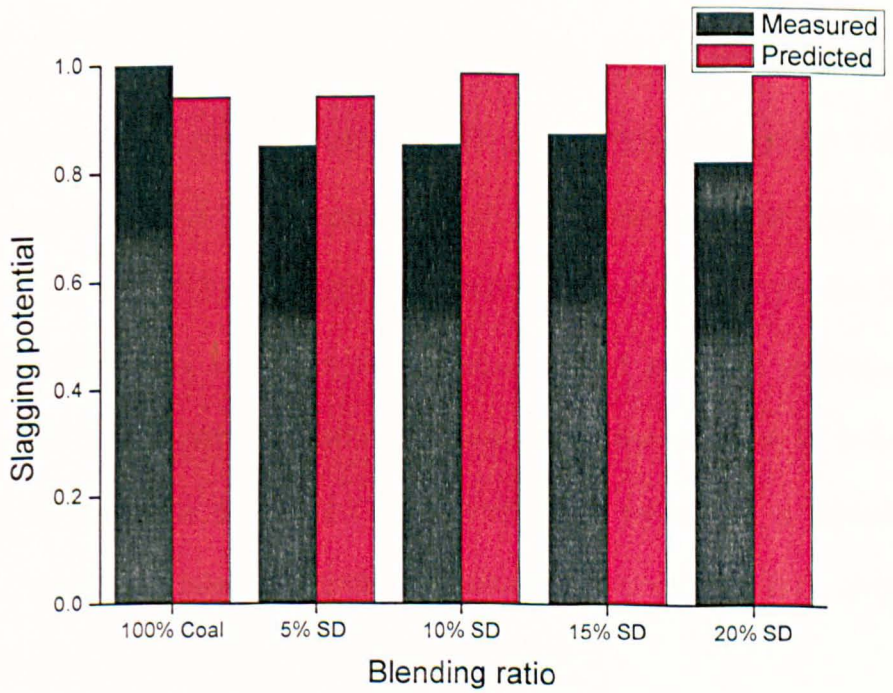

Fig. 7.3 Normalized values for the measured and predicted slagging potential of coal/biomass blends for test Case 1 (SD).

Although the reported increases in the content of alkali metals when biomass addition is greater than 15% may result in increased slagging, the significant reduction in the ash content and the content of Fe_2O_3 in the ash may decrease the slagging potential, and the predicted result for 20% BR is consistent with the both the measurements and predictions in Case 1 (with SD). Therefore, the predictions of the coal/SD blends using the proposed co-firing slagging index are also considered to be accurate.

In Fig. 7.5, the normalized values for the measured and predicted slagging potential of coal and white pine pellets blends for the Case 3 (Shao *et al.*, 2010) are shown. For BR greater than 20%, the model predicted almost a linear decrease in the slagging potential of the blends, and this trend agrees with the experimental data.

The decrease in the slagging potential with an increase in the BR is not unexpected since the biomass used in this case (white pine wood) has a very low ash content (3.1 wt %) compared to the ash content for the lignite coal (22 wt %) (Shao *et al.*, 2010). Although there are no data between 0% and 20% BR, the experimental data suggests an increase in the slagging potential of the blends which is in agreement with the measured data in Case 2. It is evident here that the model is consistent in its predictions when BR is between 15% and 20%, and the three experimental cases on woody biomass show some inconsistencies.

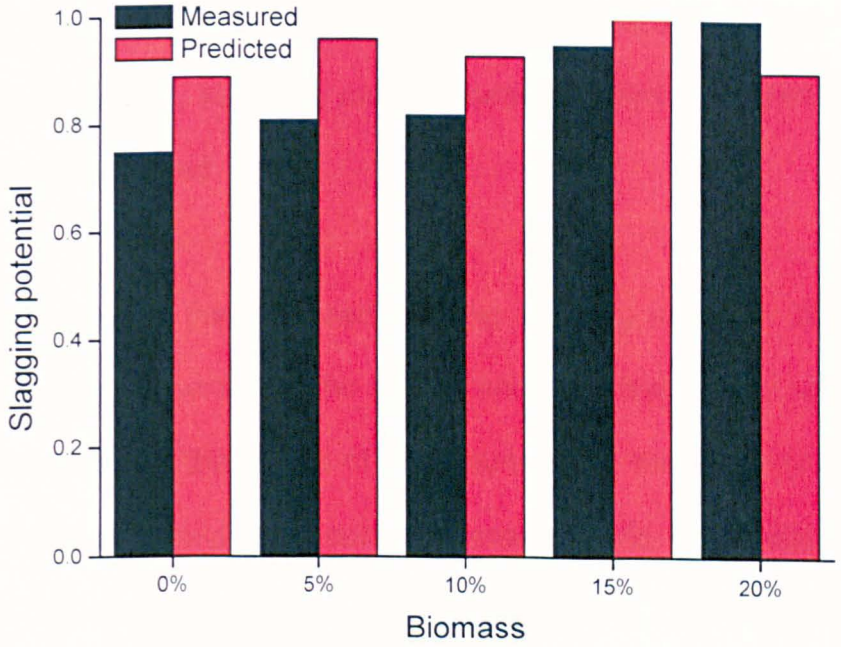

Fig. 7.4 Normalized values for the measured and predicted slagging potential of coal/biomass blends for test Case 2.

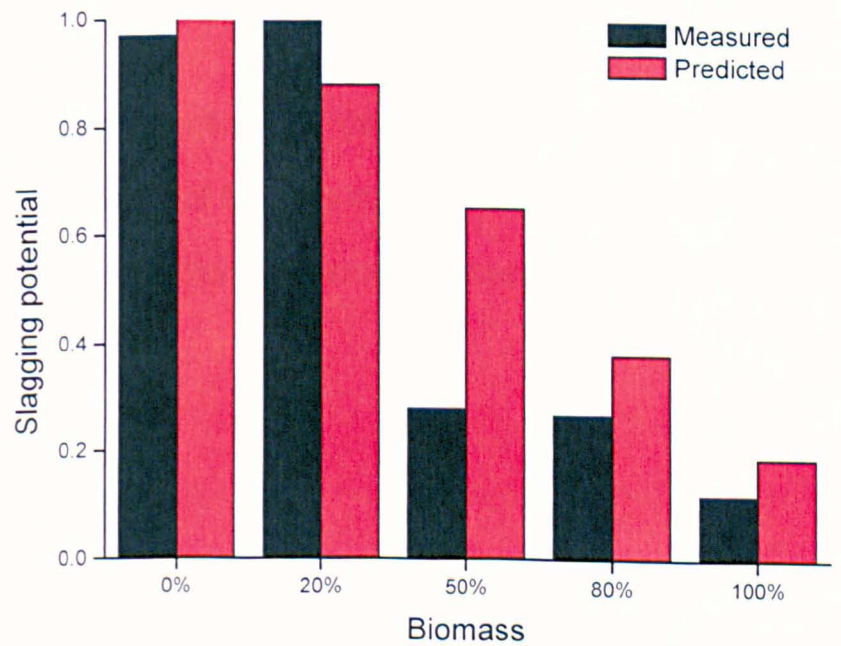

Fig. 7.5 Normalized values for the measured and predicted slagging potential of coal/biomass blends for test Case 3.

Some of the potential transformations and association that are likely to occur when the content of the biomass in the blend becomes significant, such as the formation of eutectic, sulfation, reaction between silica and alkali metals, etc., need to be investigated.

The performance of the proposed co-firing slagging index on different blends depends on the properties of the blends and the properties of their respective ashes. For example, the results of predictions using the index on coal/saw dust blends in Cases 1 and 2 produced different results. For Case 1, the index predicted 0.52 and 0.53 slagging potential for 5% and 10% BR (not normalised). Similarly, the index predicted 0.62 and 0.60 for 5% and 10% BR in Case 2. The prediction results show that the blend in Case 2 has higher slagging potential. This may be attributed to the high ash content in Case 2 (14.6 wt %) compared to that of Case 1 ((10.64 wt %).

It is important to mention that the model was successful in predicting a high percentage (> 20%) of biomass in the blend by simply assessing the softening temperatures of the biomass which is subsequently correlated to the BR in the blends.

7.6 Challenges

i. Although the ash viscosity may be sufficient to determine the sticking tendency of coal ash, which is predominantly alumino-silicate, the softening temperature of the biomass particle may not be sufficient to

determine its sticking tendency. Therefore, there is the need to understand the potential interactions between the coal and the biomass elements and incorporate them into the model for better predictions.

ii. Two of the available co-firing cases that have been tested in this investigation are basically woody biomass, whose ash is less complex compared to other forms of biomass. Although sewage sludge has also been investigated, there is a need to test other forms of available biomasses in order to draw a general conclusion. Also, it is important to investigate blends with not more than 20% BR, this is because at this stage the emphasis has been on 20% BR.

iii. The availability of data on industrial scale co-firing slagging is also considered as a limitation to the implementation of the proposed co-firing numerical slagging index. It is expected that further enhancement of the features of this model will assist in the assessment of the slagging potential of coal and biomass co-firing. Also, with a better understanding of the slagging mechanism of the blends, its use can be extended to higher values of BR.

7.7 Conclusions

i. The existing coal slagging index has been modified in order to predict the slagging potential of coal/biomass blends. The working principles of the modified slagging index are based on the weight of ash and the heating value of the individual fuels, as well as their individual softening temperatures.

ii. The model has satisfactory predicted the slagging potential of coal/biomass blends, especially for BR < 20%. The results of the prediction using the modified index are in very good agreement with the measured data, especially with sewage sludge and woody biomass.

iii. Although the experimental results show some inconsistencies when the BR is greater than 15%, the predicted results are consistent with all the experimental results that are reported.

iv. Some minor discrepancies between the measured and predicted results do exist, especially where the difference in the reported experimental results for two successive blending ratios is insignificant.

v. The content of some of the ash elements in the blends, such as potassium, titanium and iron, correlate with the overall ash slagging behaviour.

vi. The weight of the incoming ash has a significant influence on the slagging potential of the blends. This has been shown by both the experiments and the predictions.

vii. The potential interaction between the particles of coal and biomass in the boiler needs to be understood and integrated into the modified slagging index in order to enhance the performance of the index.

viii. There is a need for further testing of the modified slagging index to cover all types of biomass and coals.

CHAPTER 8

GENERAL CONCLUSIONS AND FUTURE WORK

In this chapter, the conclusions derived from the research findings are presented. This thesis is considered as a conceptual basis for broader research activities towards the understanding of the ash behaviour for all solid fuels. Therefore, some areas of future research work are identified and discussed at the end of this chapter.

8.1 General Conclusions

In an attempt to contribute towards a better of the boiler slagging problems, CFD techniques are used in the implementation of the ash particle deposition rate model and the numerical slagging index that have been proposed in this thesis. The two models have been validated using the available experimental data on coal combustion, and some conclusions are drawn.

8.1.1 Ash particle deposition model

The existing models for various phases of coal combustion are used in order to establish the gas phase temperature and velocity field which are necessary for ash deposition studies. The particle trajectories are predicted in a Lagrangian reference frame.

Inertial impaction has been considered as the major pathway for the transportation of particles to the boiler walls. The overall sticking tendency of the particle was determined on the basis of its calculated viscosity at impaction on the boiler walls and its tendency to rebound after impaction if it possesses excess energy.

Some of the predicted results that have been compared with the measurement data include the following: the flame temperatures in the regions of the slag panels; the heat fluxes on the three slag panels; and most importantly, the ash deposition rates on the three slag panels.

The following general conclusions are made based on the investigations performed using the proposed ash particle deposition rates model that is reported in this thesis:

- A numerical model to predict ash deposition in furnaces has been developed based on the temperature-dependent viscosity of the ash particle has been developed. The model also incorporates the particle rebound tendency after impaction on the boiler walls.
- The proposed model has successfully predicted the ash deposition rates for four Australian bituminous coals that have been tested in this investigation. The results of prediction using the deposition model correlate very well with the reported slagging performance of the coals.

- The ash particle deposition model is found suitable for the prediction of the deposition rates of homogeneous coal ash slag in a high temperature region.
- The performance of this model at the downstream boiler where temperatures are low has not been tested and therefore is not guaranteed. This is because at low temperature regions, condensation is considered as a major deposition pathway, and also, ash crystallization may occur, thereby introducing non-homogeneous characteristics in the ash. The effects of these transformations due to the change in temperature gradient are not accounted for in the model.
- The gas phase temperatures are found to have a significant effect on the ash deposition rates. The peak flame temperatures obtained vary for different coal types since the operating conditions are the same.
- Also, the heat fluxes on the walls of the ACIRL furnace are found to have a significant effect on the rates of ash deposition on the slag panels. According to reports, the heat fluxes can be used to characterize ash deposition on the water-walls of a boiler (Su *et al.*, 2001a).
- It has been observed that the viscosity of the ash particle in the furnace determine, to a large extent, the particle deposition rates. Reducing the value of the reference viscosity results in a lower rate of ash deposition. This suggests that at very low viscosity ($< 10^4$ Pa.s), little or no deposition is recorded.
- The swirling motion of the particles in the boiler seems to increase their tendency to penetrate the boundary layer and hit the heat exchange surfaces. Consequently, this increases the overall slagging propensity. In

this investigation, it has been observed that an increase in the swirl number, result in proportional increase in the rate of ash particle deposition. This is attributed to the particle entrainment due to strong recirculation zone created with high swirl numbers.

- This ash deposition model has not been tested on an industrial scale boiler due to the non availability of field performance data at the time of this investigation. However, the results of the test on the pilot-scale furnace are good representation of the large scale boilers since they are operated under similar conditions.
- An attempt to model the ACIRL furnace in 3D scale has been only successful with a low swirling velocity, and the results of the 3D calculations correlate with those of 2D calculations under the same operating conditions. This has confirmed that the ash deposition model developed in this investigation can predict in both 2D and 3D domains.

8.1.2 Coal slagging index

Also, a numerical slagging index has been proposed based on the viscosity of the ash, the softening temperature of the ash and the ash content in the coal, with some basic assumptions. The slagging index is to predict the pre-combustion slagging potential of a wide range of coals.

The model has been tested on seventeen coals with different properties, ranging from low rank coals from India to bituminous coals from Australian,

Columbia, Indonesia, South Africa, the UK and the US. The index has also been tested on some sets of coal blends in order to establish its robustness.

In order to examine the flexibility of the slagging index, it has also been tested on some sets of coal blends and satisfactory prediction results are obtained. Although nonlinear slagging performance for the coal/blends has been observed, the availability of the ash analysis for the tested blends helps in the accurate predictions using the slagging index.

In order to establish a genuine basis for comparison, the slagging performance of all the tested coals has also been evaluated using six existing coal slagging indices. The predicted results using the proposed NSI and the six existing indices have been compared with the reported slagging performance of the coals/blends, and the following conclusions are drawn:

- In the second investigation reported in this thesis, a numerical slagging index that correlates with the field performance of coals/blends has been developed. The NSI is based on the ash viscosity, ash fusibility and ash loading in coals.
- The proposed slagging index has been validated against measurement data on seventeen different coals, including lignite and bituminous coals. Although the coals tested are from different parts of the world, the NSI has been so robust to have satisfactorily predicted the slagging performance of all the coals.

- The slagging index has also been tested on some few sets of Australian coal blends. The proposed slagging index has been successful in ranking the coals/blends being investigated according to their reported field performance. When compared with the reported performance of some empirical techniques, such as TMA, SEM and ash chemistry, the proposed slagging index stands out.
- The slagging index predicted increased slagging potential with increase in the percentage of the incoming ash. While decreased slagging has been predicted with increase in the viscosity of the ash.
- In comparison, the six existing slagging indices that have been tested only accurately predicted the performance of UK and US coals.
- In addition to the chemistry of the ash, the mineral distributions and associations, the ash loading in the coals have a significant effect on the rate of the ash accumulation in the boilers.
- The presence of low-viscosity materials and the ash content in coals/blends enhance the slagging propensity.
- The performance of blends may not be interpreted linearly from that of their parent coals.
- The proposed numerical slagging index is a step forward in the drive for a more generic method of predicting the pre-combustion slagging behaviour of coals in boilers.
- It should be noted that the interaction of different ash particles on the deposit surface and how this affects deposit build-up needs to be better understood, in order to provide a better prediction tool for coals and blends.

8.1.3 Co-firing slagging index

The coal numerical index has been modified to predict the slagging potential of coal and biomass blends. The softening temperatures, ash composition and the content of ash of the individual fuels have been considered in modelling the co-firing index.

The proposed co-firing slagging index has been tested on some sets coal blends with sewage sludge and woody biomass. The results of prediction using the co-firing index correlate very well with the reported experimental data, and therefore, the following conclusions are made:

- A coal slagging tool developed reported in this thesis has been modified to predict the slagging potential of coal and biomass blends. The ash of the blend is considered both as individual fuel ash and a mixture ash. Also, the behaviour of the ash elements are considered in the numerical modelling.
- The proposed model has satisfactory predicted the slagging potential of coal and biomass blends, particularly the blend of coal and saw-dust and that of coal and sewage sludge.
- Although the model has successfully predicted the slagging potential of blends with higher percentage of biomass than coal, it is originally designed to predict blends with < 20% BR whose ash is assumed to be predominantly alumino-silicate.

- In order to improve the performance of the model, the potential interaction between coal and biomass particles needs to be accounted for.

8.2 Future Work

In this thesis, two numerical models have been developed; one is to predict the coal ash particles deposition rates in the upstream burner region of a furnace, and the other, is to predict the slagging potential of a wide range of coals. The coal slagging model has been modified to predict coal and biomass blends. The successful testing of these models informed the need for further investigations along the same line. Thus, the following investigations can take bases from the content of this report:

i. The ash deposition rates model has only been tested on a pilot-scale furnace because there was no experimental deposition data on industrial scale boilers that was ready available at the time of this investigation. Therefore, there will be the need to run the ash deposition model on a full 3D industrial scale boiler when data is available.

ii. The ash deposition model can be extended to predict the ash deposition in the convective section of a boiler. This can be achieved by incorporating the effect of the factors that can influence deposition at low temperatures, such as condensation and agglomeration. For a

successful implementation of the model at the downstream boiler, it is essential to consider the heterogeneous nature of the coal ash.

At the convective section of the boiler, the slag begins to solidify due to decrease in the temperatures. The solid crystals that may form due to the decrease in the temperatures will form part of the slag. Therefore, the slag will now contain both liquid and solid particles. At this stage, the slag flow will not longer be Newtonian, and therefore, the viscosity method of predicting slagging potential may not be sufficient to yield accurate results.

So far, some attempts have been made in order to describe the non-Newtonian behaviour of the ash at low temperatures. According to the reported empirical investigations, the ash behaviour can be predicted if the concentration of the particle in the slurry is determined (Kondratiev & Jak, 2001). Although there are criticism that the determination of the concentrations of the particles is done using a prediction tool, the technique will provide a better understanding of the non-Newtonian slag flow in the downstream boiler.

iii. The 3D calculations using the deposition model need improvement. There is a need to model an industrial boiler in full 3D domain in order to predict high swirling scenario.

iv. The use of the ash deposition model can be extended to biomass provided that the ash properties of biomass are fully integrated into the model. However, some major changes have to take place. For example, in biomass, ash elements such as potassium, phosphorus, ammonia, etc., are said to have significant effect on the ash deposition.

Also, the stickiness of the ash particle is determined based on the melt fraction of the particle unlike the silica-rich particle, where the particle sticking tendency is determined by its viscosity. In some case where the biomass particle is not completely burnt, the melt fraction of the particle is also used in order to determine its stickiness. Some research reports suggest that when 30% of the particle has melted it is completely sticky (Ma *et al.*, 2006).

The relatively large size of biomass pellets is another issue to worry about. Owing to its large size, the biomass particle may posses adequate inertial force to transverse the boundary layer and impact on the boiler walls, which may result in increased slagging potential.

v. The proposed coal slagging index has also been tested on some coal blends, and the predicted results are encouraging. After little modification, the numerical slagging index has successfully predicted the slagging potential of coal and biomass blends with < 20 BR. This suggest that, with more investigations on the biomass ash behaviour and the coal biomass interaction, the features of the numerical slagging index can be

extended to predict the slagging potential of coal and /biomass blends with higher percentage of BR.

REFERENCES

Abolhassan, J. S., & Stewart, J. E. (1994). Surface grid generation in a parameter space. *Journal of Computational Physics*, 113, 112-121.

Alecci, M., Cammarata, G. & Petrone, G. (2005). Analysis and modelling of a low NOx swirl burner. *Excerpt from the Proceedings of the COMSOL Multiphysics User's Conference*, Stockholm, 2005.

American Coal Foundation, 2010. Converting coal into electricity.

Aslanyan, G. S., & Maikov, I. L. (1994). Simulation of pulverized coal combustion in a turbulent flow. *Combustion, Explosion and Shock Waves,* 30(4), 448-453.

Arvelakis, s., Folkedahl, B., Dam-Johansen, K., & Hurley, J. 2006). Study of the melting behaviour of coal, biomass and coal/biomass ash using viscosity and heated stage XRD date. *Energy & Fuel*, 20, 1329-1340.

Backreedy, R. I., Fletcher, L. M., Jones, J. M., Ma, L., Pourkashanian, M., & Williams, A. (2005). Co-firing pulverized coal and biomass: a modelling approach. *Proceedings of Combustion Institute*, 30, 2955 - 2964.

Backreedy, R. I., Fletcher, L. M., Ma, L., Pourkashanian, M., & Williams, A. (2006). Modelling pulverized coal combustion using a detailed coal combustion model. *Combustion Sci. & Tech.*, 178, 2955 - 2964.

Badzioch, S., & Hawksley, P. G. W. (1970). Kinetics and thermal decomposition of pulverized coal particles. *Industrial Engineering Chemistry*, 9(4), 521-530.

Barths, H., Hosse, C., & Peters, N. (2000). CFD modelling of non-premixed combustion in direct injection diesel engines. *Int. J. Engine Research*, 1(3), 249-267.

Basu, P., Kefa, C., & Jestin, L. (1946). Boilers and Burners. Springer- Verlag, New York.

Baum, M. M., & Street, P. J. (1971). Predicting the combustion behaviour of coal particle. *Combustion Science and Technology*, 3(5), 231-243.

Baxter, L. (2005). Biomass-coal co-firing: opportunity for affordable renewable energy. *Fuel*, 84, 1295-1302.

Baxter, L. L., & DeSollar, R. W. (1993). A mechanistic description of ash deposition during pulverized coal combustion: predictions compared with observations. *Fuel*, 72 (10), 1411-1418.

Benson, S. A., Sondreal, E. A., & Hurley, J. P. (1995). Status of coal ash behaviour research. *Fuel Processing Technology*, 44, 1-12.

Biferale, L., Boffetta, G., Celani, A., Lanotte, A., & Toschi, F. (2005). Particle trapping in three-dimensional fully developed turbulence. *Physics of Fluids*, 17, 021701.

Brewster, B. S., Baxter, L. L., & Smoot, L. D. (1988). Treatment of coal devolatilization in comprehensive combustion modelling. *Energy Fuels*, 2(4), 362-370.

Browning, G. J., Bryant, G. W., Hurst, H. J., Lucas, J. A., & Wall, T. F. (2003). An empirical method for the prediction of coal ash slag viscosity. *Energy and Fuel*, 17, 731-737.

Byers, R. L. & Calvert, S. (1969). Particle deposition from turbulent streams by means of thermal force. *Ind. Eng. Chem. Fundamen.*, 8(4), 646-655.

Chui, E. H., & Raithby, G. D. (1993). Computation of radiant heat transfer on a non-orthogonal mesh using the finite-volume method. *Numerical Heat Transfer, Part B*, 23, 269-288.

Coal Science (2011). Coal rank. http://www.coalscience.com/rank.htm. Retrieved: September 02, 2011.

Costen, P. G., Lockwood, F. C., & Saddique, M. M. (2000). Mathematical modelling of ash deposition in pulverized fuel-fired combustor. *Proceedings of the Combustion Institute*, 28, 2243-2250.

Degereji, M. U., Ingham, D. B., Ma, L., Pourkashanian, M., Williams, A. (2011). Prediction of ash slagging propensity in a pulverized coal combustion furnace. *Fuel (2011)*, doi:10.1016/j.fuel.2010.12.038.

Dhumal, S. S., & Saha, R. K. (2007). A one dimensional model of pulverized coal combustion in a cylindrical furnace and its experimental validation. *Journal of Energy and Environment*, 6, 72-86.

Dinesh, K. K. J. R., Malalasekera, W., Ibrahim, S. S., & Kirkpatrick, M. P. (2005). Large eddy simulation of isothermal swirling flows. *5th Asia-Pacific Conference on Combustion,* the University of Adelaide, Australia, 17-20 July, 2005.

Eaton, M. A., Smoot, L. D., Hill, S. C., & Eatongh, C. N. (1999). Components, formulations, solutions, evaluation and applications of comprehensive combustion models. *Process in Energy & Combustion Science*, 25, 387-436.

Eghlimi, A., Lu, L., Sahawalla, V., & Harris, D. (1999). Computational modelling of char combustion based on the structure of char particles. *2nd International Conference on CFD in the Mineral and Processing Industries*, CSIRO, Melbourne, Australia. 6-8 Dec. 1999.

Elberling, B., Nicholson, R. V., & Schaver, J. M. (1994). The combined kinetic and diffusion model for pyrites oxidation in tailings: a change in controls with time. *Journal of Hydrology*, 157, 47-60.

Eldrainy, Y. A., Jaafar, M. N. M., & Lazim, T. M. (2010). Cold flow investigation of primary zone characteristics in combustor utilizing axial air swirler. *International Journal of Mechanical & Material Engineering*, 1(4), 257-263.

Energy Information Administration (2010). International energy outlook, Energy Information Administration, USA, DOE.

Energy Information Administration (2010) International energy statistics, Energy Information Administration, USA, DOE.

Erickson, T. A., Allan, S. E., McCollor, D. P., Hurley, J. P., Srinivasachar, S., Kang, S. G., Baker, J. E., Morgan, M. E., Johnson, S. A., & Borio, R. (1995). Modelling of fouling and slagging in coal fired utility boilers. *Fuel Processing Technology*, 44, 155-171.

Field, M. A. (1969). Rate of combustion of size-graded fraction of char from a low rank coal between 1200K-2000K. *Combustion & Flame*, 13, 237-252.

Filkoski, R. V., Belosevic, S. V., Petrovski, I. J., Oka, S. N., & Sijercic, M. A. (2006). Computational fluid dynamics techniques as a tool for description of the phenomena occurring in pulverized coal combustion systems. *Journal of Power & Energy*, 221, 399-409.

Finkelman, R. B. (2004). Potential health impacts of burning coal beds and waste banks. *Int. Journal of Coal Geology*, 59, 19-24.

Fletcher, T. H., & Kerstein, A. R. (1990). Chemical percolation model for devolatilization 2. Temperature and heating rate effects on products yields. *Energy & Fuel*, 4(1), 54-60.

Fluent Inc. (2009). *ANSYS Fluent User's Guide*, Release 12.0, Fluent Inc., Lebanon, NH.

Forstner, M., Hofmeister, G., Joller, M., Dahl, J., Braun, M., Kleditzsch, S., Scharler, R., & Obernberger, I. (2006). CFD simulation of ash deposit formation in fixed bed biomass furnaces and boilers. *Progress in Computational Fluid Dynamics*, 6 (4/5), 248-261.

Ghenai, C., & Janajreh, I. (2009). CFD analysis of the effect of co-firing biomass and coal. *GCREEDER* 2009, Amman-Jordan, March 31-April 2.

Gupta, S. K., Wall, T. F., Creelman, R. A., & Gupta, R. P. (1998). Ash fusion temperatures and the transformations of coal ash particles to slag. *Fuel Processing Technology*, 56, 33-43.

Habib, R. S. (2001). An advanced coal combustion model. *Unpublished PhD Thesis submitted to the Fuel & Energy Department*, University of Leeds, March 2001.

Habibi, A., Merci, B., & Heynderickx, G. J. (2007). Impact of radiation models in CFD simulations of steam cracking furnaces. *Computers & Chemical Engineering,* 31, 1389-1406.

Harb, J. N., Zygarlicke, C. J., & Richards, G. H. (1993). The effect of particle composition of two western US coals in a laminar drop-tube furnace. *Journal of the Institute of Energy*, 66, 91-98.

Heinzel, T., Siegle, V., Spliethoff, H., & Hein, K. R. G. (1998). Investigation of slagging in pulverized fuel co-combustion of biomass and coal at pilot-scale test facility. *Fuel Processing Technology*, 54, 109-125.

Huang, L. Y., Norman, J. S., Pourkashanian, M., & Williams, A. (1996). Prediction of Ash deposition on superheater tubes from pulverized coal combustion. *Fuel*, 73(3), 271-279.

Hubner, A. W., Tummers, M. J., Hanjalic, K., & van der Meer, T. H. (2003). Experiments on rotating-pipe swirl burner. *Experimental, Thermal & Fluid Science*, 27, 481-489.

Israel, R., & Rosner, D. E. (1983). Use of a generalized Stokes number to determine the aerodynamic capture efficiency of non-Stokesian particles from a compressible gas flow. *Aerosol Science & Technology*, 2, 45-51.

Jayanti, S., Maheswaran, K., & Saravanan, V. (2007). Assessment of the effect of high ash content in pulverized coal combustion. *Applied Mathematical Modelling*, 31, 934-953.

Joller, M., Brunner, T., & Obernberger, I. (2005). Modelling of aerosol formation during biomass combustion in grate furnaces and comparison with measurements. *Energy & Fuels*, 19, 311-323.

Jones, J. M., Darvell, L. I., Bridgeman, T. G., Pourkashanian, M. & Williams, A. (2007). An investigation of the thermal and catalytic behaviour of potassium in biomass combustion. *Proceeding of the Combustion Institute*, 31(2), 1955-1963.

Jung, B., & Schobert, H. H. (1992). Improved prediction of coal ash slag viscosity by thermodynamic modelling of liquid-phase composition. *Energy and fuel*, 6, 387-398.

Jones, W. P. & Whitelaw, J. H. (1984). Modelling and measurement in turbulent combustion. *20th International Symposium on Combustion*, 233-249.

Komatina, M., Manovic, V., & Saljinikov, A. (2006). Temperature of coal particle during devolatilization in fluidized bed combustion reactor. *Energy Sources, Part A: recovery, utilization and environmental effects*, 28(15), 1387-1396.

Kondratiev, A., & Jak, E. (2001). Predicting coal ash flow characteristics (viscosity model for the Al_2O_3-CaO-'FeO-SiO_2 system). *Fuel*, 80 (14), 1989-2000.

Kucukbayrak, S., Acma, H. H., Mericboyu, A. E., & Yaman, S. (2001). Effect of lignite properties on reactivity of lignite. *Energy Conversion and Management*, 42, 613-626.

Kupka, T., Mancini, M., Irmer, M., & Weber, R. (2008). Investigation of ash deposit formation during co-firing of coal with sewage sludge, saw-dust and refuse derived fuel. *Fuel*, 87, 2824-2837.

Kwark, J. H., Jeong, Y. K., Jeon, C. H., & Chang, Y. J. (2004). Effect of swirl intensity on the flow and combustion of turbulent non-premixed flat flame. *Flow, Turbulence & Combustion*, 73, 231-257.

Lapple, C. E., & Shepherd, C. B. (1940). Calculation of particle trajectories. *Industrial & Engineering Chemistry*. 32(5), 605-617. 1155 Sixteenth Street N.W., Washington, DC 20036.

Launder, B. E., & Spalding, D. B. (1972). *Lectures in Mathematical Models of Turbulence*. Academic press, London, England.

Laursen, K., Frandsen, F., & Larsen, O. H. (1998). Ash deposition trials at three power stations in Denmark. *Fuel & energy*. 12, 429-442.

Lawn, C. J. (1987). *Principles of Combustion Engineering for Boilers.* Academic Press, Harcourt Jovanovich Publishers, London.

Lawrence, A., Kumar, R., Nandakumar, K., & Narayanan, K. (2008). A novel tool for assessing slagging propensity of coals in pf boiler. *Fuel*, 87, 946-950.

Li, Z. Q., Wei, F., & Jin, Y. (2003). Numerical simulation of pulverized coal combustion and NO formation. *Chemical Engineering Science*, 58, 5161-5171.

Lin, J., Tsai, C., Tung, K., & Chiang, H. (2008). Thermophoretic particle deposition efficiency in turbulent tube flow. *Journal of Chinese Institute of Chemical Engineers*. 39, 281-285.

Lee, B., Song, J., Kim, R., Kim, S., Kim, Y., Chang, Y., & Jeon, C. (2010). Simulation of the influence of the coal volatile matter content on fuel NO emissions in drop-tube furnace. *Energy Fuel*, 24, 4333-5340.

Lee, F. C. C., & Lockwood, F. C. (1999). Modelling ash deposition in pulverized coal-fired applications. *Progress in Energy and Combustion Science*, 25, 117-132.

Lokare, S. S., Dunaway, J. D., Moulton, D., Rogers, D., Tree, D. R., & Baxter, L. L. (2006). Investigation of ash deposition rates for a suite if biomass fuels and fuel blends. *Energy & Fuel*, 20, 1008-1014.

Luo, X. Y., Hinton, J. S., Liew, T. T., & Tan, K. K. (2004). LES modelling of flow in a simple airway model. *Medical engineering and physics*, 26, 403-413.

Luxsanayotin, A., Pipatmanomai, S., & Bhattacharya, S. (2010). Effects of mineral oxides on slag formation tendency of Mae Moh lignites. *Songklanakarin J. Sci. Technol.*, 32(4), 403-412.

Ma, L., Poukashanian, M., Williams, A., & Jones, J. M. (2006). A numerical model for predicting biomass particle deposition in a pf furnace. *Proceedings of ASME*, Barcelona, Spain, 8-11 May 2006.

Mason, D. M., & Gandhi, K. N. (1983). Formulas for calculating the calorific value of coal and coal char: development, test and uses. *Fuel Proc. Tech.*, 7, 11-22.

Mao, T., Kuhn, D. C. S., & Tran, H. (1997). Spread and rebound of liquid droplets upon impact on flat surfaces. *AlchE Journal*, 43(9), 2169 – 2179.

McLennen, A. R., Bryant, G. W., Bailey, C. W., Stanmore, B. R., & Wall, T. F. (2000). Index for iron-based slagging for pulverized coal firing in oxidizing and reducing conditions. *Energy & Fuel*, 14, 349-354.

Melchior, T., Putz, G., & Muller, M. (2009). Surface tension measurements of coal ash slag under reducing conditions at atmospheric pressure. *Energy fuel*, 23, 4540 – 4546.

Miessen, G. Behrendt, F., Deutschmann, O., & Warnatz, J. (2001). Numerical studies of the heterogeneous combustion of char using detailed chemistry. *Chemosphere*, 42, 609-613.

Molcan, P., Lu, G., Bris, T. L., Yan, Y., Taupin, B., & Caillat, S. (2009). Characterization of biomass and coal co-firing on a 3 MWth combustion test facility using flame imaging and gas/ash sampling techniques. *Fuel*, 88, 2328-2334.

Moore, E. S. (1922). *Coal*, London: John Wiley & Sons Inc.

Morsi, S. A., & Alexander, A. J. (1972). *An* investigation of particle trajectories in two-phase flow systems. *Journal of Fluid Mechanics,* 55(2), 193-208.

Mshelia, E. D. (1997). Nuclear science and technology in human progress. *Inaugural Lecture Series No.3* Abubakar Tafawa Balewa University, Bauchi, Nigeria.

Mueller, C., Skrifvars, B. J., Backman, R., & Hupa, M. (2003). Ash deposition prediction in biomass fired fluidized bed boiler-combustion of CFD and advanced fuel analysis. *Progress in CFD*, 3(2-4), 112-120.

Mueller, C., Selenius, M., Theis, M., Skrifvars, B. J., Backman, R., Hupa, M., & Tran, H. (2005). Deposition behaviour of molten alkali-rich fly ashes; development of submodel for CFD applications. *Proceeding of the Combustion Institute*, 30, 2991-2998.

Munir, S., Nimmo, W., & Gibbs, B. M. (2010a). co-combustion of agricultural residues with coal: Turning waste into energy. *Energy Fuel*, 24, 2146-2153.

Munir, S., Nimmo, W., & Gibbs, B. M. (2010b). Potential slagging and fouling problems associated with biomass-coal blends in coal-fired boilers. *Journal of the Pakistan Institute of Chemical Engineers*, 38(1).

Murphy, J. J., & Shaddix, C. R. (2006). Combustion kinetics of coal chars in oxygen – enriched environments. *Combustion & Flame, 144*, 710 - 729.

Naganuma, H., Ikeda, N., Kawai, T., Takuwa, T., Ito, T., Igarashi, Y., Yoshiie, R., & Naruse, I. (2009). Control of ash deposition in pulverized coal-fired boiler. *Proceedings of the Coal Combustion Institute.*

Naruse, I., Kamihashira, D., Khairil, Miyauchi, Y., Kato, Y., Yamashita, T., & Tominaga, H. (2005). Fundamental ash deposition characteristics in pulverized coal reaction under high temperature conditions. *Fuel*, 84, 405-410.

Nutalapati, D., Gupta, R., Maghataderi, B., & Wall, T. F. (2009). Assessing slagging and fouling during biomass combustion: A thermodynamic approach allowing for alkali/ash reactions. *Fuel Processing Technology*, 88, 1044-1052.

Oh, M. S., Brooker, D. D., De Paz, E. F., Brady, J. J., & Decker, T. R. (1995). Effect of crystalline phase formation on coal slag viscosity. *Fuel Processing Technology*, 44, 191199.

Pimentel, D., Rodriques, G., Wang, T., Abrams, R., Goldberg, K., Staecker, H., Ma, E., Brueckner, L., Trovato, L., Chow, C., Govindarajulu, U., & Boerke, S. (1994). Renewable energy: Economic and environmental issues. *Bioscience,* 44 (8), 536-547.

Plaza, P., Griffiths, A. J., Syred, N., & Rees-Gralton, T. (2009). Use of a predictive model for the impact of co-firing coal/biomass blends on slagging and fouling propensity. *Energy & Fuels*, 23, 3437-3445.

Raask, E. (1979). Sintering characteristics of coal ashes by simultaneous dilatometry-electrical conductance measurements. *Journal of Thermal Analysis,* 16, 91-102.

Rushdi, A., Gupta, R., Sharma, A., & Holcombe, D. (2005). Mechanistic prediction of ash deposition in a pilot-scale test facility. *Fuel,* 84, 1246-1258.

Saljnikov, A., Komatina, M., & Goricanec, D. (2006). Verification of the mathematical model of pulverized coal combustion in swirl burners. *FME Transactions*, 34,45-52.

Samareh, J. A. (1998). Geometry modelling and grid generation for design and optimization. *ICASE/LaRC/NSF/ARO Workshop on Computational Aerosciences in the 21st Century*. Hampton, Virginia. April 22-24.

Sami, M., Annamali, K., & Wooldridge, M. (2001). Co-firing of coal and biomass fuel blends. *Progress in Energy and Combustion Science*, 27, 171-214.

Sazhin, S. S., Sazhina, E. M., Saravelon, . F., & Wild, P. (1996). The P-1 model for thermal radiation transfer: advantages and limitations. *Fuel* 75(3), 289-294.

Scaroni, A. W. (1989). Coal combustion – old and new challenges. *Preprints, Amer. Chem. Soc. Div. Fuel Chem.*, 34(1), 256 – 262.

Senior, C. L., & Srinivasachar, S. (1995). Viscosity of ash particles in combustion systems for prediction of particle sticking. *Energy & Fuel*, 9, 277-283.

Shao, Y., Xu, C., Zhu, J., Preto, F., Wang, J., Tourigny, G., Badour, C., & Li, H. (2010). Ash deposition during co-firing biomass and coal in a fluidized-bed combustor. *Energy Fuels*, 24, 4681-4688.

Sheng, C., Moghataderi, B., Gupta, R., & Wall, T. F. (2004). A CFD based study of combustion characteristics of coal blends in pulverized coal – fired furnace. *Fuel*, 83, 1543 – 1552.

Sivathanu, Y. R., & Faeth, G. M. (1990). Generalized state relationships for scalar properties in non-premixed hydrocarbon/air flames. *Combustion & Flame*, 82, 211-230.

Smith, I. W. (1982). The combustion rates of coal chars: a review. *19th Symposium (Int.) on Combustion / the Combustion Institute*, pp. 1045-1065.

Smoot, L. D., & Smith, P. J. (1985). *Coal Combustion and Gasification.* The Plenum Chemical Engineering Series. Plenum publishing corporation. 233 Spring Street, New York NY 10013.

Speight, J. M. (2005). *Handbook of Coal Analysis.* John Wiley & Sons. www.knovel.com.

Srinivasachar, S., Helble, J. J., & Boni, A. A. (1990). An experimental study of the deposition of ash under coal combustion. In: *Proceedings of the 23rd International Symposium on Combustion.* The combustion institute.

Sroda, S., Makipaa, M., Cha, S., & Spiegel, M. (2006). The effect of ash Stephenson, P. L. (2003). Mathematical modelling of semi-anthracite combustion in a single burner furnace. *Fuel*, 82, 2069-2073.

Stam, A. F., Livingston, W. R., Cremers, & M. F. G., Brem, G., (2009). Review of models and tools for slagging and fouling prediction for biomass co-combustion. http://www.ieabcc.nl/publications/slagging_fouling_in_cofiring.pdf. Retrieved June 24, 2011.

Strandstorm, K., Mueller, C., & Hupa, M. (2007). Development of an ash particle deposition model considering build-up and removal mechanisms. *Fuel Processing Technology*, 88, 1053-1060.

Strezov, V., Lucas, J. A., Evans, T. J., & Strezov, L. (2004). Effect of heating rate on the thermal properties and devolatilization of coal. *Journal of Thermal Analysis and Calorimetry,* 78, 385–397.

Su, S., Pohl, J. H., Holcombe, D., & Hart, J. A. (2001a). A comparison of thermal conditions between pilot and full-scale furnaces for studying slagging and fouling propensity in PF boilers. *Combustion Science & Technology*, 165, 129-150.

Su, S., Pohl, J. H., Holcombe, D., & Hart, J. A. (2001b). Slagging propensities of blended coals. *Fuel*, 80, 1351-1360.

Tsai, W. B., Hsieh, C. J., & Chieng, C. C. (2005). Parallel computation of electro-osmotic flow in L-shaped micro-channels. *6th World congress of structural and multidisciplinary optimization*. Rio de Janeiro, Brazil, 30 May – 03 June, 2005.

Takuwa, T., Mkilaha, I. S. N., & Naruse, I. (2006). Mechanism of fine particulate formation with alkali metal compound during coal combustion. *Fuel*, 85, 671-678.

Tillman, D., Conn, R., & Duong, D. (2009). Coal characteristics and biomass firing in pulverized coal boilers. Presented at *Coal Gen 2009*. Charlotte, North Carolina, USA. 18-21 August, 2009.

Truelove, J. S., & Holcombe, D. (1990). Measurement and modelling of coal flame stability in a pilot-scale combustor. *23rd Symposium (international) on Combustion / the Combustion Institute,* pp. 963 – 971.

Turns, S. R. (2006). *An Introduction to Combustion*. (2nd ed.). Singapore: McGraw-Hill.

Vargas, S., Frandsen, F. J., & Dam-Johansen, K. (2001). Rheological properties of high - temperature melts of coal ashes and other silicates. *Progress in Energy and Combustion Science*, 27, 237 – 429.

Versteeg, H. G.,& Malalasekera, W. (2007). *An introduction to Computational Fluid Dynamics*. (2nd ed.). Essex: Pearson Educational Limited.

Vassilev, S. V., Baxter, D., Anderson, L. K., & Vassileva, C. G. (2010). An overview of the chemical composition of biomass. *Fuel*, 89, 913 – 933.

Vuthaluru, R., & Vuthaluru, H. B. (2006). Modelling of a wall fired furnace for different operating conditions using FLUENT. *Fuel Processing Technology*, 87, 633-639.

Wang, H., & Harb, J. N. (1997). Modelling of ash deposition in large-scale combustion facilities burning pulverized coal. *Prog. Energy Combust. Sci.*, 23, 267-282.

Watt, J. D., & Fereday, F. (1969). The flow properties of slag formed from the ashes of British coals: Part 1: Viscosity of homogeneous liquid slag in relation to slag composition. *J. Inst. Fuel,* 42, 99-103.

Wigley, F., Williamson, J., & Jones, A. R. (1990). Slagging indices for UK coals and their relationship with mineral matter. *Fuel Processing Technology*, 24, 383-389.

Wigley, F., & Williamson, J. (1998). Modelling fly ash generation for pulverized coal. *Prog. Energy Combustion Science*, 24, 337-343.

Wigley, F., Williamson, J., Malmgren, A., & Riley, G. (2007). Ash deposition at higher levels of coal replacement by biomass. *Fuel Processing Technology*, 88, 1148-1154.

Williams, A., Backreedy, R., Habib, R., Jones, J. M., & Pourkashanian, M. (2002). Modelling coal combustion: the current position. *Fuel*, 81, 605-618.

Williams, A., Pourkashanian, M., & Jones, J. M. (2000). The combustion of coal and some other solid fuels. *Proceedings of the Combustion Institute*, 28, 2141-2162.

Williamson, D. L., Drake, J. B., Hack, J. J., Jakob, R., & Swarz-trauber, P. N. (1992). A standard test set for numerical approximations to the shallow water equations in spherical geometry. *J. Comput. Phys.*, 102, 211-224.

World Coal Institute, 2010. Coal & electricity.

World Coal Institute, 2010. Coal information.

Xiaohong, H., Zhaohui, L., Jing, L., Ming, Y., Yunye, S., & Chuguang, Z. (2011). Ignition behaviour of pulverized coal in lower oxygen content O2/CO2 atmosphere. *Energy Procedia* 00 (2011) 000-000.

Xu, M., He, X., Azevedo, L. T., & Carvalho, M. G. (2002). An advanced model to assess fouling and slagging in coal fired boilers. *Int. J. Energy Res.*, 26, 1221 – 1236.

Yin, C., Luo, Z., Ni, M., & Cen, K. (1998). Predicting coal ash fusion temperature with a back-propagation neutral network model. *Fuel*, 77 (15), 1777 – 1782.

You, C., & Zhou, Y. (2006). Effects of operation parameters on the slagging near swirl coal burner throat. *Energy & Fuel*, 20, 1855-1861.

Zhang, H., & Ahmadi, G. (2001). Particle transport and deposition in the hot-gas filter vessel at Wilsonville. *Powder Technology*, 116, 53-68.

Zhang, L., & Jahanshahi, S. (2001). Modelling viscosity of alumina-containing silicate melts. *Scandinavian Journal of Metallurgy*, 30, 364 – 369.

Zhao, B., & Wu, J. (2006). Modelling particle deposition onto rough walls in ventilation duct. *Atmosphere Environment*, 40, 6918-6927.

Zheng, Y., Jensen, P. A., Jensen, A. D., Sander, B., & Junker, H. (2007). Ash transformation during co-firing coal and straw. *Fuel*, 86, 1008-1020.

Zhou, H., Jensen, P. A., & Frandsen, F. J. (2007). Dynamic mechanistic model of super-heater deposit growth and shedding in a biomass fired gate boiler. *Fuel*, 86, 1519-1533.

Zygarlicke, C. J., Pavlish, J. H., Gunderson, J. R., & McCollor, D. P. (2000). Ash behaviour and combustion performance during the co-firing of rice straw lignin and coal. In *proceedings of the 9th Biennial Bioenergy Conference: Moving Technology into the Marketplace*; Buffalo, NY, Oct 15–19, 2000;